Canadian Science Publishing

ARTICLE

The mid-Cretaceous Peninsular Ranges orogeny: a new slant on Cordilleran tectonics? I: Mexico to Nevada[1]

Robert S. Hildebrand and Joseph B. Whalen

Abstract: The Peninsular Ranges orogeny occurred during the mid-Cretaceous at ~100 Ma and affected rocks from southern Mexico to Alaska. The event resulted from the closing of an Early Cretaceous marine arc trough, named the Bisbee–Arperos seaway in Mexico and Arizona, and the Cinko Lake arc trough in the Sierra Nevada. The trough was an ocean that formed after the Late Jurassic – Early Cretaceous Nevadan orogeny and associated post-collisional magmatism. It was open for ~40 million years and closed by westward subduction. Here, we focus initially on the most complete cross section, located in southwestern Mexico, where a west-facing Albian carbonate platform, with subjacent siliciclastic rocks built on the western margin of North America, was pulled down into a trench at 100 Ma, buried in hemipelagic mud and Cenomanian flysch, then overthrust from the west by rocks of the 140–100 Ma Santiago Peak – Alisitos arc and its substrate, the Guerrero Superterrane, which collectively document westerly subduction. This tectonically thickened collision zone was exhumed and intruded by 99–84 Ma distinctive post-collisional tonalite–granodiorite plutonic complexes, all with Sr/Y > 20, Sm/Yb > 2.5, Nb/Y > 0.4, and La/Yb > 10. These geochemical features are typical of slab failure, not arc magmas. The post-collisional plutons, previously considered to represent arc flare-ups, were derived from melting of the descending slab following arc-continent collision. Remnants of the arc, basin, related east-vergent 100 Ma thrusts, flexural foredeep, and 99–84 Ma slab failure plutons are traced from the Peninsular Ranges, through the Mojave Desert to the Sierra Nevada where similar rocks, relations, and ages occur. Along the western, back-arc, side of the orogen after collision and slab break-off, but during exhumation, east-dipping reverse faults with >10 km of east-side up movement shed 100–85 Ma plutonic and other debris westward from the hinterland into troughs such as the Valle and Great Valley. We extend our synthesis northward, from west-central Nevada to Alaska, in Part II.

Key words: orogeny, North American Cordillera, arc magmatism, arc-continent collision, slab failure magmatism, Peninsular Ranges orogeny.

Résumé : L'orogenèse des chaînes péninsulaires s'est produite durant le Crétacé moyen, vers 100 Ma, et a touché des roches allant du sud du Mexique à l'Alaska. Elle est le résultat de la fermeture d'une fosse d'arc marine d'âge crétacé précoce, appelée le bras de mer Bisbee–Arperos au Mexique et en Arizona et la fosse de l'arc de Cinko Lake dans les Sierra Nevada. La fosse était un océan formé après l'orogenèse névadienne d'âge jurassique tardif à crétacé précoce et le magmatisme post-collision associé. Elle est demeurée ouverte pendant ~40 millions d'années et s'est refermée par subduction vers l'ouest. Nous nous concentrons dans un premier temps sur la coupe la plus complète, située dans le sud-ouest du Mexique, où une plateforme carbonatée albienne faisant face à l'ouest, avec des roches silicoclastiques sous-jacentes accumulées sur la marge occidentale de l'Amérique du Nord, a été attirée dans une fosse à 100 Ma, ensevelie par des boues hémipélagiques et un flysch cénomanien, puis charriée vers l'est par des roches de l'arc de Santiago Peak – Alisitos de 140–100 Ma et son substrat, le superterrane de Guerrero, qui documentent collectivement une subduction vers l'ouest. Cette zone de collision épaissie tectoniquement a été exhumée et recoupée par des complexes plutoniques à tonalites-granodiorites post-collision distinctifs de 99–84 Ma qui présentent tous des rapports Sr/Y > 20, Sm/Yb > 2,5, Nb/Y > 0,4 et La/Yb > 10. Ces caractéristiques géochimiques sont typiques des magmas de rupture de plaque et non des magmas d'arc. Les plutons post-collision, auparavant considérés représenter des sursauts de magmatisme d'arc, sont dérivés de la fusion de la plaque descendante dans la foulée de la collision arc-continent. Des restes de l'arc, du bassin, de chevauchements vers l'est reliés de 100 Ma, de l'avant-fosse formée par flexion et de plutons associés à la rupture de la plaque de 99–84 Ma peuvent être suivis des chaînes péninsulaires au désert du Mojave et jusque dans les Sierra Nevada, où de roches, relations et âges semblables sont observés. Le long du côté ouest d'arrière-arc de l'orogène après la collision et la rupture de la plaque, mais durant l'exhumation, des failles inverses à pendage vers l'est montrant >10 km de déplacement du bloc est vers le haut ont évacué vers l'ouest des débris plutoniques de 100–85 Ma et d'autres débris de l'arrière-pays jusque dans des fosses comme la Valle et la Grande vallée. Dans la deuxième partie, nous élargissons notre synthèse vers le nord, du centre-ouest du Nevada jusqu'en Alaska. [Traduit par la Rédaction]

Mots-clés : orogenèse, cordillère nord-américaine, magmatisme d'arc, collision arc-continent, magmatisme de rupture de plaque, orogenèse des chaînes péninsulaires.

Received 20 August 2020. Accepted 7 December 2020.

R.S. Hildebrand. Tucson, Arizona, USA.
J.B. Whalen. Geological Survey of Canada, 601 Booth Street, Ottawa, ON K1A 0E8, Canada.
Corresponding author: Robert S. Hildebrand (email: bob@roberthildebrand.com).

[1]This paper is one of two companion papers published in this issue of Canadian Journal of Earth Sciences (Hildebrand and Whalen 2021. Canadian Journal of Earth Sciences. This issue. doi:dx.doi.org/10.1139/cjes-2021-0006).

It ain't what you know that gets you into trouble. It's what you know for sure that just ain't so.

—Mark Twain

Introduction

In 1969, Warren Hamilton published two seminal papers in which he inferred — based in part on the Cenozoic volcanic belt of the Andes — that thousands of kilometres of oceanic lithosphere were swept against, and subducted beneath, western North America to generate the great Mesozoic batholithic belt and the ensimatic and chaotic Franciscan Formation (Hamilton 1969*a*, 1969*b*). At about the same time, Dickinson (1970) noted the similarity of ages across California and so linked strongly deformed rocks of the high-pressure, low-temperature Franciscan complex with sedimentary rocks of the Great Valley Group and plutons of the Sierran-Klamath batholith as a trench fill – forearc basin – arc batholith tectonic association (Fig. 1). This concept quickly evolved into a more generalized hypothesis in which the trench fill – forearc basin – batholithic assemblage, interpreted to be the products of eastward subduction beneath western Laurentia, had an associated fold-thrust belt, located well to the east, with mostly westerly dipping thrust faults developed in heated retro-arc crust, and an adjacent, but even more easterly, foreland basin (Burchfiel and Davis 1972; Armstrong and Dick 1974; Dickinson 1976). A half century later, the essence of this model is still in vogue and rarely challenged, so the notion of eastward subduction beneath North America — especially for the great batholithic belts of the Sierra Nevada, Peninsular Ranges, and Coast plutonic complex — has become a formidable paradigm.

Although several contributions have challenged this paradigm (Moores 1970; Mattauer et al. 1983; Chamberlain and Lambert 1985; Lambert and Chamberlain 1988; Johnston 2008; Hildebrand 2009, 2013; Hildebrand and Whalen 2014*a*, 2014*b*, 2017; Hildebrand et al. 2018), they were, in many cases, broad syntheses covering several orogenies through time and so these ideas failed to generate traction within the Cordilleran community. In the aftermath of the recent kerfuffle about the polarity of subduction in the northern Cordillera (Sigloch and Mihalynuk 2020; Pavlis et al. 2020*a*, 2020*b*), it seemed to us worthwhile and timely to describe a little known, mid-Cretaceous orogeny that can be traced along the length of the North American Cordillera from southern Mexico to Alaska, and perhaps beyond, as it provides evidence on the polarity of subduction in the northern Cordillera. We call it the Peninsular Ranges orogeny after the region where we first recognized it and because the most-complete cross sections of the orogen are exposed there and in adjacent Mexico.

Although we have argued that other orogenies within the Cordillera involved eastward-facing arcs, we focus on the Peninsular Ranges orogen because it entailed several of the world's most impressive Cordilleran type batholiths, which, for over 50 years, have been taken as proof-positive evidence for eastward subduction beneath North America. We approach the overall geology of the orogen from south to north, and our goal is to demonstrate why we find the long-ingrained hypothesis for eastward subduction flawed and untenable.

The Peninsular Ranges orogen in its type area

In Southern and Baja California, the largely chaparral-covered mountains expose remnants of the Early Cretaceous Santiago Peak – Alisitos arc terrane, comprising shallow-marine clastic and carbonate sedimentary rocks, deep-water turbiditic fan deposits, basaltic to rhyolitic volcanic rocks, and 128–99 Ma calcic, epizonal intrusions ranging from gabbro to granite (Allison 1974; White and Busby-Spera 1987; Almazán-Vásquez 1988*a*, 1988*b*; Johnson et al. 2003; Wetmore et al. 2005; Busby et al. 2006; Herzig and Kimbrough 2014; Clausen et al. 2014; Morris et al. 2019). In California, the basement to the volcano-sedimentary cover is dominantly composed of metamorphosed and deformed Jurassic to Triassic metaturbidites, migmatitic schists, gneisses, and granodioritic plutons, but farther south on the Baja Peninsula of Mexico, carbonates and quartzites of Paleozoic age also occur (Shaw et al. 2003; Todd 2004; Gastil and Miller 1981; Gastil et al. 1991; Gastil 1993). Near San Diego, an uppermost Jurassic succession of marine volcaniclastic rocks, collectively named the Peñasquitos Formation, was folded, in places even overturned, prior to deposition of the Santiago Peak rocks (Kimbrough et al. 2014). To the south in Baja California (Fig. 2), arc successions overstep several subterrane boundaries within the Guerrero superterrane (Centeno-García et al. 2008), and after Cenozoic opening of the Gulf of California is restored, form a continuous lithostratigraphic unit onto the mainland in Zihuatanejo (Centeno-García et al. 2011; Duque-Trujillo et al. 2015). Thus, the arc formed atop and intruded rocks of the Guerrero superterrane as noted by Dickinson and Lawton (2001*a*).

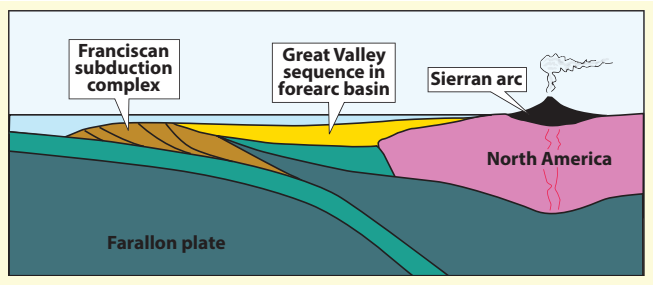

Fig. 1. Cartoon illustrating the fundamental western triad of the Sierran paradigm. [Colour online.]

The intrusions, dated at 128–99 Ma (Todd et al. 2003; Wetmore et al. 2005; Premo et al. 2014; Shaw et al. 2014), were informally termed the Escondido plutons (Clausen et al. 2014) whereas we called the same bodies, the Santa Ana suite (Hildebrand and Whalen 2014*b*). These plutons are both normally and reversely zoned, isotropic to foliated, locally protomylonitic, sheeted intrusive complexes, varying in composition from tonalite through quartz diorite and granodiorite to leucomonzogranite, locally with abundant wall rock screens and mafic inclusions, and containing varying proportions of mafic enclaves (Todd et al. 2003; Todd 2004).

Morton et al. (2014) noted that the westernmost intrusions are isotropic whereas those farther east are foliated, so that there is a megascopically visible deformation gradient from west to east, especially evident in enclaves. In the east, cumulate layering in gabbroic plutons is now mostly steeply dipping; intrusive contacts are folded, in many places isoclinally, along with their wall rocks. The mineral foliation is steep and commonly transects external contacts, and dykes of one pluton within another are isoclinally folded (Todd and Shaw 1979).

In Baja California, large pre-100 Ma plutons are also strongly deformed with concordant contacts, transecting cleavage, and folded wallrocks (Murray 1979; Johnson et al. 1999, 2003). Some bodies there were recumbently folded (Johnson et al. 2002). Overall, the data provide compelling evidence that intrusions of the Santiago Peak – Alisitos arc are complexly folded sills or sheets (Hildebrand and Whalen 2014*b*).

Age of deformation

Premo and Morton (2014) examined a variety of rocks in the Peninsular Ranges where they found and dated zircon in a pre- to syn-metamorphic diorite dyke, which yielded an age of 103.3 ± 0.7 Ma. They also dated zircon in a post-metamorphic pegmatite dyke to be 97.53 ± 0.18 Ma, which they interpreted to have been

Fig. 2. Sketch map illustrating key geological units of the Peninsular Ranges batholith and Aptian–Albian volcano-sedimentary rocks of the Alisitos – Santiago Peak arc, various terranes of the Guerrero superterrane, and Albian carbonate platforms, mostly located west of the younger Laramide suture and its related fold-and-thrust belt. The Peninsular Ranges batholith continues the length of Baja California, as indicated by a conspicuous aeromagnetic anomaly (Langenheim et al. 2014), but the batholith is buried by younger volcanic rocks south of the state line. Red dots represent drilled and dated core from La Posta plutons (Duque-Trujillo et al. 2015). Rocks of similar age and lithology to those of the Peninsular Ranges batholith crop out in Zihuatanejo (Centeno-García et al. 2011). Westward-facing Albian carbonate banks of the Sonora and Guerrero–Moreles platforms were pulled westward beneath rocks of the Guerrero superterrane at 100 Ma during closure of the Bisbee–Arperos seaway. Box labeled "TP" shows location of Fig. 5. [Colour online.]

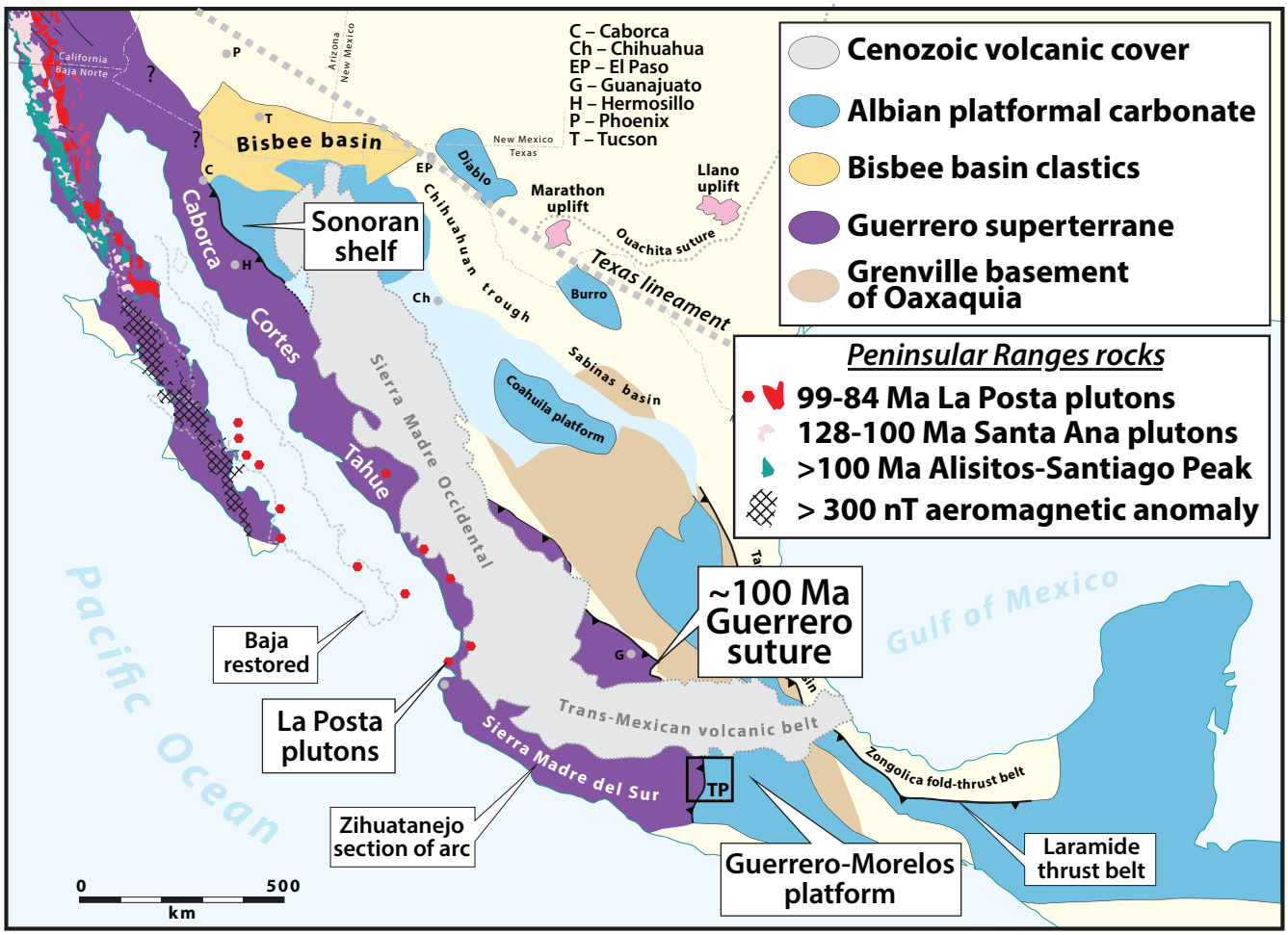

emplaced soon after metamorphism. Additionally, they dated more than 30 hornblende separates and determined that metamorphism took place at or before 100.1 ± 0.6 Ma. These age data are consistent with data collected farther south in the Sierra de San Pedro Mártir of Baja California, where the age of the deformation is tightly constrained by plutons. There, 100 Ma gabbro, as well as a 101 Ma gabbro–tonalite–trondhjemite body, are compositionally linked to the arc, strongly deformed, and folded (Johnson et al. 2002; Alsleben et al. 2008; Schmidt et al. 2009) whereas the post-deformational Sierra San Pedro de Mártir intrusive complex yields U–Pb zircon ages as old as 96 Ma (Gastil et al. 2014; Ortega-Rivera et al. 1997). Thus, we consider the deformational age of the arc rocks to be tightly constrained at 100 Ma, roughly coincident with the Albian–Cenomanian boundary (Cohen et al. 2013).

Bisbee–Arperos seaway

The Santiago Peak – Alisitos arc developed along the western margin of an elongate trough or seaway, termed the Bisbee–Arperos seaway, after the transborder Bisbee basin and the Arperos basin farther south, which we interpret to have been parts of the same basin (Hildebrand and Whalen 2014*b*). The Bisbee–Arperos basin developed during rifting of the western part of North America following the ~153 Ma Nevadan orogeny and a younger Early Cretaceous event, possibly as young as about 140 Ma.

In southern Arizona, coarse clastic sedimentation and eruption of bimodal volcanic rocks in the Bisbee basin were traditionally considered to have started at around 150 Ma, following Early to mid-Jurassic arc magmatism (Bilodeau et al. 1987; Krebs and Ruiz 1987; Lawton and McMillan 1999; Dickinson and Lawton 2001*b*). However, the oldest sedimentary rocks within the basin were recently shown by detrital zircon studies and dating of intercalated volcanic rocks to have been deposited between 136 and 125 Ma (Peryam et al. 2012). Within the Bisbee Basin, the lowermost clastic rocks have bimodal northeast–southwest paleocurrents and reflect shelf, lagoonal, tidal flat, and fluvial environments (Klute 1991), but pass stratigraphically upwards into an eastward-transgressive sequence of fining-upwards fluvial to shallow marine deposits (Peryam et al. 2012). A recent stratigraphic, detrital

Fig. 3. Block diagram modified from Martini et al. (2014) illustrating the dual nature of sedimentation within the Bisbee–Arperos seaway of southern Mexico and the 100 Ma collision between the Guerrero superterrane and North America. Where sufficient data exist, these relations are consistent from southern Mexico to Alaska. [Colour online.]

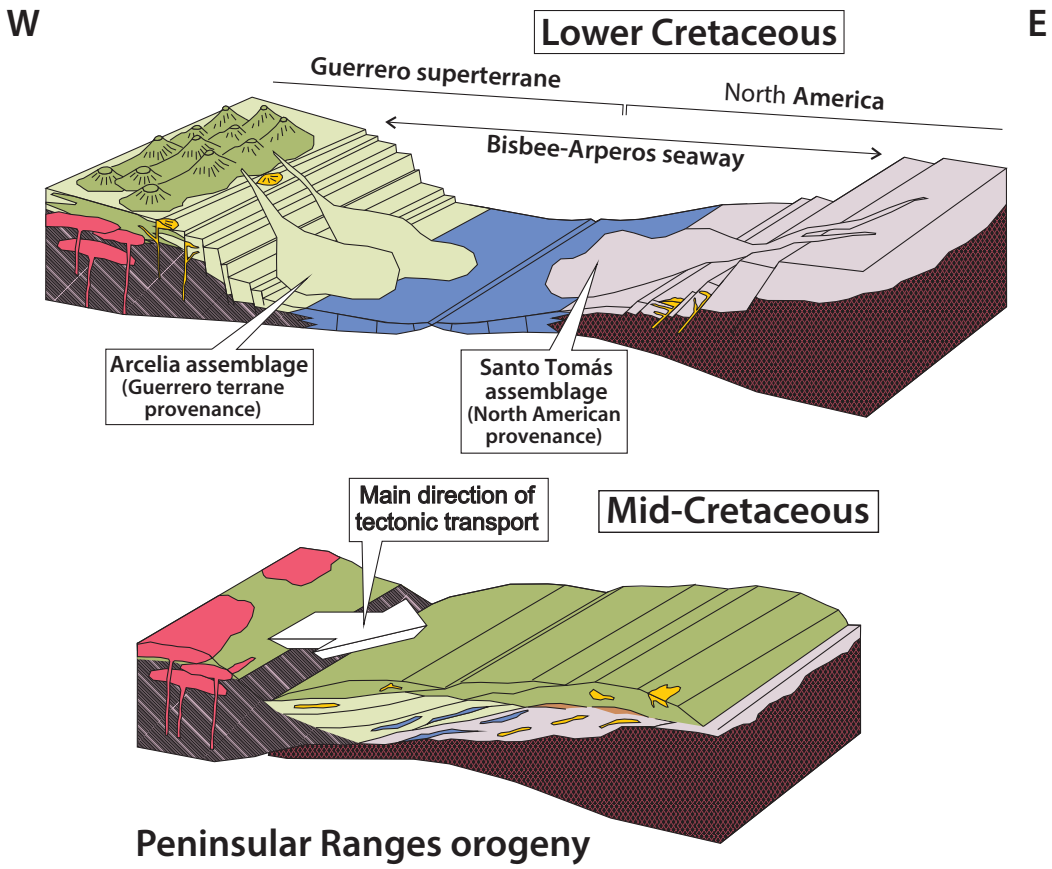

zircon, and provenance study of the basal siliciclastic unit in the basin, the Morita Formation, determined maximum depositional ages (MDAs) for the lower part of the unit to range from 131 to 125 Ma depending on the location (González-León et al. 2020). The overlying carbonate platform, known in northern Mexico as the Sonoran shelf, had a well-developed reefal rim or ramp along its southwest side (González-León et al. 2008).

In Sonora, the rocks of the Bisbee Basin sit unconformably atop deformed Jurassic arc rocks and isoclinally folded, Oxfordian to Tithonian, marine clastic rocks of the Cucurpe Formation, which were largely derived from post-160 Ma plutonic rocks of the bimodal Ko Vaya suite (Mauel et al. 2011; Lawton et al. 2020). We interpret rocks of the Cucurpe Formation to be consanguineous with the Tithonian Peñasquitos Formation of the western Peninsular Ranges near San Diego (Kimbrough et al. 2014), as both formations have similar basements and contain comparable rocks of the same age. Furthermore, both successions were deformed between about 145 and 139 Ma and are both unconformably overlain by 130–125 Ma rocks. In the east, the Curcurpe Formation is overlain by rocks of the Bisbee margin; and to the west, rocks of the Peñasquitos Formation are overlain by the Santiago Peak volcano-sedimentary arc complex. Kimbrough et al. (2014) noted that another succession, the Mariposa Formation of the western Sierra Nevada, is also of the same age (Snow and Ernst 2008), has a similar detrital zircon profile, and was intruded by 125–120 Ma plutonic rocks of the westernmost Sierran batholith (Lackey et al. 2012*a*, 2012*b*).

Farther south, much of east-central Mexico, such as Oaxaquia, Central, and Mixteca terranes (Ortega-Gutiérrez et al. 1995; Centeno-García 2005; Keppie et al. 2012), formed a coherent block and was covered by a westward-thickening siliciclastic prism capped by a west-facing Albian carbonate platform (Fig. 2), known as the Guerrero–Morelos platform in southern Mexico as well as the Valles – San Luis and El Doctor platform in central Mexico (Lapierre et al. 1992; Monod et al. 1994; Centeno-García et al. 2008; Martini et al. 2012). The platform was built upon about 1000 m of Lower Cretaceous red beds, alluvial sandstone, and conglomerate with thick evaporite deposits and an older metamorphic basement (Fries 1960).

Martini et al. (2014) demonstrated that calcareous and siliciclastic metaturbidites of the eastern Santo Tomás assemblage, deposited on easterly derived submarine fans within the basin, were exclusively derived from North American sources, such as Oaxaquia and the Acatlán and Taray complexes, and were sedimentologically disconnected from mafic to intermediate volcanic sources in the arc to the west (Fig. 3).

The western margin of the Arperos Basin, now preserved in eastward-vergent thrust sheets, is represented by the Arcelia and Arperos assemblages, which comprise Aptian volcaniclastic metaturbidites derived from the west, and are intercalated with intraplate and oceanic basalts (Tardy et al. 1994; Martini et al. 2012). Overall, the basin shows a clear provenance asymmetry with sediments derived from the Guerrero terrane and its carapace of arc rocks to the west and mainland-derived sediments to the east (Fig. 3), so that the Bisbee–Arperos seaway separated the Guerrero superterrane and its arc from the Lower Cretaceous passive margin of North America (Martini et al. 2014; Hildebrand and Whalen 2014*b*).

Fig. 4. Detailed cross section of the uppermost few metres of the west-facing Guerrero–Morelos carbonate platform showing the rapid transition from carbonate shelf to orogenic deposits near Concordia, Estado de Guerrero. Hoffman (2012) presents an excellent overview of the process of platform foundering at the beginning of orogenesis. Figure modified from Monod et al. (2000). For location of section, see Fig. 5. [Colour online.]

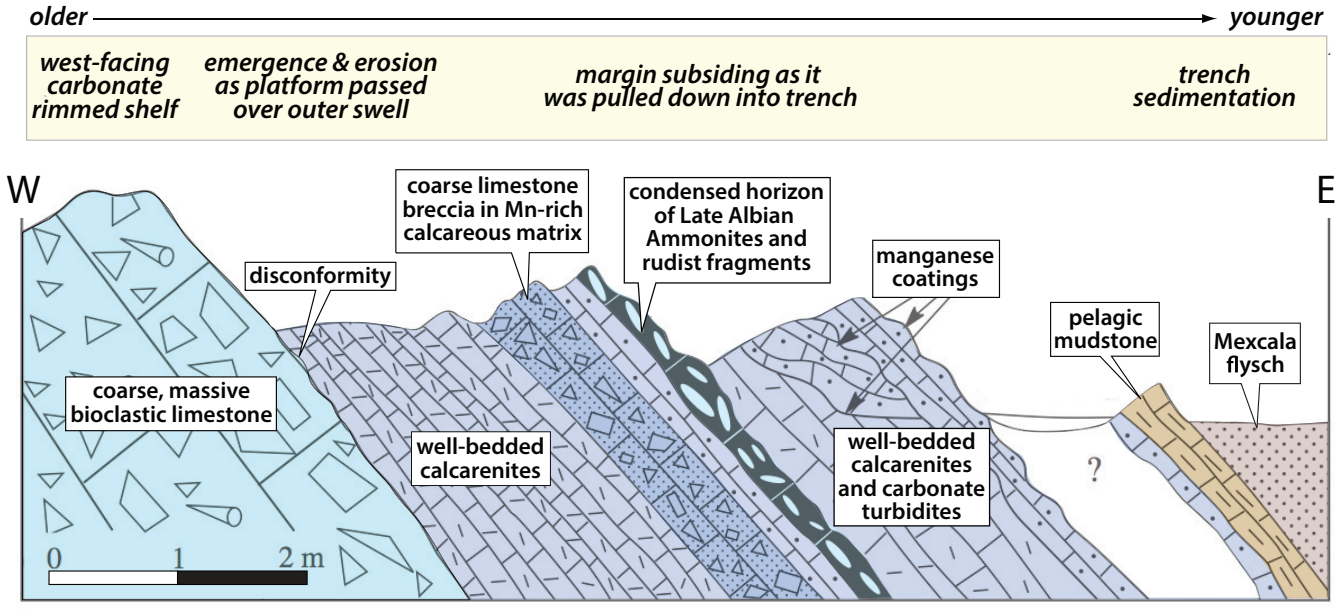

Closure of the Bisbee–Arperos seaway and arc-continent collision

Perhaps the best cross section of the orogen in southern and central Mexico is that of the Sierra Madre del Sur, located south of the Trans Mexico volcanic belt (Fig. 2). There, beginning in the late Albian, upward growth of the west-facing carbonate platform stopped, as marked by a disconformity atop massive bioclastic carbonate and below a few metres of well-laminated beds of detrital carbonate, breccias, condensed horizons rich in Albian faunal debris, and ultimately by hemipelagic shale overlain by Mexcala flysch (Monod et al. 2000). The disconformity, as well as the rapid tectonic subsidence and burial of the carbonate platform by hemipelite and orogenic flysch, are easily explained by transport of the platform over the outer bulge to a trench, where it was eroded; then, as the platform was pulled into the trench, it was covered by a thin veneer of hemipelagic mud deposited on the starved outer-trench slope, only to be overwhelmed by trench-fill turbidites upon arrival in the trench axis (Fig. 4). Easterly vergent thrust faults inverted the basin and thrust basinal facies rocks and basement of the Guerrero superterrane onto the North American margin, where it originated prior to rifting and formation of the basin (Fig. 3).

To the west of the carbonate platform, several kilometres of calc-alkaline and tholeiitic metavolcanic and metasedimentary rocks of various arc assemblages within the Guerrero superterrane (Centeno-García et al. 2008), including, from west to east, the Zihuatanejo, Arcelia, Taxco – Taxco Viejo, and Teloloapan assemblages, have U–Pb ages and prominent age peaks ranging from 141 to 124 Ma (Talavera-Mendoza et al. 2007; Campa-Uranga et al. 2012), the same age as the passive margin succession on the eastern side of the Bisbee–Arperos trough. The easternmost units of the Teloloapan terrane were thrust over the west-facing, dominantly Albian Guerrero–Morelos carbonate platform and its synorogenic cover of Cenomanian Mexcala flysch (Fig. 5) at about 100 Ma. Some researchers (Mendoza and Suastegui 2000; Guerrero-Suasegui 2004; Talavera-Mendoza et al. 2007) argued that the easternmost Teloloapan metavolcanics, which are penetratively deformed and recumbently folded, but at relatively low metamorphic grade, were overlain by a different, but much lesser deformed, carbonate platform just west of the Guerrero–Morelos platform and place the suture along its eastern boundary. Here we note that because both carbonate platformal successions formed during the Albian and are overlain by similar Cenomanian clastic successions, we interpret them as formerly continuous units dismembered by thrust faults. We locate the suture along the Teloloapan thrust (Fig. 5), which places the older volcanic successions eastward over the Albian carbonate platform and its overlying orogenic Mexcala flysch as originally envisioned by Campa and Coney (1983).

In the north, the Sonoran platform was buried by at least 1500 m of westerly derived Cenomanian and Turonian flysch, termed the Cintura and Mojado formations, and deposited in a flexural foredeep (Mack 1987; González-Léon and Jacques-Ayala 1988). The most southwestern exposures of Cintura Formation are in excess of 2000 m thick and are overlain gradationally by latest Albian – early Cenomanian fluvio-deltaic sandstone with sparse pebbles of quartzite and limestone, and overthrust from the southwest by plutonic rocks (Jacques-Ayala 1992; T. Lawton, personal communication 2014). Lawton et al. (2020) established the temporal correlation between the Mojado and Cintura formations by U–Pb studies of detrital zircons and ash beds, which aid in understanding the nature of the foredeep as far to the east as El Paso, Texas.

The tectonic subsidence was caused by downward flexure of the lithosphere when the leading edge of the North American margin was subducted beneath the Guerrero superterrane and its Lower Cretaceous arc carapace (Pubellier et al. 1995; Martini et al. 2014). The Cintura Formation is overlain in Sonora by conglomerate of the Cocóspera Formation interbedded with andesitic lava dated by $^{40}Ar/^{39}Ar$ as 93.3 ± 0.7 Ma (González-León et al. 2011). Anderson et al. (2005) also described the thrust belt in some detail and, based on the age of a pluton that cuts mylonites of the zone, determined that the deformation was older than 84 Ma.

Taken in its entirety, the evidence in western Mexico suggests that the Alisitos – Santiago Peak arc, and its basement, collided with a west-facing passive margin at about 100 Ma during the

Fig. 5. Geological sketch map showing relations near Teloloapan, west-central Mexico, illustrating metavolcanic and metasedimentary rocks of the Roca Verde, Taxco–Viejo, and Teloloapan arc assemblages thrust over the west-facing Guerrero–Morelos carbonate platform and its overlying syntectonic cover of Mexcala flysch along the Teloloapan thrust. Modified from Cabral-Cano et al. (2000). Detailed section at Concordia (Fig. 4) marked by star. See Fig. 2 for location of figure. [Colour online.]

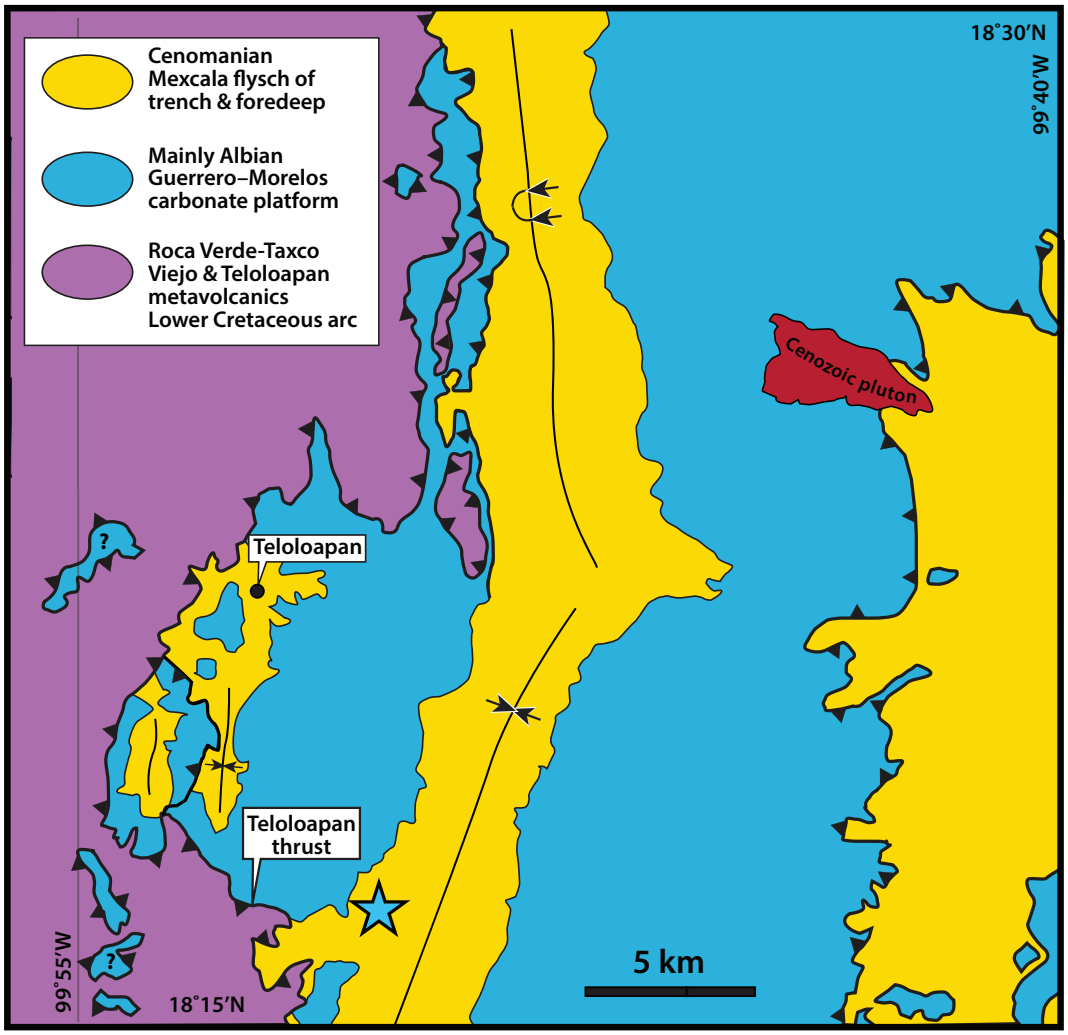

Peninsular Ranges orogeny. The polarity of subduction was clearly westward and the western edge of the North American passive margin was partially subducted beneath the arc. The basin was apparently a linear trough of unknown width that was open for at least 30 million years, but it must have been sufficiently wide to be floored by oceanic crust to drive the 100 Ma collision. If we assume that half of the 30 million year timespan was spreading, then at moderate spreading and convergence rates of 5 cm/year (Müller et al. 2008), the basin would have been about 750 km wide: about three-quarters the maximum width of the Sea of Japan.

Post-collisional plutonism and exhumation of the orogenic hinterland

Soon after collision and terminal closure of the basin, seemingly within a million years, the collisional hinterland was intruded by a voluminous suite of post-collisional 99–86 Ma mesozonal to catazonal plutons (Fig. 6). The bodies were intruded during a period of rapid exhumation when rocks at depths of 15–23 km were brought to the surface in less than 10 million years by detachment faulting and collapse (Krummenacher et al. 1975; Ortega-Rivera et al. 1997; Ortega-Rivera 2003; Miggins et al. 2014). Rapid exhumation is also documented by abundant coarse plutonic debris of the Valle Formation, such as boulder beds containing clasts up to 2.5 m in diameter, as well as abundant 100–90 Ma detrital zircons deposited during the Cenomanian–Turonian, in a basin located to the west of the collision zone (Kimbrough et al. 2001). As this basin was located west of the former arc and collision zone, that is, on the opposite side of the arc from the trench, it cannot have been a forearc basin. The debris was probably shed from reverse fault scarps, some with 3–4 kbar of 100–86 Ma exhumation across them, that bounded the hinterland belt to the west (Schmidt and Paterson 2002; Schmidt et al 2014; see also Supplementary Fig. S1[2]).

The post-collisional intrusions form a group of gregarious plutons, collectively termed the La Posta suite, after a compositionally zoned intrusive complex that spans the international border (Walawender et al. 1990). The plutons are mesozonal to catazonal, range in age from 99 to 86 Ma (Premo et al. 2014), possibly

[2]Supplementary data are available with the article at https://doi.org/10.1139/cjes-2020-0154.

Fig. 6. U–Pb zircon ages with 2σ errors for the Peninsular Ranges batholith plotted versus general longitude. Modified from Premo et al. (2014) with additional ages from Shaw et al. (2014), Gastil et al. (2014), and Wetmore et al. (2005). The pluton ages prior to 100 Ma are not aligned by geography, but by age, because most researchers recognized that the western Santa Ana arc suite did not migrate with time (Silver and Chappell 1988; Shaw et al. 2014). [Colour online.]

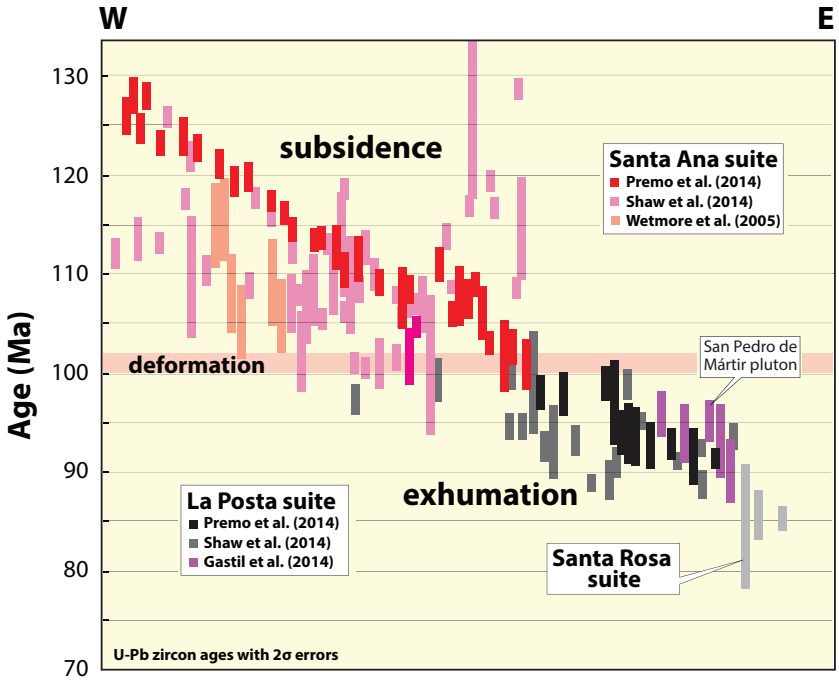

young eastward (Ortega-Rivera 2003), and are dominated by large, concentrically zoned complexes comprising biotite–hornblende-bearing, tonalitic marginal phases grading inward over several decametres to granodiorite and cored by granite, in places containing both biotite and muscovite (Hill 1984; Silver and Chappell 1988; Walawender et al. 1990). A diagnostic characteristic of the bodies in the field is the presence of euhedral titanite (Silver and Chappell 1988).

The plutons were emplaced mostly to the east of the Santiago Peak – Alisitos arc, although a few intrude the easternmost arc plutons. Thus, there are two, side-by-side intrusive suites, the arc-related Escondido / Santa Ana and the post-collisional La Posta. Plutons of the Escondido / Santa Ana arc suite are mainly epizonal and compositionally more variable, ranging from gabbro to granite, than the younger, post-collisional La Posta plutons, which are dominantly granodioritic to tonalitic.

These two different intrusive suites, each with different ages, depth of emplacement, and composition have been recognized for some time (Buddington 1927; Larsen 1948; Silver et al. 1979; Silver and Chappell 1988; Gromet and Silver 1987; Gastil et al. 1975, 1990; Kimbrough et al. 2001; Tulloch and Kimbrough 2003; Ortega-Rivera 2003). Most researchers agree that the older Santiago Peak – Alisitos rocks represents a magmatic arc, but also infer that the younger La Posta magmatism represented a continuation of arc magmatism, despite development of numerous models that invoke closure of back-arc basins and collisions just prior to their emplacement (Silver and Chappell 1988; Gastil et al. 1981; Gromet and Silver 1987; Todd et al. 1988; Walawender et al. 1990; Busby et al. 1998; Johnson et al. 1999; Ortega-Rivera 2003; Schmidt et al. 2014).

Kimbrough et al. (2001) tied together many critical elements, including the post-deformational nature of the La Posta suite, the rapid exhumation, and coeval sedimentation to the west, which they viewed as the fore-arc region, but they attributed the La Posta suite to a transient episode of high-flux magmatism. Tulloch and Kimbrough (2003) expanded on the earlier model by recognizing that the La Posta suite was a high Na, Sr and low Y suite and so created a model in which the older, western and low Sr, Y Santiago Peak – Alisitos arc was underthrust beneath the mainland arc during slab-flattening, which shut off normal arc magmatism and generated the burst of La Posta magmatism. In a more recent contribution, Centeno-García et al. (2011, p. 1793) noted the strong ties between the history of Baja California and the Guerrero composite terrane of mainland Mexico and so speculated that the arc was separated from the continent by a marginal basin, which closed "when the Early Cretaceous Alisitos fringing arc underthrust the Mexican continental margin and the crust was greatly thickened" also without explaining how the arc ended up on the lower plate and the continental margin on the upper.

Hildebrand and Whalen (2014*b*) examined recent inductively coupled plasma – mass spectrometry geochemical data and, to resolve the tectonomagmatic difficulties, proposed that the two plutonic suites were emplaced in two different tectonic regimes separated by a 100 Ma arc-continent collision. The collision resulted from the closure of the Bisbee–Arperos seaway, which had formed along the western North America margin at about 140 Ma (Fig. 4). That the plutons were emplaced during rapid exhumation suggested to us that the post-collisional bodies formed by some mechanism related to slab break-off (Sacks and Secor 1990; Davies and von Blanckenburg 1995). It is the depth of break-off that largely controls the width of the orogen, for it is the rebound of the partially subducted continent that will lead to the region of intense uplift and exhumation (Duretz et al. 2011, 2012; Duretz and Gerya 2013). Thus, shallow break-off creates narrow orogens, lower-grade metamorphism, and intense, rapid, and higher rates of exhumation, whereas deep break-off creates broad orogens with higher grades of metamorphism and slow, more subdued rebound (Duretz et al. 2011).

The process of arc-continent collision and slab failure, or break-off, involves the pulling of the leading edge of the continent beneath the arc. When the competing buoyancy forces

Fig. 7. Plutonic samples with SiO_2 >60% from the Peninsular Ranges batholith plotted on five discrimination diagrams modified from Hildebrand and Whalen (2014*b*, 2017) and Whalen and Hildebrand (2019). The Nb vs. Y and Ta vs. Yb discrimination diagrams were modified from Pearce et al. (1984) by addition of fields for post-collisional and arc plutons based empirically on samples from the Peninsular Ranges batholith. ORG, within-plate granite. Alisitos volcanic arc data are generally more mafic and are from Morris et al. (2019). [Colour online.]

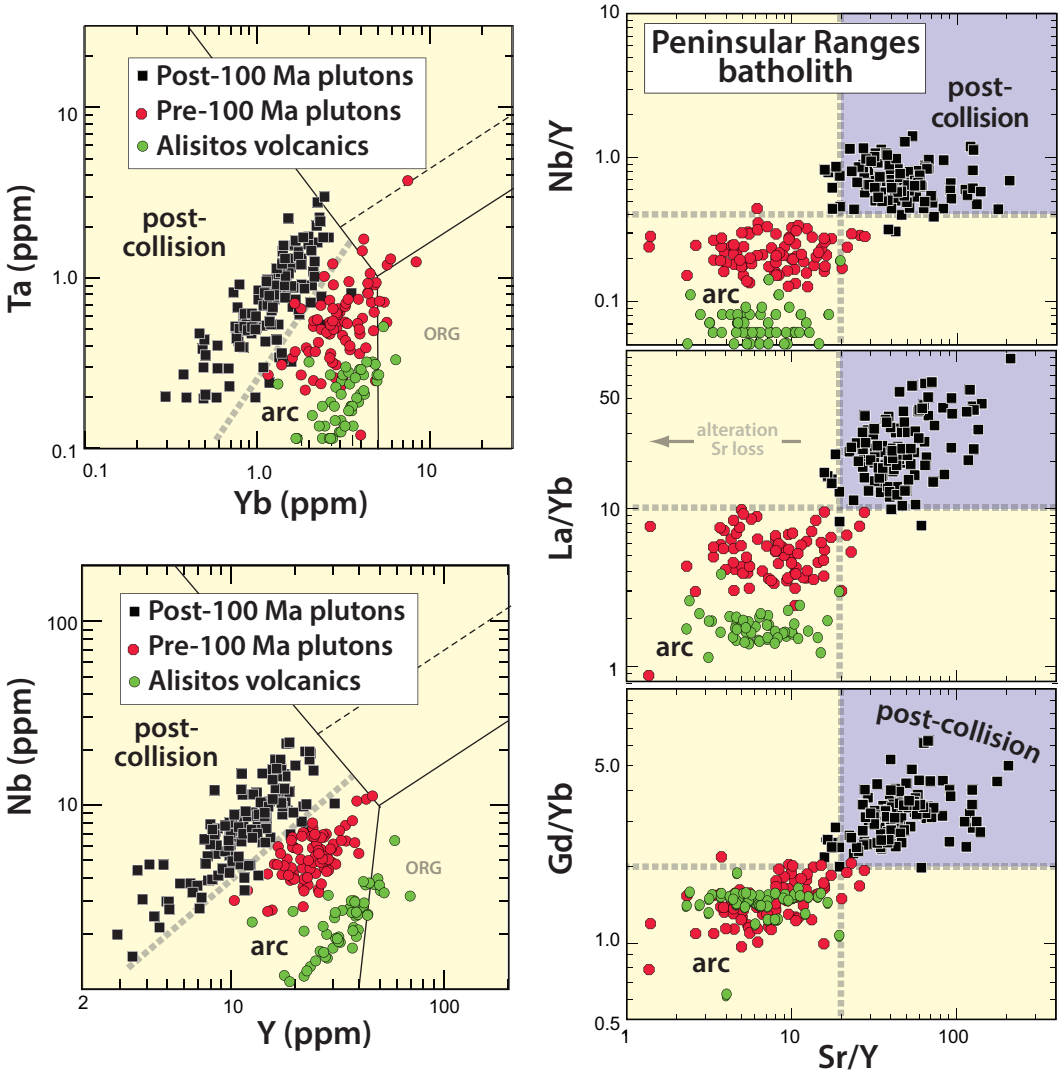

between the oceanic and continental lithosphere are overcome, the sinking slab tears from the lower continental plate and sinks into the mantle. Unless the tear is diachronous, the collision stops at this time, the trench dies, and the continental margin, now free of its oceanic anchor, rapidly rises thereby generating extreme exhumation rates in the collision belt. Well-understood ongoing arc-collision belts, such as Taiwan, provide a timeline of 4–5 million years for arc-continent collision in the south, slab break-off, collapse of the mountain belt in the northern part of the island, and initiation of oppositely directed subduction beneath the Ryukyu arc (Viallon et al. 1986; Suppe 1987; Lallemand et al. 2001; Huang et al. 2006; Teng 1996). In the case of the Peninsular Ranges orogen, the short time from initial collision of the arc, which had relatively thin crust, as documented by the presence of intercalated marine sedimentary rocks in the arc, to slab break-off — as well as other severe problems discussed by Hildebrand (2013, p. 82) — preclude crustal thickening by arc magmas and melting of underthrust cratonic crust, both of which are integral components to the cyclic arc model of DeCelles et al. (2009).

The recognition that the two magmatic suites were emplaced in contrasting tectonic settings led to the construction of a variety of geochemical discrimination diagrams (Fig. 7) that provide evidence for the distinction between arc and post-collisional plutons, and are especially useful where the geology is difficult, obscure, or incomplete. These discrimination diagrams were verified with Cenozoic arc and post-collisional rocks where the tectonic setting is independently known (Hildebrand and Whalen 2017; Hildebrand et al. 2018). We also devised a protocol for their use (Whalen and Hildebrand 2019), and then tested their usability with multiply deformed and metamorphosed volcanic and plutonic rocks in the Paleozoic Taconic orogen (Hildebrand and Whalen 2020). We discuss our model for the petrogenesis of these rocks following a description of the Sierra Nevada where additional data from plutons in a similar tectonomagmatic regime helps to unravel their petrogenesis.

As we describe parts of the orogen farther north, it is important to keep in mind that the best exposed cross section of the orogen is in Mexico and not all of the more northerly cross sections are as complete, or obvious, as they are complicated by

Fig. 8. Similarities along strike within the Peninsular Ranges orogen, from Mexico to Alaska, of major sedimentological, magmatotectonic, and tectonic packages arranged from west to east, along with their age constraints, where known. Note the coeval nature of most units along strike. The absence of a foreland basin north of the Lewis and Clark line in Idaho/Montana is attributed to uplift and erosion during the younger Laramide orogeny.

West → East

North ↑ South

Location	Western retroarc debris 99-83 Ma	Back-arc Reverse faults	Arc terrane 130-100 Ma	Syn-arc basin 140-100 Ma	Age of Collision	Metamorphic hinterland	Post-collision plutonism 99-84 Ma	Easterly vergent fold-thrust belt ~100 Ma	Foredeep <100 Ma
Mainland Alaska	McHugh complex	Yes	133-98 Ma Chisana	Kahiltna	103-97 Ma	amphibolite	94-88 Ma Tok-Tetlin Gardiner Crk. ?	yes	unknown
Insular Alaska	Queen Charlotte Group	Yes	Muir-Chichagof suite & Gravina	Gravina	105-95 Ma	amphibolite granulite	95-90 Ma Moth Bay & many others	yes	unknown
Coast Plutonic belt, BC	Nainaimo Group	Yes	Gambier Group Firvale & Desire plutonic suites	Gambier Group	101-97 Ma	amphibolite granulite	Ecstall & many others 99-85 Ma	yes	unknown
Cascades	Cascade River Skagit gneiss ?	NR	Chiwaukum schist	Nooksack	108-96 Ma	amphibolite	Many plutons 96-89 Ma	unknown	unknown
Idaho & Montana	unknown	NR	Little Goose Hazard Creek 120-108 Ma	unknown	100-91 Ma	amphibolite	Atlanta lobe Payette-Rat Cr. 98-84 Ma	Yes	Flint Crk. basin Frontier Fm. Bighorn basin
Nevada/UT	unknown	NR	King Lear 125-123 Ma	Newark Canyon ?	101-96 Ma	amphibolite	Many plutons 98-84 Ma	Sevier fold & thrust belt: Pavant & Nebo thrusts	Frontier Sanpete Dakota Mancos Indianola
Sierra Nevada	Eastern Great Valley Group	NR	western arc terrane & Cinko Lake arc	Cinko Lake trough	103-98 Ma	amphibolite	Sierran Crest 99-84 Ma		
Mojave Desert	unknown	NR	Delfonte volcanics 100.5±2 Ma	not recognized	100.5-98 Ma	amphibolite	Teutonia & others 98-85 Ma	New York Mtns Mezcals-Spring & Muddy Mtns	Willow Tank Baseline etc
Peninsular Ranges Mexico & USA	Valle Gp	Yes	128-100 Ma Santiago Peak & Alisitos	Bisbee-Arperos trough	103-98 Ma	amphibolite	La Posta 99-84 Ma	Yes	Cintura Mojada Mexcala

Laramide overprint

BC–British Columbia | UT–Utah | NR–Not Recognized | Crk–Creek

younger orogenic events, intrusions, or cover. Nevertheless, we find that along strike, sufficient components of the orogen exist to ascertain that it is continuous and coeval from Mexico to Alaska (Fig. 8). In most locations, several of the following features exist and collectively constitute a rationale for correlation and continuity along strike.

1. The occurrence of an Early Cretaceous trough, 140–100 Ma, comprising volcano-sedimentary arc successions formed on a substrate of Jurassic orogenic rocks, commonly atop Paleozoic cover.
2. A >100 Ma arc with magmatism that overlaps temporally with sedimentation in the trough and is located along the western margin of it.
3. Sedimentation within the trough that deposited different age debris adjacent to opposite sides of the basin.
4. The consilience of deformation of the volcano-sedimentary arc successions, shutdown of arc magmatism, eastward-verging thrusting, and formation of an orogenic foredeep — all at about 100 Ma.
5. Post-deformational plutons, with compositions distinct from arc plutons, and ranging in age from 99 to 84 Ma, were emplaced into an orogenic hinterland during rapid exhumation.
6. Reverse faults, typically with 6–10 km of east side up separation, formed along the western margin of the orogenic hinterland.
7. Sedimentary rocks, most commonly Cenomanian to Santonian, containing abundant post-collisional plutonic debris were shed westward into the back-arc region during exhumation of the hinterland to the east.

Whereas the trough opened along a largely Jurassic accretionary margin, it contained a wide variety of rocks ranging in age from Precambrian to Cretaceous and grouped in many ways from area to area. In some places, such as Mexico, the Guerrero terrane refers to the westernmost outboard terrane, but in other places along strike, rocks had not been grouped into older terranes and groups, or were previously part of named terranes, but were dismembered and now occur on both sides of the trough. For example, in the Canadian Cordillera, the more easterly Intermontane and westerly Insular superterranes collided during the Jurassic, but rifting during opening of the seaway at 140–135 Ma, did not occur at precisely the same location(s) as the previous suture, so although the western block was dominated by rocks of the Insular terrane, it could contain fragments of Intermontane terrane and form a new western composite terrane. The lack of recognition of this 100 Ma suture zone led to some implausible models involving reversed basins and large-magnitude strike-slip faults (Monger et al. 1994; Gehrels et al. 2009). By recognizing the existence of the Early Cretaceous seaway, we resolve these types of problems to some degree, but the problem of previously defined terranes occurring on opposite sides of the basin is an artifact of problems inherent in the existing nomenclature. To resolve these issues, we refer to all of the rocks on the outboard arc-bearing block, which appear to have formed a continuous ribbon continent, as the Peninsular Ranges composite terrane, although we still utilize the original names wherever reasonable to do so, such as with local basement-cover relations.

Mojave Desert sector

The thrust belt in Sonora can be traced northward to about the United States border where it is transected by a segment of the younger, and somewhat sinuous, Laramide orogen, which trends nearly east–west across southern Arizona and California (Hildebrand 2015). To the north, the 80–70 Ma post-deformational intrusions of the Laramide are progressively less common (Fig. 9) and the 100–85 Ma post-deformational plutons reappear to the

Fig. 9. Map modified from Wells (2016) and Hildebrand and Whalen (2017) on a geological base provided by Sue Beard (US Geological Survey) showing the location of sites near Las Vegas, Nevada, with evidence for 100 Ma thrusting as red stars, and location of 100–85 Ma plutons described in text as blue stars. WCT, Wilson Cliffs thrust; RST, Red Springs thrust; WPT, Wheeler Pass thrust. [Colour online.]

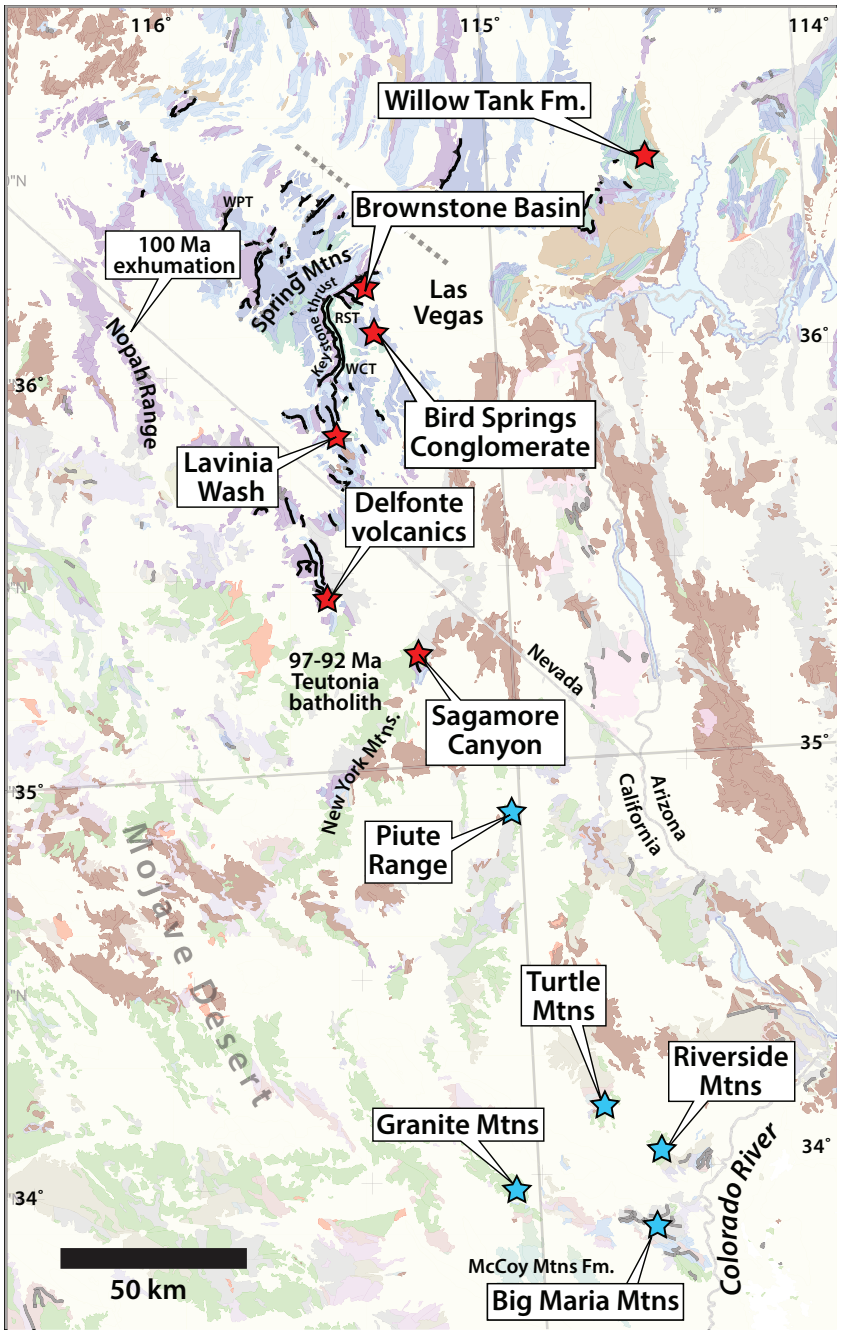

north of the Laramide McCoy Mountains Formation, and to the west within California in the Big Maria Mountains, where a 86 Ma granodiorite was folded during the Laramide orogeny (Hamilton 1964; Stone 2006). Just to the north in the Turtle and Riverside mountains, several intrusions are in the 100–85 Ma range (Allen et al. 1995). One granodioritic pluton, in the Granite Mountains, just north of Palen Pass, is undated, but cuts Jurassic rocks and generally contains a mylonitic foliation with a mineral lineation (Stone and Kelly 1989) so is likely another member of the 100–84 Ma suite. Near the northern end of the Piute Range, the 85 ± 7 Ma East Piute body is weakly to strongly peraluminous, undeformed to mylonitic, and predates the Laramide deformation (Fletcher and Karlstrom 1990; Miller et al. 1990).

Some researchers recognized the lithological similarities of the 100–84 Ma Mojave plutons (for example, Allen et al. 1995) with those of the Sierra Nevada and Peninsular Ranges batholiths and wondered why they were so far out of line with those belts. Faults or tears in the subducting plate might be responsible for apparent jumps across strike.

The mid-Cretaceous thrust belt of the US Cordillera, commonly referred to as the Sevier fold-thrust belt (Armstrong 1968), reappears in the New York Mountains of California (Burchfiel and Davis 1977), where highly strained metavolcanic rocks range in age from 98.4 to 97.6 Ma, whereas associated metasedimentary rocks of Sagamore Canyon (Fig. 9) have MDAs of 98 Ma (Wells 2016). Thrust faults cut the volcanic rocks and are cut by 90.4 ±

0.8 Ma Mid Hills monzogranite, which is one of several plutons of the 98–90 Ma Teutonia batholith (Beckerman et al., 1982; Miller et al. 2007; Haxel and Miller 2007; Wells 2016).

In the Mezcal Range to the northwest, a sequence of 100.5 ± 2 Ma basaltic lavas and epiclastic rocks overlain by plagioclase porphyritic ignimbrites and lavas known as the Delfonte volcanics (Fig. 9), was detached, folded, and transported eastward on thrust faults (Fleck et al. 1994; Walker et al. 1995) prior to the emplacement of the Teutonia batholith. Other allochthons in the area carry deformed plutons dated between 150 and 140 Ma (Walker et al. 1995).

In the southern Spring Mountains just southwest of Las Vegas (Page et al. 2005), nonmarine sedimentary and volcaniclastic rocks of the Lavinia Wash sequence (Fig. 9), interpreted as synorogenic deposits by Carr (1980), lie structurally below the contact thrust plate. A rhyolitic boulder in conglomerate of the Lavinia Wash sequence was dated at 98.0 Ma, and plagioclase within an ignimbrite in the sequence yielded a $^{40}Ar/^{39}Ar$ age of 99.0 ± 0.4 Ma (Fleck and Carr 1990). Two different ages of thrusts are well mapped and described in the area of the Spring Mountains, Nevada (Burchfiel et al. 1974, 1998; Axen 1987; Walker et al. 1995; Page et al. 2005), where the spectacularly exposed Keystone thrust is a classic example of a younger and "out-of-sequence" thrust (Longwell 1926; Davis 1973; Burchfiel et al. 1998).

A conglomerate unit within Brownstone Basin (Fig. 9), sits structurally beneath the Red Spring thrust and contains cobbles and pebbles apparently derived from the Wheeler Pass thrust plate to the west (Axen 1987), as well as detrital zircons as young as 103–102 Ma (Wells 2016). The Wheeler Pass thrust sheet itself (Fig. 9), where exposed in the Spring Mountains, contains evidence for exhumation during the Late Jurassic (Giallorenzo 2013), which perhaps reflects the Nevadan event; however, zircon (U–Th)/He thermochronology from the thrust sheet, where exposed in the Nopah Range to the southwest (Fig. 9), shows that exhumation started there at ~100 Ma (Giallorenzo 2013).

In both the Caborca region of Sonora and the Spring Mountains – Death Valley area west of Las Vegas, distinctive Neoproterozoic and Cambrian sedimentary rocks, such as the Noonday Dolomite, Johnnie Formation, and Stirling Quartzite, unknown from autochthonous North America, were transported eastward in allochthons, although they were originally hypothesized to be offset by the enigmatic Mojave–Sonora megashear (Stewart 2005). The Neoproterozoic successions, as well as 150–140 Ma plutons, and the 100.5 Ma Delfonte volcanics, were likely situated at or near the leading edge of the arc terrane during basin closure. However, without Lower Cretaceous cover on the eastern North American block, precisely which thrust fault marks the suture is not obvious.

Northeast of Las Vegas (Fig. 9), the upper Albian to Cenomanian Willow Tank Formation and Baseline Conglomerate, interpreted as synorogenic foreland deposits, rest unconformably on Middle Jurassic Aztec sandstone in the Valley of Fire region, and were dated as 98–96 Ma (Fleck 1970; Bohannon 1983; Bonde 2008; Pape et al. 2011). More recent studies of detrital zircons from these and other local formations — as well as zircons from plutons and volcanic rocks — bracket deformation from 102 to 96 Ma (Troyer et al. 2006; Bonde et al. 2012; Wells 2016).

Farther north in east-central Nevada, eastward-vergent thrust faults within the Garden Valley thrust system (Bartley and Gleason 1990), part of the Central Nevada fold and thrust system (Speed et al. 1988; Long 2015), are cut by the ~98 Ma Lincoln stock and the ~86 Ma Troy granite (Taylor et al. 2000). Basinal sedimentary rocks of the westerly derived Newark Canyon Formation are exposed within the Central Nevada fold and thrust belt in east-central Nevada and were deposited from about 106 Ma until just after 99 Ma (Di Fiori et al. 2020). The rocks could be a remnant of the throughgoing pre-collisional seaway as they appear to be too old to be part of the foredeep succession. The Nevada data are consistent with folds and thrusts active at about 100 Ma in eastern Nevada, but the northward continuation of the Sevier fold-thrust belt from the Las Vegas area lies farther east in Utah and will be examined after descriptions and discussion of the Sierra Nevada arc.

The Sierra Nevada

The geology of the Sierra Nevada is similar to the Peninsular Ranges in that it has a 130–100 Ma volcano-plutonic arc complex, built largely on Jurassic to Paleozoic basement, and situated west of a 100–82 Ma suite of dominantly granodioritic–tonalitic intrusions. One fundamental difference is located in the western Sierran foothills where at least three different arc terranes (Supplementary Fig. S2[2]), younging westward and each accreted during the Jurassic, serve to document westerly subduction, because arcs are the upper plate in collisions (Brown et al. 2011; Hildebrand 2013). Each accretionary event was followed by an interval of post-collisional plutonism that spanned several adjacent terranes (Supplementary Fig. S2[2]), which is typical for slab failure magmatism (Hildebrand and Whalen 2017).

Early Cretaceous arc rocks are less abundant in the Sierra Nevada than in the Peninsular Ranges batholith, but many intrusive rocks of that age exist and are widely distributed (Bateman 1992). Perhaps the best-studied example of Early Cretaceous plutonic rocks was by Clemons-Knott, who mapped a group of ~120 Ma ring complexes, known as the Stokes Mountain complex, and produced geochemical analyses and isotopic data (Clemens-Knott 1992; Clemens-Knott and Saleeby 1999). Other examples of 130–100 Ma rocks occur as roof pendants within the batholith.

Saleeby et al. (1990) described the geology of the Boyden Cave and Oak Creek pendants (Fig. 10; Supplementary Fig. S3[2]), both located in Sequoia – Kings Canyon National Park. In the Boydon Cave pendant, a variety of <110 Ma metavolcanic and metasedimentary rocks — as well as Paleozoic and Jurassic metasedimentary rocks — are intruded by a number of highly strained 103 Ma hypabyssal intrusions and by post-deformational plutons at about 100 Ma. The Oak Creek pendant, located to the west on the Sierran Crest, comprises Jurassic metavolcanic rocks overlain with angular unconformity by deformed and metamorphosed <110 Ma basaltic to rhyolitic tuff, breccia, and lava, cut by hypabyssal sills, and intruded by plutons dated at 106–105 Ma. Chen and Moore (1982) obtained a slightly discordant U–Pb age on zircon of 103–100 Ma from an leucogranite body that cuts the sequence.

Memeti et al. (2010), in trying to define the location of the cryptic Snow Lake shear zone of Lahren and Schweickert (1989), collected and analyzed detrital zircons from several pendants, two of which are applicable to our study. The first is at Cinko Lake, located to the northeast of the Snow Lake pendant, where a sequence of metavolcanic and metasedimentary rocks, folded about northwest axes, have MDAs of 103 Ma; were intruded by a 101.8 ± 0.2 Ma pluton, also metamorphosed and deformed; and cut by the voluminous post-deformational 94–84 Ma Tuolumne intrusive complex and the 96 Ma Kinney Lakes granodiorite of the Sonoran Pass intrusive complex (Fig. 11). Just a few kilometres to the southeast and along the eastern contact of the Tuolumne complex, Cao et al. (2015) obtained an MDA of 117.4 ± 2 Ma from volcanogenic sandstones cut by a 97.4 ± 0.4 Ma pluton. Deformed metasedimentary rocks in both the Strawberry Mine and Cinko Lakes pendants produced U–Pb zircon age peaks of 117, 116, 112, 108, 103, 99, and 96 Ma, consistent with local Aptian–Albion arc sources (Memeti et al. 2010). We call the magmatic and related sedimentary rocks the Cinko Lake arc trough after dated exposures at Cinko Lake.

Farther south in the Mineral King pendant (Supplementary Fig. S3[2]), Sisson and Moore (2013) report U–Pb zircon ages for metarhyolitic tuffs and andesitic lavas of 111–102 Ma, with older metarhyolites and siliceous sills ranging back to 140 Ma. They also reported that a 98 Ma granodiorite cuts vertical metasedimentary rocks, which are also cut by isoclinally folded aplites, one of which produced a U–Pb zircon age of about 98 Ma.

Fig. 10. Sketch map showing four post-collisional centered complexes of the Sierra Nevada. These are only a few of the post-collisional plutons. See Supplementary Fig. S3[2] for a more detailed view of the southern sector of the batholith. Location of Fig. 11, Cinco Lake pendant, as well as location of Boyden Cave and Oak Creek pendants, are starred. Modified from Davis et al. (2012). [Colour online.]

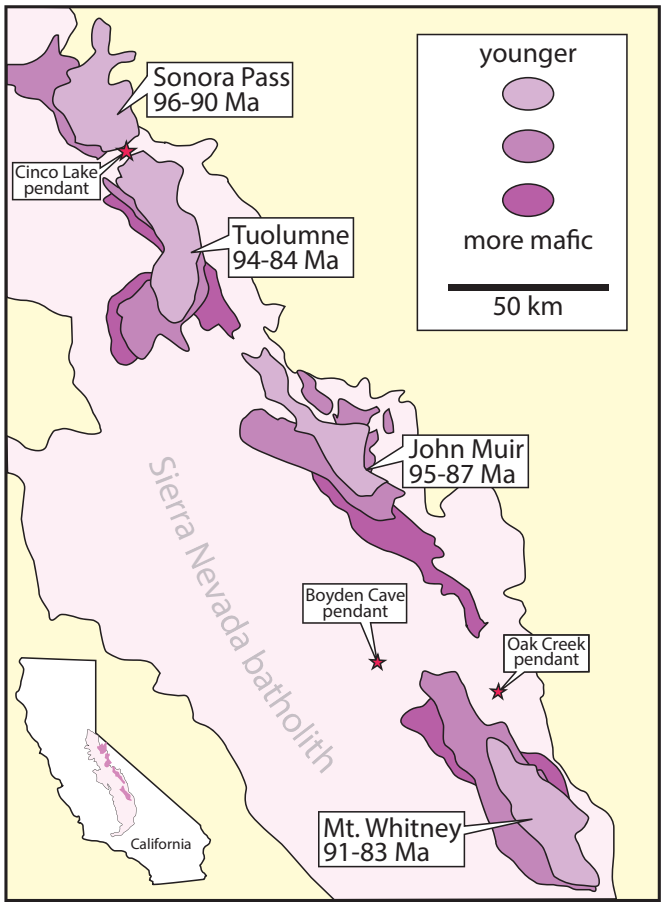

Near the southern end of the batholith, where it outcrops along the Kern Canyon fault (Supplementary Fig. S3[2]), the Erskine Canyon sequence comprises 105–102 Ma siliceous ignimbrites and subordinate intermediate lava flows, along with associated hypabyssal rocks (Saleeby et al. 2008). These authors also document several plutons with ages ranging from 105 to 103 Ma cropping out to the west and a 98 Ma granodiorite to the east. Even farther south, in the Tehachepi Mountains, Wood (1997) mapped and dated by U–Pb zircon methods, several isoclinally and recumbently folded gabbroic, dioritic, and tonalitic plutons of the Tehachapi intrusive complex, which yielded ages of about 100 Ma, and sit close to the Oaks metavolcanics (Supplementary Fig. S3[2]) dated at 103 Ma (Chapman 2012). Thus, widespread pendants within the main Sierran block consistently contain evidence for the existence of Early Cretaceous volcanic and epiclastic rocks that were deformed at about 100 Ma prior to emplacement of post-deformational plutons as old as 98–96 Ma.

In the northern Sierra (Supplementary Fig. S3[2]), northwest of Lake Tahoe, Lower to Upper Jurassic metavolcanic and metasedimentary rocks of the Eastern Mesozoic belt (Christe and Hannah 1990) are unconformably overlain by a sequence of Barremenian prehnite–pumpellyite grade metasedimentary and metavolcanic rocks collectively known as the Evans Peak sequence (Christe 2011). Lower units in the sequence comprise chert-pebble conglomerate and quartzose sandstones, which are overlain by coarse-grained plagioclase-rich sandstone, tuffaceous shales, green siliceous tuff, volcanic cobbly conglomerate and ~128 Ma ignimbrites, overturned beneath the west-dipping Taylorsville fault, which places Paleozoic rocks of the northern Sierra terrane atop the early Cretaceous sequence (Moores and Day 1984; Christe 2010, 2011). Although we only have a maximum age, it is possible that the Taylorsville thrust is a 100 Ma structure and the rocks of the Evans Peak sequence might be the oldest known supracrustal rocks of the Early Cretaceous Cinco arc and trough in the Sierra Nevada. Additional studies in the area are warranted.

At the northernmost end of the White Mountains, west of White Mountain peak, (Supplementary Fig. S3[2]) is an overturned section of metasedimentary and volcaniclastic rocks, containing detrital zircons derived mostly from local 120–115 Ma volcanic sources, that sit beneath a low angle fault carrying the Jurassic Barcroft pluton (Scherer et al. 2008). If the entire section, including the Jurassic rocks in the upper plate is overturned, then the fault is likely to be a normal fault; otherwise, it is, as queried by Scherer et al. (2008), a west-vergent thrust. Whatever its kinematics, this low-angle fault is transected by a body dated by U–Pb to be 100 ± 1 Ma (Hanson et al. 1987).

Although the age of deformation is tightly constrained by metasedimentary, metavolcanic, and plutonic rocks to be about 100 Ma, another line of evidence supports both age and subduction polarity in the Sierran sector of the Peninsular Ranges orogen.

Chin et al. (2013) document granulite quartzite xenoliths (T = 700–800 °C and P = 7–10 kbar), brought to the surface in a Miocene diatreme of the central Sierra Nevada, that contain zircons with Proterozoic and Archean cores, but with rims that yield a mean metamorphic age of 103 Ma. They interpreted the Proterozoic and Archean U–Pb crystallization ages found in the cores of detrital zircon grains, and Hf isotopic ratios like those from Proterozoic basement east of the Sierra Nevada, as the vestiges of rocks deposited along the North American passive margin that were transported deep beneath the arc where they were metamorphosed at about 100 Ma. As the North American platform is unknown west of the Sierra Nevada, we infer that the rocks were underthrust beneath the Cinko Lake arc from the east.

From the above, it appears that the age of deformation in rocks of the Sierran batholith is coeval with rocks of the Peninsular Ranges batholith (Memeti et al. 2010; Chin et al. 2013), as well as easterly vergent thrust faults located in eastern California and in the Spring Mountains of Nevada discussed earlier. By analogy, we suggest that within the Sierra Nevada, subduction of the leading edge of North America beneath the Cinco Lake arc during closure of the basin led to break-off of the North American oceanic lithosphere, and its descent, along with perhaps part of the rift complex, into the mantle. Thus, even though the Cretaceous passive margin succession on the eastern side of the basin is not exposed, the overwhelming geological and temporal similarities lead us to conclude that the Cretaceous Sierra Nevada and broader Great Basin are part of the Peninsular Ranges orogen. We now briefly describe and examine the post-deformational magmatic suite within the Sierra Nevada to demonstrate that rocks of the suite are compositionally and temporally similar to the post-collisional La Posta plutonic suite, located farther south. We then utilize the geochemical and isotopic variations, as well as the timing from both suites, to constrain the origin of post-collisional magmatism by slab break-off.

The post-collisional Sierran Crest magmatic suite

Largely outcropping east of the 130–100 Ma Cinco arc assemblage, dozens of post-deformational 99–84 Ma tonalitic–granodioritic plutons (Supplementary Fig. S3[2]) are known collectively as the Sierran Crest magmatic suite (Coleman and Glazner 1998). Just as early researchers recognized that there were two intrusive suites in the Peninsular Ranges batholith, researchers in the Sierra Nevada

Fig. 11. Geological sketch map of the Snow Lake and western Cinco Lake pendant (Lahren et al. 1990; Wahrhaftig 2000; Memeti et al. 2010; Leopold 2016), showing ages of folded metavolcanic, metaplutonic, and metasedimentary rocks and their truncation by younger post-collisional plutonic complexes, which constrain the age of deformation to be between 102 and 96 Ma. DV, Death Valley. [Colour online.]

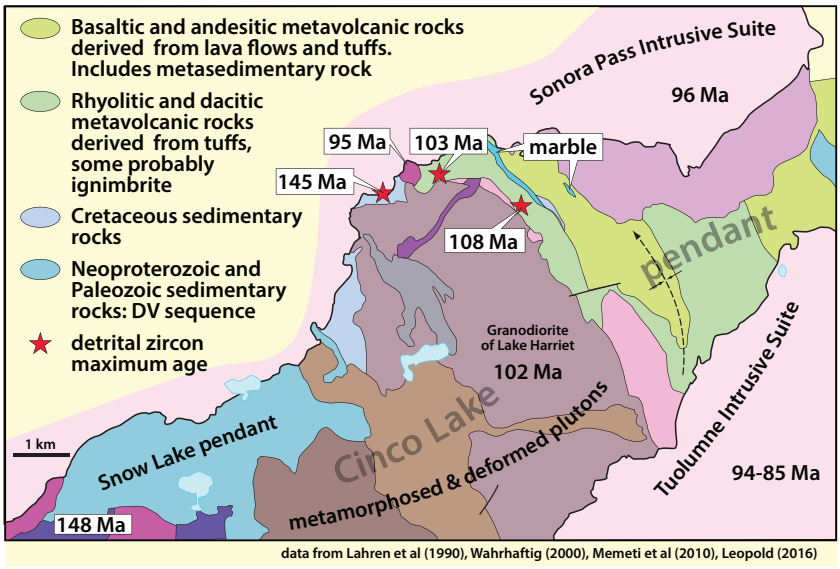

understood that the more mafic plutons within the Sierra Nevada batholith occur west of more intermediate-composition bodies (Lindgren 1915; Buddington 1927; Moore 1959; Moore et al. 1961). Many researchers have since confirmed that the intrusions of the Sierra Nevada are readily divisible into older western and younger eastern sectors (Fig. 12) on the basis of geochemistry, magnetic susceptibility, age, and both radiometric and stable isotope ratios (Chen and Tilton 1991; Bateman et al. 1991; Kistler 1990, 1993; Saleeby et al. 2008; Lackey et al. 2008, 2012*a*, 2012*b*; Chapman et al. 2012). But, like rocks of the Peninsular Ranges, the deformation that occurred between the two magmatic suites went largely unrecognized, or was considered to be related to the emplacement of the plutons (Bateman 1992).

The post-collisional plutonic rocks within the Sierran Batholith range in composition from gabbro to leucogranite, but the most common rocks are tonalite, granodiorite, and granite (Bateman and Wahrhaftig 1966; Bateman et al. 1963; Bateman 1992; Ross 1989). In general, the hundreds of mesozonal intrusions within the post-100 Ma composite batholith have sharp contacts with one other, or are separated by minor screens of older metamorphic rock (Bateman 1992; Bartley et al. 2012).

Bateman (1992) distinguished several intrusive suites of cogenetic, but not necessarily comagmatic, plutons that have distinctive petrographic, compositional, and textural characteristics, as well as spatial proximity. The best known are the <100 Ma compositionally zoned complexes of the Sierran Crest magmatic suite (Coleman and Glazner 1998), such as the Tuolumne intrusive suite, the Mount Whitney Suite, the John Muir suite, and the Sonora Pass intrusive suite (Fig. 10), all of which consist of seemingly nested units that are progressively younger and more leucocratic inward (Calkins 1930; Leopold 2016; Bateman and Chappell 1979; Huber et al. 1989; Hirt 2007). Plutons of the Sierran Crest magmatic suite, were emplaced along the eastern Sierran crest between 98 and 84 Ma, and many are characterized by an outer, older tonalite and granodiorite in sharp contact with an inner younger hornblende porphyritic granodiorite, and cored by even younger K-feldspar megacrystic granite and granodiorite (Bateman 1992; Coleman and Glazner 1998; Hirt 2007).

Besides a spatial centering, it is unclear whether or not individual plutons within any of the so-called "nested" complexes are related, other than by source. Originally, Bateman and Chappell (1979) argued that the compositional zoning within the Tuolumne intrusive complex resulted from crystal fractionation of a single voluminous influx of magma. However, subsequent isotopic work (Kistler et al. 1986) ruled out this possibility, and U–Pb zircon age determinations demonstrated that the complex was emplaced over 10 million years from 95 to 85 Ma (Coleman et al. 2004) thereby negating the two-component mixing scheme favoured by Kistler et al. (1986). Instead, Coleman et al. (2004) argued for incremental emplacement of stacked intrusive sheets.

Fig. 12. West–east section vs. age showing U–Pb zircon ages for plutons in the central Sierra Nevada (from Beck 2013) and their temporal relation to the ca. 100 Ma deformational event. Note the similar ages and relations as plutons in the Peninsular Ranges batholith in Fig. 5.

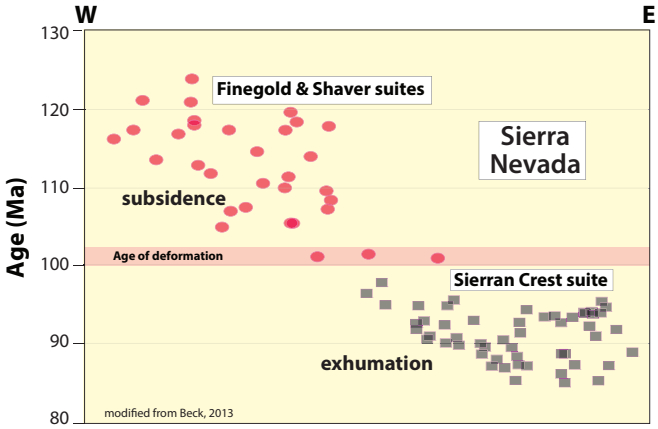

Geochemistry and origin of the post-collisional plutons

Since the early days of plate tectonics, most researchers have developed models for the North American Cordillera where the older arc-related magmatism developed above an eastwardly dipping subduction zone and that shallowing subduction forced arc magmatism to prograde eastwardly into the western margin of North America, where it interacted with, and assimilated, older

cratonic crust (Bateman and Clark 1974; Kistler and Peterman 1978; Kistler 1990; Gastil et al. 1981; Saleeby et al. 1990; Walawender et al. 1990; Chen and Tilton 1991; Johnson et al. 1999; Todd et al. 2003; Grove et al. 2003; Ortega-Rivera 2003; Ducea and Barton 2007; Paterson et al. 2014; Schmidt et al. 2014; Cao et al. 2015; Ducea et al. 2015).

Our analysis challenges this paradigm and proposes that the arc and post-collisional suites were derived from the mantle directly, without extensive crustal interaction (Hildebrand and Whalen 2017; Hildebrand et al. 2018). Furthermore, these data unexpectedly suggested to us that post-collisional magmatism was likely responsible for producing at least half of all continental crust and by doing so resolves the long-standing crustal composition paradox (Rudnick 1995).

On our discrimination diagrams, the Sierra plutons plot in the same fields as those of the rocks from the Peninsular Ranges (Fig. 13, Supplementary Fig. S4[2]). Although arc and post-collisional bodies are superficially similar in field characteristics, there are consistent major and minor geochemical differences between the >100 Ma arc and <100 Ma post-collisional suites (Hildebrand and Whalen 2014*b*). For example, most rocks of the La Posta and Sierran Crest magmatic suites contain 60%–70% SiO_2 whereas the arc suite displayed a continuous range from basalt to rhyolite (Fig. 14). Relative to the arc rocks, members of the La Posta – Sierran Crest suites were generally more enriched in incompatible elements, as well as Sr, Na, and Nb, have minor to negligible Eu anomalies, and are depleted in Y and heavy rare earth elements as recognized over 30 years ago by Gromet and Silver (1987). They proposed that, although the western pre-100 Ma rocks are typical arc rocks, the eastern, post-100 Ma plutons were derived from a plagioclase-free, garnet-bearing source — most likely eclogite or metabasalt. They suggested that altered basaltic magma ponded at the base of the crust and thickened it, only to be remelted later to create the post-100 Ma suite; although the process by which basalts might have been emplaced at the base of the arc crust prior to arc magmatism in the east remained unanswered. While certainly attractive, models that involve melting of basalt accumulated at the base of the arc are unsatisfactory because the post-100 Ma rocks are post-tectonic, and at the time of that magmatism, the leading edge of the continental margin had already been subducted beneath the arc, effectively isolating the arc from the mantle. And the switchover to post-collisional magmatism happened far too rapidly for accumulations of basalt to build up, as even the youngest arc rocks are intercalated with marine sedimentary rocks in both the Peninsular Ranges (Allison 1974; Phillips 1993; Busby et al. 2006) and Sierra Nevada (Nokleberg 1981; Saleeby et al. 2008; Memeti et al. 2010).

Putirka (1999) modeled aggregate melts using polybaric partial melting of mantle rocks transported from their source to the base of the lithosphere and found that Sm/Yb ratios increases with depth of melting in peridotite, eclogite, and garnet pyroxenite, as well as with greater lithospheric thickness. On a La/Sm vs. Sm/Yb diagram (Fig. 15), slab failure suites consistently have higher Sm/Yb than arc suites, indicative of initial melting at greater depths, which led us to test and utilize this diagram as another discriminator between the two suites, with a Sm/Yb boundary of 2.5.

Isotopic constraints

Lackey et al. (2008) showed that intrusions of the post-100 Ma Sierran Crest magmatic suite had $\delta^{18}O_{zircon}$ within, and close to, the range of mantle $\delta^{18}O_{zircon}$ values. For example, Tuolumne plutons have $\delta^{18}O_{zircon}$ ratios of 6.0‰–6.6‰, Mount Whitney zircons are 5.67‰–5.90‰, and other intrusive bodies emplaced at 96 Ma range as low as 4.21‰. The sub-mantle values probably represent melting of hydrothermally altered rocks that had previously interacted with low $\delta^{18}O$ meteoric water at high temperature (see Bindeman 2008). Overall, these data suggest that the

Fig. 13. Nb vs. Y discrimination diagram from Hildebrand and Whalen (2017) for various Sierra Nevada and northwestern Nevada plutonic suites: pre-collisional 120 Ma Sierran Stokes Mountain complex arc rocks (Clemens-Knott 1992), 94–84 Ma postcollisional Tuolumne intrusive suite (Memeti 2009), Sahwave intrusive suite of northwestern Nevada (Van Buer and Miller 2010), and Onion Valley hornblende gabbro (Sisson et al. 1996) plus northern Nevada plutonic rocks (du Bray 2007). WPG, within-plate granite; ORG, ocean-ridge granite. [Colour online.]

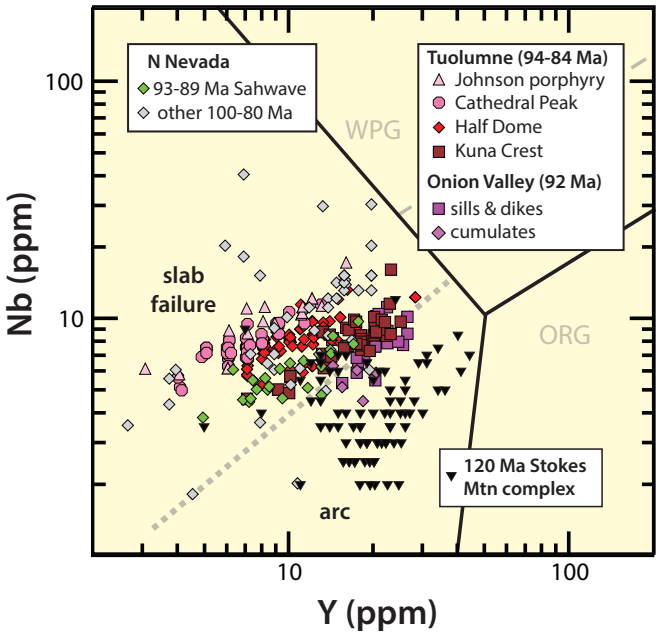

Fig. 14. Representative samples from the arc and post-collisional plutonic suites from the Peninsular Ranges and Sierra Nevada plotted on the normative Q′ vs. ANOR classification diagram (Streckeisen and LeMaitre 1979). We use the Whalen and Frost (2013) compositional trends. Note that the plutons of the Peninsular Ranges arc define the calcic trend, as do the Sierran arc samples, and both extend from granite to gabbro, whereas the post-collisional plutonic suites have more limited ranges of silica and tend to be more alkalic. [Colour online.]

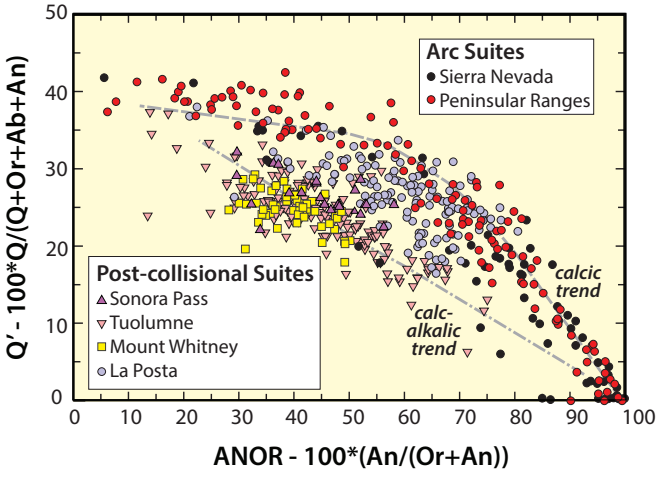

Fig. 15. Rocks from both pre- and post-100 Ma suites from the Peninsular Ranges batholith plotted in La/Sm vs. Sm/Yb space. Sm/Yb ratios are one measure of partial melting depth in the mantle (Putirka 1999). Rocks older than 100 Ma have Sm/Yb values <2.5, whereas younger rocks have Sm/Yb >2.5. The differences presumably reflect depth of melting of the original source magmas and thus whether garnet was stable in the source. According to Putirka (personal communication, 2016), partial melts of spinel peridotite should produce more melt due to larger degrees of partial melting than the deeper garnet peridotites, most partial melts of spinel peridotite will have Sm/Yb less than ~2.5. Based on values from hundreds of younger arc rocks from the GEOROC database, Hildebrand and Whalen (2017) found Sm/Yb = 2.5 to be an effective dividing line between arc and post-collisional rocks. [Colour online.]

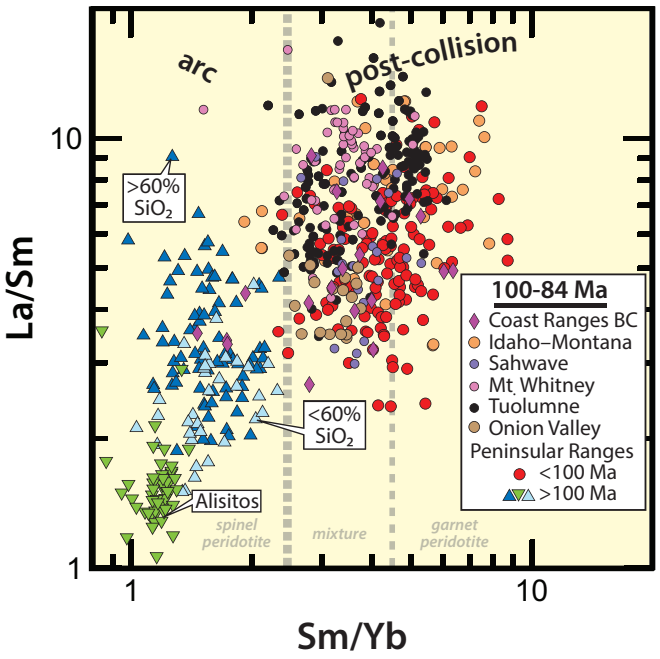

magmas were dominantly mantle derived but with some contamination by source rocks that had previously interacted with hot meteoric water.

Plutonic rocks of the post-100 Ma La Posta suite in the Peninsular Ranges batholith have heavier whole rock $\delta^{18}O$ with values between 8‰ and 11‰ (Taylor and Silver 1978). These values led Lackey et al. (2008) to argue that relatively young, hydrothermally altered oceanic crust was the most plausible source of the magmatism as hydrothermally altered, oceanic basalt has whole rock $\delta^{18}O$ ~10‰ (Eiler 2001; Bindeman et al. 2005).

Some of the most obvious differences between the arc and post-collisional magmas are their different initial Nd and Sr isotopic ratios in that the post-collisional rocks typically have negative εNd_T and $^{87}Sr/^{86}Sr_i > 0.706$, whereas the arc rocks have positive εNd_T and less evolved $^{87}Sr/^{86}Sr_i$ (Fig. 16). As mentioned earlier, the more evolved ratios are classically interpreted to represent assimilation of continental crust as the subducted slab shallowed (Kistler and Peterman 1978; DePaolo 1980, 1981; Bateman 1992; Ducea and Barton 2007; DeCelles et al. 2009), but additional data suggest another plausible source.

Mid-Cretaceous mantle-derived ~100 Ma pyroxenite xenoliths carried to the surface by Cenozoic basaltic magmas in the Sierra Nevada have dominantly mantle $\delta^{18}O$ values (Lackey et al. 2008; Ducea and Saleeby 1998), but many also have negative $\varepsilon Nd_{(0)}$ and $^{87}Sr/^{86}Sr_i > 0.706$ (Fig. 16). Both the plutons and the pyroxenite

Fig. 16. εNd_T vs. $^{87/86}Sr_i$ plot of various arc and slab failure plutonic and volcanic suites of the Peninsular Ranges and Sierra Nevada compared with some Cenozoic basalts of western North America (modified from Hildebrand and Whalen 2017), illustrating the isotopic differences between arc suites and slab failure suites and the isotopic similarities of the Peninsular Ranges and Sierran post-collisional slab failure suites with basalts from the Snake River Plain (Jean et al. 2014; Hanan et al. 2008) and Big Pine volcanic field (Blondes et al. 2008). Fields for two Cascade arc volcanoes (CL, Crater Lake and Lassen) from Bacon et al. (1994), Sierran mantle xenoliths from Ducea and Saleeby (1998). CHUR, chondritic uniform reservoir. [Colour online.]

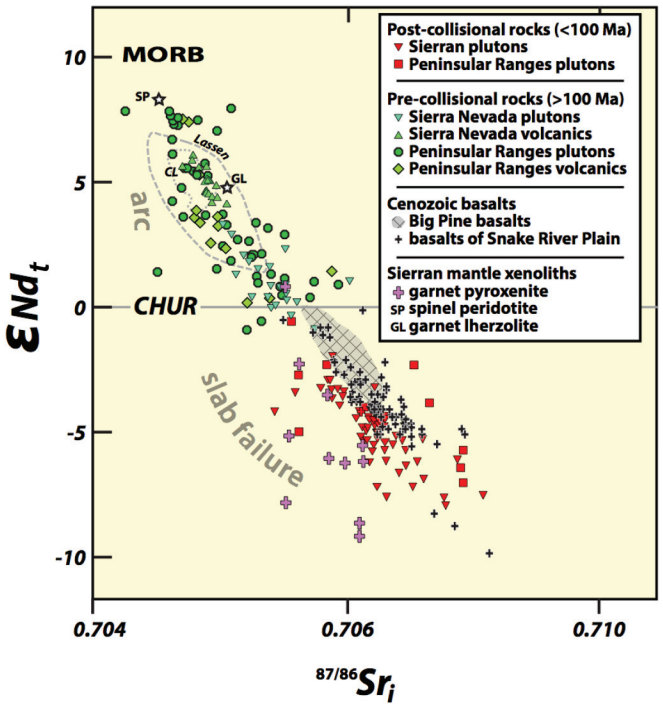

xenoliths also have Nd and Sr isotopic values similar to much younger basalts widely erupted in western North America (Fig. 16), including those of the <17 Ma Snake River Plain (Hanan et al. 2008) and the 44–7 ka Big Pine volcanic field, erupted along the eastern Sierran fault scarps (Blondes et al. 2008; Ormerod et al. 1991). Three-component isotopic mixing models, utilizing (1) the oceanic island basalt–like Steens–Imnaha lava, erupted west of the inferred continental edge, to represent the asthenospheric (Yellowstone plume) component, (2) old lithosphere like that of the Wyoming craton, and (3) younger Paleoproterozoic-like lithosphere, show that >97% of the variability can be accounted for by progressive incorporation of older subcontinental mantle lithosphere (SCLM) eastward along the Yellowstone hot spot track (Jean et al. 2014). Thus, we infer that the Sr and Nd isotopic ratios of the post-100 Ma plutonic rocks of the Sierra Nevada and Peninsular Ranges batholiths were derived from fractional melting of old, enriched SCLM.

Other post-collisional suites, such as the 100–85 Ma plutons within the Coast Range batholith of British Columbia have positive εNd_T and $Sr_i < 0.704$ (Girardi et al. 2012; Wetmore and Ducea 2011) similar to Steens basalt (Camp and Hanan 2008), but contain typical slab failure trace element signatures (Hildebrand and Whalen 2017), so apparently do not have old, enriched SCLM beneath them.

The contrasting isotopic signatures of arc and post-collisional magmatism can be explained by a scenario in which the arc magmas rose through juvenile arc lithosphere, and so exhibit non-radiogenic values. However, after collision subcontinental mantle

typically belongs to the lower plate, which, if cratonic, isolates the arc from its formerly subjacent mantle. Thus, magmas triggered by slab failure may have very different (more radiogenic) isotopic ratios because enriched mantle lithosphere was pulled beneath the arc just prior to slab failure. Likewise, where both upper and lower plates are young, they both should exhibit non-radiogenic isotope ratios (Hildebrand et al. 2018).

Geochemistry and isotopic analyses suggest that pre- and post-collisional magmas were derived from two different sources at different depths as previously envisioned for the Peninsular Ranges by Gromet and Silver (1987). They also noted, as have Girardi et al. (2012) in the Coastal batholith of British Columbia, that the post-collisional rocks have minor to negligible Eu anomalies, which is the general case for post-collisional slab-failure-derived magmas (Hildebrand and Whalen 2014*b*, 2017). The lack of a Eu anomaly suggests the absence of residual plagioclase in the source.

Hildebrand and Whalen (2017) showed that most slab window adakitic rocks have trace element concentrations and ratios similar to slab failure rocks with mantle-like Sr and Nd isotopic concentrations, except for those of western North America, which have isotopic compositions typical of the Snake River Plain, Sierran Crest magmatic suite, and the Big Pine volcanic field. These results support a slab failure model that involves melting of the oceanic slab at depths sufficient for partial melting of garnetiferous, plagioclase-free rocks to produce the observed trace element profiles in both adakites and slab failure rocks, as well as the unradiogenic Sr and radiogenic Nd ratios in regions without old, enriched SCLM.

In regions where there was enriched SCLM, we found that Nd and Sr isotopes were more evolved so we suggested that the rising magmas fractionally melted the SCLM to produce the more evolved isotopic signatures, as well as the general lack of correlation between silica and incompatible elements (see Supplementary Fig. S5[2]; Hildebrand and Whalen 2017; Hildebrand et al. 2018).

Great Valley Group

Although the Sierra Nevada is characterized by voluminous 130–100 Ma arc magmatism, no temporally equivalent arc debris occurs in the adjacent Great Valley Group located on the western side of the arc terrane, and in fact, there are no Early Cretaceous sedimentary rocks known even in drill core from the eastern Central Valley of California (Ojakangas 1968; Reid 1988; DeGraaff-Surpless et al. 2002; Orme and Graham 2018). Additionally, rocks of the Great Valley Group and their basement along the western margin of the Central Valley (Constenius et al. 2000) show no evidence of deformation related to the Nevadan orogeny (Wright and Wyld 2007), or the 100 Ma deformational event of the Sierra Nevada (Hildebrand 2013). These observations are consistent with the model of Wright and Wyld (2007) in which the western Great Valle Group, Coast Ranges ophiolite, and the Early Cretaceous part of the Franciscan complex migrated into the area at about 100 Ma.

Exhumation of the hinterland in the Sierra Nevada region and emplacement of plutons of the Sierran Crest magmatic suite appear to have been contemporaneous with deposition of thick Cenomanian–Turonian clastic successions to the west (Mansfield 1979; Surpless et al. 2006) just as in the Peninsular Ranges. This same contrasting feature occurs at a few localities to the north, such as the Coast Ranges batholith of British Columbia and Wrangellia in south-central Alaska (Hildebrand and Whalen 2021 (this issue)). Examination of the 12-4 Ma Central Range orogeny of Papua, New Guinea (Cloos et al. 2005), shows that about 25 km of denudation occurred on the northern slope of the highest mountains and plateaux (Fig. 17), which rise to nearly 5 km elevation and contain many post-collisional intrusions rich in Cu and Au (Doucette 2000; McMahon 2000, 2001; Cloos and Housh 2008). Sediment transport was into the back-arc region.

The suture zone preserved?

The southernmost part of the Sierran batholith in the Tehachapi and San Emigdio mountains, which abut the San Andreas and Garlock faults to the south (Supplementary Fig. S3[2]), is dominated by amphibolite- and granulite-grade metamorphic rocks with paleopressures as high as 10–11 kbar (Pickett and Saleeby 1993; Chapman et al. 2012). Structurally beneath the high-grade rocks (Fig. 18), which have ages ranging from 136 to 101 Ma, and separated from them by the Rand fault, is the San Emigdio schist (Chapman and Saleeby 2012), which contains detrital zircons ranging mostly from 120 to 100 Ma (Jacobson et al. 2011). The few zircons younger than 100 Ma appear to be metamorphic (A. Chapman and C. Jacobson, personal communication, 2020), which indicates that, at an age of 100 Ma, the San Emigdio schist is older than, and unrelated to, the Pelona–Orocopia–Swakane schists elsewhere. Precambrian detrital zircons are plentiful within the schist, comprising ~25% of the zircons in one sample (Fig. 18), which suggests that these rocks were deposited within the seaway and do not represent material deposited on the open seafloor to the west, where there was no likely source for Precambrian zircons.

According to Chapman et al. (2011), the San Emigdio schist comprises over 75% interbedded metapsammite and metasandstone with much lesser amounts of metabasalt and talc–actinolite schist. They documented peak metamorphic assemblages as garnet + plagioclase + biotite + quartz ± muscovite ± kyanite with limited melt pods near the top. Paleopressures range from 11 to 9 kbar and paleotemperatures were inverted, ranging from 600 °C near the exposed base to 700 °C at the top.

The Antimony Peak tonalite sits above the Rand thrust with paleopressures of 10 kbar and magmatic epidote (Chapman et al. 2011). U–Pb analyses of zircons revealed 136–135 Ma cores surrounded by 103–99 Ma rims (Chapman et al. (2012), which along with the results of Chin et al. (2013) from granulite xenoliths, described earlier, constrain peak metamorphism at about 101–100 Ma.

The schist structurally overlies a terrane comprising 5–10 km long slabs of marble, quartzite, and metasandstone, as well as a variety of schists (Chapman and Saleeby 2012). Their geologic map (Fig. 18) lists the large 92–88 Ma Lebec Granodiorite as having paleopressures of 3 kbar, which implies a high rate of exhumation, one similar to that seen elsewhere along the orogen (Hildebrand and Whalen 2021, this issue). Chapman et al. (2011) argued that deposition, deep subduction, and exhumation to mid-crustal depths took <3 million years, whereas Chapman et al. (2012) suggested exhumation of rocks from 9–11 kbar at 98 Ma to mid-crustal levels by about 95 Ma. These exhumation rates are typical of slab break-off at the end of collision when the cratonic lower plate is freed of its oceanic anchor and rises rapidly to exhume the collision zone (Hildebrand and Whalen 2017).

Considering the above, we suggest that the San Emigdio Mountains exposes an oblique north–south section through the 100 Ma suture consisting of (1) lower plate North American Paleozoic basement slabs, some as long as 10 km, of quartzite, metasandstone, schist, and marble, upward through (2) the San Emigdio schists, likely remnants of material eroded from the arc and deposited within the seaway, and finally up into (3) the lowermost part of the upper-plate arc, which expose abundant Early Cretaceous plutons and gneisses, with some as young as 101 Ma, at ~11 kbar paleopressures. By at least 92 Ma, rocks of the suture were exhumed to 3 kbar.

In either our collisional model or in the eastward subduction and underplate model presented by Chapman et al. (2012), the ~10 kbar paleopressures for the schist correspond to the base of the Sierran crust at 100 Ma. Thus, at that time the crust

Fig. 17. Modern topography and differences in depth of denudation in the Central Range orogen of Papua, New Guinea, modified from Cloos et al. (2005), and illustrating ~25 km exhumation on the opposite side of the orogen from the foreland. Large rivers have transported most debris northward to the North Coast basin because the nearly 5 km high Central Range blocks drainage to the south. We see this as a more modern example of the post-collisional sedimentation in the back-arc region, such as the <100 Ma Valle and Great Valley rocks, caused by slab break-off and consequent exhumation of the hinterland belt. [Colour online.]

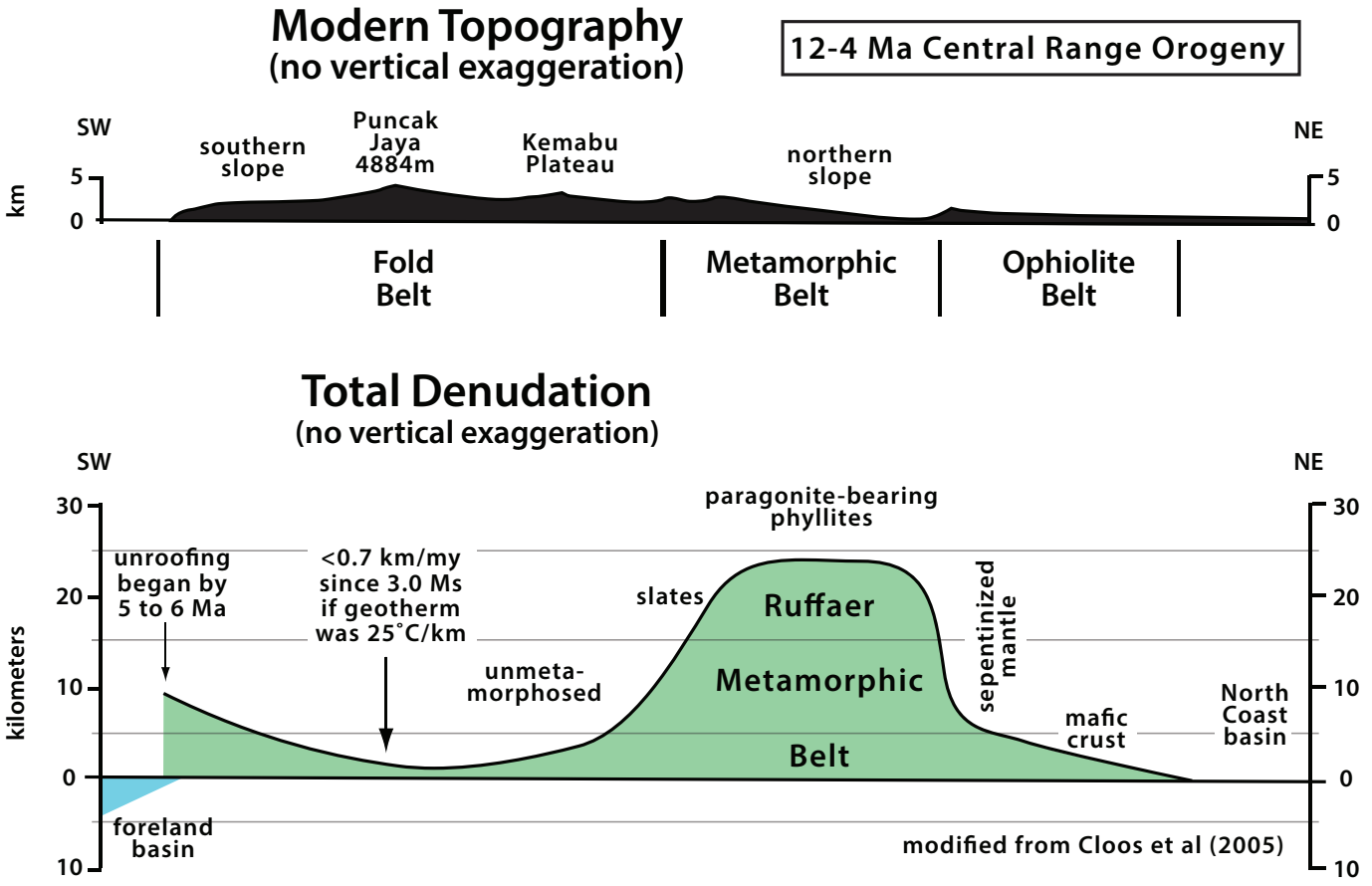

beneath the Sierra Nevadan arc was about equal to, or slightly less than, the average thickness of continental crust (Hacker et al. 2015). This negates models that require a thickened arc crust to remove fractionated cumulates formed during arc magmatism (Ducea and Saleeby 1998; DeCelles et al. 2009) and supports the Hildebrand et al. (2018) model that most continental and oceanic arcs are built on normal to thinned crust.

The San Emigdio collisional suture and surrounding rocks were rotated clockwise from a more northerly orientation after 80 Ma (Kanter and McWilliams 1982) and the entire southerly Sierran Nevada batholith and basal suture were uplifted during the east–west-trending Late Cretaceous Laramide orogeny (Wood and Saleeby 1998; Chapman et al. 2012), which we have argued was also collisional (Hildebrand and Whalen 2017; Hildebrand 2015). When displacements on the faults of southern California are restored (Powell 1993; Nourse 2002), the similar Pelona–Orocopia schists form an east–west band extending across much of southern California and western Arizona, and so they might in some cases represent suture zone rocks rather than the product of east-directed flat subduction as commonly hypothesized (Grove et al. 2003; DeCelles et al. 2009; Jacobson et al. 2011; Chapman et al. 2011, 2012).

Sevier fold-thrust belt

If the complex zone described above represents the basal suture of the Sierran arc system, then where to the east does it surface? In other words, where is the easternmost exposure of the contact zone?

Although there are many thrust faults known in the Great Basin region east of the Sierras, temporal data suggest that the zone could lie well to the east in eastern California, the Spring Mountains just west of Las Vegas, and northward into Utah and Idaho, where the thrusts are collectively known as the Sevier fold-thrust belt (Armstrong 1968). Hildebrand (2014) pointed out that the oldest thrusts of the Sevier belt were synchronous with the first deformational thickening to affect the North American platform terrace.

In southeastern California and southern Nevada, and as described in the Mojave Desert section of the paper, a sequence of 100.5 ± 2 Ma basaltic lavas and epiclastic rocks overlain by plagioclase porphyritic ignimbrites and lavas known as the Delfonte volcanics (Fig. 9), was detached, folded, and transported eastward on thrust faults (Fleck et al. 1994; Walker et al. 1995) prior to the emplacement of the 98–90 Ma Teutonia batholith. Other allochthons in the area carry deformed plutons dated between 150 and 140 Ma (Walker et al. 1995).

The earliest of the Utah thrusts, the Canyon Range thrust, was emplaced at about 125 Ma (DeCelles 2004; DeCelles and Coogan 2006) and the resultant synorogenic foredeep was filled during the Aptian–Albian mainly by the Cedar Mountain and San Pitch formations (Lawton et al. 2010) and so predates the 100 Ma collision. The thrust was unconformably overlain and sealed by upper Albian? – Cenomanian conglomerate (DeCelles and Coogan 2006; Lawton et al. 2007).

The next youngest thrust system of south-central Utah, known as the Pavant–Nebo thrust system, transported Neoproterozoic

Fig. 18. Simplified geological map of the San Emigdio Mountains (modified from Chapman and Saleeby 2012), where we infer 11–9 kbar San Emigdio schist to represent deformed metasedimentary rocks of the Lower Cretaceous Cinco Lake arc trough caught between the pre-100 Ma high-grade base of the Cinco Lake arc and lower plate North America comprising megaslabs of Paleozoic metasedimentary rocks. Cenozoic faults, mainly related to compression adjacent to the San Andreas fault, are not shown as they appear to have little separation (Chapman and Saleeby 2012) and only limited effect on the regional tectonostratigraphy. Schematic section in upper left (*a*) illustrates the inferred geological relations. (*b*) Detrital zircon profiles illustrating the similarities of zircons in the Salt Creek pendant compared with a composite of sandstones in the Death Valley region to the east from Chapman et al (2012). (*c*) Subfigure in lower right shows cumulative distribution of detrital zircons from two samples of the San Emigdio schist replotted from Jacobson et al. (2011) and interpreted to represent metasedimentary fill of the Cinko Lake arc trough. Note the presence of sparse Precambrian zircons, which were probably derived from North America as opposed to open seafloor to the west of the arc. These relations all support our model for westward subduction of the leading edge of the North American craton and its Lower Cretaceous sedimentary cover beneath the 140–100 Ma Cinko arc. [Colour online.]

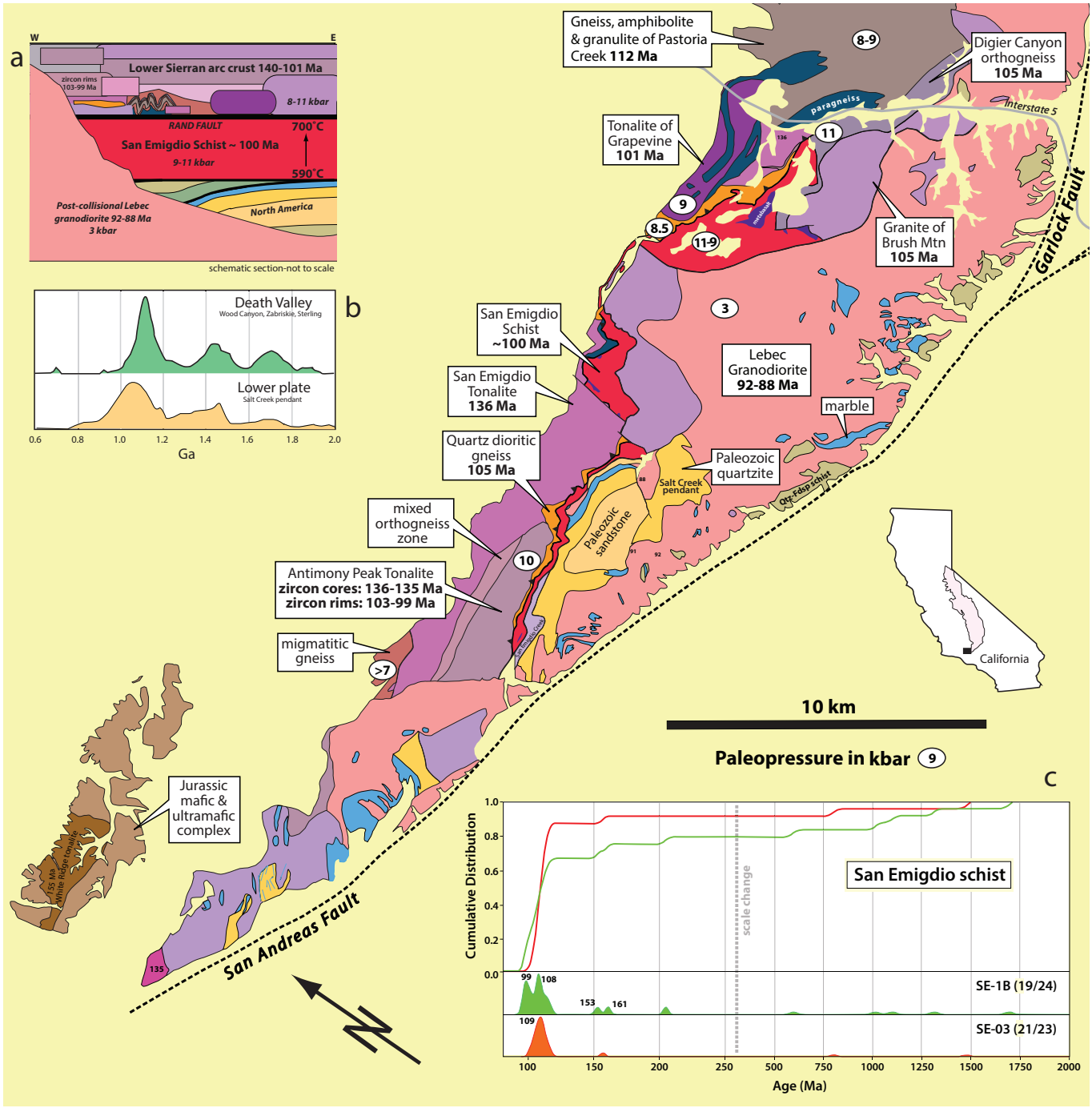

metasedimentary rocks, Paleoproterozoic crystalline basement of the Santequin complex (Nelson et al. 2002), and a Phanerozoic sedimentary succession, eastward, and led to the development of a large overturned, nearly recumbent anticline. The Pavant sector of the system deformed and elevated the Canyon Range thrust into an antiformal culmination during its emplacement (DeCelles and Coogan 2006). Zircon (U/Th)/He ages from the Pavant–Nebo thrust sheets document emplacement and exhumation of the thrust sheets between 102 and 96 Ma (Pujols et al. 2020). Using detrital zircon He, they also found that active thrust belt deformation was concurrent with sediment dispersal eastward into the Cenomanian Dakota Formation, the temporally equivalent foredeep stratigraphic unit. Thus, the Pavant–Nebo thrust system was active at about 100 Ma. To the south in southwestern Utah, the Iron Springs thrust was recently dated to be about 100 Ma on the basis of 100.18 ± 0.04 Ma zircons extracted from a dacitic tuff intercalated with coarse syn- to post-orogenic debris of the Iron Springs Formation (Quick et al. 2020).

In northern Utah, major thrust activity and cooling of the ~125 Ma Willard thrust also occurred at 105–95 Ma, which led to increased subsidence to the east and deposition of the 100–96 Ma Aspen and Frontier formations in the foreland basin (Yonkee et al. 2019; Pujols et al. 2020). A thrust duplex of Paleoproterozoic crystalline rocks known as the Farmington complex seemingly sits on Archean basement of the Wyoming – Grouse Creek block (Mueller et al. 2011; Yonkee et al. 2003). The band of Paleoproterozoic crystalline rocks likely continues northward into Idaho, where Paleoproterozoic crystalline basement occurs within the Cabin – Medicine Lake thrust system just east of the Idaho batholith (Skipp 1987) and the Tendoy thrust of southwestern Montana (Skipp and Hait 1977; DuBois 1982).

Hi-flux magmatic events

Our data suggest that the so-called hi-flux magmatic events of arcs (Gehrels et al. 2009) are not arc-related, but instead occur from slab failure during collision. Some researchers recognized that flare-ups coincide with episodes of crustal thickening (Ducea and Barton 2007; Ducea et al. 2015) but interpreted the thickening to reflect retro-arc thrusting (DeCelles et al. 2009). Other researchers (Ducea and Saleeby 1998; Jagoutz and Behn 2013; Lee and Anderson 2015) suggest crustal thickening in the arc by magmatic underplating, commonly accompanied by foundering of dense cumulates, but these models fail because the arc is underplated by the lower plate lithosphere prior to the hi-flux event so there is insufficient time for magmatic underplating. In our model (Hildebrand and Whalen 2017), arc-continent collision shuts down arc magmatism, and due to the buoyancy contrast between the continental and oceanic lithosphere, the subducting plate fails and the oceanic sector, possibly plus some thin lithosphere of the rifted margin, sinks into the mantle, where the upper basaltic–gabbroic part of the oceanic slab melts to produce post-collisional magmatism. The change from arc magmatism to slab failure magmatism happens rapidly, typically within a couple of million years, so there is no time, given the low thermal diffusivity of rocks, for underthrust material to heat up and melt sufficiently to produce the quantity of observed magmatism.

The key difference between our model and those of others is that we recognize the post-collisional nature of the hi-flux magmatism and relate it to melting of the subducting slab. We utilized the timing and composition of the magmatism to resolve the crustal composition paradox because we maintain that most magmas are not arc derived (as commonly hypothesized), but instead formed during the waning stages of collision and consequent slab failure (Hildebrand et al. 2018). Because the batholiths typically have silica contents >60% and are derived directly from the mantle, we argue that they create large amounts of continental crust. In fact, on the basis of detrital zircon peaks that largely coincide with periods of continental amalgamation (Condie et al. 2009, 2017; Hawkesworth et al. 2010, 2016), we suggest that post-collisional magmatism might have created more than half of all continental crust.

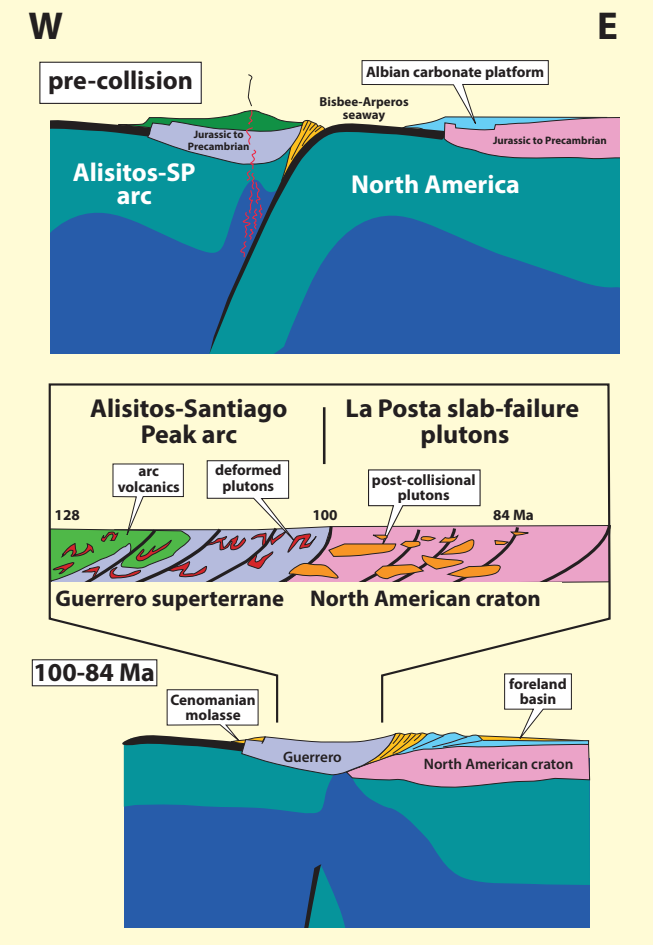

Fig. 19. Our tectonic plate scale model for the Peninsular Ranges orogeny involves closure of a Lower Cretaceous seaway by west-directed subduction and arc magmatism from ~140 Ma until the collision of the arc with North America at 100 Ma. The competing buoyancies of the oceanic and cratonic lithosphere led to rapid tearing and break-off of the subducted plate and an influx of 99–84 Ma post-collisional magmatism during exhumation of the orogenic hinterland. During exhumation and plutonism, between 99–90 Ma molasse was shed westward into the old back-arc region. [Colour online.]

Conclusions

1. The Peninsular Ranges orogen is a ~100 Ma orogenic belt that extends from Mexico to Alaska, but here we discussed only the Peninsular Ranges, Mojave, and Sierran sectors of the orogen. The orogen formed when a marine trough, open for about 40 million years along the western margin of North America, closed by westerly subduction, which pulled a passive continental margin, capped by a west-facing Albian carbonate platform built on the eastern North American side of the trough, beneath an Early Cretaceous arc complex, built on the western side of the trough (Fig. 19).
2. About a million years or so following the collision, the collisional hinterland was exhumed and intruded by a swarm of

tonalite–granodiorite–granite plutons. The timing suggests that the plutons and exhumation formed in tandem when the oceanic lithosphere broke off from the partially subducted North American plate (Fig. 19).

3. The large mid-Cretaceous batholiths of the Peninsular Ranges and Sierra Nevada are composed of two contrasting magmatic suites derived from distinct mantle sources and emplaced at different times. The older arc suite represents a generally low-standing marine arc built on thinned lithosphere over a westward-dipping subduction zone, whereas the younger suite was post-collisional and invaded the orogenic hinterland during exhumation due to break-off and melting of the subducting slab.
4. Models that utilize Andino-type or cyclic hi-magmatic flux models for the development of Cordilleran batholiths, fail to recognize that the transition from arc magmatism to post-collisional hi-flux magmatism occurred rapidly, perhaps in about a million years, so that there is insufficient time to thicken the crust by underplating or for heat transfer by conduction to melt underthrust cratonic material.
5. The post-collisional magmas appear to have been derived from melting of the basaltic–gabbroic upper part of the subducted oceanic lithosphere augmented by assimilation due to fractional melting of the SCLM as they rose toward the crust. Thus, slab break-off magmas have trace element concentrations and ratios similar to slab window rocks, but where they rise through old and enriched cratonic lithosphere they acquire an enriched radiogenic signature.
6. There is no compelling evidence along the western edge of the Peninsular Ranges and Sierra Nevada for a fore-arc basin or accretionary prism during Early Cretaceous arc magmatism. Instead, voluminous quantities of material were shed westward into the back-arc region after the 100 Ma collision and termination of arc magmatism, when abundant detrital zircons from the 100–90 Ma post-collisional plutons document rapid exhumation of the orogenic hinterland.
7. An implication of our model is that retro-arc models for the Sevier thrust-fold belt should be reconsidered, as there was no eastward subduction beneath North America at about 120 Ma when the Sevier thrusting initiated. We claim there is compelling evidence that the 130–100 Ma arc magmatism in the Peninsular Ranges and Sierra Nevada were built above westward, not eastward, subduction zones (Fig. 19).
8. In the San Emigdio mountains, the ∼100 Ma San Emigdio schist, with an inverse temperature gradient and paleopressures of 11–9 kbar, lies between a basal terrane comprising slabs, up to 10 km long, of marble, quartzite, schist and metasandstone, and the base of the Sierran arc, consisting of 136–101 Ma plutons and gneisses originally at pressures of 10–11 kbar. We interpret these relations to represent an oblique cross section through the uplifted 100 Ma collisional suture zone, which was exhumed to mid crustal depths by ∼95 Ma. Their paleopressures suggest Sierran crust of normal, or lesser, thickness.
9. The so-called "flare-up" events in Cordilleran arcs are the result of collision followed by slab break-off magmatism.
10. In Part II, we explore the more northerly continuation of the Peninsular Ranges orogen and demonstrate that overall it extends from southern Mexico to Alaska, with geological relations and timing in the northern sector similar to the Peninsular Ranges and Sierra Nevada.

Acknowledgements

Eldridge, this is for you! Paul Link and Tim Lawton helped with detrital zircon plotting and discussions. Several phone conversations during Covid-19 sequestration on the geology of Nevada with C.J. Northrup were very useful. Bob Hatcher and Brendan Murphy commented on an early draft of the manuscript. Since 2014, ongoing discussions with Tim Lawton on all matters of foredeeps and basins have been incredibly helpful. Thoughtful reviews by Michaelangelo Martini and Basil Tikoff helped us to improve both papers.

References

Allen, C., Wooden, J.L., Howard, K.A., Foster, D.A., and Tosdal, R.M. 1995. Sources of the early Cretaceous plutons in the Turtle and West Riverside mountains, California: Anomalous Cordilleran interior intrusions. Journal of Petrology, **36**: 1675–1700. doi:10.1093/oxfordjournals.petrology.a037270.

Allison, F.C. 1974. The type Alisitos formation (Cretaceous, Aptian–Albian) of Baja California and its bivalve fauna, *In* Geology of Peninsular California. *Edited by* G. Gastil and J. Lillegraven. AAPG-SEPM-SEG Pacific Section 49th Annual Meeting Field Trip Guidebook. pp. 20–59.

Almazán-Vásquez, E. 1988*a*. Marco paleosedimentario y geodinámico de la Formación Alisitos en la península de Baja California. Universidad Nacional Autónoma de México, Instituto de Geología, Revista, **7**: 41–51.

Almazán-Vásquez, E. 1988*b*. Geoquímica de las rocas volcánicas de la Formación Alisitos del Arroyo La Bocana en el Estado de Baja California Norte. Universidad Nacional Autónoma de México, Instituto de Geología, Revista, **7**: 78–88.

Alsleben, H., Wetmore, P.H., Schmidt, K.L., Paterson, S.R., and Melis, E.A. 2008. Complex deformation during arc–continent collision: Quantifying finite strain in the accreted Alisitos arc, Peninsular Ranges batholith, Baja California. Journal of Structural Geology, **30**: 220–236. doi:10.1016/j.jsg.2007.11.001.

Anderson, T.H., Rodríguez-Castañeda, J.L., and Silver, L.T. 2005. Jurassic rocks in Sonora, Mexico: Relations to the Mojave-Sonora megashear and its inferred northwestward extension. *In* The Mojave-Sonora Megashear Hypothesis: Development, Assessment, and Alternatives. *Edited by* T.H. Anderson, J.A. Nourse, J.W. McKee, and M.B. Steiner. Geological Society of America Special Papers, 393. pp. 51–95. doi:10.1130/0- 8137-2393-0.51.

Armstrong, R.L. 1968. Sevier orogenic belt in Nevada and Utah. Geological Society of America Bulletin, **79**: 429–458. doi:10.1130/0016-7606(1968)79[429:SOBINA]2.0.CO;2.

Armstrong, R.L., and Dick, H.J.B. 1974. A model for the development of thin overthrust sheets of crystalline rock. Geology, **2**: 35–40. doi:10.1130/0091-7613(1974)2<35:AMFTDO>2.0.CO;2.

Axen, G.J. 1987. The Keystone and Red Spring thrust faults in the La Madre Mountain area, eastern Spring Mountains, Nevada. *In* Centennial field guide. *Edited by* M.L. Hill. Geological Society of America, North American Geology, 1: pp. 57–60.

Bacon, C.R., Gunn, S.H., Lanphere, M.A., and Wooden, J.L. 1994. Multiple isotopic components in Quaternary volcanic rocks of the Cascade arc near Crater Lake, Oregon. Journal of Petrology, **35**: 1521–1556. doi:10.1093/petrology/35.6.1521.

Bartley, J.M., and Gleason, G.C. 1990. Tertiary normal faults superimposed on Mesozoic thrusts, Quinn Canyon and Grant Ranges, Nye County, Nevada. *In* Basin and Range Extensional Tectonics near the Latitude of Las Vegas. *Edited by* B.P. Wernicke. Geological Society of America Memoir, **176**: 195–212. doi:10.1130/MEM176-p195.

Bartley, J.M., Glazner, A.F., and Mahan, K.H. 2012. Formation of pluton roofs, floors, and walls by crack opening at Split Mountain, Sierra Nevada, California. Geosphere, **8**(5): 1086–1103. doi:10.1130/GES00722.1.

Bateman, P.C. 1992. Plutonism in the Central Part of the Sierra Nevada Batholith. U.S. Geological Survey Professional Paper 1483. 186pp.

Bateman, P.C., and Chappell, B.W. 1979. Crystallization, fractionation, and solidification of the Tuolumne intrusive series, Yosemite National Park, California. Geological Society of America Bulletin, **90**: 465–482. doi:10.1130/0016-7606(1979)90<465:CFASOT>2.0.CO;2.

Bateman, P.C., and Clark, L.D. 1974. Stratigraphic and structural setting of the Sierra Nevada batholith, California. Pacific Geology, **8**: 79–89.

Bateman, P.C., and Wahrhaftig, C. 1966. Geology of the Sierra Nevada. *In* Geology of Northern California. *Edited by* E.H. Baily. California Division of Mines and Geology Bulletin 190. pp. 107–172.

Bateman, P.C., Clark, L.D., Huber, N.K., Moore, J.G., and Rinehart, C.D. 1963. The Sierra Nevada Batholith—A Synthesis of Recent Work across the Central Part. U.S. Geological Survey Professional Paper 414-D, 46 p.

Bateman, P.C., Dodge, F.C.W., and Kistler, R.W. 1991. Magnetic susceptibility and relation to initial $^{87}Sr/^{86}Sr$ for granitoids of the central Sierra Nevada, California. Journal of Geophysical Research, **96**: 19,555–19,568. doi:10.1029/91JB02171.

Beck, C.L. 2013. New insights into migration of the cretaceous Sierran Arc using high-precision U-Pb geochronology. M.S. thesis, University of North Carolina, Chapel Hill, North Carolina. 49pp.

Beckerman, G.M., Robinson, J.P., and Anderson, J.L. 1982. The Teutonia batholith: A large intrusive complex of Jurassic and Cretaceous age in the eastern Mojave Desert, California, *In* Mesozoic–Cenozoic tectonic evolution of the Colorado River region, California, Arizona, and Nevada. *Edited by* E.G. Frost and D.L. Martin. Cordilleran Publishers, San Diego, California, pp. 205–220.

Bilodeau, W.L., Kluth, C.F., and Vedder, L.K. 1987. Regional stratigraphic, sedimentologic, and tectonic relationships of the Glance Conglomerate in south-eastern Arizona. *In* Mesozoic rocks of southern Arizona adjacent areas. *Edited by* W.R. Dickinson and M.F. Klute. Arizona Geological Society, Digest 18. pp. 229–256.

Bindeman, I. 2008. Oxygen isotopes in mantle and crustal magmas as revealed by single crystal analysis. Reviews in Mineralogy and Geochemistry, **69**: 445–478. doi:10.2138/rmg.2008.69.12.

Bindeman, I.N., Eiler, J.M., Yogodzinski, G.M., Tatsumi, Y., Stern, C.R., Grove, T.L., et al. 2005. Oxygen isotope evidence for slab melting in modern and ancient subduction zones. Earth Planetary Science Letters, **235**: 480–496. doi:10.1016/j.epsl.2005.04.014.

Blondes, M.S., Reiners, P.W., Ducea, M.N., Singer, B.S., and Chesley, J. 2008. Temporal–compositional trends over short and long time-scales in basalts of the Big Pine volcanic field, California. Earth and Planetary Science Letters, **269**: 140–154. doi:10.1016/j.epsl.2008.02.012.

Bohannon, R.G. 1983. Mesozoic and Cenozoic tectonic development of the Muddy, North Muddy, and northern Black Mountains, Clark County, Nevada, *In* Tectonic and stratigraphic studies in the Eastern Great Basin. *Edited by* D.M. Miller, V.R. Todd, and K.A. Howard. Geological Society of America Memoir 157. pp. 125–148. doi:10.1130/MEM157-p125.

Bonde, J.W. 2008. Paleoecology and Taphonomy of the Willow Tank Formation (Albian), Southern Nevada. M.Sc. thesis, Montana State University, Bozeman, Montana. 96pp.

Bonde, J.W., Varricchio, D.J., Bryant, G., and Jackson, F.D. 2012. Mesozoic vertebrate paleontology of Valley of Fire State Park, Clark County, Nevada. *In* Field Guide for the 71st Annual Meeting of the Society of Vertebrate Paleontology. *Edited by* J.W. Bonde, and A.R.C. Milner. Nevada State Museum Paleontological Paper Number 1. pp. 108–126.

Brown, D., Ryan, P.D., Afonso, J.C., Boutelier, D., Burg, J.P., Calvert, A., et al. 2011. Arc–continent collision: the making of an orogen. *In* Arc-continent collision. *Edited by* D. Brown and P.D. Ryan. Springer-Verlag, Berlin. pp. 477–493.

Buddington, A.F. 1927. Coast Range intrusives of southeastern Alaska. Journal of Geology, **35**: 224–246. doi:10.1086/623404.

Burchfiel, B.C., and Davis, G.A. 1972. Structural framework and evolution of the southern part of the Cordilleran orogeny, western United States. American Journal of Science, **272**: 97–118. doi:10.2475/ajs.272.2.97.

Burchfiel, B.C., and Davis, G.A. 1977. Geology of the Sagamore Canyon-Slaughterhouse Spring area. New York Mountains. California. Geological Society of America Bulletin, **88**: 1623–1640. doi:10.1130/0016-7606(1977)88<1623:GOTSCS>2.0.CO;2.

Burchfiel, B.C., Fleck, R.J., Secor, D.T., Vincelette, R.R., and Davis, G.A. 1974. Geology of the Spring Mountains, Nevada. Geological Society of America Bulletin, **85**: 1013–1022. doi:10.1130/0016-7606(1974)85<1013:GOTSMN>2.0.CO;2.

Burchfiel, B.C., Cameron, C.S., and Royden, L.H. 1998. Geology of the Wilson Cliffs–Potosi Mountain area, southern Nevada. *In* Integrated Earth and environmental evolution of the southwestern United States: The Clarence A. Hall Jr., volume. *Edited by* W.G. Ernst and C.A. Nelson. Columbia, Maryland, Bellwether Publishing for the Geological Society of America. pp. 203–227.

Busby, C., Smith, D., Morris, W., and Fackler-Adams, B. 1998. Evolutionary model for convergent margins facing large ocean basins: Mesozoic Baja California, Mexico. Geology, **26**: 227–230. doi:10.1130/0091-7613(1998)026<0227:EMFCMF>2.3.CO;2.

Busby, C.J., Adams, B.F., Mattinson, J., and Deoreo, S. 2006. View of an intact oceanic arc, from surficial to mesozonal levels: Cretaceous Alisitos arc, Baja California. Journal of Volcanology and Geothermal Research, **149**: 1–46. doi:10.1016/j.jvolgeores.2005.06.009.

Cabral-Cano, E., Lang, H.R., and Harrison, C.G.A. 2000. Stratigraphic assessment of the Arcelia±Teloloapan area, southern Mexico: implications for southern Mexico's post-Neocomian tectonic evolution. Journal of South American Earth Sciences, **13**: 443–457. doi:10.1016/S0895-9811(00)00035-3.

Calkins, F.C. 1930. The granitic rocks of the Yosemite region. *In* Geologic history of the Yosemite Valley. *Edited by* F.E. Matthes. United States Geological Survey Paper 160. pp. 120–129.

Camp, V.E., and Hanan, B.B. 2008. A plume-triggered delamination origin for the Columbia River Basalt Group. Geosphere, **4**: 480–495. doi:10.1130/GES00175.1.

Campa, M.F., and Coney, P.J. 1983. Tectono-stratigraphic terranes and mineral resource distributions in Mexico. Canadian Journal of Earth Sciences, **20**(6): 1040–1051. doi:10.1139/e83-094.

Campa-Uranga, M.F., Torres de León, R., Iriondo, A., and Premo, W.R. 2012. Caracterización geológica de los ensambles metamórficos de Taxco y Taxco el Viejo, Guerrero, México. Boletín de la Sociedad Geológica Mexicana, **64**: 369–385.

Cao, W., Paterson, S., Memeti, V., Mundil, R., Anderson, J.L., and Schmidt, K. 2015. Tracking paleodeformation fields in the Mesozoic central Sierra Nevada arc: Implications for intra-arc cyclic deformation and arc tempos. Lithosphere, **7**: 296–320. doi:10.1130/L389.1.

Carr, M.D. 1980. Upper Jurassic to Lower Cretaceous (?) synorogenic sedimentary rocks in the southern Spring Mountains. Geology, **8**: 385–389. doi:10.1130/0091-7613(1980)8<385:UJTLCS>2.0.CO;2.

Centeno-García, E. 2005. Review of Upper Paleozoic and Lower Mesozoic stratigraphy and depositional environments of central and west Mexico: Constraints on terrane analysis and paleogeography. *In* The Mojave-Sonora Megashear Hypothesis: development, assessment, and alternatives. *Edited by* T.H. Anderson. Geological Society of America Special Paper 393. pp. 233–258.

Centeno-García, E., Guerrero-Suastegui, M., and Talavera-Mendoza, O. 2008. The Guerrero composite terrane of western Mexico: Collision and subsequent rifting in a supra-subduction zone. *In* Formation and applications of the sedimentary record in arc collision zones. *Edited by* A.E. Draut, P.D. Clift, and D.W. Scholl. Geological Society of America Special Paper 436. pp. 279–308. doi:10.1130/2008.2436(13).

Centeno-García, E., Busby, C., Busby, M., and Gehrels, G. 2011. Evolution of the Guerrero composite terrane along the Mexican margin, from extensional fringing arc to contractional continental arc. Geological Society of America Bulletin, **123**: 1776–1797. doi:10.1130/B30057.1.

Chamberlain, V.E., and Lambert, R.S.J. 1985. Cordilleria, a newly defined Canadian microcontinent. Nature, **314**: 707–713. doi:10.1038/314707a0.

Chapman, A.D., and Saleeby, J. 2012. Geologic map of the San Emigdio Mountains, southern California. Geological Society of America Map and Chart 101. doi:10.1130/2012.MCH101.

Chapman, A.D., Luffi, P., Saleeby, J., and Petersen, S. 2011. Metamorphic evolution, partial melting, and rapid exhumation above an ancient flat slab: Insights from the San Emigdio Schist, southern California. Journal of Metamorphic Geology, **29**: 601–626. doi:10.1111/j.1525-1314.2011.00932.x.

Chapman, A.D., Saleeby, J.B., Wood, D.J., Piasecki, A., Kidder, S., Ducea, M.N., and Farley, K.A. 2012. Late Cretaceous gravitational collapse of the southern Sierra Nevada batholith, California. Geosphere, **8**: 314–341. doi:10.1130/GES00740.1.

Chen, J.H., and Moore, J.G. 1982. Uranium-lead ages from the Sierra Nevada batholith, California. Journal of Geophysical Research, **87**: 4761–4784. doi:10.1029/JB087iB06p04761.

Chen, J.H., and Tilton, G.R. 1991. Applications of lead and strontium isotopic relationships to the petrogenesis of granitoid rocks, central Sierra Nevada batholith, California. Geological Society of America Bulletin, **103**: 439–447. doi:10.1130/0016-7606(1991)103<0439:AOLASI>2.3.CO;2.

Chin, E.J., Lee, C.-T.A., Tollstrup, D.L., Xie, L., Wimpenny, J.B., and Yin, Q.-Z. 2013. On the origin of hot metasedimentary quartzites in the lower crust of continental arcs. Earth and Planetary Science Letters, **361**: 120–133. doi:10.1016/j.epsl.2012.11.031.

Christe, G. 2010. U/Pb ages of Kettle Rock and Mount Jura sequence volcanic rock, eastern Mesozoic belt, northern Sierra Nevada, California: A revised understanding of the age relationship of volcanism, plutonism, and tectonism within successive Jurassic arc sequences. Geological Society of America Abstracts with Programs, **42**(4): 110.

Christe, G. 2011. New U-Pb ages for the Eastern Mesozoic Belt of northeastern California: Implications for stratigraphy, tectonic evolution, terrane assignment and possible correlation with Mesozoic units in the western Great Basin of Nevada. *In* Great Basin Evolution and Metallogeny. *Edited by* R. Steininger. Geological Society of Nevada Symposium, Vol. 1. pp. 257–288.

Christe, G., and Hannah, J.L. 1990. High-K, continental-arc volcanism in the Kettle Rock Sequence of the Eastern Mesozoic Belt, northern Sierra Nevada, California: Implications for lower Mesozoic Cordilleran Tectonics. *In* The nature and origin of Cordilleran magmatism. *Edited by* J.L. Anderson. Geological Society of America, Memoir 174, Boulder, Colorado. pp. 315–329.

Clausen, B.L., Morton, D.M., Kistler, R.W., and Lee, C.T.A. 2014. Low-initial-Sr felsic plutons of the northwestern Peninsular Ranges batholith, southern California, and the role of mafic-felsic magma mixing in continental crust formation. *In* Peninsular Ranges Batholith, Baja California and Southern California. *Edited by* D.M. Morton and F.K. Miller, Geological Society of America Memoir 211. pp. 317–344.

Clemens-Knott, D. 1992. Geologic and isotopic investigations of the Early Cretaceous Sierra Nevada Batholith, Tulare County, California, and the Ivrea Zone, northwest Italian Alps: examples of interaction between mantle-derived magma and continental crust. Ph.D. thesis, California Institute of Technology, Pasadena, California. 389pp.

Clemens-Knott, D., and Saleeby, J.B. 1999. Impinging ring dike complexes in the Sierra Nevada batholith, California: Roots of the Early Cretaceous volcanic arc. Geological Society of America Bulletin, **111**: 0484–0496.

Cloos, M., and Housh, T.B. 2008. Collisional delamination: Implications for porphyry-type Cu-Au ore formation in New Guinea. *In* Ores and orogenesis: Circum-Pacific tectonics, geologic evolution, and ore deposits. *Edited by* J.E. Spencer and S.R. Titley. Arizona Geological Society Digest. Vol. 22. pp. 235–244.

Cloos, M., Sapiie, B., van Ufford, A.Q., Weiland, R.J., Warren, P.Q., and McMahon, T.P. 2005. Collisional delamination in New Guinea: the geotectonics of subducting slab breakoff. Geological Society of America Special Paper 400. 51pp.

Cohen, K.M., Finney, S.C., Gibbard, P.L., and Fan, J.-X. 2013. The ICS International Chronostratigraphic Chart. Episodes, **36**: 199–204. doi:10.18814/epiiugs/2013/v36i3/002.

Coleman, D.S., and Glazner, A.F. 1998. The Sierra Crest magmatic event: rapid formation of juvenile crust during the Late Cretaceous in California. *In* Integrated earth and environmental evolution of the southwestern United States: the Clarence A. Hall Jr., Volume. *Edited by* W.G. Ernst

and C.A. Nelson. Bellwether Publishing for the Geological Society of America, Columbia, Maryland. pp. 253–272.
Coleman, D.S., Gray, W., and Glazner, A.F. 2004. Rethinking the emplacement and evolution of zoned plutons: Geochronologic evidence for incremental assembly of the Tuolumne intrusive suite, California. Geology, **32**: 433–436. doi:10.1130/G20220.1.
Condie, K.C., Belousova, E., Griffin, W.L., and Sircombe, K.N. 2009. Granitoid events in space and time: constraints from igneous and detrital zircon age spectra. Gondwana Research, **15**: 228–242. doi:10.1016/j.gr.2008.06.001.
Condie, K.C., Arndt, N., Davaille, A., and Puetz, S.J. 2017. Zircon age peaks: production or preservation of continental crust? Geosphere, **13**: 227–234. doi:10.1130/GES01361.1.
Constenius, K.N., Johnson, R.A., Dickinson, W.R., and Williams, T.A. 2000. Tectonic evolution of the Jurassic–Cretaceous Great Valley forearc, California: Implications for the Franciscan thrust-wedge hypothesis. Geological Society of America Bulletin, **112**: 1703–1723. doi:10.1130/0016-7606(2000)112<1703:TEOTJC>2.0.CO;2.
Davies, J.H., and von Blanckenburg, F. 1995. Slab break-off: A model of lithosphere detachment and its test in the magmatism and deformation of collisional orogens. Earth and Planetary Science Letters, **129**: 85–102. doi:10.1016/0012-821X(94)00237-S.
Davis, G.A. 1973. Relations between the Keystone and Red Spring faults, eastern Spring Mountains, Nevada. Geological Society of America Bulletin, **84**: 3709–3716. doi:10.1130/0016-7606(1973)84<3709:RBTKAR>2.0.CO;2.
Davis, J.W., Coleman, D.S., Gracely, J.T., Gaschnig, R., and Stearns, M. 2012. Magma accumulation rates and thermal histories of plutons of the Sierra Nevada batholith, CA. Contributions to Mineralogy and Petrology, **163**: 449–465. doi:10.1007/s00410-011-0683-7.
DeCelles, P.G. 2004. Late Jurassic to Eocene evolution of the Cordilleran thrust belt and foreland basin system, western USA. American Journal of Science, **304**: 105–168. doi:10.2475/ajs.304.2.105.
DeCelles, P.G., Ducea, M.N., Kapp, P., and Zandt, G. 2009. Cyclicity in Cordilleran orogenic systems. Nature Geoscience, **2**: 251–257. doi:10.1038/ngeo469.
DeCelles, P.G., and Coogan, J.C. 2006. Regional structure and kinematic history of the Sevier fold-and-thrust belt, central Utah. Geological Society of America Bulletin, **118**: 841–864. doi:10.1130/B25759.1.
DeGraaff-Surpless, K., Graham, S.A., Wooden, J.L., and McWilliams, M.O. 2002. Detrital zircon provenance analysis of the Great Valley Group, California: Evolution of an arc-forearc system. Geological Society of America Bulletin, **114**: 1564–1580. doi:10.1130/0016-7606(2002)114<1564:DZPAOT>2.0.CO;2.
DePaolo, D.J. 1980. Crustal growth and mantle evolution: inferences from models of element transport and Nd and Sr isotopes. Geochimica et Cosmochimica Acta, **44**: 1185–1196. doi:10.1016/0016-7037(80)90072-1.
DePaolo, D.J. 1981. A neodymium and strontium isotopic study of the Mesozoic calc-alkaline granitic batholiths of the Sierra Nevada and Peninsular Ranges, California. Journal of Geophysical Research, **86**(10): 10470–10410. doi:10.1029/JB086iB11p10470.
Dickinson, W.R. 1970. Relations of andesites, granites, and derivative sandstones to arc-trench tectonics. Reviews of Geophysics, **8**: 813–860. doi:10.1029/RG008i004p00813.
Dickinson, W.R. 1976. Sedimentary basins developed during evolution of Mesozoic–Cenozoic arc-trench system in western North America. Canadian Journal of Earth Sciences, **13**(9): 1268–1287. doi:10.1139/e76-129.
Dickinson, W.R., and Lawton, T.F. 2001*a*. Carboniferous to Cretaceous assembly and fragmentation of Mexico. Geological Society of America Bulletin, **113**: 1142–1160. doi:10.1130/0016-7606(2001)113<1142:CTCAAF>2.0.CO;2.
Dickinson, W.R., and Lawton, T.F. 2001*b*. Tectonic setting and sandstone petro-facies of the Bisbee basin (USA–Mexico). Journal of South American Earth Sciences, **14**: 475–504. doi:10.1016/S0895-9811(01)00046-3.
Di Fiori, R.V., Long, S.P., Fetrow, A.C., Snell, K.E., Bonde, J.W., and Vervoort, J. 2020. Syn-contractional deposition of the Cretaceous Newark Canyon Formation, Diamond Mountains, Nevada: Implications for strain partitioning within the U.S. Cordillera. Geosphere, **16**: 546–566. doi:10.1130/GES02168.1.
Doucette, J. 2000. A petrochemical study of the Mount Fubilan intrusion and associated ore bodies, Papua New Guinea. Unpublished Ph.D. thesis, Oregon State University. 400pp.
DuBois, D.P. 1982. Tectonic framework of basement thrust terrane, northern Tendoy Range, southwest Montana. *In* Geologic studies of the Cordilleran Thrust Belt. *Edited by* R.B. Powers. Rocky Mountain Association of Geologists. pp. 145–158.
du Bray, E.A. 2007. Time, space, and composition relations among northern Nevada intrusive rocks and their metallogenic implications. Geosphere, **3**: 381–405. doi:10.1130/GES00109.1.
Ducea, M.N., and Barton, M.D. 2007. Igniting flare-up events in Cordilleran arcs. Geology, **35**: 1047–1050. doi:10.1130/G23898A.1.
Ducea, M.N., and Saleeby, J.B. 1998. The age and origin of a thick mafic-ultramafic keel from beneath the Sierra Nevada batholith. Contributions to Mineralogy and Petrology, **133**: 169–185. doi:10.1007/s004100050445.
Ducea, M.N., Paterson, S.R., and DeCelles, P.G. 2015. High-volume magmatic events in subduction systems. Elements, **11**: 99–104. doi:10.2113/gselements.11.2.99.
Duque-Trujillo, J., Ferrari, L., Orozco-Esquivel, T., López-Martínez, M., Lons-Dale, P., Bryan, S.E., et al. 2015. Timing of rifting in the southern Gulf of California and its conjugate margins: Insights from the plutonic record. Geological Society of America Bulletin, **127**: 702–736. doi:10.1130/B31008.1.
Duretz, T., and Gerya, T.V. 2013. Slab detachment during continental collision: Influence of crustal rheology and interaction with lithospheric delamination. Tectonophysics, **602**: 124–140. doi:10.1016/j.tecto.2012.12.024.
Duretz, T., Gerya, T.V., and May, D.A. 2011. Numerical modelling of spontaneous slab breakoff and subsequent topographic response. Tectonophysics, **502**: 244–256. doi:10.1016/j.tecto.2010.05.024.
Duretz, T., Schmalholz, S.M., and Gerya, T.V. 2012. Dynamics of slab detachment. Geochemistry, Geophysics, Geosystems, **13**. doi:10.1029/2011GC004024.
Eiler, J.M. 2001. Oxygen isotope variations of basaltic lavas and upper mantle rocks. *In* Stable isotope geochemistry. *In* Mineralogical Society of America Reviews in Mineralogy and Geochemistry. *Edited by* J.W. Valley and D.R. Cole. Vol. 43. pp. 319–364. doi:10.2138/gsrmg.43.1.319.
Fleck, R.J. 1970. Tectonic style, magnitude, and age of deformation in the Sevier orogenic belt in southern Nevada and eastern California. Geological Society of America Bulletin, **81**: 1705–1720. doi:10.1130/0016-7606(1970)81[1705:TSMAAO]2.0.CO;2.
Fleck, R.J., and Carr, M.D. 1990. The age of the Keystone thrust: Laser-fusion $^{40}Ar/^{39}Ar$ dating of foreland basin deposits, southern Spring Mountains, Nevada. Tectonics, **9**: 467–476. doi:10.1029/TC009i003p00467.
Fleck, R.J., Mattinson, J.M., Busby, C.J., Carr, M.D., Davis, G.A., and Burchfiel, B.C. 1994. Isotopic complexities and the age of the Delfonte volcanic rocks, eastern Mescal Range, southeastern California: Stratigraphic and tectonics implications. Geological Society of America Bulletin, **106**: 1242–1253. doi:10.1130/0016-7606(1994)106<1242:ICATAO>2.3.CO;2.
Fletcher, J.M., and Karlstrom, K.E. 1990. Late Cretaceous ductile deformation, metamorphism and plutonism in the Piute Mountains, eastern Mojave Desert. Journal of Geophysical Research, **95**: 487–500. doi:10.1029/JB095iB01p00487.
Fries, C., Jr. 1960. Geología del Estado de Morelos y de Partes Adyacentes de México y Guerrero, Región Central Meridional de México. Boletín del Instituto de Geología, Universidad Nacional Autónoma de México. Vol. 60. 236pp.
Gastil, R.G. 1993. Prebatholithic history of peninsular California. *In* The prebatholithic stratigraphy of peninsular California. *Edited by* R.G. Gastil and R.H. Miller. Geological Society of America Special Paper 279. pp. 145–156. doi:10.1130/SPE279-p145.
Gastil, R.G., and Miller, R.H. 1981. Lower Paleozoic strata on the Pacific Plate of North America. Nature, **292**: 828–830. doi:10.1038/292828a0.
Gastil, R.G., Phillips, R.P., and Allison, E.C. 1975. Reconnaissance geology of the state of Baja California. Geological Society of America Memoir, **140**: 201. doi:10.1130/MEM140-p1.
Gastil, R.G., Morgan, G., and Krummenacher, D. 1981. The tectonic history of Peninsular California and adjacent Mexico. *In* The Geotectonic Development of California, Rubey Volume 1. *Edited by* W.G Ernst. Prentice-Hall, Englewood Cliffs, New Jersey. pp. 284–306.
Gastil, R.G., Diamond, J., Knaack, C., Walawender, M., Marshall, M., Boyles, C., et al. 1990. The problem of the magnetite/ilmenite boundary in southern and Baja California. *In* The nature and origin of Cordilleran magmatism. *Edited by* J.L. Anderson. Geological Society of America Memoir 174. pp. 19–32. doi:10.1130/MEM174-p19.
Gastil, R.G., Miller, R., Anderson, P., Crocker, J., Campbell, M., Buch, P., et al. 1991. The relation between the Paleozoic strata on opposite sides of the Gulf of California. *In* Studies of Sonoran Geology. *Edited by* E. Pérez-Segura and C. Jacques-Ayala. Geological Society of America Special Paper 254. pp. 7–18. doi:10.1130/SPE254-p7.
Gastil, R.G., Kimbrough, D.L., Kimbrough, J.M., Grove, M., and Shimizu, M. 2014. The Sierra San Pedro Mártir zoned pluton, Baja California, Mexico. *In* Peninsular Ranges Batholith, Baja California and southern California. *Edited by* D.M. Morton and F.K. Miller. Geological Society of America Memoir 211. pp. 739–758. doi:10.1130/2014.1211(24).
Gehrels, G., Rusmore, M., Woodsworth, G., Crawford, M., Andronicos, C., Hollister, L., et al. 2009. U–Th–Pb geochronology of the Coast Mountains batholith in north-coastal British Columbia: constraints on age and tectonic evolution. Geological Society of America Bulletin, **121**: 1341–1361. doi:10.1130/B26404.1.
Girardi, J.D., Patchett, P.J., Ducea, M.N., Gehrels, G.E., Cecil, M.R., Rusmore, M.E., et al. 2012. Elemental and isotopic evidence for granitoid genesis from deep-seated sources in the Coast Mountains batholith, British Columbia. Journal of Petrology, **53**: 1505–1536. doi:10.1093/petrology/egs024.
Giallorenzo, M. 2013. Application of (U-Th)/He and 40Ar/39Ar Thermochronology to the age of thrust faulting in the Sevier orogenic belt. Ph.D. dissertation, University of Nevada, Las Vegas, Nevada. 281pp.
González-Léon, C., and Jacques-Ayala, C. 1988. Estratigrafía de las rocas cretácicas del área de Cerro de Oro, Sonora Central. Boletín de Departmento de Universidad Sonora, **5**: 1–23.
González-Léon, C.M., Scott, R.W., Löser, H., Lawton, T.F., Robert, E., and Valencia, V.A. 2008. Upper Aptian- Lower Albian Mural Formation: stratigraphy, biostratigraphy and depositional cycles on the Sonoran shelf, northern México. Cretaceous Research, **29**: 249–266. doi:10.1016/j.cretres.2007.06.001.
González-León, C.M., Solari, L., Solé, J., Ducea, M.N., Lawton, T.F., Bernal, J.P., et al. 2011. Stratigraphy, geochronology, and geochemistry of the Laramide magmatic arc in north-central Sonora, Mexico. Geosphere, **7**: 1392–1418. doi:10.1130/GES00679.1.

González-León, C.M., Madhavaraju, J., Ramírez Montoya, E., Solari, L.A., Villanueva-Amadoz, U., Monreal, R., and Sánchez Medrano, P.A. 2020. Stratigraphy, detrital zircon geochronology and provenance of the Morita formation (Bisbee Group) in northeastern Sonora, Mexico. Journal of South American Earth Sciences, **103**: 102761. doi:10.1016/j.jsames.2020.102761.

Gromet, L.P., and Silver, L.T. 1987. REE variations across the Peninsular Ranges Batholith: Implications for batholithic petrogenesis and crustal growth in magmatic arcs. Journal of Petrology, **28**: 75–125. doi:10.1093/petrology/28.1.75.

Grove, M., Lovera, O., and Harrison, M. 2003. Late Cretaceous cooling of the east-central Peninsular Ranges Batholith (33 degrees N): Relationship to La Posta pluton emplacement, Laramide shallow subduction, and forearc sedimentation. *In* Tectonic Evolution of Northwestern Mexico and the Southwestern USA. *Edited by* S.E. Johnson, S.R. Patterson, J.M. Fletcher, G.H. Girty, D.L. Kimbrough, and A. Martín-Barajas. Geological Society of America Special Paper 374. pp. 355–379. doi:10.1130/0-8137-2374-4.355.

Guerrero-Suasegui, M. 2004. Depositional and tectonic history of the Guerrero terrane, Sierra Madre del Sur; with emphasis on sedimentary successions of the Teloloapan area, southwestern Mexico. Unpublished Ph.D. thesis, Memorial University of Newfoundland. 332pp.

Hacker, B.R., Kelemen, P.B., and Behn, M.D. 2015. Continental lower crust. Annual Review of Earth and Planetary Science, **43**: 167–205. doi:10.1146/annurev-earth-050212-124117.

Hamilton, W.B. 1964. Geologic map of the Big Maria Mountains NE quadrangle, California. USGS Map GQ-350, scale 1:24,000.

Hamilton, W.B. 1969*a*. Mesozoic California and the underflow of Pacific mantle. Geological Society of America Bulletin, **80**: 2409–2430. doi:10.1130/0016-7606(1969)80[2409:MCATUO]2.0.CO;2.

Hamilton, W.B. 1969*b*. The volcanic central Andes, a modern model for the Cretaceous batholiths and tectonics of western North America. Oregon Department of Geology and Mineral Industries Bulletin, **65**: 175–184.

Hanan, B.B., Shervais, J.W., and Vetter, S.K. 2008. Yellowstone plume–continental lithosphere interaction beneath the Snake River Plain. Geology, **36**: 51–54. doi:10.1130/G23935A.1.

Hanson, R.B., Saleeby, J.B., and Fates, D.G. 1987. Age and tectonic setting of Mesozoic metavolcanic and metasedimentary rocks, northern White Mountains, California. Geology, **15**: 1074–1078. doi:10.1130/0091-7613(1987)15<1074:AATSOM>2.0.CO;2.

Hawkesworth, C.J., Dhuime, B., Pietranik, A.B., Cawood, P.A., Kemp, A.I.S., and Storey, C.D. 2010. The generation and evolution of the continental crust. Journal of the Geological Society of Society, **167**: 229–248. doi:10.1144/0016-76492009-072.

Hawkesworth, C.J., Cawood, P.A., and Dhuime, B. 2016. Tectonics and crustal evolution. GSA Today, **26**: 4–11. doi:10.1130/GSATG272A.1.

Haxel, G.B., and Miller, D.M. 2007. Mesozoic rocks. *In* Geology and mineral resources of the East Mojave National Scenic Area, San Bernardino County, California. *Edited by* T.G. Theodore. United States Geological Survey Bulletin, 2160: 59-66.

Herzig, C.T., and Kimbrough, D.L. 2014. Santiago Peak volcanics: Early Cretaceous arc volcanism of the western Peninsular Ranges batholith, southern California. *In* Peninsular Ranges Batholith, Baja California and southern California. *Edited by* D.M. Morton and F.K. Miller. Geological Society of America Memoir 211. pp. 345–363. doi:10.1130/2014.1211(09).

Hildebrand, R.S. 2009. Did westward subduction cause Cretaceous–Tertiary orogeny in the North American Cordillera? Geological Society of America Special Paper, **457**: 71. doi:10.1130/2009.2457.

Hildebrand, R.S. 2013. Mesozoic assembly of the North American Cordillera. Geological Society of America Special Paper, **495**: 169. doi:10.1130/2013.2495.

Hildebrand, R.S. 2014. Geology, mantle tomography, and inclination corrected paleogeographic trajectories support westward subduction during Cretaceous orogenesis in the North American Cordillera. Geoscience Canada, **41**: 207–224. doi:10.12789/geocanj.2014.41.032.

Hildebrand, R.S. 2015. Dismemberment and northward migration of the Cordilleran orogen: Baja-BC resolved. GSA Today, **25**(11): 4–11. doi:10.1130/GSATG255A.1.

Hildebrand, R.S., and Whalen, J.B. 2014*a*. Arc and slab-failure magmatism in Cordilleran batholiths I—The Cretaceous Coastal batholith of Peru and its role in South American orogenesis and hemispheric subduction flip. Geoscience Canada, **41**: 255–282. doi:10.12789/geocanj.2014.41.047.

Hildebrand, R.S., and Whalen, J.B. 2014*b*. Arc and slab-failure magmatism in Cordilleran batholiths II—The Cretaceous Peninsular Ranges batholith of Southern and Baja California. Geoscience Canada, **41**: 399–458. doi:10.12789/geocanj.2014.41.059.

Hildebrand, R.S., and Whalen, J.B. 2017. The tectonic setting and origin of Cretaceous batholiths within the North American Cordillera: the case for slab failure magmatism and its signifcance for crustal growth. Geological Society of America Special Paper, **532**: 113.

Hildebrand, R.S., and Whalen, J.B. 2020. Arc and slab-failure magmatism of the Taconic Orogeny, western New England, USA. *In* Pannotia to Pangaea: Neoproterozoic and Paleozoic orogenic cycles in the Circum-Atlantic Region Murphy. *Edited by* J.B. Strachan, R.A. Strachan, and C.A. Quesada Mateo. Geological Society of London Special Publication 503. doi:10.1144/SP503-2019-247.

Hildebrand, R.S., and Whalen, J.B. 2021. The mid-Cretaceous Peninsular Ranges orogeny: a new slant on Cordilleran tectonics? II: northern United States and Canada. Canadian Journal of Earth Sciences. [This issue.] doi:10.1139/cjes-2021-0006.

Hildebrand, R.S., Whalen, J.B., and Bowring, S.A. 2018. Resolving the crustal composition paradox by 3.8 billion years of slab failure magmatism and collisional recycling of continental crust. Tectonophysics, **734-735**: 69–88. doi:10.1016/j.tecto.2018.04.001.

Hill, R.I. 1984. Petrology and Petrogenesis of Batholithic Rocks, San Jacinto Mountains, Southern California: Unpublished Ph.D. thesis, California Institute of Technology, Pasadena, Calif. 660pp.

Hirt, W.H. 2007. Petrology of the Mount Whitney Intrusive Suite, eastern Sierra Nevada, California: Implications for the emplacement and differentiation of composite felsic intrusions. Geological Society of America Bulletin, **119**: 1185–1200. doi:10.1130/B26054.1.

Hoffman, P.F. 2012. The Tooth of Time: How do passive margins become active? Geoscience Canada, **39**: 67–73.

Huang, C.-Y., Yuan, P.B., and Tsao, S.-J. 2006. Temporal and spatial records of active arc-continent collision in Taiwan: A synthesis. Geological Society of America Bulletin, **118**: 274–288. doi:10.1130/B25527.1.

Huber, N.K., Bateman, P.C., and Wahrhaftig, C. 1989. Geologic map of Yosemite National Park and vicinity, California. U.S. Geological Survey Miscellaneous Investigations Series Map I-1874, scale 1:125,000.

Jacobson, C.E., Grove, M., Pedrick, J.N., Barth, A.P., Marsaglia, K.M., Gehrels, G.E., and Nourse, J.A. 2011. Late Cretaceous–early Cenozoic tectonic evolution of the southern California margin inferred from provenance of trench and forearc sediments. Geological Society of America Bulletin, **123**: 485–506. doi:10.1130/B30238.1.

Jacques-Ayala, C. 1992. Stratigraphy of the Lower Cretaceous Cintura Formation, Sierra El Chanate, northwestern Sonora, Mexico. Universidad Nacional Autónoma de México, Instituto de Geologia Revista, **10**: 129–136.

Jagoutz, O., and Behn, M.D. 2013. Foundering of lower island-arc crust as an explanation for the origin of the continental Moho. Nature, **504**: 131–134. doi:10.1038/nature12758. PMID:24305163.

Jean, M.M., Hanan, B.B., and Shervais, J.W. 2014. Yellowstone hotspot– continental lithosphere interaction. Earth and Planetary Science Letters, **389**: 119–131. doi:10.1016/j.epsl.2013.12.012.

Johnson, S.E., Tate, M.C., and Fanning, C.M. 1999. New geologic mapping and SHRIMP U–Pb zircon data in the Peninsular Ranges batholith, Baja California, Mexico: Evidence for a suture? Geology, **27**: 743–746. doi:10.1130/0091-7613(1999)027<0743:NGMASU>2.3.CO;2.

Johnson, S.E., Schmidt, K.L., and Tate, M.C. 2002. Ring complexes in the Peninsular Ranges Batholith, Mexico and the USA: magma plumbing systems in the middle and upper crust. Lithos, **61**: 187–208. doi:10.1016/S0024-4937(02)00079-8.

Johnson, S.E., Fletcher, J.M., Fanning, C.M., Paterson, S.R., Vernon, R.H., and Tate, M.C. 2003. Structure and emplacement of the San Jose tonalite pluton, Peninsular Ranges batholith, Baja California, Mexico. Journal of Structural Geology, **25**: 1933–1957. doi:10.1016/S0191-8141(03)00015-4.

Johnston, S.T. 2008. The Cordilleran ribbon continent of North America. Annual Review of Earth and Planetary Sciences, **36**: 495–530. doi:10.1146/annurev.earth.36.031207.124331.

Kanter, L.R., and McWilliams, M.O. 1982. Rotation of the southernmost Sierra Nevada, California. Journal of Geophysical Research, **87**: 3819–3830. doi:10.1029/JB087iB05p03819.

Keppie, J.D., Murphy, J.B., Nance, R.D., and Dostal, J. 2012. Mesoproterozoic Oaxaquia-type basement in peri-Gondwanan terranes of Mexico, the Appalachians and Europe: T_{DM} age constraints on extent and significance. International Geology Review, **54**: 313–324. doi:10.1080/00206814.2010.543783.

Kimbrough, D.L., Smith, D.P., Mahoney, J.B., Moore, T.E., Grove, M., Gastil, R.G., et al. 2001. Forearc-basin sedimentary response to rapid Late Cretaceous batholith emplacement in the Peninsular Ranges of southern and Baja California. Geology, **29**: 491–494. doi:10.1130/0091-7613(2001)029<0491:FBSRTR>2.0.CO;2.

Kimbrough, D.L., Abbott, P.L., Balch, D.C., Bartling, S.H., Grove, M., Mahoney, J.B., and Donohue, R.F. 2014. Upper Jurassic Peñasquitos Formation—Forearc basin western wall rock of the Peninsular Ranges batholith. *In* Peninsular Ranges Batholith, Baja California and southern California. *Edited by* D.M. Morton and F.K. Miller. Geological Society of America Memoir 211. pp. 625–643. doi:10.1130/2014.1211 (19).

Kistler, R.W. 1990. Two different lithosphere types in the Sierra Nevada, California. *In* The nature and origin of Cordilleran magmatism. *Edited by* J.L. Anderson. Geological Society of America Memoir 174. pp. 271–281. doi:10.1130/MEM174-p271.

Kistler, R.W. 1993. Mesozoic intrabatholithic faulting, Sierra Nevada, California. *In* Mesozoic paleogeography of the western United States—II. *Edited by* G. Dunne,and K. McDougall. Society of Economic Paleontologists and Mineralogists, Pacific Section Book 71. pp. 247–262.

Kistler, R.W., and Peterman, Z.E. 1978. Reconstruction of crustal rocks of California on the basis of initial strontium isotopic compositions of Mesozoic granitic rocks. United States Geological Survey Professional Paper 1071. 17pp.

Kistler, R.W., Chappell, B.W., Peck, D.L., and Bateman, P.C. 1986. Isotopic variation in the Tuolumne intrusive suite, central Sierra Nevada, California. Contributions to Mineralogy and Petrology, **94**: 205–220. doi:10.1007/BF00592937.

Klute, M.A. 1991. Sedimentology, sandstone petrofacies, and tectonic setting of the late Mesozoic Bisbee Basin, southeastern Arizona. Ph.D. thesis, University of Arizona, Tucson, Ariz. 268pp.

Krebs, C.K., and Ruiz, J. 1987. Geochemistry of the Canelo Hills volcanics and implications for the Jurassic tectonic setting of southeastern Arizona. *In* Mesozoic rocks of southern Arizona and adjacent areas. *Edited by* W.R. Dickinson and M.A. Klute. Arizona Geological Society Digest 18. pp. 139–151.

Krummenacher, D., Gastil, R.G., Bushee, J., and Doupont, J. 1975. K–Ar apparent ages, Peninsular Ranges batholith, southern California and Baja California. Geological Society of America Bulletin, **86**: 760–768. doi:10.1130/0016-7606(1975)86<760:KAAPRB>2.0.CO;2.

Lackey, J.S., Valley, J.W., Chen, J.H., and Stockli, D.F. 2008. Dynamic magma systems, crustal recycling, and alteration in the central Sierra Nevada batholith: The oxygen isotope record. Journal of Petrology, **49**: 1397–1426. doi:10.1093/petrology/egn030.

Lackey, J.S., Cecil, R., Windham, C.J., Frazer, R.E., Bindeman, I.N., and Gehrels, G.E. 2012*a*. The Fine Gold intrusive suite: The roles of basement terranes and magma source development in the Early Cretaceous Sierra Nevada batholith. Geosphere, **8**: 292–313. doi:10.1130/GES00745.1.

Lackey, J.S., Eisenberg, J.I., and Sendek, C.L. 2012*b*. Day 2: The Fine Gold intrusive suite—Records of the nascent Cretaceous arc. *In* Formation of the Sierra Nevada Batholith: magmatic and tectonic processes and their tempos. *Edited by* V. Memeti, S.R. Paterson, and K.D. Putirka. Geological Society of America Field Guide 34. pp. 2-1–2-23. [Now supplanted by GSA Field Guide 34.]

Lahren, M.M., and Schweickert, R.A. 1989. Proterozoic and Lower Cambrian passive margin rocks of Snow Lake pendant, Yosemite-Emigrant Wilderness, Sierra Nevada, California: Evidence for major Early Cretaceous dextral translation. Geology, **17**: 156–160. doi:10.1130/0091-7613(1989)017<0156:PALCMR>2.3.CO;2.

Lahren, M.M., Schweickert, R.A., Mattinson, J.M., and Walker, J.D. 1990. Evidence of uppermost Proterozoic to Lower Cambrian miogeoclinal rocks and the Mojave–Snow Lake fault: Snow Lake pendant, central Sierra Nevada, California. Tectonics, **9**: 1585–1608. doi:10.1029/TC009i006p01585.

Lallemand, S., Font, Y., Bijwaard, H., and Kao, H. 2001. New insights on 3-D plates interaction near Taiwan from tomography and tectonic implications. Tectonophysics, **335**: 229–253. doi:10.1016/S0040-1951(01)00071-3.

Lambert, R.S.J., and Chamberlain, V.E. 1988. Cordilleria revisited, with a three-dimensional model for Cretaceous tectonics in British Columbia. The Journal of Geology, **96**: 47–60. doi:10.1086/629192.

Langenheim, V.E., Jachens, R.C., and Aiken, C. 2014. Geophysical framework of the Peninsular Ranges batholith— Implications for tectonic evolution and neotectonics. *In* Peninsular Ranges Batholith, Baja California and Southern California. *Edited by* D.M. Morton and F.K. Miller. Geological Society of America Memoir 211. pp. 1–20. doi:10.1130/2014.1211(01).

Lapierre, H., Tardy, M., Coulon, C., Ortiz Hernandez, E., Bourdier, J.-L., Martínez Reyes, J., and Freydier, C. 1992. Caractérisation, genèse et évolution géodynamique du terrain de Guerrero (Mexique occidental). Canadian Journal of Earth Sciences, **29**(11): 2478–2489. doi:10.1139/e92-194.

Larsen, E.S., Jr. 1948. Batholith and associated rocks of Corona, Elsinore, and San Luis Rey quadrangles, southern California. Geological Society of America Memoir 29. **29**: 185. doi:10.1130/MEM29.

Lawton, T.F., and McMillan, N.J. 1999. Arc abandonment as a cause for passive continental rifting: Comparison of the Jurassic Mexican Borderland rift and the Cenozoic Rio Grande rift. Geology, **27**: 779–782 doi:10.1130/0091-7613(1999)027<0779:AAAACF>2.3.CO;2.

Lawton, T.F., Sprinkel, D.A., and Waanders, F.L. 2007. The Cretaceous Canyon Range Conglomerate, central Utah: Stratigraphy, structure and significance. *In* Central Utah – Diverse Geology of a Dynamic Landscape. *Edited by* G.C. Willis, M.D. Hylland, D.L. Clark, and T.C. Chidsey, Jr. Utah Geological Association Publication, **36**: 101–122.

Lawton, T.F., Hunt, G.J., and Gehrels, G.E. 2010. Detrital zircon record of thrust belt unroofing in Lower Cretaceous synorogenic conglomerates, central Utah. Geology, **38**: 463–466. doi:10.1130/G30684.1.

Lawton, T.F., Amato, J.M., Machin, S.E.K., Gilbert, J.C., and Lucas, S.G. 2020. Transition from Late Jurassic rifting to middle Cretaceous dynamic foreland, southwestern U.S. and northwestern Mexico. Geological Society of America Bulletin, **132**: 2489–2516. doi:10.1130/B35433.1.

Lee, C.-T.A., and Anderson, D.L. 2015. Continental crust formation at arcs, the arclogite "delamination" cycle, and one origin for fertile melting anomalies in the mantle. Science Bulletin, **60**: 1141–1156. doi:10.1007/s11434-015-0828-6.

Leopold, M.B. 2016. Structure, construction, and emplacement of the Late Cretaceous Sonora Pass intrusive suite: Central Sierra Nevada batholith, California. M.S. thesis, San José State University, San José, California. 100pp.

Lindgren, W. 1915. The igneous geology of the Cordilleras and its problems. *In* Problems of American geology. *Edited by* W.N. Rice, F.D. Adams, A.P. Coleman, and C.D. Walcott. Yale University Press, New Haven, Connecticut. pp. 234–286.

Long, S.P. 2015. An upper-crustal fold province in the hinterland of the Sevier orogenic belt, eastern Nevada, U.S.A.: A Cordilleran Valley and Ridge in the Basin and Range. Geosphere, **11**: 404–424. doi:10.1130/GES01102.1.

Longwell, C.R. 1926. Structural studies in southern Nevada and western Arizona. Geological Society of America Bulletin, **37**: 551–584. doi:10.1130/GSAB-37-551.

Mack, G.H. 1987. Mid-Cretaceous (late Albian) change from rift to retroarc foreland basin in southwestern New Mexico. Geological Society of America Bulletin, **98**: 507–514. doi:10.1130/0016-7606(1987)98<507:MLACFR>2.0.CO;2.

Mansfield, C.F. 1979. Upper Mesozoic subsea fan deposits in the southern Diablo Range, California: Record of the Sierra Nevada magmatic arc. Geological Society of America Bulletin, **90**: 1025–1046. doi:10.1130/0016-7606(1979)90<1025:UMSFDI>2.0.CO;2.

Martini, M., Fitz, E., Solari, L., Camprubi, A., Hudleston, P.J., Lawton, T.F., et al. 2012. The Late Cretaceous fold-thrust belt in the Peña de Bernal–Tamazunchale area and its possible relationship to the accretion of the Guerrero terrane. *In* The Southern Cordillera and Beyond. *Edited by* J.J. Aranda-Gómez, G.G. Tolson, and R.S. Molina-Garza. Geological Society of America Field Guide. Vol. 25. 19–38. doi:10.1130/2012.0025(02).

Martini, M., Solari, L., and Lopez-Martínez, M. 2014. Correlating the Arperos Basin from Guanajuato, central Mexico, to Santo Tomás, southern Mexico: implications for the paleogeography and origin of the Guerrero terrane. Geosphere, **10**: 1385–1401. doi:10.1130/GES01055.1.

Mattauer, M., Collot, B., and Van den Driessche, J. 1983. Alpine model for the internal metamorphic zones of the North American Cordillera. Geology, **11**: 11–15. doi:10.1130/0091-7613(1983)11<11:AMFTIM>2.0.CO;2.

Mauel, D.J., Lawton, T.F., González-Léon, C., Iriondo, A., and Amato, J.M. 2011. Stratigraphy and age of Upper Jurassic strata in north-central Sonora, Mexico: southwestern Laurentian record of crustal extension and tectonic transition. Geosphere, **7**: 390–414. doi:10.1130/GES00600.1.

McMahon, T.P. 2000. Magmatism in an arc-continent collision zone: an example from Irian Jaya (western New Guinea), Indonesia. Buletin Geologi, **32**: 1–22.

McMahon, T.P. 2001. Origin of a collision-related ultrapotassic to calc-alkaline magmatic suite: the latest Miocene Minjuah volcanic field, Irian Jaya, Indonesia. Buletin Geologi, **33**: 47–77.

Memeti, V. 2009. Growth of the Cretaceous Tuolumne Batholith and Synchronous Regional Tectonics, Sierra Nevada, CA: A Coupled System in a Continental Margin Arc Setting. Ph.D. thesis, University of Southern California, Los Angeles, California. 282 pp.

Memeti, V., Gehrels, G.E., Paterson, S.R., Thompson, J.M., Mueller, R.M., and Pignotta, G.S. 2010. Evaluating the Mojave–Snow Lake fault hypothesis and origins of central Sierran metasedimentary pendant strata using detrital zircon provenance analyses. Lithosphere, **2**: 341–360. doi:10.1130/L58.1.

Mendoza, O.T., and Suastegui, M.G. 2000. Geochemistry and isotopic composition of the Guerrero Terrane (western Mexico): implications for the tectonomagmatic evolution of southwestern North America during the Late Mesozoic. Journal of South American Earth Sciences, **13**: 297–324. doi:10.1016/S0895-9811(00)00026-2.

Miggins, D.P., Premo, W.R., Snee, L.W., Yeoman, R., Naeser, N.D., Naeser, C.W., and Morton, D.M. 2014. Thermochronology of Cretaceous batholithic rocks in the northern Peninsular Ranges batholith, southern California: Implications for the Late Cretaceous tectonic evolution of southern California. *In* Peninsular Ranges Batholith, Baja California and Southern California. *Edited by* D.M. Morton and F.K. Miller. Geological Society of America Memoir 211. pp. 199–261. doi:10.1130/2014.1211(06).

Miller, C.F., Wooden, J.L., Bennett, V.C., Wright, J.E., Solomon, G.C., and Hurst, R.W. 1990. Petrogenesis of the composite peraluminous-metaluminous Old Woman–Piute Range batholith, southeastern California: Isotopic constraints. *In* The nature and origin of Cordilleran Magmatism. *Edited by* J.L. Anderson. Geological Society of America Memoir 174. pp. 99–109.

Miller, D.M., Miller, R.J., Nielson, J.E., Wilshire, H.G., Howard, K.A., and Stone, P. 2007. Geologic map of the East Mojave National Scenic Area, California. *In* Geology and mineral resources of the East Mojave National Scenic Area, San Bernardino County, California. *Edited by* T.G. Theodore. United States Geological Survey Bulletin 2160. Scale 1:125,000.

Monger, J.W.H., Heyden, P.V.D., Journeay, J.M., Evenchick, C.A., and Mahoney, J.B. 1994. Jurassic-Cretaceous basins along the Canadian Coast Belt: Their bearing on pre-mid-Cretaceous sinistral displacements. Geology, **22**: 175–178. doi:10.1130/0091-7613(1994)022<0175:JCBATC>2.3.CO;2.

Monod, O., Faure, M., and Salinas, J.-C. 1994. Intra-arc opening and closure of a marginal sea: The case of the Guerrero terrane (SW Mexico). The Island Arc, **3**: 25–34. doi:10.1111/j.1440-1738.1994.tb00002.x.

Monod, O., Busnardo, R., and Guerrero-Suastegui, M. 2000. Late Albian ammonites from the carbonate cover of the Teloloapan arc volcanic rocks (Guerrero State, Mexico). Journal of South American Earth Sciences, **13**: 377–388. doi:10.1016/S0895-9811(00)00030-4.

Moore, J.G. 1959. The quartz boundary line in the western United States. The Journal of Geology, **67**: 198–210. doi:10.1086/626573.

Moore, J.G., Grantz, A., and Blake, M.C., Jr. 1961. The Quartz Diorite Boundary Line in northwestern North America. United States Geological Survey Professional Paper 424-C. pp. 87–90.

Moores, E.M. 1970. Ultramafics and orogeny, with models of the U.S. Cordillera and Tethys. Nature, **228**: 837–842. doi:10.1038/228837a0. PMID:16058720.

Moores, E.M., and Day, H.W. 1984. Overthrust model for Sierra Nevada. Geology, **12**: 416–419. doi:10.1130/0091-7613(1984)12<416:OMFTSN>2.0.CO;2.

Morris, R.A., DeBari, S.M., Busby, C., Medynski, S., and Jicha, B.R. 2019. Building arc crust: plutonic to volcanic connections in an extensional oceanic arc, the southern Alisitos arc, Baja California. Journal of Petrology, **60**: 1195–1228. doi:10.1093/petrology/egz029.

Morton, D.M., Miller, F.K., Kistler, R.W., Premo, W.R., Lee, C.-T.A., Langenheim, V.E., et al. 2014. Framework and petrogenesis of the northern Peninsular Ranges batholith, southern California. *In* Peninsular Ranges Batholith, Baja California and southern California. *Edited by* D.M. Morton and F.K. Miller. Geological Society of America Memoir 211. pp. 61–143. doi:10.1130/2014.1211(03).

Mueller, P.A., Wooden, J.L., Mogk, D.W., and Foster, D.A. 2011. Paleoproterozoic evolution of the Farmington zone: Implications for terrane accretion in southwestern Laurentia. Lithosphere, **3**: 401–408. doi:10.1130/L161.1.

Müller, R.D., Sdrolias, M., Gaina, C., and Roest, W.R. 2008. Age, spreading rates, and spreading asymmetry of the world's ocean crust. Geochemistry Geophysics Geosystems, **9**: Q04006. doi:10.1029/2007GC001743.

Murray, J.D. 1979. Outlines of the structure and emplacement history of a tonalite pluton in the Peninsular Ranges batholith, northern Baja California, Mexico. *In* Mesozoic crystalline rocks. *Edited by* P.L. Abbott and V.R. Todd. California State University, Department of Geological Sciences, San Diego, Calif. pp. 163–176.

Nelson, S., Harris, R., Dorais, M., Heizler, M., Constenius, K., and Barnett, D. 2002. Basement complexes in the Wasatch fault, Utah, provide new limits on crustal accretion. Geology, **30**: 831–834. doi:10.1130/0091-7613(2002)030<0831:BCITWF>2.0.CO;2.

Nokleberg, W.J. 1981. Stratigraphy and structure of the Strawberry Mine roof pendant, central Sierra Nevada, California. United States Geological Survey Professional Paper 1154. 18pp.

Nourse, J.A. 2002. Middle Miocene reconstruction of the central and eastern San Gabriel Mountains, southern California, with implications for the evolution of the San Gabriel fault and Los Angeles basin, *In* Contributions to crustal evolution of the southwestern United States. *Edited by* A. Barth. Geological Society of America Special Paper 365. pp. 161–185.

Ojakangas, R.W. 1968. Cretaceous sedimentation, Sacramento Valley, California. Geological Society of America Bulletin, **79**: 973–1008. doi:10.1130/0016-7606(1968)79[973:CSSVC]2.0.CO;2.

Orme, D.A., and Graham, S.A. 2018. Four-dimensional model of Cretaceous depositional geometry and sediment flux in the northern Great Valley forearc, California. *In* Tectonics, sedimentary basins, and provenance: a celebration of William R. Dickinson's career. *Edited by* R.V. Ingersoll, T.F. Lawton, and S.A. Graham. Geological Society of America Special Paper 540. pp. 409–424. doi:10.1130/2018.2540(18).

Ormerod, D.S., Rogers, N.W., and Hawkesworth, C.J. 1991. Melting in the lithospheric mantle: Inverse modelling of alkali-olivine basalts from the Big Pine volcanic field, California. Contributions to Mineralogy and Petrology, **108**: 305–317. doi:10.1007/BF00285939.

Ortega-Gutiérrez, F., Ruiz, J., and Centeno-García, E. 1995. Oaxaquia, a Proterozoic microcontinent accreted to North America during the late Paleozoic. Geology, **23**: 1127–1130. doi:10.1130/0091-7613(1995)023<1127:OAPMAT>2.3.CO;2.

Ortega-Rivera, A. 2003. Geochronological constraints on the tectonic history of the Peninsular Ranges Batholith of Alta and Baja California: Tectonic implications for western México, *In* Tectonic Evolution of Northwestern Mexico and the Southwestern USA. *Edited by* S.E. Johnson, S.R. Patterson, J.M. Fletcher, G.H. Girty, D.L. Kimbrough, and A. Martín-Barajas. Geological Society of America Special Paper 374. pp. 297–335. doi:10.1130/0-8137-2374-4.297.

Ortega-Rivera, A., Farrar, E., Hanes, J.A., Archibald, D.A., Gastil, R.G., Kimbrough, D.L., et al. 1997. Chronological constraints on the thermal and tilting history of the Sierra San Pedro Mártir pluton, Baja California, Mexico, from U-Pb, $^{40}Ar/^{39}Ar$ and fission-track geochronology. Geological Society of America Bulletin, **109**: 728–745. doi:10.1130/0016-7606(1997)109<0728:CCOTTA>2.3.CO;2.

Page, W.R., Lundstrom, S.C., Harris, A.G., Langenheim, V.E., Wotkman, J.B., Mahan, S.A., et al. 2005. Geologic and Geophysical Maps of the Las Vegas 30′ × 60′ Quadrangle, Clark and Nye Counties, Nevada, and Inyo County, California. U.S. Geological Survey Scientific Investigations Map 2814, scale 1:100,000.

Pape, D.E., Spell, T.L., Bonde, J.W., Fish, B., and Rowland, S.M. 2011. $^{40}Ar/^{39}Ar$ isotopic dates for the fossiliferous Willow Tank Formation (Cretaceous) in Valley of Fire State Park, Nevada. Geological Society of America Abstracts with Programs, 43(5): 586.

Paterson, S.R., Memeti, V., Anderson, L., Cao, W., Lackey, J.S., Putirka, K.D., et al. 2014. Day 6: Overview of arc processes and tempos. *In* Formation of the Sierra Nevada Batholith: magmatic and tectonic processes and their tempos. *Edited by* V. Memeti, S.R. Paterson, and K.D. Putirka. Geological Society of America Field Guide 34. pp. 87–116. doi:10.1130/2014.0034(06).

Pavlis, T.L., Amato, J.M., Trop, J.M., Ridgway, K.D., Roeske, S.M., and Gehrels, G.E. 2020*a*. Subduction polarity in ancient arcs: A call to integrate geology and geophysics to decipher the Mesozoic tectonic history of the northern Cordillera of North America: Reply. GSA Today, **29**: 4–10. doi:10.1130/GSATG465Y.1.

Pavlis, T.L., Amato, J.M., Trop, J.M., Ridgway, K.D., Roeske, S.M., and Gehrels, G.E. 2020*b*. Subduction polarity in ancient arcs: A call to integrate geology and geophysics to decipher the Mesozoic tectonic history of the northern Cordillera of North America: Reply. GSA Today, **30**: e51. doi:10.1130/GSATG465Y.1.

Pearce, J.A., Harris, N.B.W., and Tindle, A.G. 1984. Trace element discrimination diagrams for the tectonic interpretation of granitic rocks. Journal of Petrology, **25**: 956–983. doi:10.1093/petrology/25.4.956.

Peryam, T.C., Lawton, T.F., Amato, J.M., González-León, C.M., and Mauel, D.J. 2012. Lower Cretaceous strata of the Sonora Bisbee Basin: A record of the tectonomagmatic evolution of northwestern Mexico. Geological Society of America Bulletin, **124**: 532–548. doi:10.1130/B30456.1.

Phillips, J.R. 1993. Stratigraphy and structural setting of the mid-Cretaceous Olvidada Formation, Baja California Norte, Mexico. *In* Prebatholithic Stratigraphy of Peninsular California. *Edited by* R.G. Gastil and R.H. Miller. Geological Society of America Special Paper 279. pp. 97–106.

Pickett, D.A., and Saleeby, J.B. 1993. Thermobarometric constraints on the depth of exposure and conditions of plutonism and metamorphism at deep levels of the Sierra Nevada Batholith, Tehachapi Mountains, California. Journal of Geophysical Research: Solid Earth, **98**: 609–629. doi:10.1029/92JB01889.

Powell, R.E. 1993. Balanced palinspastic reconstruction of pre–late Cenozoic paleogeography, southern California: Geologic and kinematic constraints on evolution of the San Andreas fault system. *In* The San Andreas Fault System: displacement, palinspastic reconstruction, and geologic evolution. *Edited by* R.E. Powell, R.J.H. Weldon, and J.C. Matti. Geological Society of America Memoir 178. pp. 1–106. doi:10.1130/MEM178-p1.

Premo, W.R., and Morton, D.M. 2014. SHRIMP-RG U–Pb ages of provenance and metamorphism from detrital zircon populations and Pb–Sr–Nd signatures of prebatholithic metasedimentary rocks at Searl Ridge, northern Peninsular Ranges batholith, southern California: Implications for their age, origin, and tectonic setting. *In* Peninsular Ranges Batholith, Baja California and southern California. *Edited by* D.M. Morton and F.K. Miller. Geological Society of America Memoir 21. pp. 449–498. doi:10.1130/2014.1211(14).

Premo, W.R., Morton, D.M., Wooden, J.L., and Fanning, C.M. 2014. U–Pb zircon geochronology of plutonism in the northern Peninsular Ranges batholith, southern California. *In* Peninsular Ranges Batholith, Baja California and southern California. *Edited by* D.M. Morton and F.K. Miller. Geological Society of America Memoir 211. pp. 145–180. doi:10.1130/2014.1211(04).

Pubellier, M., Rangin, C., Rascon, B., Chorowicz, J., and Bellon, H. 1995. Cenomanian thrust tectonics in the Sahuaria region, Sonora: Implications about northwestern Mexico megashears. *In* Studies on the Mesozoic of Sonora and Adjacent Areas. *Edited by* C. Jacques-Ayala, C.M. González-León, and J. Roldán-Quintana. Geological Society of America Special Paper 301. pp. 111–120. doi:10.1130/0-8137- 2301-9.111.

Pujols, E.J., Stockli, D.F., Constenius, K.N., and Horton, B.K. 2020. Thermochronological and geochronological constraints on Late Cretaceous unroofing and proximal sedimentation in the Sevier orogenic belt, Utah. Tectonics, **39**: e2019TC005794. doi:10.1029/2019TC005794.

Putirka, K. 1999. Melting depths and mantle heterogeneity beneath Hawaii and the East Pacific Rise: constraints from Na/Ti and rare earth element ratios. Journal of Geophysical Research, **104**: 2817–2829. doi:10.1029/1998JB900048.

Quick, J.D., Hogan, J.P., Wizevich, M., Obrist-Farner, J., and Crowley, J.L. 2020. Timing of deformation along the Iron Springs thrust, southern Sevier fold-and-thrust belt, Utah: evidence for an extensive thrusting event in the mid-Cretaceous. Rocky Mountain Geology, **55**: 75–89. doi:10.24872/rmgjournal.55.2.75.

Reid, S.A. 1988. Late Cretaceous and Paleogene sedimentation along the east side of the San Joaquin basin. *In* Studies of the geology of the San Joaquin Basin. *Edited by* S.A Graham, Pacific Section S.E.P.M, 60: 157-171.

Ross, D.C. 1989. The Metamorphic and Plutonic Rocks of the Southernmost Sierra Nevada, California, and Their Tectonic Framework. United States Geological Survey Professional Paper 1381. 159pp.

Rudnick, R.L. 1995. Making continental crust. Nature, **378**: 571–578. doi:10.1038/378571a0.

Sacks, P.E., and Secor, D.T., Jr. 1990. Delamination in collisional orogens. Geology, **18**: 999–1002. doi:10.1130/0091-7613(1990)018<0999:DICO>2.3.CO;2.

Saleeby, J.B., Kistler, R.W., Longiaru, S., Moore, J.G., and Nokleberg, W.J. 1990. Middle Cretaceous silicic metavolcanic rocks in the Kings Canyon area, central Sierra Nevada, California. *In* The nature and origin of Cordilleran magmatism. *Edited by* J.L. Anderson. Geological Society of America Memoir 174. pp. 251–271. doi:10.1130/MEM174-p251.

Saleeby, J.B., Ducea, M.N., Busby, C.J., Nadin, E.S., and Wetmore, P.H. 2008. Chronology of pluton emplacement and regional deformation in the southern Sierra Nevada batholith, California. *In* Ophiolites, arcs, and batholiths: a tribute to Cliff Hopson. *Edited by* J.E. Wright and J.W. Shervais. Geological Society of America Special Paper 438. pp. 397–427. doi:10.1130/2008.2438(14).

Scherer, H.H., Ernst, W.G., and Hanson, R.B. 2008. Geologic implications of new zircon U-Pb ages from the White Mountain Peak Metavolcanic Complex, eastern California. Tectonics, **27**. doi:10.1029/2007TC002141.

Schmidt, K.L., and Paterson, S.R. 2002. A doubly vergent fan structure in the Peninsular Ranges batholith: transpression or local complex flow around a continental margin buttress? Tectonics, **21**: 14-1–14-19. doi:10.1029/2001TC001353.

Schmidt, K.L., Paterson, S.R., Blythe, A.E., and Kopf, C. 2009. Mountain building across a lithospheric boundary during arc construction: The Cretaceous Peninsular Ranges batholith in the Sierra San Pedro Mártir of Baja California, Mexico. Tectonophysics, **477**: 292–310. doi:10.1016/j.tecto.2009.04.020.

Schmidt, K.L., Wetmore, P.H., Alsleben, H., and Paterson, S.R. 2014. Mesozoic tectonic evolution of the southern Peninsular Ranges batholith, Baja California, Mexico: Long-lived history of a collisional segment in the Mesozoic Cordilleran arc. *In* Peninsular Ranges Batholith, Baja California and southern California. *Edited by* D.M. Morton, and F.K. Miller. Geological Society of America Memoir 211. pp. 645–668. doi:10.1130/2014.1211.

Shaw, S.E., Todd, V.R., and Grove, M. 2003. Jurassic peraluminous gneissic granites in the axial zone of the Peninsular Ranges, southern California. *In* Tectonic Evolution of Northwestern Mexico and the Southwestern USA. *Edited by* S.E. Johnson, S.R. Patterson, J.M. Fletcher, G.H. Girty, D.L. Kimbrough, and A. Martín-Barajas. Geological Society of America Special Paper 374. pp. 157–183. doi:10.1130/0-8137-2374-4.157.

Shaw, S.E., Todd, V.R., Kimbrough, D.L., and Pearson, N.J. 2014. A west-to-east geologic transect across the Peninsular Ranges batholith, San Diego County, California: Zircon $^{176}Hf/^{177}Hf$ evidence for the mixing of crustal- and mantle-derived magmas, and comparisons with the Sierra Nevada batholith. *In* Peninsular Ranges Batholith, Baja California and Southern California. *Edited by* D.M. Morton and F.K. Miller. Geological Society of America Memoir 211. pp. 499–536. doi:10.1130/2014.1211(15).

Sigloch, K., and Mihalynuk, M.G. 2020. Comment on GSA Today article by Pavlis et al., 2019: "Subduction Polarity in Ancient Arcs: A Call to Integrate Geology and Geophysics to Decipher the Mesozoic Tectonic History of the Northern Cordillera of North America". GSA Today, **30**: e47. doi:10.1130/GSATG431C.1.

Silver, L.T., and Chappell, B. 1988. The Peninsular Ranges batholith: An insight into the Cordilleran batholiths of southwestern North America. Earth and Environmental Science Transactions of the Royal Society of Edinburgh, **79**: 105–121. doi:10.1017/S0263593300014152.

Silver, L.T., Taylor, H.P., Jr., and Chappell, B. 1979. Some petrological, geochemical and geochronological observations of the Peninsular Ranges batholith near the international border of the U.S.A. and Mexico. *In* Mesozoic Crystalline Rocks. *Edited by* P.L. Abbott, and V.R. Todd, California State University, Department of Geological Sciences, San Diego, Calif. pp. 83–110.

Sisson, T.W., and Moore, J.G. 2013. Geologic map of the southwestern Sequoia National Park. United States Geological Survey, Open-File Report 2013-1096, scale 1:24,000.

Sisson, T.W., Grove, T.L., and Coleman, D.S. 1996. Hornblende gabbro sill complex at Onion Valley, California, and a mixing origin for the Sierra Nevada batholith. Contributions to Mineralogy and Petrology, **126**: 81–108. doi:10.1007/s004100050237.

Skipp, B. 1987. Basement thrust sheets in the Clearwater orogenic zone, central Idaho and western Montana. Geology, **15**: 220–224. doi:10.1130/0091-7613(1987)15<220:BTSITC>2.0.CO;2.

Skipp, B., and Hait, M.H., Jr. 1977. Allochthons along the northeast margin of the Snake River plain, Idaho, *In* Rocky Mountain Thrust Belt Geology and Resources. *Edited by* E.L. Heisey, and D.E. Lawson, D.E. Wyoming Geological Association, Annual Field Conference, 29: 499–516.

Snow, C.A., and Ernst, W.G. 2008. Detrital zircon constraints on sediment distribution and provenance of the Mariposa Formation, central Sierra Nevada Foothills, California. *In* Ophiolites, arcs, and batholiths: a tribute to Cliff Hopson. *Edited by* J.E. Wright and J.W. Shervais. Geological Society of America Special Paper 438. pp. 311–330. doi:10.1130/2008.2438(11).

Speed, R.C., Elison, M.W., and Heck, R.R. 1988. Phanerozoic tectonic evolution of the Great Basin. *In* Metamorphism and crustal evolution of the western United States, Rubey Volume 7. *Edited by* W.G. Ernst. Prentice Hall, Englewood Cliffs, N.J. pp. 572–605.

Stewart, J.H. 2005. Evidence for Mojave-Sonora megashear — Systematic left-lateral offset of Neoproterozoic to Lower Jurassic strata and facies, western United States and northwestern Mexico. *In* The Mojave-Sonora Megashear Hypothesis: Development, Assessment, and Alternatives. *Edited by* T.H. Anderson, J.A. Nourse, J.W. McKee, and M.B. Steiner. Geological Society of America Special Paper, **393**: 209–231. doi:10.1130/0-8137-2393-0.209.

Stone, P. 2006. Geologic map of the west half of the Blyth 30' by 60' quadrangle, Riverside County, California and La Paz County, Arizona. United States Geological Survey Scientific Investigation Map 2922, scale 1:100,000.

Stone, P., and Kelly, M.M. 1989. Geologic map of the Palen Pass quadrangle, Riverside County, California. United States Geological Survey Miscellaneous Field Studies Map MF-2020, scale 1:24,000.

Streckeisen, A.L., and LeMaitre, R.W. 1979. Chemical approximation to modal QAPF classification of the igneous rocks. Neus Jahrbuch fur Mineralogie, **136**: 169–206.

Suppe, J. 1987. The active Taiwan mountain belt In Anatomy of Mountain Ranges. *Edited by* J.P. Schaer and J. Rodgers. Princeton University Press, Princeton, New Jersey. pp. 277–293.

Surpless, K.D., Graham, S.A., Covault, J.A., and Wooden, J.L. 2006. Does the Great Valley sequence contain Jurassic strata?: Reevaluation of the age and early evolution of a classic forearc basin. Geology, **34**: 21–24. doi:10.1130/G21940.1.

Talavera-Mendoza, O., Ruiz, J., Gehrels, G.E., Valencia, V.A., and Centeno-García, E. 2007. Detrital zircon U/Pb geochronology of southern Guerrero and western Mixteca arc successions (southern Mexico): new insights for the tectonic evolution of southwestern North America during the late Mesozoic. Geological Society of America Bulletin, **119**: 1052–1065. doi:10.1130/B26016.1.

Tardy, M., Lapierre, H., Freydier, C., Coulon, C., Gill, J.-B., Mercier de Lep- Inay, B., et al. 1994. The Guerrero suspect terrane (western Mexico) and coeval arc terranes (the Greater Antilles and the Western Cordillera of Colombia): A late Mesozoic intra-oceanic arc accreted to cratonal America during the Cretaceous. Tectonophysics, **230**: 49–73. doi:10.1016/0040-1951(94)90146-5.

Taylor, H.P., and Silver, L.T. 1978. Oxygen isotope relationships in plutonic igneous rocks of the Peninsular Ranges batholith, Southern and Baja California. *In* Short Papers of the Fourth International Conference on Geochronology, Cosmochronology, Isotope Geology, 1978. *Edited by* R.E. Zartman. United States Geological Survey Open-File Report 78-701. pp. 423–426.

Taylor, W.J., Bartley, J.M., Martin, M.W., Geissman, J.W., Walker, J.D., Armstrong, P.A., and Fryxell, J.E. 2000. Relations between hinterland and foreland shortening: Sevier orogeny, central North American Cordillera. Tectonics, **19**: 1124–1143. doi:10.1029/1999TC001141.

Teng, L.S. 1996. Extensional collapse of the northern Taiwan mountain belt. Geology, **24**: 949–952. doi:10.1130/0091-7613(1996)024<0949:ECOTNT>2.3.CO;2.

Todd, V.R. 2004. Preliminary geologic map of the El Cajon 30′ x 60′ quadrangle, southern California. United States Geological Survey Open-File Report 2004-1361.

Todd, V.R., and Shaw, S.E. 1979. Structural, metamorphic, and intrusive framework of the Peninsular Ranges batholith in southern San Diego County, California. *In* Mesozoic crystalline rocks. *Edited by* P.L. Abbott and V.R. Todd. California State University, Department of Geological Sciences, San Diego, Calif. pp. 177–231.

Todd, V.R., Erskine, B.G., and Morton, D.M. 1988. Metamorphic and tectonic evolution of the northern Peninsular Ranges batholith, southern California. *In* Metamorphism and Crustal Evolution of the Western United States, Rubey Volume VII. *Edited by* W.G. Ernst, W.G. Prentice Hall, Englewood Cliffs, New Jersey. pp. 894–937.

Todd, V.R., Shaw, S.E., and Hammarstrom, J.M. 2003. Cretaceous plutons of the Peninsular Ranges batholith, San Diego and westernmost Imperial Counties, California: Intrusion across a Late Jurassic continental margin. *In* Tectonic evolution of northwestern Mexico and the southwestern USA. *Edited by* S.E. Johnson, S.R. Patterson, J.M. Fletcher, G.H. Girty, D.L. Kimbrough, and A. Martín-Barajas. Geological Society of America Special Paper 374. pp. 185–235. doi:10.1130/0-8137-2374-4.185.

Troyer, R., Barth, A.P., Wooden, J.L., and Jacobson, C. 2006. Provenance and timing of Sevier foreland basin sediments in the Valley of Fire, southern Nevada, from U-Pb geochronology. Geological Society of America Abstracts with Programs, **38**(7): 369.

Tulloch, A.J., and Kimbrough, D.L. 2003. Paired plutonic belts in convergent margins and the development of high Sr/Y magmatism: Peninsular Ranges batholith of Baja-California and Median batholith of New Zealand. *In* Tectonic evolution of northwestern Mexico and the southwestern USA. *Edited by* S.E. Johnson, S.R. Patterson, J.M. Fletcher, G.H. Girty, D.L. Kimbrough, and A. Martín-Barajas. Geological Society of America Special Paper 374. pp. 275–295. doi:10.1130/0-8137-2374-4.275.

Van Buer, N.J., and Miller, E.L. 2010. Sahwave batholith, NW Nevada: Cretaceous arc flare-up in a basinal terrane. Lithosphere, **2**: 423–446. doi:10.1130/L105.1.

Viallon, C., Huchon, P., and Barrier, E. 1986. Opening of the Okinawa basin and collision in Taiwan: A retreating trench model with lateral anchoring. Earth and Planetary Science Letters, **80**: 145–155. doi:10.1016/0012-821X(86)90028-2.

Wahrhaftig, C. 2000. Geologic map of the Tower Peak Quadrangle, central Sierra Nevada, California. United States Geological Survey, Geologic Investigations Series Map I-2697, scale 1:62,500.

Walawender, M.J., Gastil, R.G., Clinkenbeard, J.P., McCormick, W.V., Eastman, B.G., Wernicke, R.S., et al. 1990. Origin and evolution of the zoned La Posta–type plutons, eastern Peninsular Ranges batholith, southern and Baja California. *In* The Nature and Origin of Cordilleran Magmatism. *Edited by* J.L. Anderson. Geological Society of America Memoir 174. pp. 1–18. doi:10.1130/MEM174-p1.

Walker, J.D., Burchfiel, B.C., and Davis, G.A. 1995. New age controls on initiation and timing of foreland belt thrusting in the Clark Mountains, southern California. Geological Society of America Bulletin, **107**: 742–750. doi:10.1130/0016-7606(1995)107<0742:NACOIA>2.3.CO;2.

Wells, M.L. 2016. A major mid-Cretaceous shortening event in the southern Sevier orogenic belt: Continental record of global plate reorganization. Geological Society of America Abstracts with Programs, **48**(7). doi:10.1130/abs/2016AM-287809.

Wetmore, P.H., and Ducea, M.N. 2011. Geochemical evidence of a near-surface history for source rocks of the central Coast Mountains Batholith, British Columbia. International Geology Review, **51**: 1–26. doi:10.1080/00206810903028219.

Wetmore, P.H., Alsleben, H., Paterson, S.R., Ducea, M.N., Gehrels, G.E., and Valencia, V.A. 2005. Field Trip to the Northern Alisitos Arc Segment: Ancestral Agua Blanca Fault Region. *In* Field Conference Guidebook for the VII International Meeting of the Peninsular Geological Society. Peninsular Geological Society, Ensenada, Baja California, Mexico. 39pp.

Whalen, J.B., and Frost, C.D. 2013. The Q-ANOR diagram: A tool for the petrogenetic and tectonomagmatic characterization of granitic suites. Geological Society of America Abstracts with Programs, **45**(3): 24.

Whalen, J.B., and Hildebrand, R.S. 2019. Trace element discrimination of arc, slab failure, and A-type granitic rocks. Lithos, **348-349**: 105179. doi:10.1016/j.lithos.105179.

White, J.D.L., and Busby-Spera, C.J. 1987. Deep marine arc apron deposits and syndepositional magmatism in the Alisitos Group at Punta Cono, Baja California, Mexico. Sedimentology, **34**: 911–927. doi:10.1111/j.1365-3091.1987.tb00812.x.

Wood, D.J. 1997. Geology of the eastern Tehachapi Mountains and Late Cretaceous–Early Cenozoic tectonics of the southern Sierra Nevada region, Kern County, California. Ph.D. thesis, California Institute of Technology, Pasadena, Calif. 287pp.

Wood, D.J., and Saleeby, J.B. 1998. Late Cretaceous–Paleocene extensional collapse and disaggregation of the southernmost Sierra Nevada batholith. *In* Integrated Earth and Environmental Evolution of the Southwestern United States: The Clarence A. Hall Jr. Volume. *Edited by* W.G. Ernst and C.A. Nelson. Columbia, Maryland, Bellwether Publishing for the Geological Society of America. pp. 289–325.

Wright, J.E., and Wyld, S.J. 2007. Alternative tectonic model for Late Jurassic through Early Cretaceous evolution of the Great Valley Group, California. *In* Convergent margin terranes and associated regions: a tribute to W.G. Ernst. *Edited by* M. Cloos, W.D. Carlson, Gilbert, J.G. Liou, and S.S. Sorensen. Geological Society of America Special Paper 419. pp. 81–95. doi:10.1130/2007.2419(04).

Yonkee, W.A., Parry, W.T., and Bruhn, R.L. 2003. Relations between progressive deformation and fluid-rock interaction during shear zone growth in a basement-cored thrust sheet, Sevier orogenic belt, Utah. American Journal of Science, **303**: 1–59. doi:10.2475/ajs.303.1.1.

Yonkee, W.A., Eleogram, B., Wells, M.L., Stockli, D.F., Kelley, S., and Barber, D.E. 2019. Fault slip and exhumation history of the Willard thrust sheet, Sevier fold-thrust belt, Utah: relations to wedge propagation, hinterland uplift, and foreland basin sedimentation. Tectonics, **38**: 2850–2893. doi:10.1029/2018TC005444.

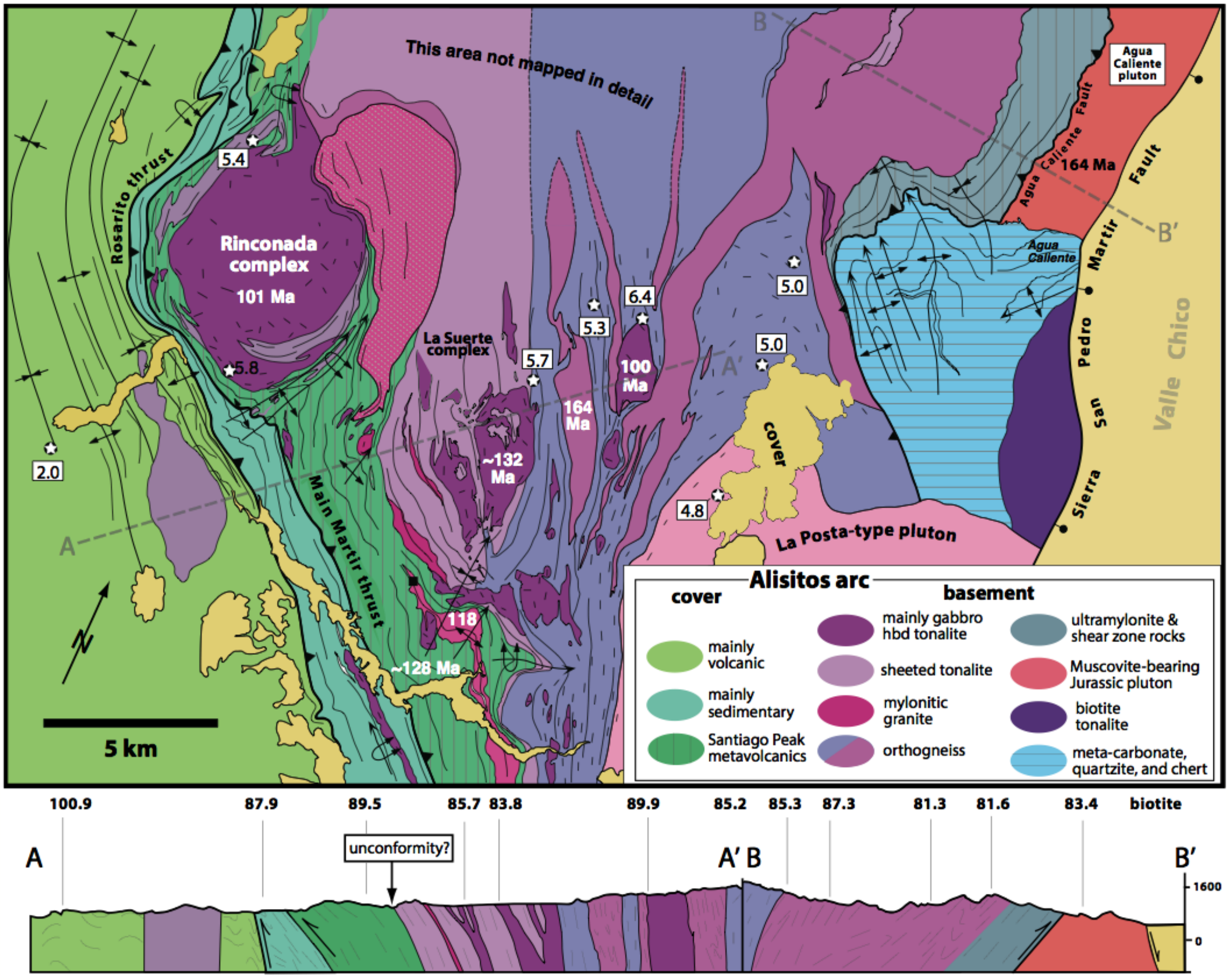

Supplemental Figure 1. Geological sketch map and section from Schmidt and Paterson (2002); Schmidt et al. (2014) showing the location and reverse faults along the western margin of the orogenic hinterland in Baja California. Numbers in boxes are paleopressures in Kbar. Note the jump in metamorphic grade across the Rosarito and Main Martir thrusts.

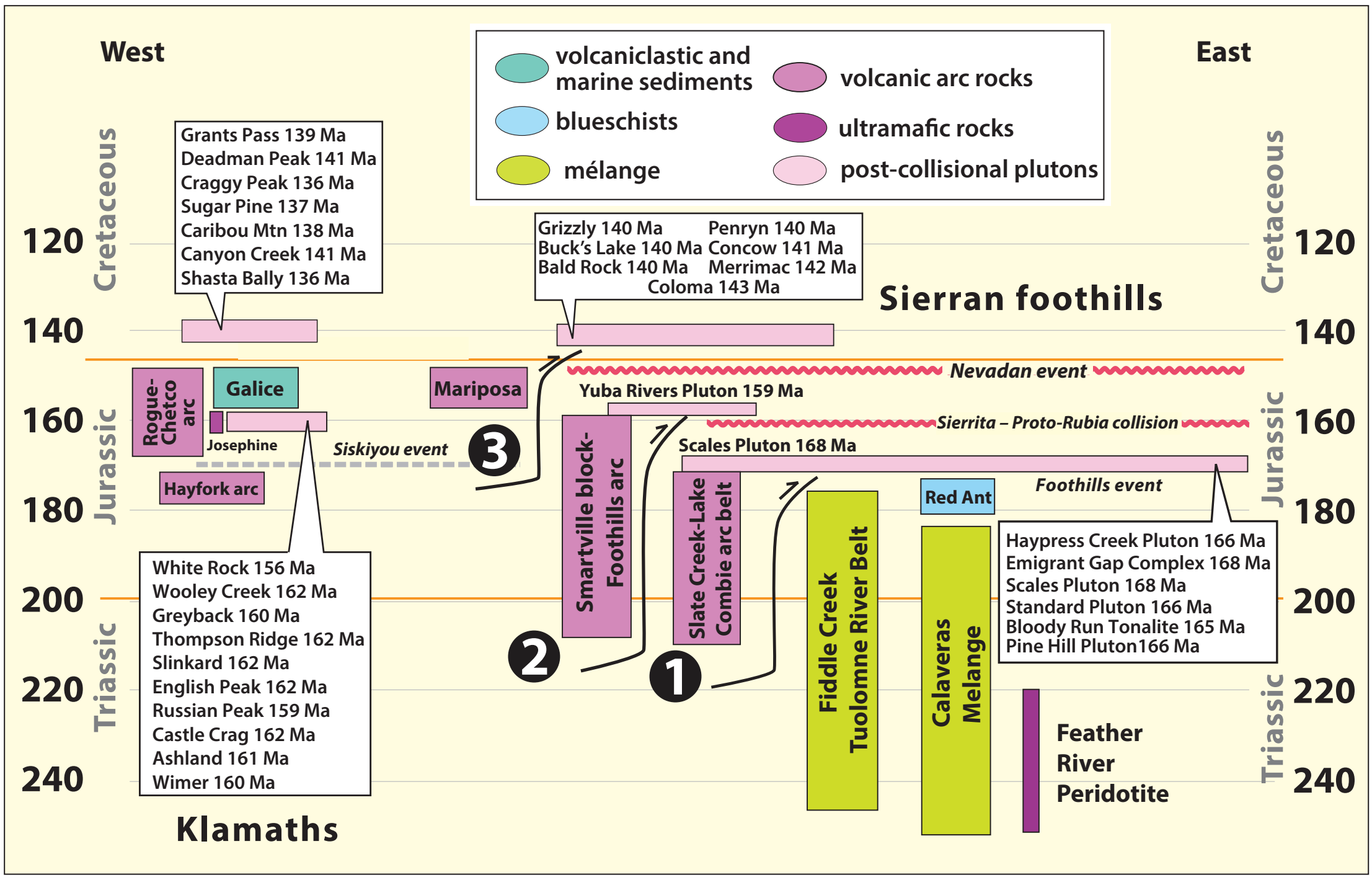

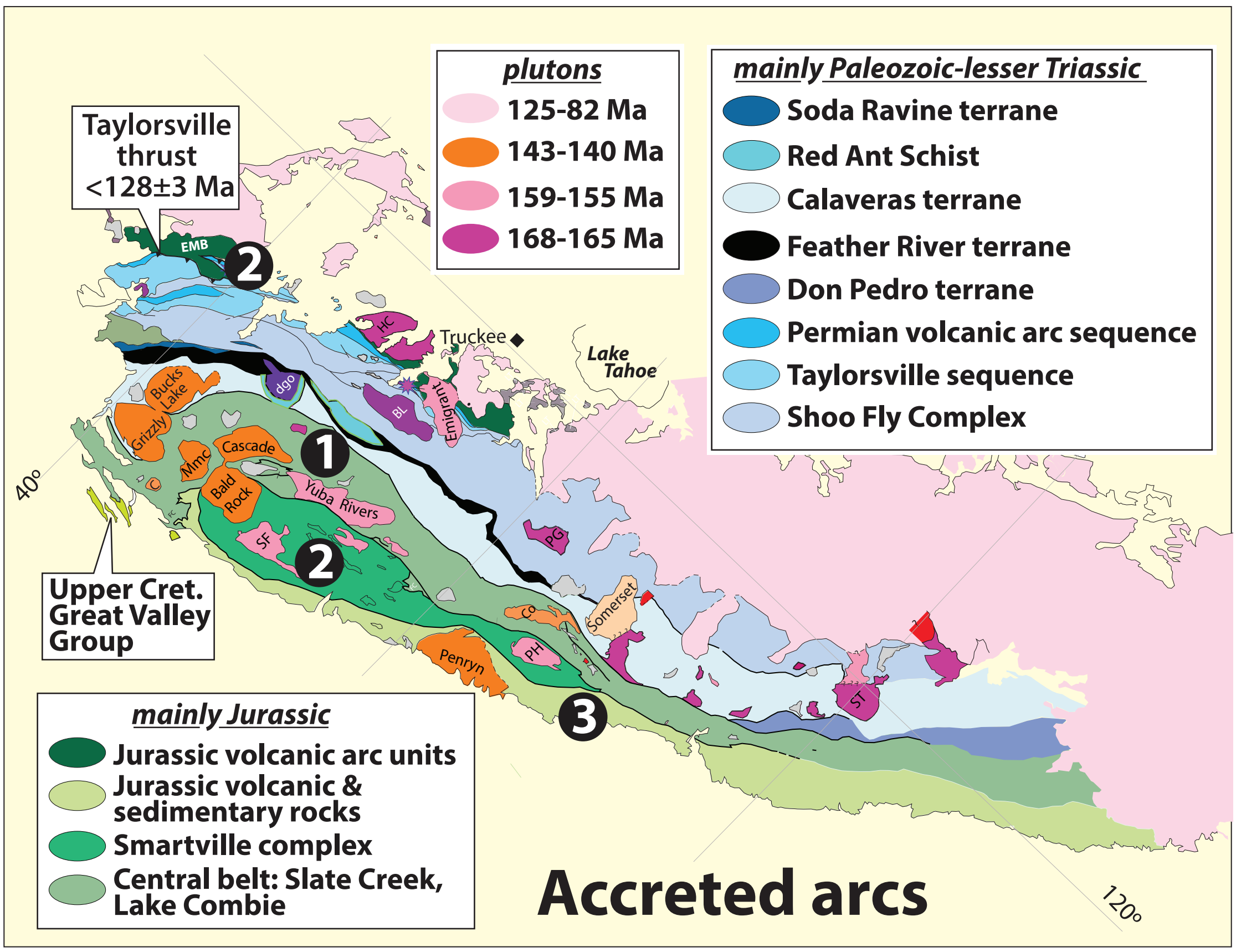

Supplemental Figure 2. Geological sketch map and time line for Jurassic and lowermost Cretaceous of the Sierra Nevada and Klamaths, illustrating the accretion of three arc suites from the west, each followed by the emplacement of postcollisional plutonic suites. The Jurassic suites are described in Hildebrand (2013). Figure concept is from Dickinson (2008). CRO—Coast Range ophiolite.

Supplemental Figure 3. Geologic sketch map of a section of the Sierra Nevada batholith compiled from from USGS quadrangle maps, showing ages of pre- and post-100 Ma plutons, with ages from papers by Coleman and Glazner (1988), Chen & Moore (1982), southern Sierran ages from Saleeby et al. (2008). Ages from Mineral King area (Sisson and Moore, (2013). For sources of Tuolumne and surrounding rocks see Hildebrand and Whalen (2018, Figure 17); Bass Lake tonalite from Lackey et al. (2012); Academy pluton from Mack et al. (1979); Mount Givens granodiorite from Frazer et al. (2014); Stokes Mountain complex from Clemens-Knott (1992); Sonora Pass intrusive suite (Leopold, 2016); San Emigdio Mountains from Chapman and Saleeby (2012). BCP—Boyden Cave pendant; MKP—Mineral King pendant; OCP—Oak Creek pendant, CLP—Cinco Lake pendant; RRP—Rugged Rock pendant. Although the Tuolumne and Mount Whitney suites are commonly mentioned in the literature, there remain many other post 100 Ma plutons that remain unstudied and generally unknown. Please note that this is a working sketch map, and is included as a helpful, not definitive. document

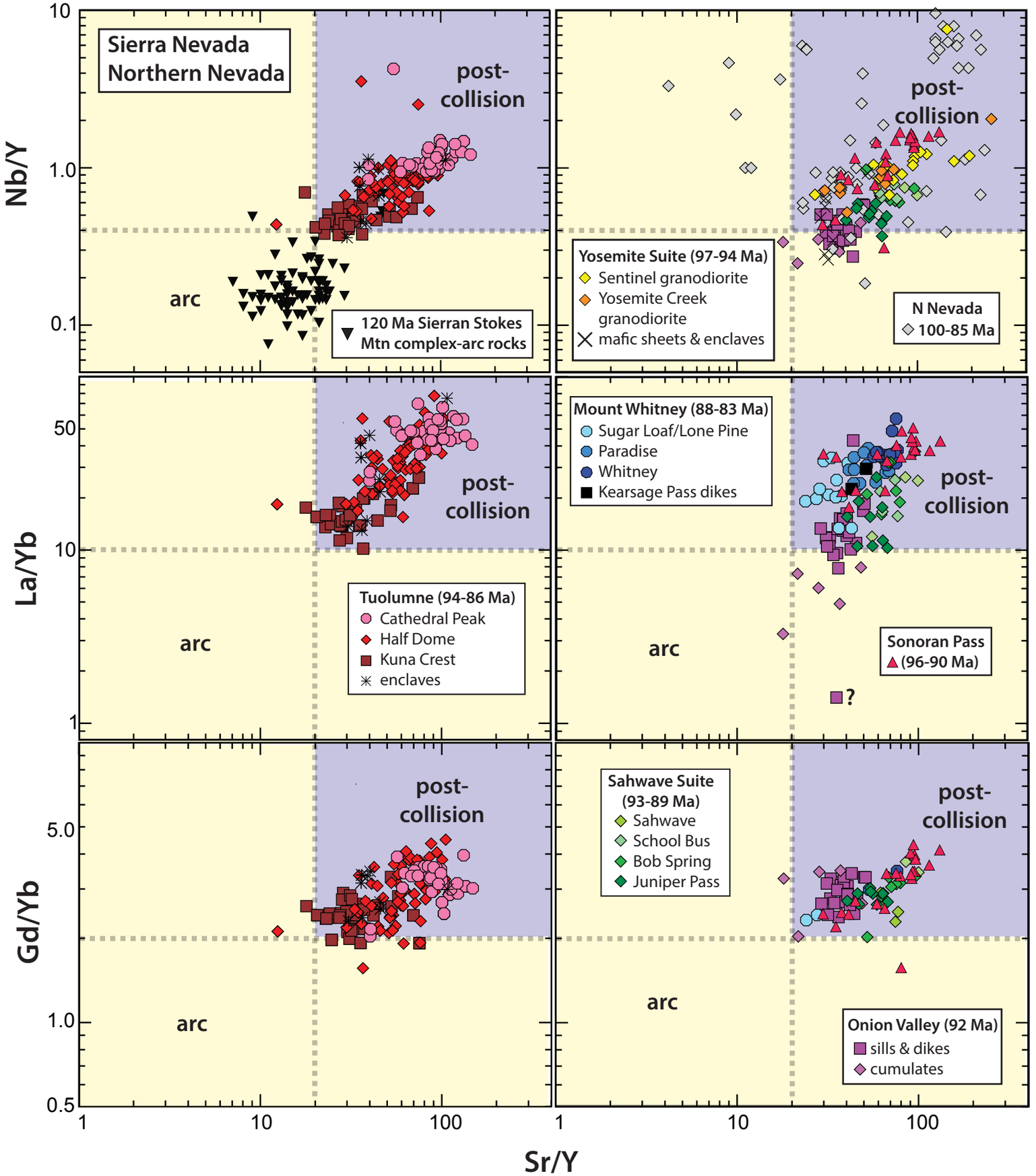

Supplemental Figure 4. Nb/Y, La/Yb, and Gd/Yb vs. Sr/Y discrimination diagrams for various Sierra Nevada and Nevadan plutonic suites, including pre-collisional 120 Ma Sierran Stokes Mountain complex arc rocks (Clemens-Knott, 1992), 100–84 Ma postcollisional Tuolumne intrusive suite (Memeti, 2009), Mount Whitney (Hirt, 2007), Sahwave intrusive suite of NW Nevada (Van Buer and Miller, 2010), Sonoran Pass intrusive suite (Alasino. 2019), and Onion Valley hornblende gabbro (Sisson et al., 1996) plus northern Nevada plutonic rocks (du Bray, 2007), illustrating that the pre–100 Ma arc rocks of the Stokes Mountain complex and the remaining plutonic units (100–80 Ma) are consistent with those of the Peninsular Ranges.

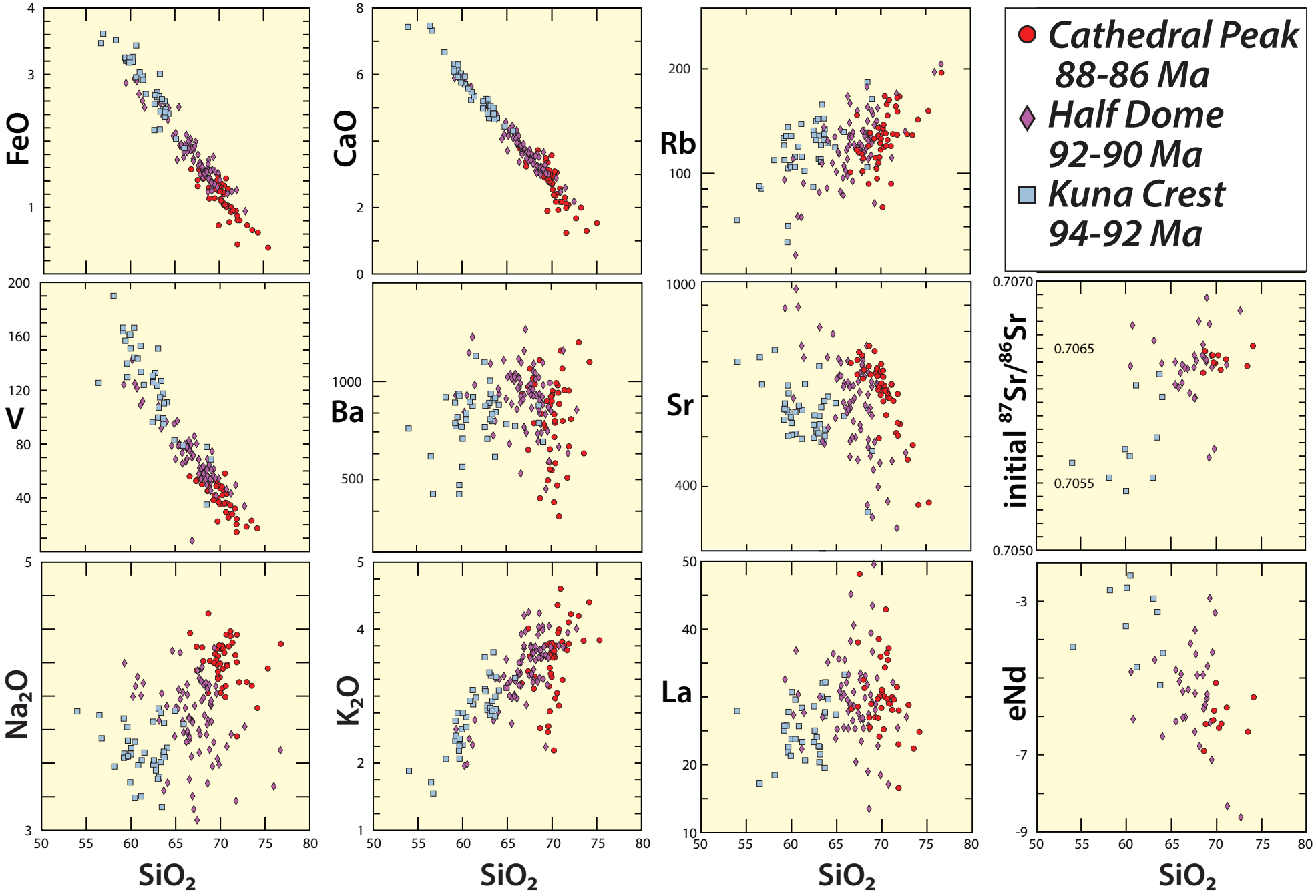

Supplemental Figure 5. Examples of major and trace elements plotted on Harker variation diagrams (majors in wt% oxide; traces in ppm) for Kuna Crest, Half Dome, and Cathedral Peak phases of the 94–84 Ma post- collisional Tuolumne intrusive suite of the Sierra Nevada batholith. Note that major and compatible trace elements form linear trends but that Na_2O, as well as incompatible trace elements (LIL) and light rare earth elements (LREE), are widely scattered and decoupled from the bulk of major and compatible trace elements, as are Nd and Sr isotopes. Data are from Memeti (2009).

The mid-Cretaceous Peninsular Ranges orogeny: a new slant on Cordilleran tectonics? I: Mexico to Nevada

HILDEBRAND, Robert S.,* 1401 N. Camino de Juan, Tucson, AZ 85745 USA
WHALEN, Joseph B., Geological Survey of Canada, 601 Booth Street, Ottawa, ON K1A 0E8, Canada

Supplemental File 1

Schmidt, K.L., and Paterson, S.R. 2002. A doubly vergent fan structure in the Peninsular Ranges batholith: Transpression or local complex flow around a continental margin buttress? Tectonics, **21**: 1050, http://dx.doi.org/ 10.1029/2001TC001353.

Schmidt, K.L., Wetmore, P.H., Alsleben, H., and Paterson, S.R. 2014. Mesozoic tectonic evolution of the southern Peninsular Ranges batholith, Baja California, Mexico: Long-lived history of a collisional segment in the Mesozoic Cordilleran arc. *In* Peninsular Ranges Batholith, Baja California and Southern California. *Edited by* D.M. Morton, and F.K. Miller, Geological Society of America Memoir **211**, 645–668, doi.org/10.1130/2014.1211.

Supplemental File 2

Dickinson, W.R. 2008. Accretionary Mesozoic–Cenozoic expansion of the Cordilleran continental margin in California and Oregon. Geosphere, **4**: 329–353. doi:10.1130/GES00105.1.

Hildebrand, R.S. 2013. Mesozoic Assembly of the North American Cordillera: Geological Society of America Special Paper **495**, 169 p.. doi:10.1130/2013.2495.

Supplemental File 3

Armin, R.A., John, D.A. 1983. Geologic map of the Freel Peak 15-minute Quadrangle, California and Nevada, U.S. Geological Survey Miscellaneous Investigations Series Map I-1424.

Armin, R.A., John, D.A., Moore, W.J. 1984. Geologic map of the Markleeville 15-minute Quadrangle, Alpine County, California. U.S. Geological Survey Geologic Quadrangle Map I-1474.

Bateman, P.C, Lockwood, J.P., Lydon, P.A. 1971. Geologic map of the Kaiser Peak Quadrangle, central Sierra Nevada, California. U.S. Geological Survey Geologic Quadrangle Map GQ-0894.

Bateman, P.C, Wones, D.R. 1972. Geologic map of the Huntington Lake Quadrangle, central Sierra Nevada, California. U.S. Geological Survey Geologic Quadrangle Map GQ-0987.

Bateman, P.C. 1965. Geologic map of the Blackcap Mountain Quadrangle, Fresno County, California. U.S. Geological Survey Geologic Quadrangle Map GQ-0428.

Bateman, P.C. 1989. Geologic map of the Bass Lake Quadrangle, west-central Sierra Nevada, California, U.S. Geological Survey Geologic Quadrangle Map, GQ-1656.

Bateman, P.C., Busacca, A. J. 1982. Geologic map of the Millerton Lake Quadrangle, west-central Sierra Nevada, California. U.S. Geological Survey Geologic Quadrangle Map GQ-1548.

Bateman, P.C., Busacca, A.J., Marchand, D.E., Sawka, W.N. 1982. Geologic map of the Raymond Quadrangle, Madera and Mariposa counties, California.U.S. Geological Survey Geologic Quadrangle Map GQ-1555.

Bateman, P.C., Kistler, R.W., Peck, D.L., Busacca, A.J. 1983. Geologic map of the Tuolumne Meadows Quadrangle, Yosemite National Park, California. U.S. Geological Survey Geologic Quadrangle Map GQ-1570.

Bateman, P.C., Krauskopf, K.B. 1987. Geologic map of the El Portal Quadrangle, west-central Sierra Nevada, California, U.S. Geological Survey Miscellaneous Field Studies Map MF-1998.

Bateman, P.C., Moore, J.G. 1965. Geologic map of the Mount Goddard Quadrangle, Fresno and Inyo counties, California. U.S. Geological Survey Geologic Quadrangle Map GQ-0429.

Carr, M.D., Christiansen, R.L., Poole, F.G., and Goodge, J.W. 1997. Bedrock geologic map of the El Paso Mountains in the Garlock and El Paso Peaks 7-1/2' quadrangles, Kern County, California. United States Geological Survey Miscellaneous Investigations Series Map I-2389, scale 1:24,000.

Chapman, A.D., and Saleeby, J. 2012. Geologic map of the San Emigdio Mountains, southern California. Geological Society of America Map and Chart **101**, doi: 10.1130/2012.MCH101.

Chen, J.H., and Moore, J.G. 1982. Uranium-lead ages from the Sierra Nevada batholith, California. Journal of Geophysical Research, **87**: 4761– 4784, doi:10.1029/JB087iB06p04761.

Clemens-Knott, D. 1992. Geologic and Isotopic Investigations of the Early Cretaceous Sierra Nevada Batholith, Tulare County, California, and the Ivrea Zone, Northwest Italian Alps: Examples of Interaction Between Mantle-Derived Magma and Continental Crust. Ph.D. thesis, California Institute of Technology, Pasadena, California, 389 p.

Coleman, D.S., and Glazner, A.F. 1998. The Sierra Crest magmatic event: rapid formation of juvenile crust during the Late Cretaceous in California. *In* Integrated Earth and Environmental Evolution of the Southwestern United States: The Clarence A. Hall Jr. Volume. *Edited by* W.G. Ernst and C.A. Nelson, Bellwether Publishing for the Geological Society of America, Columbia, Maryland, 253–272.

Crowder, D.F, Robinson, P.T, Harris, Dahl, L. 1972. Geologic map of the Benton Quadrangle, Mono County, California, and Esmeralda and Mineral counties, Nevada. U.S. Geological Survey Geologic Quadrangle Map GQ-1013.

Crowder, D.F., Sheridan, M.F. 1972. Geologic map of the White Mountain Peak Quadrangle, Mono County, California. U.S. Geological Survey Geologic Quadrangle Map GQ-1012.

Dodge, F.C.W., Calk, L.C. 1987. Geologic map of the Lake Eleanor Quadrangle, central Sierra Nevada, California. U.S. Geological Survey Geologic Quadrangle Map GQ-1639.

du Bray, E.A., Moore, J.G. 1985. Geologic map of the Olancha Quadrangle, southern Sierra Nevada, California. U.S. Geological Survey Geologic Quadrangle Map MF-1734.

Giusso, J.R. 1981. Preliminary geologic map of the Sonora Pass 15-minute Quadrangle, California.U.S. Geological Survey Geologic Quadrangle Map OF 81-1170.

Hildebrand, R.S., Whalen, J.B. 2017. The Tectonic Setting and Origin of Cretaceous Batholiths Within the North American Cordillera: The Case for Slab Failure Magmatism and Its Signifcance for Crustal Growth. Geological Society of America Special Paper **532**, 113 p.

Huber, N.K. 1968. Geologic map of the Shuteye Peak Quadrangle, Sierra Nevada, California. U.S. Geological Survey Geologic Quadrangle Map GQ-0728.

Huber, N.K. 1983. Preliminary geologic map of the Dardanelles Cone Quadrangle, central Sierra Nevada, California, U.S. Geological Survey Geologic Quadrangle Map MF-1436.

Huber, N.K. 1983. Preliminary geologic map of the Pinecrest Quadrangle, central Sierra Nevada, California. U.S. Geological Survey Geologic Quadrangle Map MF-1437.

Huber, N.K., Rinehart, C.D. 1965. Geologic map of the Devils Postpile Quadrangle, Sierra Nevada, California, U.S. Geological Survey Geologic Quadrangle Map GQ-437.

John, D.A., Giusso, J., Moore, W.J., Armin, R.A. 1981. Reconnaissance geologic map of the Topaz Lake 15-minute quadrangle, California-Nevada. U.S. Geological Survey Geologic Quadrangle Map OF 81-0273.

Kistler, R.C. 1973. Geologic map of the Hetch Hetchy Reservoir Quadrangle, Yosemite National Park, California, U.S. Geological Survey Geologic Quadrangle Map GQ-1112.

Kistler, R.W. 1966. Geologic map of the Mono Craters Quadrangle, Mono and Tuolumne counties, California. U.S. Geological Survey Geologic Quadrangle Map GQ-0462.

Krauskopf, K.B, Bateman, P.C., 1977.Geologic map of the Glass Mountain Quadrangle, Mono County, California, and Mineral County, U.S. Geological Survey Geologic Quadrangle Map GQ-1099.

Krauskopf, K.B. 1971. Geologic map of the Mount Barcroft Quadrangle, California-Nevada. U.S. Geological Survey Geologic Quadrangle Map GQ-0960.

Krauskopf, K.B. 1985. Geologic map of the Mariposa Quadrangle, Mariposa and Madera counties, California. U.S. Geological Survey Geologic Quadrangle Map GQ-1586.

Lackey, J.S., Cecil, R., Windham, C.J., Frazer, R.E., Bindeman, I.N., and Gehrels, G.E. 2012a The Fine Gold intrusive suite: The roles of basement terranes and magma source development in the Early Cretaceous Sierra Nevada batholith. Geosphere, **8**: 292–313, doi:10.1130/GES00745.1.

Lackey, J.S., Eisenberg, J.I., and Sendek, C.L. 2012b. Day 2: The Fine Gold intrusive suite—Records of the nascent Cretaceous arc. *In* Formation of the Sierra Nevada Batholith: Magmatic and Tectonic Processes and Their Tempos. *Edited by* V. Memeti, S.R. Paterson, and K.D. Putirka. Geological Society of America Field Guide **34**, 2-1–2-23 (now supplanted by GSA Field Guide 34).

Leopold, M.B. 2016. Structure, construction, and emplacement of the Late Cretaceous Sonora Pass intrusive suite: Central Sierra Nevada batholith, California. M.S. thesis. San José State University, San José, California, 100 p.

Lockwood, J.P., Bateman, P.C. 1976. Geologic map of the Shaver Lake Quadrangle, central Sierra Nevada, California. U.S. Geological Survey Geologic Quadrangle Map GQ-1271.

Lockwood, J.P., Lydon, P.A. 1975. Geologic map of the Mount Abbot Quadrangle, central Sierra Nevada,

California. U.S. Geological Survey Geologic Quadrangle Map GQ-1155.
Mack, S., Saleeby, J.B., and Farrell, J.E. 1979. Origin and Emplacement of the Academy Pluton, Fresno County, California. Geological Society of America Bulletin, **90**: 633-694, doi.org/10.1130/GSAB-P2-90-633.
McKee, E.H., Nelson, C.A. 1967. Geologic map of the Soldier Pass Quadrangle, California and Nevada. U.S. Geological Survey Geologic Quadrangle Map GQ-0654.
Moore, J.G, Nokleberg, W.J. 1991. Geologic map of the Tehipite Dome Quadrangle, Fresno County, California.U. S. Geological Survey, Report: GQ-1676.
Moore, J.G. 1978. Geologic map of the Marion Peak Quadrangle, Fresno County, California. U.S. Geological Survey Geologic Quadrangle Map GQ-1399.
Moore, J.G. 1981 Geologic map of the Mount Whitney Quadrangle, Inyo and Tulare counties, California. U.S. Geological Survey Geologic Quadrangle Map GQ-1545.
Moore, J.G., Sisson, T.W. 1985. Geologic map of the Kern Peak Quadrangle, Tulare County, California. U.S. Geological Survey Geologic Quadrangle Map GQ-1584.
Moore, J.G., Sisson, T.W. 1987. Geologic map of the Triple Divide Peak Quadrangle, Tulare County, California. U.S. Geological Survey Geologic Quadrangle Map GQ-1636.
Nelson, C.A. 1966. Geologic map of the Blanco Mountain Quadrangle, Inyo and Mono counties, California, U.S. Geological Survey Geologic Quadrangle Map GQ-0529.
Nelson, C.A. 1966. Geologic map of the Waucoba Mountain Quadrangle, Inyo County, California. U.S. Geological Survey Geologic Quadrangle Map GQ-0528.
Nelson, C.A. 1971. Geologic map of the Waucoba Spring Quadrangle, Inyo County, California. U.S. Geological Survey Geologic Quadrangle Map GQ-0921.
Peck, D.L 2002. Geologic map of the Yosemite Quadrangle, central Sierra Nevada, California. U.S. Geological Survey Geologic Quadrangle Map I-2751.
Peck, D.L. 1980. Geologic map of the Merced Peak Quadrangle, central Sierra Nevada, California. U.S. Geological Survey Geologic Quadrangle Map GQ-1531.
Robinson, P.T., Crowder, D.F. 1973. Geologic map of the Davis Mountain Quadrangle, Esmeralda and Mineral counties, Nevada, and Mono County, California. U.S. Geological Survey Geologic Quadrangle Map GQ-1078.
Ross, D.C. 1967. Geologic map of the Waucoba Wash Quadrangle, Inyo County, California. U.S. Geological Survey Geologic Quadrangle Map GQ-0612.
Ross, D.C. 1989. The Metamorphic and Plutonic Rocks of the Southernmost Sierra Nevada, California, and Their Tectonic Framework. United States Geological Survey Professional Paper 1381, 159 p.
Saleeby, J.B., Ducea, M.N., Busby, C.J., Nadin, E.S., and Wetmore, P.H. 2008. Chronology of pluton emplacement and regional deformation in the southern Sierra Nevada batholith, California. *In* Ophiolites, Arcs, and Batholiths: A Tribute to Cliff Hopson. *Edited by* J.E. Wright, and J.W. Shervais. Geological Society of America Special Paper **438**, 397–427, doi:10.1130/2008.2438(14).
Sisson, T.W, Moore, J.G. 1994. Geologic map of the Giant Forest Quadrangle, Tulare County, California, U.S. Geological Survey Geologic Quadrangle Map, GQ-1751.
Sisson, T.W., and Moore, J.G. 2013. Geologic map of the southwestern Sequoia National Park. United States Geological Survey, Open-File Report 2013-1096, scale 1:24,000.
Stewart, J.H., Robinson, P.T., Albers, J.P., Crowder, D.F. 1974. Geologic map of the Piper Peak Quadrangle, Nevada-California. U.S. Geological Survey Geologic Quadrangle Map GQ-1186.
Stone, P., Dunne, G.C., Moore, J.G., Smith, G.I. 2000. Geologic map of the Lone Pine 15' quadrangle, Inyo County, California. U.S. Geological Survey Geologic Quadrangle Map I-2617.
Wahrhaftig, C. 2000. Geologic map of the Tower Peak Quadrangle, central Sierra Nevada, California. U.S. Geological Survey Geologic Quadrangle Map I-2697.

Supplemental File 4

Alasino, P.H., Ardill, K., Stanback, J., Paterson, S.R., Galindo, C., and Leopold, M. 2019. Magmatically folded and faulted schlieren zones formed by magma avalanching in the Sonora Pass Intrusive Suite, Sierra Nevada, California. Geosphere, **15**: 1677–1702, doi.org/10.1130/GES02070.1.
Clemens-Knott, D. 1992. Geologic and Isotopic Investigations of the Early Cretaceous Sierra Nevada Batholith, Tulare County, California, and the Ivrea Zone, Northwest Italian Alps: Examples of Interaction Between Mantle-Derived Magma and Continental Crust. Ph.D. thesis, California Institute of Technology, Pasadena, California, 389 p.

du Bray, E.A. 2007. Time, space, and composition relations among northern Nevada intrusive rocks and their metallogenic implications. Geosphere, **3**: 381–405. doi:10.1130/GES00109.1.

Hirt, W.H. 2007. Petrology of the Mount Whitney Intrusive Suite, eastern Sierra Nevada, California: Implications for the emplacement and differentiation of composite felsic intrusions. Geological Society of America Bulletin, **119**: 1185–1200. doi.org/10.1130/B26054.1.

Memeti, V. 2009. Growth of the Cretaceous Tuolumne Batholith and Synchronous Regional Tectonics, Sierra Nevada, CA: A Coupled System in a Continental Margin Arc Setting. Ph.D. thesis, University of Southern California, Los Angeles, California, 282 p.

Sisson, T.W., Grove, T.L., and Coleman, D.S. 1996. Hornblende gabbro sill complex at Onion Valley, California, and a mixing origin for the Sierra Nevada batholith. Contributions to Mineralogy and Petrology, **126**: 81–108, doi:10.1007/s004100050237.

Van Buer, N.J., and Miller, E.L. 2010. Sahwave batholith, NW Nevada: Cretaceous arc flare-up in a basinal terrane. Lithosphere, **2**: 423–446, doi:10.1130/L105.1.

Supplemental File 5

Memeti, V. 2009. Growth of the Cretaceous Tuolumne Batholith and Synchronous Regional Tectonics, Sierra Nevada, CA: A Coupled System in a Continental Margin Arc Setting. Ph.D. thesis, University of Southern California, Los Angeles, California, 282 p.

Canadian Science Publishing

ARTICLE

The mid-Cretaceous Peninsular Ranges orogeny: a new slant on Cordilleran tectonics? II: northern United States and Canada[1]

Robert S. Hildebrand and Joseph B. Whalen

Abstract: The mid-Cretaceous Peninsular Ranges orogeny occurred in the North American Cordillera and affected rocks from Mexico to Alaska. It formed when a marine trough, open for ~35 million years, closed by westerly subduction beneath a 140–100 Ma arc complex. In Part I, we described the features of the orogen in Mexico and California, west to east: back-arc trough, magmatic arc, 140–100 Ma seaway, post-collisional 99–84 Ma granodioritic–tonalitic plutons emplaced into the orogenic hinterland during exhumation, an east-vergent thrust belt, and farther east, a flexural foredeep. In western Nevada, where the Luning–Fencemaker thrust might be a mid-Cretaceous feature, arc and post-collisional plutons occur in proximity. The orogen continues through the Helena salient and Washington Cascades. In British Columbia, rocks of the 130–100 Ma Gambier arc lie west of the exhumed orogenic hinterland and 99–84 Ma post-collisional plutons to collectively indicate westerly subduction. East-dipping reverse faults near Harrison Lake, active from ~100 Ma until ~90 Ma, shed 99–84 Ma debris westward into the Nanaimo back-arc region. Within Insular Alaska, the Early Cretaceous Gravina basinal arc assemblage was deformed at 100 Ma and flanked to the east by a high-grade hinterland cut by post-collisional plutons. In mainland Alaska, the 100 Ma collision of Wrangellia and the Yukon–Tanana–Farewell composite terrane occurred above a southward-dipping subduction zone as shown by the 130–100 Ma Chisana arc sitting on Wrangellia and southward-dipping, northerly vergent thrusts in the Lower Cretaceous Kahiltna basin to the north. The outboard back-arc region was filled with post-collisional detritus of the McHugh complex.

Key words: orogeny, North American Cordillera, arc magmatism, arc-continent collision, slab failure magmatism, Peninsular Ranges orogeny.

Résumé : L'orogenèse des chaînes péninsulaires d'âge crétacé moyen s'est produite dans la cordillère nord-américaine et a touché des roches allant du sud du Mexique à l'Alaska. Elle s'est formée quand une fosse marine, ouverte pendant ~35 millions d'années, s'est refermée par subduction vers l'ouest sous un complexe d'arc de 140–100 Ma. Dans la première partie, nous avons décrit les éléments de l'orogène au Mexique et en Californie qui comprennent, d'ouest et est, une fosse d'arrière-arc, un arc magmatique, un bras de mer de 140–100 Ma, des plutons de granodiorite–tonalite post-collision de 99–84 Ma mis en place dans l'arrière-pays orogénique durant l'exhumation, une ceinture de charriage vers l'est et, plus à l'est, une avant-fosse formée par flexion. Dans l'ouest du Nevada, où le chevauchement de Luning–Fencemaker pourrait être un élément d'âge crétacé moyen, des plutons d'arc et post-collision sont présents à proximité les uns des autres. L'orogène se poursuit par le saillant d'Helena et les montagnes Cascades de l'État de Washington. En Colombie-Britannique, des roches de l'arc de Gambier de 130–100 Ma sont présentes à l'ouest de l'arrière-pays orogénique exhumé et de plutons post-collision de 99–84 Ma, indiquant collectivement une subduction vers l'ouest. Des failles inverses à pendage vers l'est près du lac Harrison, actives de ~100 Ma à ~90 Ma, ont évacué vers l'ouest des débris de 99–84 Ma jusque dans la région de l'arrière-arc de Nanaimo. En Alaska insulaire, l'assemblage d'arc et de bassin de Gravina d'âge crétacé précoce a été déformé à 100 Ma et flanqué à l'est par un arrière-pays de haut degré de métamorphisme recoupé par des plutons post-collision. En Alaska continental, la collision à 100 Ma de la Wrangellie et du terrane composite de Yukon–Tanana–Farewell s'est produite au-dessus d'une zone de subduction à pendage vers le sud, comme l'indique l'arc de Chisana de 130–100 Ma reposant sur la Wrangellie et des chevauchements vers le nord à pendage vers le sud dans le bassin crétacé inférieur de Kahiltna au nord. La région d'arrière-arc externe a été remplie par des détritus post-collision du complexe de McHugh. [Traduit par la Rédaction]

Mots-clés : orogenèse, cordillère nord-américaine, magmatisme d'arc, collision arc-continent, magmatisme de rupture de plaque, orogenèse des chaînes péninsulaires.

Introduction

Ever since the late 1960s, protracted easterly dipping subduction beneath North America has been the standard model to explain the development of the Cordillera (Dickinson 1970). However, in a companion paper (Hildebrand and Whalen 2021, this issue) we demonstrated how the geology of the Peninsular Ranges and Sierra Nevada can be reconciled by a major orogenic event, the Peninsular Ranges orogen, which developed at 100 Ma

Received 15 January 2021. Accepted 15 January 2021.

R.S. Hildebrand. Tucson, Arizona, USA.
J.B. Whalen. Geological Survey of Canada, 601 Booth Street, Ottawa, ON K1A 0E8, Canada.
Corresponding author: Robert S. Hildebrand (email: bob@roberthildebrand.com).

[1]This paper is one of two companion papers published in this issue of Canadian Journal of Earth Sciences (Hildebrand and Whalen 2021. Canadian Journal of Earth Sciences. This issue. doi:dx.doi.org/10.1139/cjes-2020-0154).

when an east-facing, 130–100 Ma shallow marine arc collided with a west-facing Aptian–Albian passive margin of the North American plate built on the east side of the Bisbee–Arperos seaway. Following closure of the basin by westward-dipping subduction, the oceanic lithosphere, along with much of the rifted margin, broke off from the partially subducted North America plate and fell away into the mantle. This slab failure led to rapid exhumation of the collisional hinterland, which shed post-collisional, 99–84 Ma plutonic and metamorphic debris westward into the back-arc region. The debris was derived in part from a suite of 99–84 Ma mesozonal–catazonal plutons formed when the basaltic–gabbroic portion of the broken and sinking plate melted. Geochemistry and isotopic analyses suggest that pre-collisional arc and post-collisional slab break-off magmas were derived from two different sources at different depths and can be distinguished on a set of discrimination diagrams (for example, Hildebrand et al. 2018).

In Part I (Hildebrand and Whalen 2021, this issue), we showed how 100 Ma easterly vergent thrust faults, interpreted to have formed during the Peninsular Ranges orogeny, were traced north–south through eastern California, Nevada, and Utah. In this paper, we describe the northward continuation of the orogen starting in western Nevada and continuing to south-central Alaska.

Nevada

Rocks and deformation of the Peninsular Ranges orogen are exposed to the north of the Sierra Nevada through western Nevada (Fig. 1), where both arc and slab failure plutons are common, but the subcontinental lithospheric mantle (SCLM) might be different from that beneath the Sierra Nevada (Hildebrand and Whalen 2017). For example, the 93–89 Ma Sahwave intrusive suite is a large post-collisional intrusive complex that is geochemically and petrologically similar in most respects to those in the Sierra Nevada batholith farther south, such as the Tuolumne and Mount Whitney intrusive suites (Supplementary Fig. S1[2]), but has more primitive εNd_T and $^{87}Sr/^{86}Sr_i$ reflecting derivation from younger and less-radiogenic lithosphere (Van Buer and Miller 2010).

In the Santa Rosa Range and Bloody Run Hills of north-central Nevada, both located just west of the Luning–Fencemaker thrust (Fig. 1), Brown et al. (2018) identified plutons of two age groups, 105–101 and 96–93 Ma, and noted that the older plutons had positive εNd_T, ranging from 0.8 to 2.9 and $^{78}Sr/^{86}Sri$ from 0.7045 to 0.7049, whereas plutons of the younger group had εNd_T from –1.5 to −3.2 and $^{78}Sr/^{86}Sr_i$ from 0.7052 to 0.7062. Even though the plutons are close to one another, these data suggest derivation from different sources, with pre-100 Ma intrusions reflecting an arc source and the post-100 Ma plutons indicating assimilation of SCLM. Thus, the lithospheres were juxtaposed at ~100 Ma just as they were to the south in the Sierra Nevada and Peninsular Ranges. Supporting evidence for the interpretation that the Santa Rosa – Bloody Run Hills now sit atop cratonic lithosphere comes from the 248 ± 1 Ma Koipato volcanics of the Humboldt and adjacent ranges (Fig. 1), which lie to the south and southeast of the Santa Rosa Range in the footwall of the Luning–Fencemaker thrust, and have high initial Sr and negative εNd_T, which Vetz (2011) argued reflected interactions with Paleoproterozoic lithosphere.

The age of the Luning–Fencemaker thrust is poorly constrained because there are no known dikes or other intrusions that cut it and, as it carries mostly Jurassic rocks in its hanging wall, has commonly been assumed to be a Jurassic fault. However, as there are also no known 130–100 Ma arc plutons to the east of the fault, it is possible that the thrust is not Jurassic, but instead a 100 Ma thrust active during the Peninsular Ranges orogeny. Most of the samples collected for $^{40}Ar/^{39}Ar$ ages from Jurassic rocks in the Santa Rosa Range, the Jungo Hills, and the Jackson Range (Fig. 1) yielded plateau ages from 97 to 86 Ma, which are considered to represent regional heating at about 100 Ma (Wyld et al. 2003). Thus, on the basis of arc plutons located just to the west — but not to the east — of the thrust, as well as the $^{40}Ar/^{39}Ar$ plateau ages discussed above, we suggest that the Luning–Fencemaker thrust is a 100 Ma structure, not a Jurassic fault as commonly assumed (Wyld et al. 2003; DeCelles 2004).

Small areas of low-grade sedimentary rocks that fill at least one half graben in the area, are collectively known as the King Lear Formation (Fig. 1) and are dominated by conglomerate and sandstone, but contain an interbedded siliceous ignimbrite dated at 125 ± 1 Ma, as well as a hypabyssal intrusion at 123 ± 1 Ma (Martin et al. 2010). We assume, based on the age, location, and presence of volcanics, that these outcrops represent remnants of early magmatism in the Cinco arc trough.

Idaho

Northward, across the Snake River Plain, several components of the Peninsular Ranges orogen are exposed. Rocks in and adjacent to the Western Idaho shear zone, which lies along the western margin of the Atlanta lobe of the Idaho batholith, are variably deformed, and in places contain deep-seated epidote-bearing, tonalitic to granitic orthogneisses in the age range 118 ± 5 to 105 ± 1.5 Ma, cut by epidote-bearing tonalitic sheets in the age range 92 to 90 Ma (Taubeneck 1971; Hyndman 1983; Manduca et al. 1993; Giorgis et al. 2008). The Western Idaho shear zone (Supplementary Fig. S2[2]) has long been considered as the western margin of cratonic North America based largely on isotopic data (Armstrong et al. 1977; Fleck and Criss 1985, 2007; Criss and Fleck 1987; Fleck 1990; Manduca et al. 1992).

East of the main shear zone, intrusions of the western border zone of the Atlanta lobe of the Idaho batholith, as well as plutons preserved as roof pendants, termed the Early Metaluminous suite, occur within the younger Laramide sector of the batholith and range in age from 98 to 87 Ma (Gaschnig et al. 2010; Kiilsgaard et al. 2001). In addition to the larger bodies, a number of small intrusions in high-grade gneisses of the Sawtooth Range near Stanley, Idaho (Supplementary Fig. S2[2]), yield 95–92 Ma zircon ages (Ma et al. 2017). On the basis of their age, the small bodies appear to be post-collisional bodies of the Peninsular Ranges orogeny, whereas the deformation appears to be related to the Late Cretaceous Laramide orogeny as a post-deformational intrusion was dated to be 77 Ma, about the same age as other post-Laramide intrusions in the area (Hildebrand and Whalen 2017).

Transpressional deformation within the Western Idaho shear zone is older than 90 Ma U–Pb ages of granitic pegmatites that cut the fabric (Giorgis et al. 2008). However, according to Braudy et al. (2017), the shear zone likely initiated after 104 Ma on the basis of 99.5 ± 1.4 Ma and 97.3 ± 0.7 Ma Lu–Hf garnet isochrons, which they interpret to represent the time of peak metamorphism. K/Ar and $^{40}Ar/^{39}Ar$ ages in the area fall in the range 93–85 Ma and partially overlap with the emplacement of the 98–87 Ma metaluminous plutons of the Idaho batholith (Lund and Snee 1988; Manduca et al. 1993; Snee et al. 1995; Giorgis et al. 2008), suggesting that the intrusions were emplaced during exhumation within the hinterland of the Peninsular Ranges orogen. Whole-rock geochemical data of the 98–87 Ma plutonic rocks plotted on our discrimination diagrams classify them as slab failure magmas (Supplementary Fig. S3[2]). Just west of the main mass of the Atlanta lobe (Supplementary Fig. S2[2]), 98–88 Ma foliated epidote–hornblende tonalitic, quartz dioritic, and granodioritic bodies, and gneisses, including the Payette River tonalitic intrusion (91.5 ± 1.1 to 89.7 ± 1.2 Ma), are exposed (Lund and Snee 1988; Manduca et al. 1993; Giorgis et al. 2008; Unruh et al. 2008) and, on the basis of the few existing analyses, appear to be slab failure magmas as well (Supplementary Fig. S3[2]).

[2]Supplementary data are available with the article at https://doi.org/10.1139/cjes-2021-0006.

Fig. 1. Geological map, with Cenozoic cover removed, of eastern California and Nevada showing the Sierra Nevada batholith, Cretaceous plutonic rocks of Nevada, various tectonic terranes of Nevada after Crafford (2007, 2008) and northern Mojave Desert modified from Walker et al. (2002). Death Valley and White–Inyo–Esmeralda sedimentary successions from Stewart (1970). BRH, Bloody Run Hills; HR, Humboldt Range; RRP, 111 ± 2 Ma metavolcanic rocks of the Rugged Rock Pendant from Whitmarsh (1997); SC, Schoonover sequence. Jurassic 0.706 isopleth from Wyld and Wright (2019); location of 97–86 Ma $^{40}Ar/^{39}Ar$ plateau ages in Jurassic rocks west of Fencemaker thrust from Wyld et al. (2003). Ages of plutons in Nevada mainly from N. Van Buer, personal communication, 2018; D. Johns and C. Henry, personal communication, 2020; and Du Bray 2007. [Colour online.]

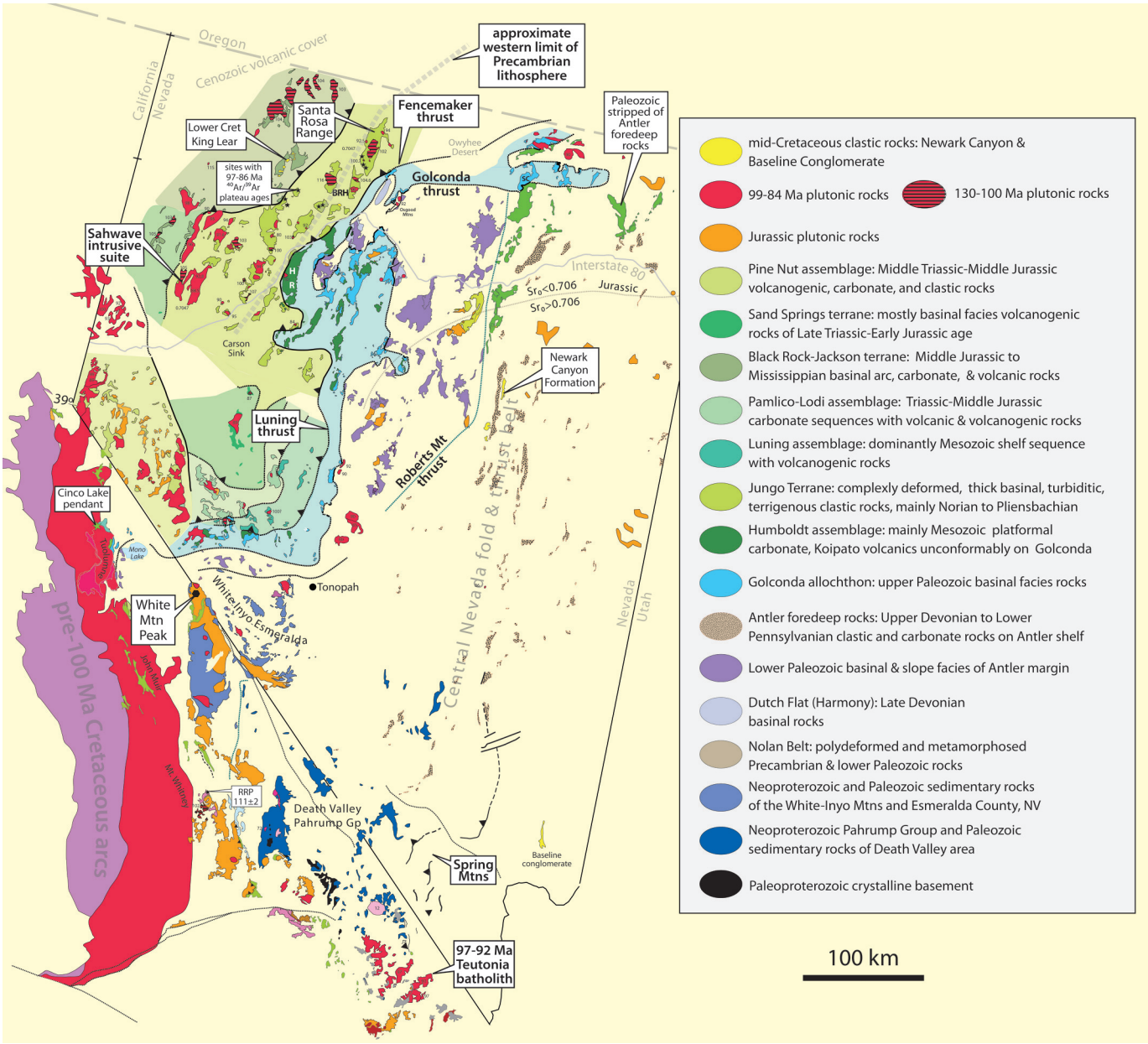

A variety of orthogneisses occur west of the Payette River tonalite (Supplementary Fig. S2[2]) as well as within the Western Idaho shear zone and the youngest unit, an undeformed biotite–hornblende granodiorite (Rat Creek granodiorite), yields U–Pb ages ranging from 89 to 84 Ma (Braudy et al. 2017). West and north of the Payette River tonalite, two deformed intrusive complexes, the Little Goose Creek and the Hazard Creek, have seven U–Pb ages ranging between 120 and 108 Ma, interpreted as emplacement ages, as well as sparse Jurassic ages, which are compatible with local basement (Patzke 2017). Unfortunately, no modern whole-rock geochemical data have been published to date.

The Potters Pond migmatitic domain (Supplementary Fig. S2[2]) contains meta-arkose metamorphosed after 96.8 ± 5.5 Ma as well as orthogneisses dated at 98.6 ± 0.6, 95.3 ± 0.9, 93.3 ± 0.7, and 92.4 ± 0.7 Ma along with seven gneisses that yielded monazite ages ranging from 98 to 91 Ma (Montz and Kruckenberg 2017). To the southwest of the Snake River Plain, in the northern Owyhee Mountains, several orthogneisses and plutons produced U–Pb zircon ages of 98–86 Ma, all with $^{87}Sr/^{86}Sr_i$ of 0.706 or higher (Benford et al. 2010).

Taken together, the abundance of 100–85 Ma intrusions emplaced during and after deformation in the transpressional Western Idaho

shear zone suggests that these intrusions are post-collisional bodies of the Peninsular Ranges orogen. Like the Sierra Nevada and Peninsular Ranges, intrusions younger than 100 Ma show the isotopic interaction with old and enriched continental lithosphere, whereas pre-100 Ma bodies located to the west are isotopically more juvenile (Armstrong et al. 1977; Fleck and Criss 1985, 2007; Criss and Fleck 1987; Manduca et al. 1992).

Foreland basin remnant

East of the Atlanta lobe of the Idaho batholith and west of the Boulder batholith in the Drummond, Montana area (Supplementary Fig. S2[2]), a succession of upper Albian to Santonian sedimentary units over 3500 m thick, likely deposited in a flexural foreland basin, were folded and thrust eastward prior to emplacement of 82 Ma intrusions (Wallace 1987; Wallace et al. 1990). The Blackleaf Formation is the basal unit, comprising three members, Flood, Taft, and Vaughn. Similar named units also occur to the east in the Montana thrust belt near Wolf Creek, but they are very much thinner, and 1–2 million years older, there (Zartman et al. 1995; Singer et al. 2021). In the thick western section, Wallace et al. (1990) pointed out that rocks of the Taft member were uplifted and eroded at about 100 Ma, but that there is no evidence of this in the thinner easterly sections. They (p. 1034) also indicated that the >3000 m thick overlying "sequence of rocks shares no similarities of lithologic succession with rocks of the upper Cretaceous" in the thrust belt north of the Lewis and Clark line and that the dominantly coarse-grained succession was deposited in shallow, brackish water compared with the thin sequence of marine Cenomanian–Santonian black shales deposited farther east (see also Fuentes et al. 2011).

We infer that the erosion of the Taft member took place as the easterly advancing thrust sheets caused the flexural bulge along the eastern flank of the foreland basin to migrate in front of it. The age of the unconformity, as well as the 3.5 km of Cenomanian–Santonian clastic sediment above it, are consistent with the 100 Ma Peninsular Ranges orogeny, not the older Sevier or younger Laramide deformation.

Detrital zircons were collected from the Vaughn member of the Blackleaf Formation and yielded a peak of 100 Ma (Stroup et al. 2008) consistent with erosional debris expected from the Peninsular Ranges orogen. They also found detrital zircons in rocks of the late Eocene Renova Formation with a distinctive 95 Ma peak dominated by zircons younger than 100 Ma, whereas they found that detrital zircons from the late Oligocene Medicine Lake beds had a 105 Ma peak dominated by detrital zircons in the age range 115–100 Ma. It appears that local drainages were able to access both arc and orogenic hinterland rocks for many millions of years after the collision.

The thrusts in the belt strike north–south and are easterly vergent (Supplementary Fig. S4[2]), whereas the younger Laramide thrusts are oriented northwest–southeast and appear to reflect the buttress effect of the Lewis and Clark lineament, located just to the north (Hildebrand 2015). The thrusts and sedimentary succession are readily interpreted to represent a foreland fold-thrust belt and related flexural foredeep of the Peninsular Ranges orogeny.

Additional sedimentary debris, likely derived from post-collisional plutonic rocks, was shed still farther inboard and is preserved in the Bighorn basin (Supplementary Fig. S2[2]) as rocks of the Mowry Shale, Frontier Formation, and Cody Shale, which yielded youngest detrital peak ages, consistent with their paleontological ages in 13 samples, ranging from 99.4 to 87.7 Ma (May et al. 2013).

Cascades

Although younger deformation and metamorphism related to the Laramide orogeny obscure and obliterate some of the older geological development of the Cascades (Miller et al. 2009 and references therein), many components of the Peninsular Ranges orogeny are preserved.

A number of Early Cretaceous metavolcanic and metasedimentary units are exposed in the generally high-grade Cascades crystalline core (Fig. 2). These include the Cascade River schist, which comprises mica schist and biotite paragneiss with lesser amounts of metaconglomerate, metavolcanic rocks, and metaperidotite (Sauer et al. 2017). One sample of the schist yielded detrital zircon populations of 120 Ma, a broad peak centered on 165 Ma, and a maximum depositional age (MDA) of 97 Ma, whereas the other sample produced a prominent peak of 93 Ma, as well as a small peak of 165 Ma, and an MDA of 91 Ma (Sauer et al. 2017). They also examined several samples from the garnet–sillimanite grade Skagit gneiss (Fig. 2) and found most detrital zircons have younger Laramide-age rims, but that the cores are mainly Early Cretaceous, Jurassic, and Triassic. Five of the samples had core MDAs of 121, 115, 112, 108, and 96 Ma, all ±2 Ma. These ages appear to reflect both arc and post-collisional magmatism related to the Peninsular Ranges orogeny.

The high-grade crystalline core was intruded by three groups of plutons with ages similar to other suites within the Cordillera (Fig. 2): plutons attributed herein to the Peninsular Ranges orogen are 96–89 Ma, Laramide bodies are 80–58 Ma, and plutons emplaced during Laramide extensional collapse are 50–45 Ma. The large 96–91 Ma Mount Stuart batholith (Matzel et al. 2006) postdates the early deformational fabric and a thrust fault, known as the Windy Pass thrust (Fig. 2), which placed rocks of the dominantly ophiolitic Ingalls complex over metamorphosed siliciclastic and metavolcanic rocks of the <125 Ma Chiwaukum schist (Miller 1985). Brown and Gehrels (2007) reported a 95 Ma dike that cut the amphibolite-grade Tonga Formation, which is a fault-bounded fragment of the Chiwaukum schist located just east of the Fraser River – Straight Creek fault zone (Fig. 2). We plotted geochemical data from several intrusions (Supplementary Fig. S5[2]), emplaced during regional amphibolite-facies metamorphism at depths of 25–35 km (Shea 2014; Miller et al. 2018) and, as consistent with their post-deformational age of emplacement, they appear to be post-collisional slab failure plutons.

West of the crystalline Cascades core, across the Straight Creek – Fraser River fault and to the west in the San Juan Islands, is an imbricate stack (Fig. 2) of units that were assembled after 110 Ma, and largely before intrusion of the 96–90 Ma plutons (Brandon et al. 1988; Brown and Dragovich 2003; Brown and Gehrels 2007) consistent with the 100 Ma orogenic event. Each thrust slice has a different metamorphic mineral assemblage, but on the whole most show evidence for high-pressure, low-temperature metamorphism (Brown et al. 1981). The lowermost unit of the stack is the Nooksack Formation, which comprises metavolcanic arc and associated metasedimentary clastic rocks with 114 and 153 Ma detrital zircon peaks and an MDA of 114 Ma (Brown and Gehrels 2007). These authors reported that the Nooksack Formation is overlain structurally, but separated by the Bell Pass mélange, from higher thrust slices containing Jurassic, but no Cretaceous, rocks. The mélange contains an incredible variety of clasts in a sandstone–argillite matrix yielding a major 119 Ma detrital zircon peak and a possible MDA of 110 Ma, but two zircons with ages of 105 Ma suggest the MDA might be younger. Individual blocks in the mélange include the 4 km × 10 km slab of Twin Sisters dunite, along with many smaller ultramafic blocks. In addition, blocks or lenses, up to a few kilometres across, of metasedimentary rocks termed the Yellow Aster complex, are dominated by detrital zircons mostly older than 1800 Ma and were strongly metamorphosed and intruded during the Devonian by gabbroic–tonalitic plutons (Brown and Gehrels 2007; Schermer et al. 2018). Other blocks include Lower Cretaceous blueschists, high-pressure, high-temperature Permian amphibolite, Triassic ribbon chert, pillow basalt of oceanic island provenance; and blocks of both underlying and overlying tectonic units. Brown and Gehrels (2007) pointed out the similarity of the

Fig. 2. Geological sketch map of northwestern Washington, illustrating the basic geology of the San Juan Islands – Northwest Cascades thrust system, the western Cascade crystalline core, and surrounding area. CB Chilliwack batholith; DF, Dirty Face pluton; GHB, Golden Horn batholith; MSB, Mount Stuart batholith; N, Nooksack Formation; SB, Snoqualmie batholith; T, Tonga Formation; TP, Ten Peak complex; WPT, Windy Pass thrust. Modified from Brown and Dragovich (2003) with ages of plutons from Miller et al. (2009) and ages of other units from Brown and Gehrels (2007) and Sauer et al. (2017). [Colour online.]

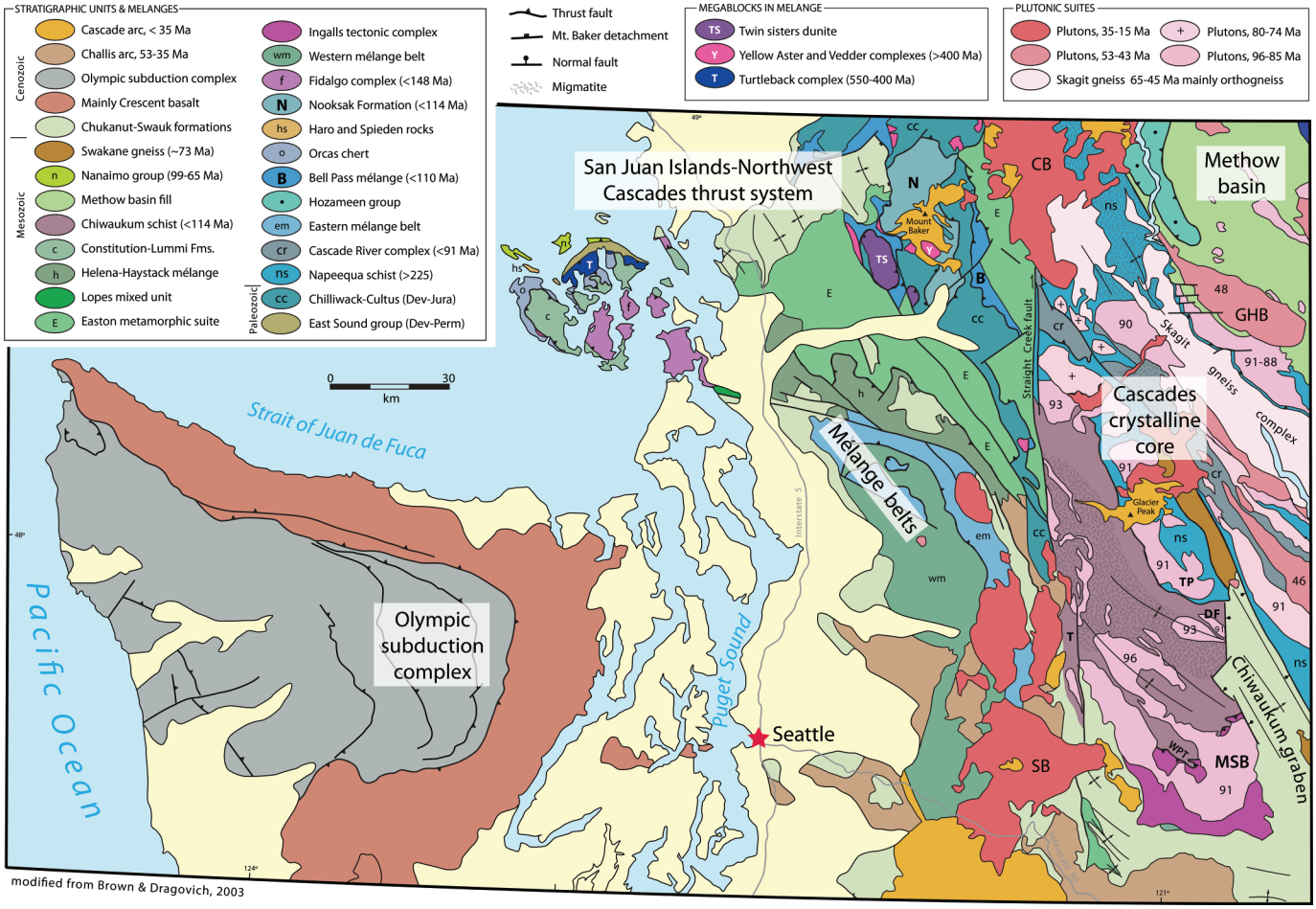

zircon age profiles in the blocks of Yellow Aster complex to many rocks of western North America, such as the older nappes in the Shoo Fly complex and the Antelope Mt. Quartzite of the Yreka terrane in the Klamaths. However, Schermer et al. (2018) suggested they are more similar to Yukon–Tanana and Alexander terranes. Because the mélange contains a wide variety of blocks from varied settings, including both continental and oceanic, as well as high-pressure, low-temperature metamorphism, we suggest that the mélange is part of the suture zone between the lower North American plate and the Peninsular Ranges arc-bearing composite terrane.

Coast Mountains batholith of British Columbia

The geology of the Coast Mountains batholith of British Columbia (Roddick and Hutchinson 1974; Roddick 1983) is similar in many aspects to that of the Peninsular Ranges and Sierra Nevada. The Coast Mountains batholith is traditionally interpreted as a manifestation of eastward subduction, initially beneath the Insular terrane, but that magmatism migrated eastward beneath Stikinia with time (Gehrels et al. 2009). The geology of the batholith is extremely complex, because not only are rocks of the Peninsular Ranges orogen present, but rocks deformed and intruded during the Campanian–Paleocene Laramide orogen (Rusmore and Woodsworth 1991), as well as an Eocene deformational and magmatic belt (Erdmer and Mortensen 1993; Johnston and Canil 2007) largely occupy the same north–south structural corridor (Hildebrand 2015; Hildebrand and Whalen 2017).

On the mainland, the westernmost parts of the Coast Mountains batholith (Fig. 3) comprise Triassic basement of Wrangellia covered by dominantly greenschist-grade metasedimentary and metavolcanic rocks of the Early to Middle Jurassic Bowen Island and Harrison Lake groups, all cut by a variety of plutons (Friedman et al. 1990; Mahoney et al. 1995). Rocks of the Bowen Island – Harrison Lake groups are overlain, along a deeply incised unconformity, by metavolcanic and metasedimentary rocks of the Gambier Group, which is divided into two formations: (1) a basal assemblage, known as the Peninsula Formation, dominantly composed of Berriasian–Valanginian conglomerate, *Buchia* coquina, and arkose, overlain by (2) rocks of the late Valanginian to Albian Brokenback Hill Formation (Fig. 3), which is a succession of submarine to subaerial volcanic and volcaniclastic rocks ranging continuously in composition from basalt to rhyolite, as well as a variety of sandstone, siltstone, black shale, and volcanic cobbly to bouldery conglomerate, containing clasts as large as 1–2 m across (Crickmay 1925; Arthur et al. 1993; Lynch 1992, 1995). The Brokenback Hill formation contains Albian fauna, rhyolite dated at 112.0 ± 0.3 Ma by U–Pb on zircon (Lynch 1992, 1995) and MDAs, determined from detrital zircon grains, of 116–114 Ma (Dorsey 2018). The Peninsular Formation was shown by Dorsey (2018) to be younger than 138 Ma.

Fig. 3. Geological sketch map of the southern portion of the Coast plutonic complex, British Columbia, modified from Friedman and Armstrong (1995), with additional ages from Gibson and Monger (2014). Note that abundant 135–100 Ma plutons, as well as arc volcanic and sedimentary rocks of the dominantly marine Gambier Group, sitting on Late Jurassic basement in pink, all lie west of the Harrison Lake structural break, whereas ~101–86 Ma post-collisional plutons, shown in brick red, span the entire area. [Colour online.]

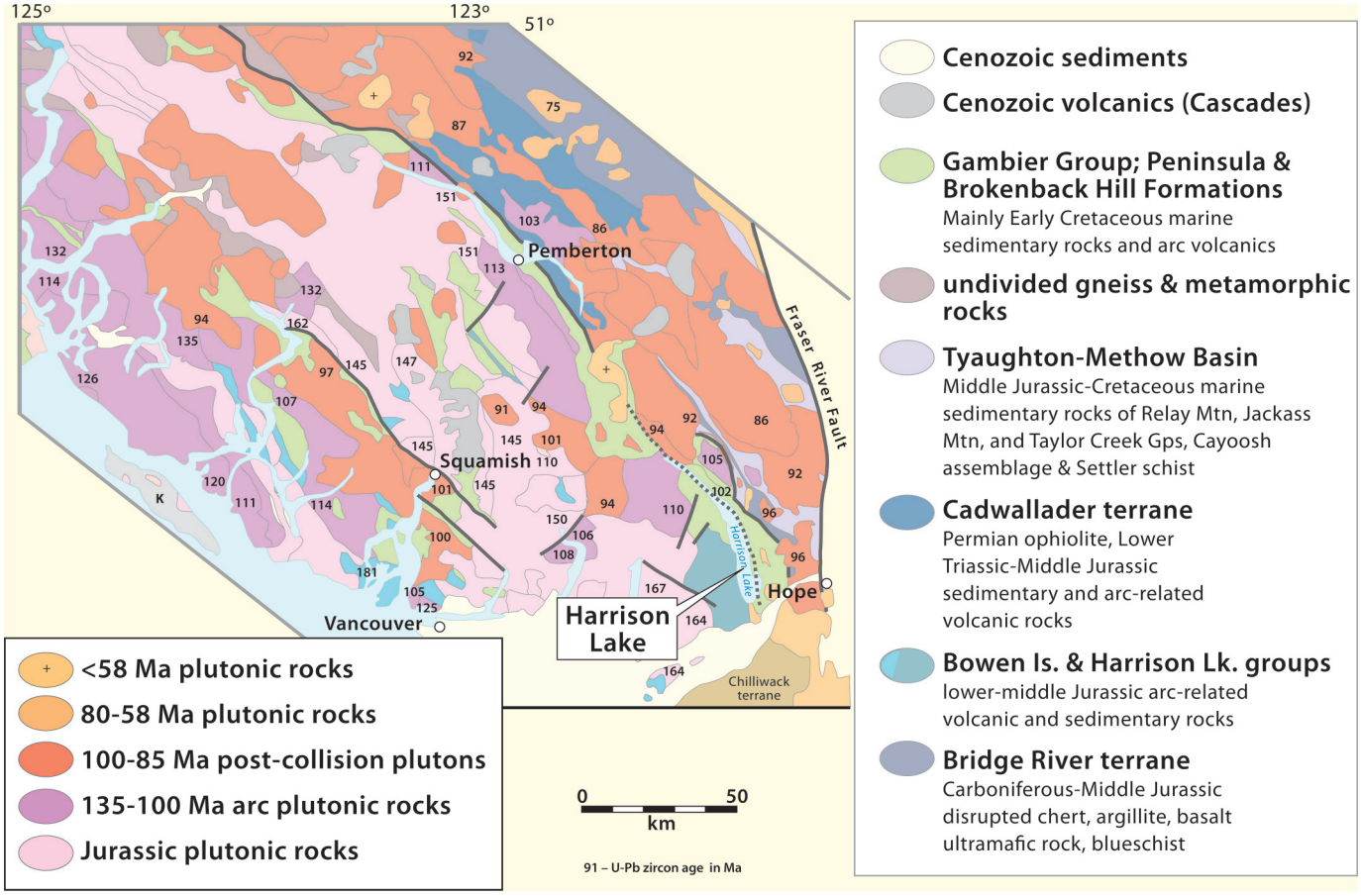

Farther north, Mahoney et al. (2009) described and grouped the Lower Cretaceous plutons in the Bella Coola region into two suites: the 141–131 Ma Firvale Suite, which consists of hornblende–biotite granodiorite to granite, and the 123–110 Ma Desire suite, a heterogeneous suite of pyroxene–hornblende- and biotite-bearing diorites and granodiorites, commonly deformed by shear zones characterized by a strong foliation and (or) locally developed mylonitic fabrics.

Early work on the structure of the southern Coast plutonic complex suggested that ~100 Ma faults along the eastern boundary of the Lower Cretaceous arc rocks in the Harrison Lake region (Fig. 3), were low-angle thrust faults that placed high-grade metamorphic rocks westward over low-grade arc rocks (Journeay and Friedman 1993), an interpretation that led to the general notion that subduction beneath the belt was eastward. However, more recent work suggests that the faults are much steeper and have over 10 km of reverse displacement (Friedman et al. 1992; Brown et al. 2000; Gibson and Monger 2014) and that the higher-grade rocks were exhumed westward and placed atop the western plutonic terrane (Fig. 4), which consists dominantly of pre-collisional Lower Cretaceous arc plutons and greenschist-grade arc volcanic and associated epiclastic rocks as discussed above.

These findings suggest that the arc was on the western block prior to collision at 100 Ma, and that the upper plate was more regionally extensive than previously thought. If so, then the reverse faults are east side up and, therefore, the collisional suture related to basinal closure, if preserved, should lie to the east, not the west.

The rocks of the Harrison Lake region (Fig. 5) constrain the age of deformation to be about 100 Ma as a 102 Ma metadacite, the 107–101 Ma Breakenridge intrusive sheets, and the 103 Ma Clear Creek pluton are all deformed, whereas the post-deformational Hornet Creek, Spuzzum, and Ascent Creek bodies are all 97–96 Ma (Brown and Walker 1993; Gibson and Monger 2014). The collision in this area represents the collision between the Peninsular Ranges composite terrane, composed of parts of the Insular and Intermontane superterranes, which had previously collided during the Jurassic (Monger et al. 1982), but were partly separated when the Lower Cretaceous trough opened.

Friedman et al. (1990) showed that tight isoclinal folds along the steeply dipping Butter Creek fault (Figs. 4 and 5), which clearly postdate the 100 Ma isoclinal folding, transposition of bedding, and thrust faults that imbricate the metavolcanic and metasedimentary rocks, as well as Breakenridge gneiss, were cut by the 91.5 ± 2 Ma Mason pluton. This implies that the majority of the exhumation within the hinterland belt took place in less than 10 million years.

Farther north, within the eastern part of the batholith, rocks of Yukon–Tanana and Stikine terranes are exposed and are generally high-grade metasedimentary migmatites and orthogneiss, typically at upper amphibolite to granulite grade with sillimanite growth after kyanite or staurolite (Hutchison 1970; Stowell and Crawford 2000; Hollister and Andronicos 2000; Rusmore et al.

Fig. 4. Cross section from west to east through the Harrison Lake fault belt illustrating the structural relief across faults. Modified from Monger and Brown (2016). [Colour online.]

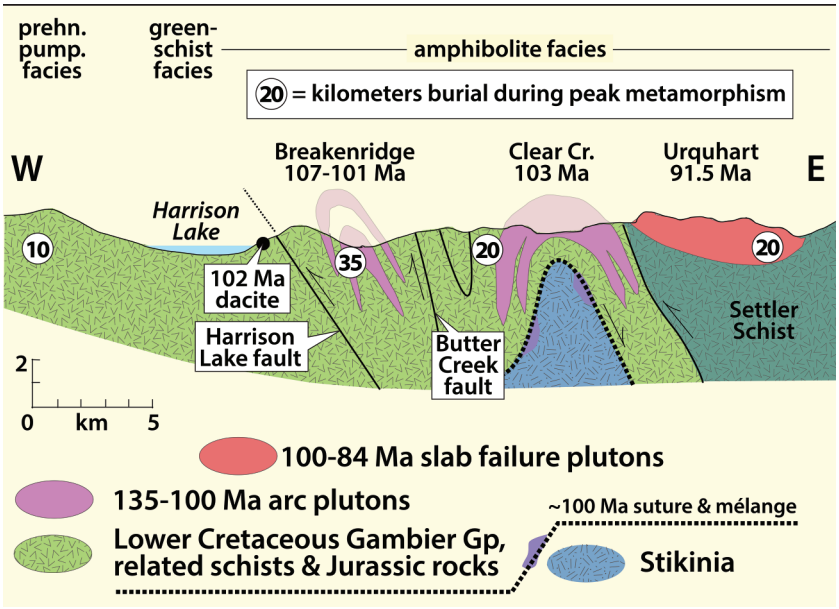

2000). Arc rocks, generally at relatively low metamorphic grade, lie to the west of the high-grade hinterland belt (Gibson and Monger 2014) and indicate that the Yukon–Tanana composite terrane was part of the lower plate in the collision and that subduction was westward beneath the arc (Fig. 6).

The post-collisional Ecstall plutonic suite

Both the hinterland and arc terranes of the Coast plutonic complex were intruded by a suite of post-collisional plutons in the age range 99–85 Ma (Brown and McClelland 2000; Brown et al. 2000; Gehrels et al. 2009; Mahoney et al. 2009; Girardi et al. 2012), just as typically occur farther south (Fig. 7). The intrusive suite consists of large homogeneous bodies of tonalite with lesser quantities of granodiorite and quartz diorite, commonly with megascopically visible euhedra of titanite and epidote (Gehrels et al. 2009). Where the bodies intruded the hinterland belt, they were emplaced into high-grade rocks during their exhumation (Crawford et al. 1987; Himmelberg et al. 2004). Mahoney et al. (2009) dated one intrusion by U–Pb zircon to be 86.8 ± 0.3 Ma and included it in his Big Snow suite.

The western part of the Coast Plutonic complex continues northward along the coast where some 50 km south of the USA–Canada international border (Fig. 7), the 20 km by >80 km, epidote-bearing, 98 ± 4 Ma hornblende dioritic–granodioritic Ecstall pluton intruded deformed and high-grade wall rocks at depths of 25–30 km and has a $^{40}Ar/^{39}Ar$ hornblende age of 90 ± 3 Ma, which indicates rapid uplift and exhumation (Woodsworth et al. 1983; Brownlee and Renne 2010) consistent with the Harrison Lake region farther south. Other U–Pb zircon data yield an age of 91 ± 0.5 Ma for the pluton (Butler et al. 2002). This age conflicts with $^{40}Ar/^{39}Ar$ hornblende ages; however, Brownlee and Renne (2010) showed that the Ar systematics were severely disturbed by younger intrusions to the east. The U–Pb ages determined by Butler et al (2002) also young eastward, so additional study is warranted. Nevertheless, the available data indicate that the pluton is no younger than 91 Ma.

The plutonic wall rocks are kyanite-bearing, metamorphosed at 30 km depth, and deformed into tight isoclines and by cleavage, both of which are transected by a more steeply dipping foliation containing steep lineations adjacent to east-dipping, westerly vergent shear zones dated at about 90 Ma by $^{40}Ar/^{39}Ar$ (Crawford et al. 1987). Crawford and Hollister (1982) pointed out that the metamorphic grade increases structurally upward from west to east, and varies from chlorite in the west to kyanite+muscovite+melt (8.1 kbar) in the east, indicating westward transport of higher over lower-grade metamorphic units. The structures responsible for this transport appear to be the typical reverse faults found along much of the western Peninsular Ranges orogen and are similar in age to those around Harrison Lake.

As the post-collisional suite was previously unnamed in the Coast plutonic complex, we name the 100–84 Ma post-collisional suite the Ecstall suite after the deep-seated Ecstall pluton. We plotted available geochemistry from the post-collisional 100–85 Ma intrusions on our discrimination diagrams and, consistent with our model, they plot as slab failure plutons (Supplementary Fig. S6[2]) as do the contemporaneous plutons farther south.

Girardi et al. (2012), who studied the geochemistry of a sector within the batholith, suggested that it is unlikely that the post 100 Ma plutons fractionated or interacted with other rocks in a significant way above the stability limit for plagioclase in these composition rocks, which, on the basis of experiments with amphibolite and eclogite, is about 100 km (Rapp et al. 1991). Overall, the geochemical data from rocks studied by Girardi et al. (2012) are similar to those of post-collisional plutons farther south, in that compatible elements vary systematically with SiO_2 but that with incompatible elements there is no correlation. The same patterns are found in the Tuolumne plutonic suite (Hildebrand et al. 2018), and indicate that as magmas rose, they modified their composition by fractional melting and assimilation of the SCLM. However, because the SCLM beneath the Coast batholith was relatively juvenile and non-radiogenic, the Nd and Sr isotopes are more juvenile, or arc-like, than plutons that interacted with old and enriched SCLM. Coast Range plutons have $\delta^{18}O$ values ranging from 7.2% to 10%, which indicates that the magmas were derived from, or interacted with, rocks that had been weathered near the surface (Wetmore and Ducea 2011). Those researchers pointed out that the high $\delta^{18}O_{quartz}$ coupled with the primitive Sr, Pb, and Nd indicate that the source of the magma must have been mainly mafic, volumetrically large, had primitive radiogenic isotopes, and were altered by low temperature meteoric or

Fig. 5. Plutons of the Coast Range plutonic complex east of Harrison Lake bracket the time of deformation to be about 100 Ma. Modified after Brown and McClelland (2000) and Brown et al. (2000). Ages from Gibson and Monger (2014). Rocks of the Slollicum schist are similar lithologically to those of the Gambier Group west of the Harrison Lake fault, but are generally at higher grade. They were shown by Dorsey (2018) to be the same age with maximum depositional ages of 120 and 112 Ma. Rocks of the Cogburn Group are a greenschist–amphibolite mélange of oceanic rocks, whereas Settler schist is composed of amphibolite-grade pelitic–psammitic metasedimentary rocks. Both are poorly dated. The Butter Creek fault (BCF) is cut by the 91.5 Mt Mason pluton; thus, the main exhumation of the hinterland took place in less than about 10 million years. B, Breakenridge pluton; CC, Clear Creek pluton; HC, Hat Creek pluton; SC, Settler Creek pluton. [Colour online.]

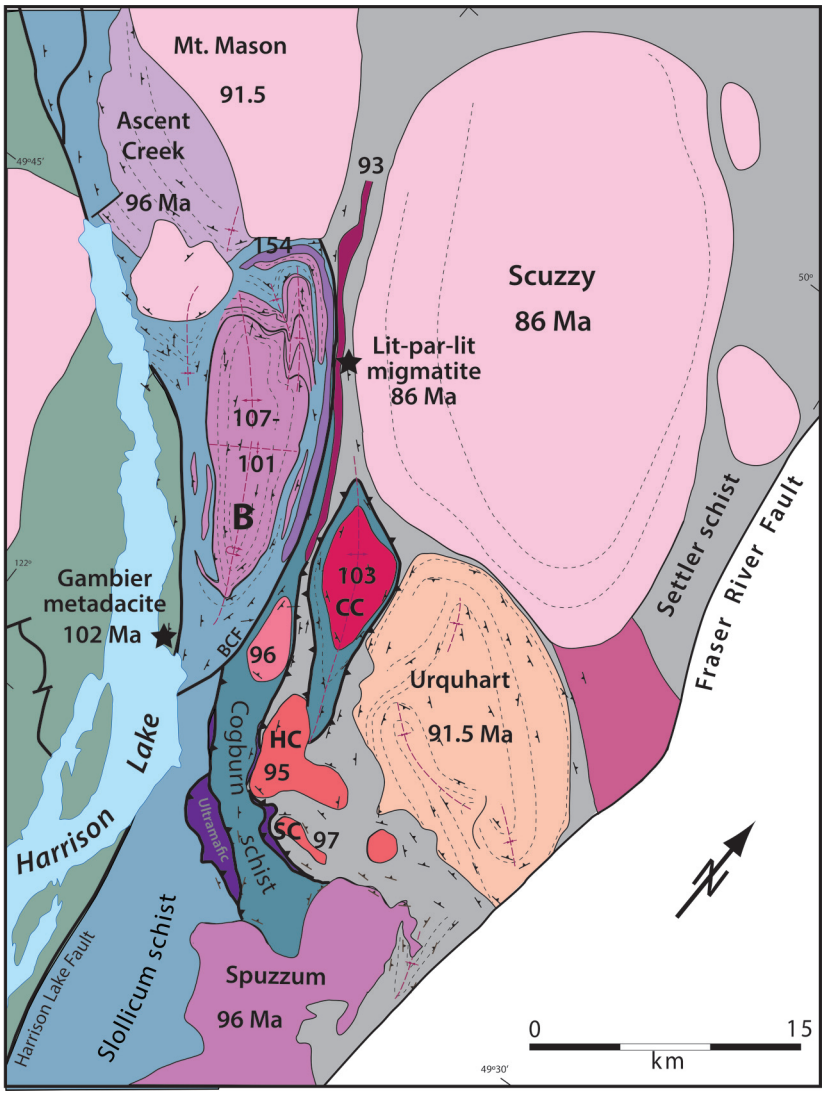

sea water. Just as with the Sierra Nevada and Peninsular Ranges batholiths, the upper basaltic–gabbroic part of oceanic crust is a potential source of these magmas. When compared with post-collisional plutons of the Sierra Nevada and Peninsular Ranges, Sr and Nd isotopes are less evolved, but Sierran plutons commonly have lower, mantle-like $\delta^{18}O$ values.

Nanaimo and Queen Charlotte groups, British Columbia

To the west of the orogen on eastern Vancouver Island, a Late Cretaceous sedimentary succession, known as the Nanaimo Group, sits unconformably upon rocks of Wrangellia (Monger et al. 1982; Mustard 1994; Mustard et al. 1995). Much like their equivalents to the south, this succession is typically considered to represent a fore-arc deposit situated west of the arc represented by the Coast Ranges batholith. However, the rocks of this succession have pronounced detrital zircon peaks (Fig. 8) between 100 and 85 Ma (Matthews et al. 2017), ages that are too young to be arc related, but do match post-collisional plutonic ages, so are interpreted here to represent debris shed from the exhumed hinterland belt.

Other researchers have noted the far-sided paleopoles for the Nanaimo Group and considered that it must have traveled from the south (Enkin et al. 2001). However, the lack of exposure between Vancouver Island and the mainland means there is no recognized fault along which this northerly rotation might have taken place. But, as discussed above, a trough with similar 100–85 Ma detrital zircons occurs all along the western side of the Peninsular Ranges orogen, obviating the requirement for Vancouver Island to have moved relative to the mainland and Coast batholith to provide the necessary-age zircons. In addition, paleomagnetic results from more interior locations, such as those obtained from rocks of the 95–85 Ma Silverquick and Powell Creek formations (Enkin et al. 2006*a*) and

Fig. 6. Cross sections through the Coast plutonic complex, modified from Gehrels et al. (2009) illustrating that the 120–100 Ma Lower Cretaceous arc plutons lie west of the collapsed Gambier basin, shown in yellow, whereas post-collisional rocks in red span the contact of the 100 Ma collision zone. These relations document that subduction was westward-dipping on the east side of the Insular superterrane prior to collision with the Intermontane terrane at 100 Ma. During the Peninsular Ranges orogeny, the leading edge of the Intermontane superterrane was pulled beneath the arc located on the Insular superterrane. Following slab failure, the area was riddled with post-collisional plutons and the collision zone exhumed to expose high-grade metamorphic rocks of the lower plate. [Colour online.]

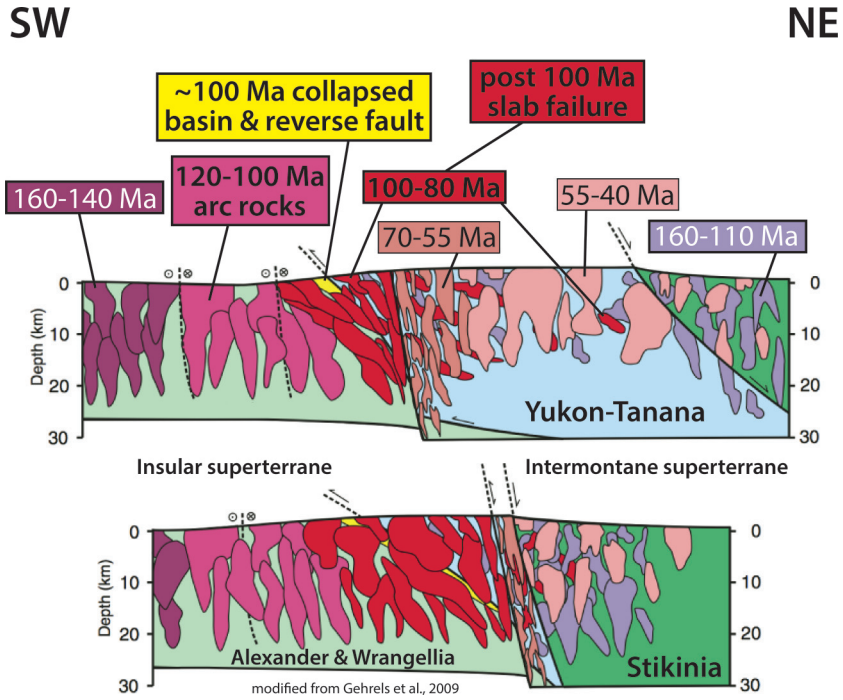

Methow block (Granirer 1985), approximate those from rocks of the Nanaimo basin (Enkin et al. 2001). Irving et al. (1995, 1996) suggested a model involving northward migration along the cryptic Intra-Quesnellia fault; whereas Hildebrand (2015) used piercing points to show how 1300 km of northerly migration could be restored along faults well inboard of those traditionally investigated for such displacements, similar to models of Enkin et al. (2006*b*) and Gladwin and Johnston (2006).

Haida Gwaii lies offshore from the region just south of the international border (Fig. 7). There, Dorsey (2019) sampled sandstones and pebbly conglomerates from the Cretaceous Queen Charlotte Group (Haggart 2004) for detrital zircons. His zircon analyses document the progressive deroofing of the arc and post-collisional hinterland belt (Fig. 7) of the Peninsular Ranges orogen at this latitude.

Trapped units

Within the northern Cordillera, the lack of recognition of a 100 Ma collision has led to difficulties in interpreting the setting of various terranes. Recognizing the rifting and spreading to form the early Cretaceous seaway and its subsequent 100 Ma demise might resolve some of these problems.

Several terranes are caught between North America and the Peninsular Ranges composite terrane. These terranes include relic parts of the Insular and Intermontane superterranes, because as discussed earlier, the two superterranes had initially collided during the Jurassic, but were subsequently dismembered during the Early Cretaceous. In this scenario, fragments of the previous Intermontane terrane could have been rifted to constitute part of the western block and, similarly, fragments of the Insular terrane could have been transferred to the eastern side of the basin. Here we briefly discuss two terranes: Spences Bridge terrane and Methow basin, both of which span the international border.

Thorkelson (1986) suggested that at least one piece of the Early Cretaceous arc, located just east of the Fraser River – Pasayten fault system in southern British Columbia (Supplementary Fig. S7[2]), and termed the Spences Bridge Group, faced westward during magmatism. Overall, the Spences Bridge Group is a late Albian two-part volcanic succession that rests unconformably on several rock units of the Intermontane superterrane and was considered to have formed by eastward subduction prior to, and after, a mid-Cretaceous collision with the Insular terrane (Thorkelson and Smith 1989).

Volcanic rocks of the group were divided into two successions: a lower unit of calc- alkaline basaltic to rhyolitic arc-type volcanic and intercalated sedimentary rocks containing late Albian fossils, overlain by more localized andesitic lava flows of a broad shield volcano interpreted to be post-collisional and cut by plutons with K–Ar ages of 98–97 Ma (Thorkelson and Smith 1989). They determined that the lower lavas have $^{87/86}Sr_i$ ranging from 0.70316 to 0.7040 and εNd_T from 5.0 to 7.8, whereas the upper andesitic rocks are more primitive with $^{87/86}Sr_i$ as low as 0.70298 and εNd_T as high as 8.8. We plotted their trace element analyses on our discrimination diagrams. Although some elements were affected by alteration, least mobile elements (Ta/Yb and La/Sm vs. Sm/Yb) support their model of arc magmatism overlain by younger andesitic magmatism derived from a different, likely deeper, mantle source. We envision that the Albian arc suite represents part of the arc built on a fragment of the Intermontane superterrane within the Peninsular Ranges composite terrane west of the seaway and that the upper suite represents early post-collisional magmas derived from beneath the collision zone during slab break-off. In a different approach to explain the location of the Spences Bridge Group, Lynch (1995) developed an arc–arc collision model with both westerly and easterly subduction.

The lack of recognition of at least one Jurassic collision followed by a 100 Ma mid-Cretaceous collision led to a complex

Fig. 7. Geological sketch map of part of the Coast plutonic complex, illustrating the various terranes, the Gravina trough assemblage and detrital zircon suites from Cretaceous sedimentary rocks of the Queen Charlotte Group on Haida Gwaii (Dorsey 2019) illustrating a progressive deroofing sequence ranging from Jurassic basement upwards through 130–100 Ma arc and 99–88 Ma post-collisional magmatism. See Supplementary Fig. S8[2] for detailed map and detrital zircon results for Gravina trough and related rocks. [Colour online.]

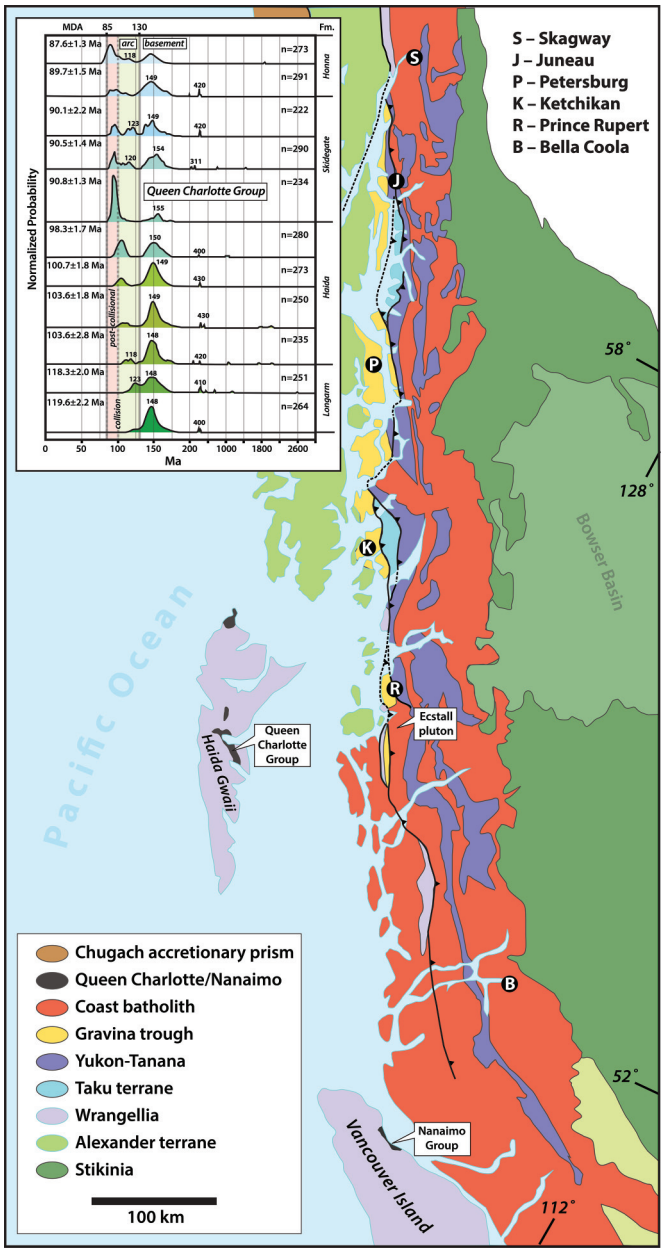

Fig. 8. Detrital zircon probability diagrams for rocks of the Nanaimo Group, illustrating the similarity of dterital ages within rocks of the Salinian block, Sierra Nevada, and Peninsular Ranges (modified from Matthews et al. 2017). Note the consistent mid-upper Jurassic peaks reflecting basement, as well as the obvious 130–100 Ma arc and 100–83 Ma post-collisional peaks. Salinia, as well as rocks of the Sierra Nevada and Peninsular Ranges, were relatively unscathed by younger Laramide deformation so their outboard regions do not contain 75 ± 5 Ma detrital zircons (see fig. 8 in Hildebrand and Whalen 2021). [Colour online.]

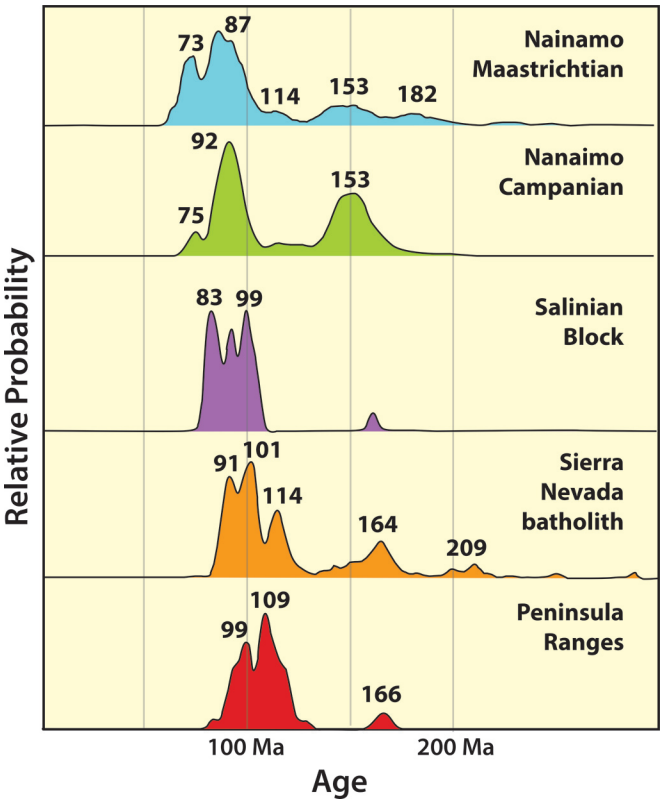

model using large-magnitude sinistral strike-slip faults to relocate the Methow basin, interpreted as a fore-arc basin, into a retro-arc position by younger dextral strike-slip faults to explain its present location on the east side of the Coast plutonic complex between the Insular and Intermontane terranes (Monger et al. 1994; Gehrels et al. 2009; Yokelson et al. 2015). The basin is a fault-bounded block (Haugerud et al. 1996) lying to the west of the Spences Bridge Group, and separated from it by the east-vergent Pasayten thrust (Umhoefer and Miller 1996). Existing data suggest that the Methow basin preserves a remnant of the Early Cretaceous arc trough. Metasedimentary rocks dominate the trough, are dominantly siliciclastic and immature with a high modal plagioclase content, and were deposited from the middle Albian to the Cenomanian atop upper Paleozoic to lower Mesozoic cherts and greenstones of the Hozameen and Bridge River groups (Kleinspehn 1985). Upper parts of the sedimentary succession were intruded by a 97.5 Ma sill (Dragovich et al. 1997) and by 96–88 Ma plutons (Haugerud et al. 1996). Detrital zircons from both northern and southern outcrop belts (Surpless et al. 2014) yield two main age peaks: an Oxfordian peak and an Early Cretaceous peak (Fig. 9). Similar profiles from several locations typically exhibit a general magmatic lull between about 140 and 125 Ma. Geochemical analyses of mudrocks from the block (Surpless et al. 2014) plot in the arc field on our discrimination plots, consistent with their presumed proximity to Lower Cretaceous arc material as well as 160 Ma Jurassic arc rocks. The uppermost unit, the Goat Wall Formation, comprises andesitic flows and siliceous ignimbrites intercalated with volcanogenic sedimentary rocks containing detrital zircons as young as 105 Ma (Surpless et al. 2014). Based on the ages and compositions of the Methow rocks, the block is interpreted to be part of the Early Cretaceous arc and seaway.

Zircons older than about 200 Ma (Fig. 9) are interpreted to have been derived from rocks well to the south, near the Gondwana–

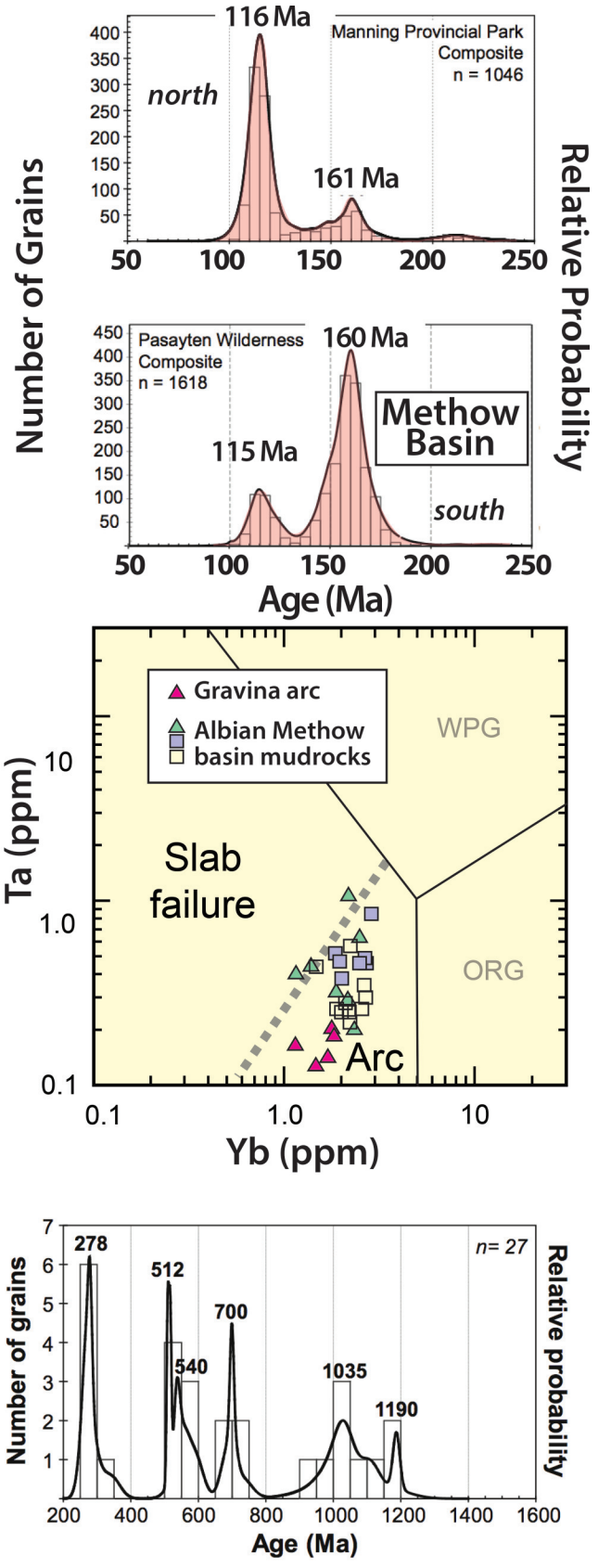

Fig. 9. Detrital zircon histograms showing relative probability vs. age for sedimentary rocks of the Methow block, modified from Surpless et al. (2014). These plots show the typical Jurassic basement peaks as well as the 130–100 Ma arc peaks. The Ta vs. Yb discrimination diagram shows that fine-grained sedimentary rocks within the basin reflect arc debris, which fits with their 130–100 Ma age. ORG, ocean-ridge granite; WPG, within-plate granite. Gravina arc samples from Rubin and Saleeby (1991). The lower plot has few total zircons, but their peaks suggest a southern Gondwana–Ouachita source. [Colour online.]

Laurussian collision zone as they contain a 278 Ma Permian peak, Cambrian peaks of 540 and 512 Ma, a 700 Ma Gondwana peak, and two Grenville age peaks of 1035 and 1190 Ma: there are no Paleoproterozoic or Archean zircons (Surpless et al. 2014). If the 700 Ma detrital zircons were derived from Gondwana, then the Methow block probably migrated northward while the basin remained open.

Gravina trough

Late Jurassic to Early Cretaceous volcaniclastic and mafic to intermediate volcanic rocks known as the Gravina succession (Fig. 7 and Supplementary Fig. S8[2]), generally interpreted to be remnants of a magmatic arc, crop out in Insular Alaska and on the mainland to the east (Berg et al. 1972; Rubin and Saleeby 1991; McClelland et al. 1992; Ricketts 2019). In the west, rocks of the Gravina succession unconformably overlie rocks of the Insular terrane, whereas to the east they sit structurally upon Permo-Triassic rocks of the Taku terrane. On the basis of Nd–Sr isotopic and detrital zircon characteristics, the Taku terrane is interpreted as part of Yukon–Tanana terrane, implying that an older suture must lie between the Insular and Intermontane superterranes in that region (Kapp and Gehrels 1998; Gehrels 2002; Giesler et al. 2016) and to the south (Crawford et al. 1987). Overall, metamorphic grade and deformation increase from west to east, reaching their peak in the high-grade gneiss complex east of the Great Tonalite Sill complex within the Coastal batholith (Brew et al. 1989).

Cohen and Lundberg (1993) demonstrated that rocks of the Gravina basin are dominantly volcaniclastic wackes and argued that they were derived from an arc terrane, which is commonly inferred to have been located to the west. More recent studies of the sedimentary rocks in the main outcrop belt, referred to as the western facies, and those in the eastern belt, showed that each belt contains different detrital zircon assemblages (Supplementary Fig. S8[2]). The western facies contains three main populations of 417–411, 165–140, and 120–105 Ma detrital zircons, whereas rocks of the eastern facies yield a pronounced Jurassic peak of 156 Ma with smaller groups of 380–310, 560–520, 1310–920, and 1955–1755 Ma, but none of Cretaceous age (Kapp and Gehrels 1998; Yokelson et al. 2015). The 120–105 Ma zircons in the western facies were likely derived from plutons of the Muir–Chichagof suite of biotite–hornblende granodioritic, tonalitic, and gabbroic plutons, located mainly to the west, along with the Jurassic 165–145 Ma Chilkut–Chichagof plutons (Brew and Morrell 1983), which are the likely source for the Jurassic detrital zircons in the western parts of the trough. Several 110–105 Ma Alaska-type mafic–ultramafic bodies crop out along the belt and attest to mafic arc magmatism (Himmelberg and Loney 1995; Rubin and Saleeby 2000). A dioritic pluton, the Jualin diorite (Supplementary Fig. S8[2]), is unconformably overlain by conglomerate holding boulders of the diorite, as well as a variety of metavolcanic and metasedimentary clasts (Redman 1984). The pluton was dated by U–Pb on zircon to be 105 ± 1 Ma (Kapp and Gehrels 1998), so provides a maximum age for the deposition of the upper units of the sedimentary succession within the Gravina basin, as well as the subsequent deformation and metamorphism.

Fig. 10. Geological sketch map of south-central Alaska illustrating the distribution of some of the geological features discussed in the text. CA, Chisana arc. Modified from Trop and Ridgway (2007). Note location of Fig. 11. [Colour online.]

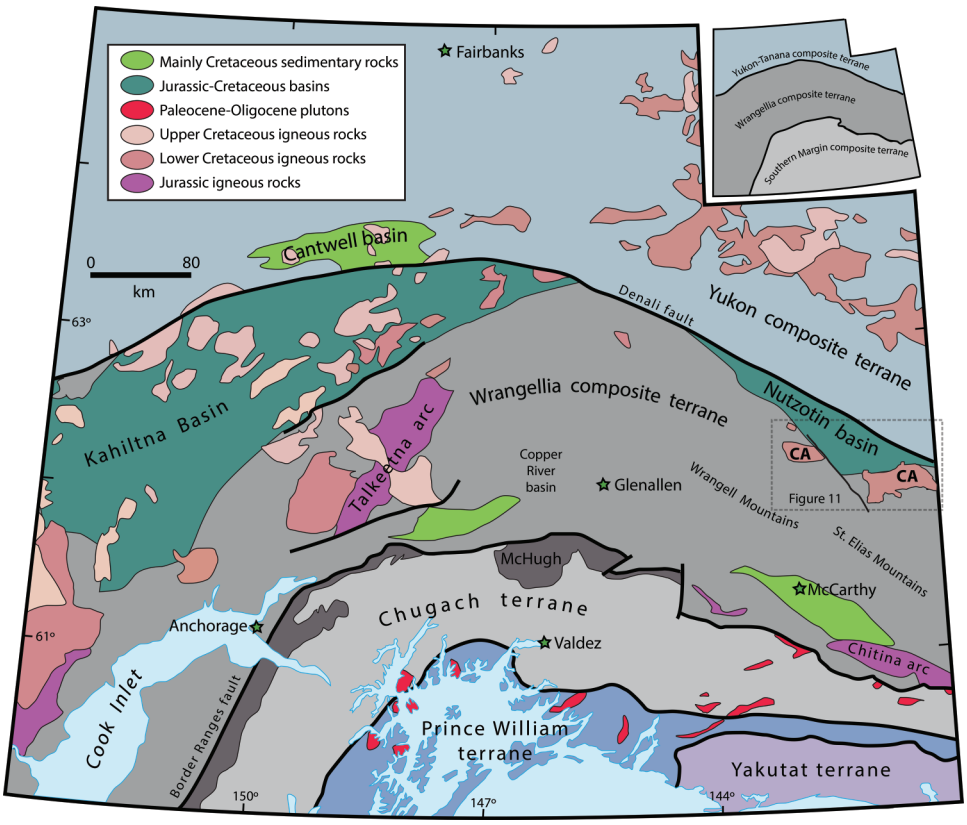

Haeussler (1992) studied the structural development of the basin and found evidence for an early extensional phase characterized by normal faults, followed by younger isoclinal folds, thrust faults, and at least one 12 km wide shear zone. The eastern margin of the basin is tectonic with east-dipping reverse, or thrust, faults placing high-grade rocks of the Coast batholith and slices of Taku terrane over rocks of the Gravina Basin to the west (Rubin et al. 1990). Eastern facies rocks are typically at higher metamorphic grade, as they commonly contain kyanite or sillimanite and are more deformed than western facies rocks. They are dominated by Jurassic detrital zircons: Lower Cretaceous zircons are absent (Yokelson et al. 2015). The dramatic grade jump from west to east suggests that the westerly vergent faults are not thrusts but are reverse faults.

Following deposition of the Gravina sequence, the rocks were metamorphosed, deformed, and then intruded by a swarm of post-deformational 95–90 Ma plutons (Haeussler 1992; Himmelberg et al. 2004; Gehrels et al. 2009). To the east, many 99–89 Ma plutons were emplaced in the high-grade hinterland of the orogen (Gehrels et al. 2009; Girardi et al. 2012). The plutons are generally plagioclase–seriate bodies of biotite–hornblende granodiorite and tonalite (Douglass et al. 1989; Himmelberg et al. 2004). Their emplacement age is poorly constrained by modern standards but appears to be between 102 and 88 Ma. The largest is the post-tectonic Moth Bay pluton (Supplementary Fig. S8[2]) (Cook et al. 1991; Saleeby 2000; Rubin and Saleeby 1987, 2000) from which a sample yielded U–Pb analyses of highly discordant zircon fractions with an age of 102 +3/−2 Ma, and a $^{40}Ar/^{39}Ar$ date of 96 ± 1 Ma (Sutter and Crawford 1985). Other plutons were dated as 90.5 and 88.5 Ma with K–Ar ages of 93–80 Ma (Saleeby 2000). The Moth Bay pluton postdates deformation and metamorphism of the schists and is a biotite–epidote–hornblende tonalite emplaced at about 9 kbar on the basis of geobarometry in kyanite–sillimanite-bearing schists in the aureole and Al-content in hornblende from the pluton (Cook et al. 1991). These data collectively demonstrate that the Gravina basin was inverted, thickened, cut by plutons, and exhumed — all in <10 million years. Sparse trace element geochemistry is only available for a few samples from the Moth Bay body and they plot as post-collisional rocks (Supplementary Fig. S8[2]).

Wrangellia – North America collision in Alaska

To the north, the Peninsular Ranges orogen continues around the Gulf of Alaska more or less parallel to its arcuate shoreline. There, an older Jurassic collision between the Peninsular and Wrangellian terranes formed what is commonly referred to as the Wrangellia composite terrane (Trop and Ridgway 2007). The area is transected and complicated by younger strike slip faults, such as the Border Ranges and Denali faults, both of which have poorly constrained displacement. The Wrangellia composite terrane is interpreted to have collided with the more northerly Yukon–Tanana terrane during closure of the siliciclastic Kahiltna basin in a double northward-dipping tectonic scheme (Pavlis et al. 2019, 2020) or in a two-phase hypothesis involving southward subduction during the Jurassic within the basin, followed by northward-directed subduction along the south side of the Wrangellia composite terrane after the collision (Sigloch and Mihalynuk 2020).

The relatively low grade Wrangellian terrane (Fig. 10) comprises carbonates and a 1–3.5 km thickness of dominantly subaerial high-Ti pillow and subaerial basalts (Lassiter et al. 1995; Greene et al. 2008). They overlie volcanic and sedimentary rocks of the Permian Skolai Group (Trop et al. 2002). Following the

Fig. 11. Geologic sketch map showing distribution and ages of 133–100 Ma Chisana arc rocks sitting unconformably upon deformed rocks of the Nutzotin basin and Wrangellia (modified from Richter et al. 2006 and Manselle 2019 with additional data from Snyder and Hart 2007). Note that both volcanic (green) and plutonic (brick red) rocks plot in the arc field on a Nb vs. Y discrimination diagram of Hildebrand and Whalen (2017). See Fig. 10 for location. bio, biotite; hbd, hornblende; WMGS, White Mountain granitoid suite. [Colour online.]

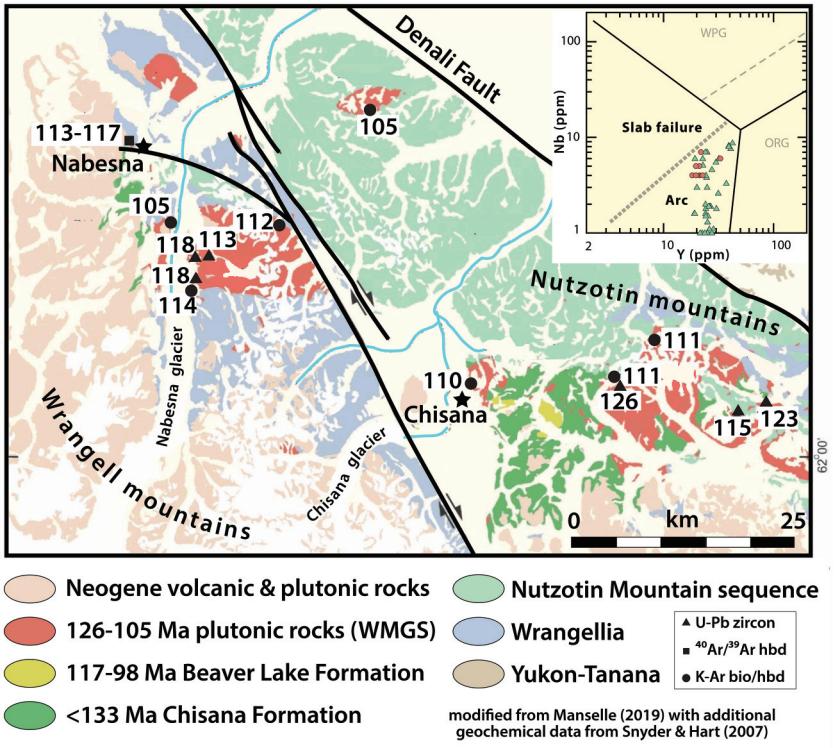

collision of Wrangellia with the Peninsular terrane, the amalgamated terrane contained a variety of Jurassic rocks, including the volcano-plutonic 202–169 Ma Talkeetna (DeBari and Coleman 1989; Clift et al. 2005; Rioux et al. 2007) and Chinitna arcs (Plafker et al. 1989), as well as mid-Jurassic sedimentary rocks of the Tuxedni Group (Trop et al. 2005; Amato et al. 2007). We plotted unpublished geochemistry from plutonic rocks associated with the Talkeetna arc (M. Rioux, personal communication, 2019) on our discrimination diagrams and found that most have arc geochemistry, but one 152.7 ± 1.3 Ma pluton, mapped as transecting the Peninsular–Wrangellia suture (Rioux et al. 2007), displays typical post-collisional slab break-off characteristics with Sm/Y > 2.5, Sr/Y > 20, and Nb/Y > 0.4. Thus, map relations, timing, and geochemistry provide a minimum age for the Penisular–Wrangellian collision. The youngest arc-like pluton dated by Rioux et al. (2007) is 168.8 Ma and provides a maximum age for collision. Following the Jurassic collision and the Early Cretaceous opening of the Kahiltna basin, rocks of the Wrangellia composite terrane lay to the south of the Kahiltna basin, whereas rocks of the Yukon composite terrane lay to the north, although the precise extent of the terrane is uncertain due to unresolved displacement on the Denali fault. We start by examining the Cretaceous rocks and their interactions, then examine the Jurassic collision as it is similar in many respects to the Peninsular Ranges orogeny.

Chisana arc

Wrangellia contains the only evidence within the region for an arc complex (Chisana arc) during the Early Cretaceous. This 133–98 Ma arc, is best exposed in the Nutzotin Mountains of south-central Alaska, where andesitic lavas, along with subordinate volcaniclastic rocks, unconformably overlie deformed sedimentary rocks of the Nutzotin basin (Fig. 11), and are intruded by calc-alkaline plutons of the White Mountain granitoid suite (Manselle 2019; Snyder and Hart 2007; Trop et al. 2020). These relations, plus detrital zircon ages from sedimentary rocks of the dismembered Dezadeaash–Nutzotin basin (Lowey 1998, 2019; Fasulo 2019) — all older than about 133 Ma — demonstrate that the Nutzotzin and Kahiltna basins were not fault-bounded segments of the same basin, or even the Gravina basin to the south, as commonly claimed (Sigloch and Mihalynuk 2017, 2020; Pavlis et al. 2019, 2020). However, correlation of the Nutzotin basin with the coeval Peñasquitos, Cucurpe, and Mariposa formations farther south is possible. These successions all carry the Tithonian bivalve, *Buchia piochii*, and were deformed by around 130 Ma, prior to the deposition of overlying rocks, which were basinal and (or) arc rocks of the Peninsular Ranges orogen (Mauel et al. 2011; Peryam et al. 2012; Kimbrough et al. 2014; Manuszak et al. 2007; Manselle 2019). Rocks of the Gravina basin show a clear gap in detrital zircon ages between 147 and 122 Ma (Yokelson et al. 2015), but there is no obvious break in the stratigraphic section (Supplementary Fig. S8[2]).

Farther west, a number of Early Cretaceous tonalite to trondhjemitic plutons (123 ± 2 Ma) intrude uppermost Middle Jurassic metasedimentary rocks of Wrangellia (Labrado et al. 2015) and may also represent arc magmas. In a recent study, using sparse geochemistry and isotopes from the intrusions, Mahar et al. (2019) suggested the intrusions might have been emplaced above a slab-window as they are isotopically primitive low-K calc-alkaline rocks. Although most of their analyzed samples show elevated Sr/Y values, all of them have Sm/Yb <2.5, which suggests that they are arc magmas (Hildebrand and Whalen 2017).

Kahiltna trough

The now collapsed and inverted Kahiltna trough (Fig. 10) lies to the north (current coordinates) and sits between more outboard Wrangellia and the inboard metamorphic Yukon–Tanana and Farewell terranes (Box et al. 2019; Kalbas et al. 2007; Trop and

Fig. 12. Modified stratigraphic chart from Amato et al. (2013), showing their concept of the relative locations of different stratigraphic packages through time. The coloured dots represent their maximum depositional ages from detrital suites and clearly show the >50 million year gap in sedimentation, which because they held to a northerly directed subduction model, were forced to attribute to subduction erosion. Our model does not require a phantom accretionary prism because we found that subduction was southerly on the other side of Wrangellia. We attribute the sedimentation of the McHugh Creek assemblage to post-collisional exhumation on the outboard side of the collision zone. The 100–90 Ma detrital zircons were derived from post-collisional plutons emplaced following slab break-off, similar to those found in areas to the south. [Colour online.]

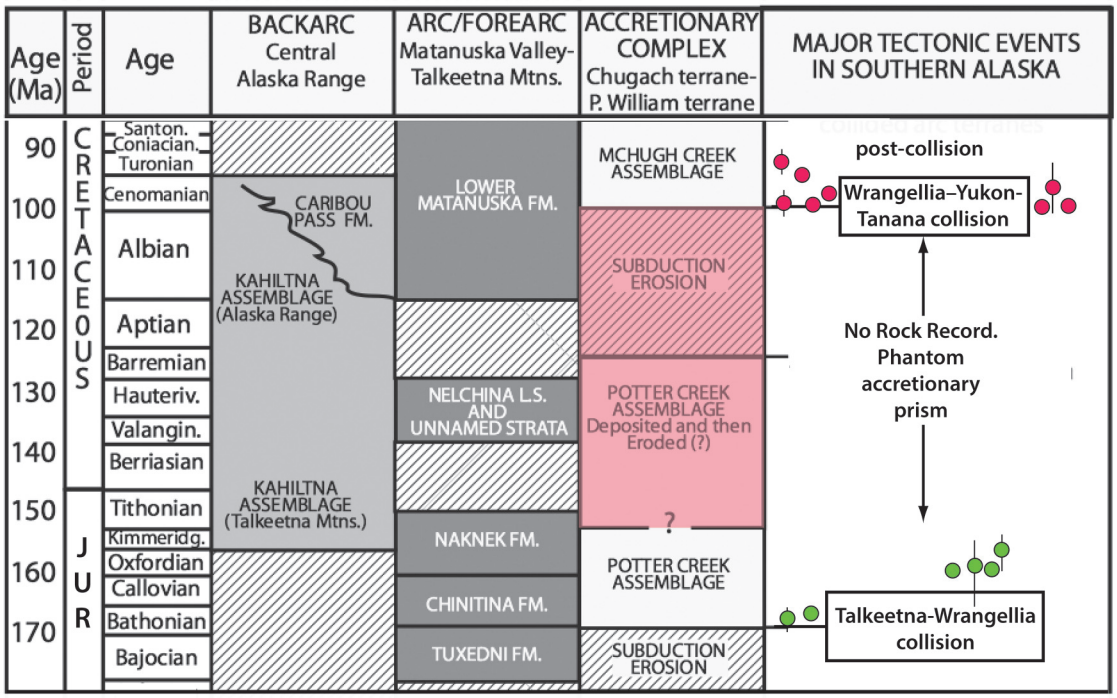

Ridgway 2007; Hampton et al. 2007, 2010). Hampton et al. (2010) measured eight sections through the basin, collected and dated detrital zircons, and found MDAs based on the weighted mean of the three youngest zircons to range from 143 to 102 Ma. Box et al. (2019), on the basis of sandstone petrography and detrital zircon age populations, divided the rocks of the basin, which are dominantly turbiditic, into three distinct petrofacies, the lower two of which remained as separate deposystems until the Late Cretaceous: (*i*) a northwestern belt with dominantly quartzose debris with MDAs all older than 100 Ma, typically 107–103 Ma; (*ii*) a southeastern belt characterized by igneous debris with detrital zircon age peaks ranging from about 170 to 142 Ma, with MDAs ranging from 146 to 103 Ma; and (*iii*) a younger belt, also dominated by igneous debris and with Late Cretaceous detrital zircon age peaks, in places accompanied by a broad 160 Ma peak, ash beds dated at 97 and 93 Ma, and Cenomanian–Turonian MDAs. Similar to more southern sectors of the basin, such as the Gravina and Arperos sectors, the basin must have been sufficiently wide, or configured such that debris from either side did not cross the basin and intermingle in any significant abundance (Box et al. 2019).

There were two obvious episodes of deformation of the basin-fill rocks, with the oldest bracketed between 103 and 97 Ma and consisting of southeast-dipping thrust faults with tight overturned folds that verge northwest, which represent deformation during the Peninsular Ranges orogeny; whereas the youngest is bracketed to be about 80 Ma (Box et al. 2019) and probably represents Laramide deformation.

Yukon–Tanana and Farewell terranes

North of the Kahiltna basin and across the Denali fault, the metamorphic Yukon–Tanana terrane and the Farewell terrane, collectively referred to as the Yukon Composite terrane (Fig. 10), are both mainly composed of Paleozoic metasedimentary and meta-igneous rocks. The more westerly Farewell terrane comprises Cambrian to Pennsylvanian carbonates, Devonian and Triassic phosphatic black shale, barite, and sandstone, with a variety of gabbroic sills and pillowed basalts (Bundtzen and Gilbert 1983; Bradley et al. 2006). The Yukon–Tanana terrane sensu lato is highly variable with complex relations and generally poor outcrop, but it is dominated by Paleozoic greenschist to amphibolite grade metamorphic rocks, in places tectonically overlain by Mississippian to Triassic oceanic igneous and metamorphic rocks (Templeman-Kluit 1979; Dusel-Bacon et al. 2006; Colpron et al. 2006). In the extreme southeastern sector of the terrane, east of Whitehorse and crossing into the Selwyn basin, are some 115–95 Ma plutons and ignimbrites with typical slab failure geochemistry; but they are likely related to the Sevier orogenic event (Hart et al. 2004; Hildebrand 2015; Hildebrand and Whalen 2017).

Cu–Au porphyry mineralization is commonly associated with slab break-off magmatism (Solomon 1990; de Boorder et al. 1998; Cloos and Housh 2008; Hildebrand 2009; Hou et al. 2015; Hildebrand and Whalen 2017) and even though the heavily mineralized 99–88 Ma Pebble porphyry complex (Supplementary Fig. S9[2]) lies several hundred kilometres to the west, it is likely also a 100–85 Ma slab failure plutonic suite (Olson 2015) related to the Wrangellia – Yukon–Tanana – Farewell composite collision.

McHugh complex

An outboard trough, exposed along the south side of Wrangellia composite terrane as the McHugh complex, was active after 101 Ma when it received detritus, including 99–82 Ma detrital zircons (Amato and Pavlis 2010; Amato et al. 2013). These workers

interpreted the McHugh complex as deposited within a fore-arc setting (Fig. 12), but temporally, spatially, and compositionally the basin is similar to the Upper Cretaceous Valle Formation of Baja California (Kimbrough et al. 2001), the Upper Cretaceous Great Valley Group of central California (Mansfield 1979), and the Upper Cretaceous Nanaimo basin of southern British Columbia (Matthews et al. 2017), all three of which developed behind the east-facing arc on the upper plate and contain Cenomanian–Turonian debris eroded from the pluton-riddled and exhuming hinterland. Additionally, plutons of the 123 ± 2 Ma tonalite–trondhjemite suite (Mahar et al. 2019), which on the basis of sparse geochemistry could be arc rocks, sit just inboard of the McHugh rocks, similar to other arc suites to the south.

As suggested earlier, these sedimentary rocks might typically be deposited in outboard troughs, or perhaps open ocean, during the later stages of arc-continent collision and mark slab failure, for it is at that time that the partially subducted lower plate is freed of its oceanic anchor, so rises rapidly (see Supplementary Fig. S10[2]). In the cases along the western margin of the Peninsular Ranges orogen, the reverse faults that separate the higher-grade hinterland from the lower-grade back-arc region probably approximate, or mark, the leading edge of the torn lower plate as it rose and exhumed the orogenic hinterland. Sedimentary debris was shed from the exhuming hinterland located to the east and deposited west of the reverse faults.

Summary of Wrangellian – Yukon–Tanana collision: implications for other models

The Cretaceous geology of south-central Alaskan parallels that seen farther south and so we include it in the Peninsular Ranges orogen. In Alaska, the Early Cretaceous seaway, recorded by strata of the Kahiltna basin, where contrasting clastic debris was shed from opposite flanks of the trough, coupled with the Early Cretaceous Chisana arc sitting on lower-grade Wrangellian basement lying to the south, and contrasting with the higher-grade metamorphic Yukon composite terrane, devoid of Early Cretaceous arc rocks, are typical relations of the Peninsular Ranges orogen farther south. The south-dipping, northward-vergent thrust faults in the basin indicate that the Yukon composite terrane was the lower plate as the basin closed, a scenario consistent with the contrasting metamorphic grades between this terrane and Wrangellia. Some possible post-collisional slab failure plutons, such as the Tok-Tetlin, the Cheslina, and the Gardiner Creek plutons have ages ranging from 94 to 88 Ma (Richter et al. 1975; Hart et al. 2004), but crop out north of the Denali fault, so may have been located elsewhere during the Upper Cretaceous.

Overall, the conjectures of Pavlis et al. (2019, 2020) fit well with the standard paradigm of eastward-dipping subduction, but are inconsistent with the geological record. For example, their model invokes two northward-dipping subduction zones, one beneath Wrangellia and another beneath Yukon–Tanana, but there is no evidence for an Early Cretaceous arc on Yukon–Tanana terrane, nor is there any evidence for an accretionary prism along the southern side of Wrangellia over the critical 150–100 Ma interval (Fig. 12). We claim that our model for west-dipping subduction beneath an Early Cretaceous arc sitting on Wrangellian basement within the Peninsular Ranges composite terrane, and attempted subduction of the higher-grade Yukon–Tanana – Farewell block during the Peninsular Ranges orogeny, is more compatible with the known geology. For example, we are not compelled to invoke any processes, such as subduction erosion, to explain the absence of an accretionary prism.

The model of Sigloch and Mihalynuk (2017, 2020) focuses largely on the Jurassic, and so does not incorporate the critical evidence for Early Cretaceous rifting and development of the arc on the western Peninsular Ranges composite terrane (Hildebrand and Whalen 2014*b*, 2017). Considerable geological evidence for the development of the Early Cretaceous seaway negates the requirement for eastward-dipping subduction beneath the amalgamated Jurassic North American block during the Cretaceous.

We agree with Sigloch and Mihalynuk (2017, 2020) that the Jurassic collision of the Talkeetna arc with Wrangellia was, in current coordinates, south-dipping (see Hildebrand 2013, p. 71). Along the north side of the Talkeetna arc, south-dipping thrust faults accompanied by deposition of clastic debris — sitting unconformably upon platformal siliciclastics and carbonate strata of Wrangellia — coarsens upward from marine mudstones and sandstones to conglomerate (Trop et al. 2002; Manuszak et al. 2007). These relations suggest that the leading edge of Wrangellia was pulled beneath the Talkeetna arc during the collision.

On the basis of our analysis of unpublished geochemical data (M. Rioux, personal communication, 2019) the youngest dated arc rock in the Talkeetna arc is a ~169 Ma quartz diorite pluton, which provides a maximum age for the collision of the arc with Wrangellia. And as noted earlier, the only post-collisional slab failure pluton yet recognized in the Talkeetna collision zone is 153 Ma, so there is a gap of some 16 million years between the youngest known arc rock (dated at 169 Ma) and the only documented post-collisional slab failure pluton. On the south side of the Talkeetna–Wrangellia collision zone, coarse 167–150 Ma batholithic debris of the Naknek Formation was shed southward from the hinterland belt as it was exhumed on north-dipping reverse faults (Trop et al. 2005). A more recent regional study of the formation (Herriott et al. 2017, 2019), including detrital zircon analyses, suggest that the trough represents the beginning of "ubiquitous batholithic provenance" generated by rapid exhumation of the plutonic roots of the Talkeetna arc with tectonism as the driving force. This scenario is precisely what occurs on the opposite side from the collisional suture and fore arc in the outboard back-arc setting along the Peninsular Ranges orogen from Mexico to Alaska or in younger arc-continent collisions like Papua, New Guinea (Supplementary Fig. S10[2]).

Thus, in contrast to Pavlis et al. (2019, 2020) and Sigloch and Mihalynuk (2020), we favour westerly dipping subduction for both the Jurassic and the Cretaceous collisions involving Wrangellia. We note that following collisions, coarse debris, including abundant material largely derived from post-collisional plutons and their wall rocks, was shed outboard (westward) from the hinterland belt as it was rapidly exhumed. In the Sierran paradigm of long-lived eastward subduction, these basins are considered fore-arc basins, but in our model, they form after collision, not when the arc was active. Thus, the basins should be dominated by post-collisional debris with detrital zircons largely derived from slab failure plutons rather than older arc magmatism. The spectrum of detrital zircons in the Chinitna and lower Naknek formations of the Naknek basin suggests that the Talkeetna–Wrangellian collision took place at about 167 Ma and that the stratigraphically lower Chinitna contains more arc debris (202–167 Ma) than the overlying Naknek Formation; but both formations are dominated by 161–157 Ma age peaks (Herriott et al. 2019), consistent with our back-arc model for deposition of debris from orogenic hinterlands.

Cordilleran outliers: Salinia and the Peruvian coastal batholith

Although here we progressed from south to north, we believe that another sector of the Peninsular Ranges orogen may have been dismembered by strike-slip fault(s) and is now divided between central California and coastal Peru (Hildebrand and Whalen 2014*a*). Located west of the Great Valley of California, and commonly considered by some to have formerly occupied the space between the Sierra Nevada and the Peninsular Ranges (Ducea 2001; Barbeau et al. 2005; Chapman et al. 2014), the Salinian block has long been recognized as an anomalous block (Ross 1978)

and comprises 3–7.5 kbar amphibolite–granulite facies gneiss and schist lacking pure quartzite and carbonate rocks characteristic of the North American margin (Ross 1977), all cut by deformed plutons in the age range of 130–103 Ma, as well as more easterly, nondeformed 100–82 Ma plutons ranging in composition from gabbro to granodiorite (Mattinson 1978, 1990; James 1992; Kistler and Champion 2001; Kidder et al. 2003; Chapman et al. 2014). The plutons with trace element geochemistry plot as slab failure rocks (Hildebrand and Whalen 2017, p. 37), but the Salinian block does not contain low-grade, pre-100 Ma volcanics and only a few 130–103 Ma arc plutons, typical of other sectors of the Peninsular Ranges orogen. This led Hildebrand and Whalen (2014*a*) to suggest that it once belonged with the Coastal batholith of Peru, which some recognized to be another anomalous block (Loewy et al. 2004). There, 7–9 km of relatively low-grade arc rocks, the mainly latest Aptian–Albian rocks of the Casma and related groups, were deposited in the Huarmey–Cañete trough (Cobbing 1978; Atherton et al. 1985; Pitcher 1993; de Haller et al. 2006), and were deformed at 100 Ma. Although the batholith contains a few post-collisional plutons, an exhumed metamorphic hinterland and voluminous 100–85 Ma slab failure plutons are absent.

We showed earlier that, except for a small gap in the Mojave Desert where the Peninsular Ranges orogen was transected by the Late Cretaceous – Paleogene Laramide orogen, the thrusts and post-collisional plutons of the Peninsular Ranges orogen are continuous from Mexico to Utah. Thus, instead of lying between the Sierra Nevada and the Peninsular Ranges batholiths, the Salinia block was more likely located to the south, and was possibly joined with the Arequipa block and its cover of Casma volcanics, which, on the basis of magmatic ages and deformation, collectively formed another sector of the Peninsular Ranges orogen (Hildebrand and Whalen 2014*a*, 2017). Although conflicting paleomagnetic data for the Salinian block exist (Champion et al. 1984; Whidden et al. 1998), paleontological data suggest that the faunal assemblage of Salinia is a reasonable match with those in the Peninsular Ranges of southern California (Elder and Saul 1993), and they are considered to be far-traveled rocks (Hagstrum et al. 1985).

Surface geology and mantle tomography

Three of the Jurassic and two — or possibly all — of the three Cretaceous arc-continent collisions were apparently built above westerly dipping subduction zones. The three Jurassic collisions, readily resolved in the western Sierra Nevada (Hildebrand 2013), likely occurred offshore from North America (Johnston 2008), and the initial docking of the partly assembled ribbon continent of Hildebrand with North America occurred during the Sevier orogeny at 124–120 Ma (Hildebrand 2013, 2014). This event was followed by the Peninsular Ranges orogeny at 100 Ma, and the Laramide during the Campanian, none of which produced an arc on cratonic North America.

Since the early 90s, a huge, steeply dipping fast zone in the mantle beneath eastern North America was recognized by tomography and interpreted as a fossil subducted slab (Grand 1994). As North America migrated westward during the opening of the Atlantic Ocean, it overrode the torn and sinking oceanic lithosphere previously located to the west. Sigloch and Mihalynuk (2013) showed how westerly — but not easterly — dipping slabs, could form steeply inclined to vertical slab walls in the mantle as North America migrated westward.

The immense size of the East Coast fast tomographic anomaly (Sigloch 2011), with a width of 8–10 degrees of longitude, which at 40°N are 85 km/degree, translate to a width of 680–850 km. Commonly, the torn and sinking slabs are shown as buckling concertina-fashion as they sink (Lee and King 2011; Sigloch and Mihalynuk 2017) to produce the required width; but in this case the anomaly probably represents an amalgamation of all the Jurassic and Cretaceous slabs, because the thickness of older oceanic lithosphere is about 80–100 km (Hamza and Vieira 2012). If subducted slabs are indeed amalgamated — or appear to be so at the current resolution of mantle tomography — and new ocean basins opened within the Cordillera, as documented here, then attempts to match mantle tomography with surface geology of the Cordillera cannot be quantitatively evaluated as claimed (Clennett et al. 2020).

Whereas the amalgamated, or tomographically irresolvable slabs, imply a long-lived zone of westerly subduction, Hildebrand and Whalen (2014*a*) noted the two long-lived mantle upwelling zones, Jason and Tuzo (Burke and Torsvik 2004; Torsvik et al. 2008; Burke 2011; Spencer et al. 2019), and postulated that a complimentary long-lived mantle downwelling zone existed to the west of North America. They speculated that it may have formed a boundary between the Panthalassic and Pacific realms, and when the various arcs and other fragments that had accumulated above the downwelling zone collided with the Americas, Panthalassa ceased to exist. The continent then overrode the torn slabs beneath the accreted collage. We wonder whether the demise of Panthalassa marks the switchover from west-dipping subduction, which appears to have dominated Panthalassic–Cordilleran interactions, to the current eastwardly dipping Pacific plates beneath the Americas.

Conclusions

In this two-part contribution, we summarized our geological evidence over the length of the Cordillera to demonstrate that the paradigm of long-lived eastward subduction runs counter to the bulk of evidence. We conclude with the following points.

1. The Peninsular Ranges orogen is a ~100 Ma orogenic belt that extends from Mexico to Alaska and beyond. The orogen formed when a trough, open for about 35 million years along the western margin of North America, closed by westerly subduction, juxtaposing a Lower Cretaceous arc complex built on the ribbon-like Peninsular Ranges composite terrane along the western side of the trough, over a passive continental margin, which was locally capped by a west-facing carbonate platform developed on the eastern North American side of the trough (Fig. 13).
2. Within a million years or so following the collision, the hinterland was exhumed and intruded by gregarious tonalite–granodiorite–granite plutons, which were emplaced over a period of 10–15 million years. The timing suggests that the plutons and exhumation formed in tandem when the oceanic lithosphere broke off from the partially subducted North American plate.
3. Because the trough formed after at least one Jurassic collision and its post-collisional magmatism, many different rocks and terranes formerly attached to North America were rifted and separated at about 135 Ma, only to return at 100 Ma, likely in different places than their original locations.
4. The large mid-Cretaceous batholiths of the North American Cordillera are composed of two contrasting magmatic suites derived from distinct mantle sources and emplaced at different times. The older arc suite, which developed on the Peninsular Ranges composite terrane from Mexico to Alaska, represents a generally low-standing marine arc built on thinned lithosphere over a westward-dipping subduction zone, whereas the younger suite was post-collisional and invaded the orogenic hinterland during exhumation due to break-off and melting of the subducting slab.
5. The so-called “flare-up” events in Cordilleran arcs are the result of collision followed by slab break-off, not arc magmatism.
6. Those who utilize Andino-type, or cyclic hi-flux, models for the development of Cordilleran batholiths, fail to recognize that the transition from arc magmatism to post-collisional

Fig. 13. Our tectonic plate scale model for the Peninsular Ranges orogeny involves closure of a Lower Cretaceous seaway by west-directed subduction and arc magmatism from ~130 Ma until the collision of the arc with North America at 100 Ma. The competing buoyancies of the oceanic and cratonic lithosphere led to rapid tearing and break-off of the subducted plate and an influx of 99–84 Ma post-collisional magmatism during exhumation of the orogenic hinterland. During exhumation and plutonism, mainly 99–90 Ma debris was shed westward into the old back-arc region. These relations hold over the length of the Cordillera, from southern Mexico to Alaska. PЄ, Precambrian. [Colour online.]

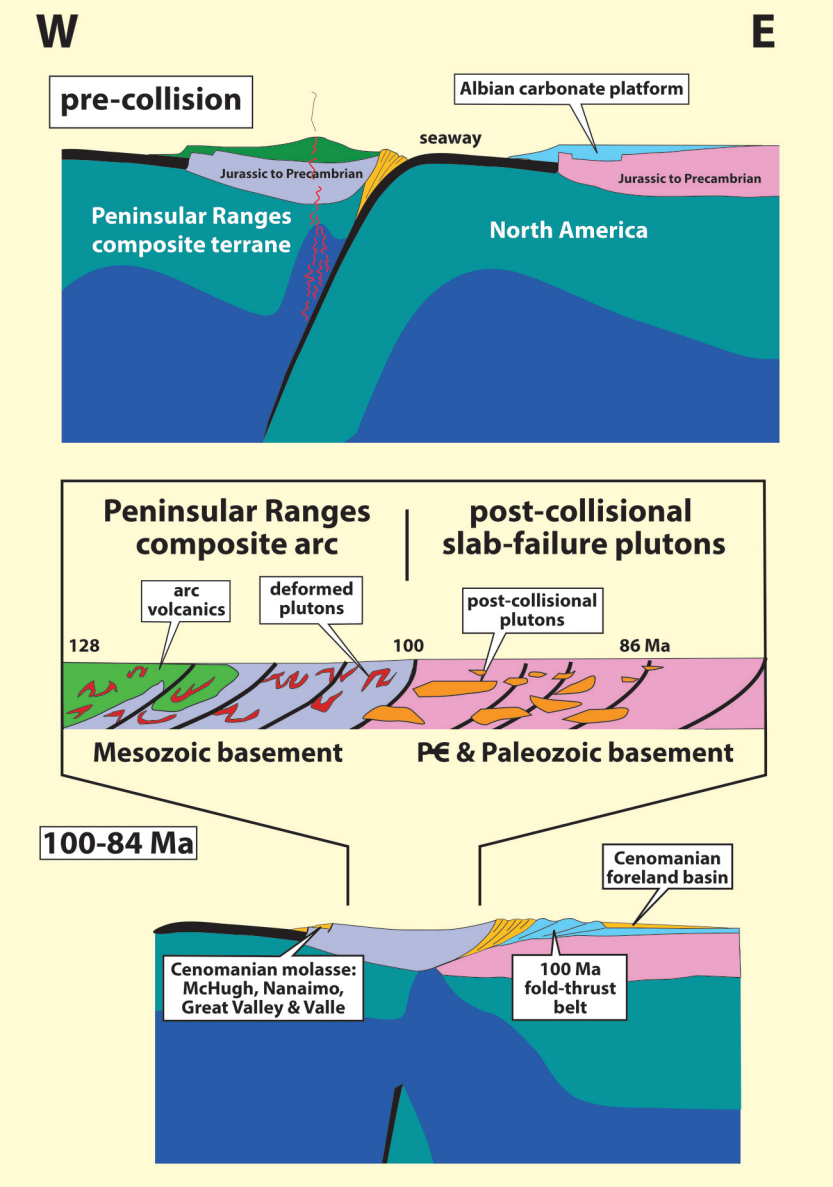

hi-flux magmatism occurred rapidly, perhaps within a million years, so that there is simply no time to thicken the crust by underplating or for heat transfer by conduction to melt underthrust cratonic material.

7. The post-collisional magmas appear to have been derived from melting of the basaltic–gabbroic upper part of the subducted oceanic lithosphere augmented by fractional melting of the SCLM as magmas rose toward the crust. Thus, slab break-off magmas have trace element concentrations and ratios similar to slab window rocks, but where they rise through old and enriched cratonic lithosphere they have enriched radiogenic isotopes.
8. There is no compelling evidence along the entire western edge of the Peninsular Ranges composite terrane for a fore-arc basin or accretionary prism during Early Cretaceous arc magmatism. Instead, voluminous quantities of material were shed westward into the back-arc region after the 100 Ma collision and termination of arc magmatism, when abundant detrital zircons from the 100–90 Ma post-collisional plutons document rapid exhumation of the orogenic hinterland.
9. Retro-arc models for the Sevier thrust-fold belt must be reconsidered, as there was no eastward subduction beneath North America at about 120 Ma when the Sevier thrusting initiated. Instead, the 130–100 Ma Alisitos and related arc segments involved in the Peninsular Ranges orogeny were built offshore above westerly, not easterly, dipping subduction zones.

10. We suggest that the huge East Coast tomographic anomaly, which underlies eastern North America, could represent several amalgamated slabs rather than a single slab that buckled. In our conception, the three westerly subducted Jurassic slabs occurred offshore beneath the ribbon continent, but failure of the west-dipping slabs, represented by the Sevier and Peninsular Ranges orogens, occurred during and after the 120 Ma Sevier collision of the ribbon with North America. As North America migrated westward, it collided with the ribbon continent and overrode the Jurassic slabs: the two Cretaceous slabs were added to the mass of subducted slabs shortly afterwards because they could not penetrate the slab wall.

Acknowledgements

Paul Link and Tim Lawton helped with detrital zircon plotting and discussions. Matt Rioux generously shared geochemical analyses from the Talkeetna plutonic rocks. Terry Pavlis is thanked for providing reprints and pointers to critical papers on Alaskan geology. Phone conversations during Covid-19 sequestration on the geology of Nevada with C.J. Northrup were very useful. Bob Hatcher and Brendan Murphy commented on an early draft of the manuscript. Since 2014, ongoing discussions with Tim Lawton on all matters of foredeeps and basins have been incredibly helpful. Thoughtful reviews by Michaelangelo Martini and Basil Tikoff helped us to improve both papers. Eldridge, this is for you!

References

Amato, J.M., and Pavlis, T.L. 2010. Detrital zircon ages from the Chugach terrane, southern Alaska, reveal multiple episodes of accretion and erosion in a subduction complex. Geology, **38**: 459–462. doi:10.1130/G30719.1.

Amato, J.M., Rioux, M.E., Kelemen, P.B., Gehrels, G.E., Clift, P.D., Pavlis, T.L., and Draut, A.E. 2007. U-Pb geochronology of volcanic rocks from the Jurassic Talkeetna Formation and detrital zircons from prearc and postarc sequences: Implications for the age of magmatism and inheritance in the Talkeetna arc. *In* Tectonic growth of a collisional continental margin: crustal evolution of south-central Alaska Ridgway. *Edited by* K.D. Trop, J.M. Glen, and J.M. O'Neill. Geological Society of America Special Paper 431. pp. 253–271. doi:10.1130/2007.2431(11).

Amato, J.M., Pavlis, T.L., Clift, P.D., Kochelek, E.J., Hecker, J.P., Worthman, C.M., and Day, E.M. 2013. Architecture of the Chugach accretionary complex as revealed by detrital zircon ages and lithologic variations: Evidence for Mesozoic subduction erosion in south-central Alaska. Geological Society of America Bulletin, **125**: 1891–1911. doi:10.1130/B30818.1.

Armstrong, R.L., Taubeneck, W.H., and Hales, P.O. 1977. Rb-Sr and K-Ar geochronometry of Mesozoic granitic rocks and their Sr isotopie composition, Oregon, Washington, and Idaho. Geological Society of America Bulletin, **88**: 397–411. doi:10.1130/0016-7606(1977)88<397:RAKGOM>2.0.CO;2.

Arthur, A.J., Smith, P.L., Monger, J.W.H., and Tipper, H.W. 1993. Mesozoic stratigraphy and Jurassic paleontology west of Harrison Lake, southwestern British Columbia. Geological Survey of Canada Bulletin 441. 62pp.

Atherton, M.P., Warden, V., and Sanderson, L.M. 1985. The Mesozoic marginal basin of central Peru: A geochemical study of within-plate-edge volcanism, *In* Magmatism at a Plate Edge: the Peruvian Andes. *Edited by* W.S. Pitcher, M.P. Atherton, E.J. Cobbing, and R.B. Beckinsale, R.B. Blackie Halstead Press, Glasgow, pp. 47–58.

Barbeau, D.L., Jr., Ducea, M.N., Gehrels, G.E., Kidder, S., Wetmore, P.H., and Saleeby, J.B. 2005. U–Pb detrital-zircon geochronology of northern Salinian basement and cover rocks. Geological Society of America Bulletin, **117**: 466–481. doi:10.1130/B25496.1.

Benford, B., Crowley, J., Schmitz, M., Northrup, C.J., and Tikoff, B. 2010. Mesozoic magmatism and deformation in the northern Owyhee Mountains, Idaho: Implications of along-zone variations for the western Idaho shear zone. Lithosphere, **2**(2): 93–118. doi:10.1130/L76.1.

Berg, H.C., Jones D.L., and Richter D.H. 1972. Gravina Nutzotin Belt—Tectonic significance of an upper Mesozoic sedimentary and volcanic sequence in southern and southeastern Alaska. United States Geological Survey Professional Paper 800-D. pp. D1–D24.

Box, S.E., Karl, S.M., Jones, J.V., III., Bradley, D.C., Haeussler, P.J., and O'Sullivan, P.B. 2019. Detrital zircon geochronology along a structural transect across the Kahiltna assemblage in the western Alaska Range: Implications for emplacement of the Alexander-Wrangellia-Peninsular terrane against North America. Geosphere, **15**: 1774–1735. doi:10.1130/GES02060.1.

Bradley, D.C., Dumoulin, J.A., Blodgett, R.B., Harris, A.G., Roeske, S.M., McClelland, W.C., and Layer, P.W. 2006. Geology and affinity of Alaska's Farewell terrane. Geological Society of America Abstracts with Programs, **38**(5): 12.

Brandon, M.T., Cowan, D.S., and Vance, J.A. 1988. The Late Cretaceous San Juan Thrust System, San Juan Islands, Washington. Geological Society of America Special Paper 221. 88pp. doi:10.1130/SPE221.

Braudy, N., Gaschnig, R.M., Wilford, D., Vervoort, J.D., Nelson, C.L., Davidson, C., et al. 2017. Timing and deformation conditions of the western Idaho shear zone, West Mountain, west-central Idaho. Lithosphere, **9**: 157–183. doi:10.1130/L519.1.

Brew, D.A., and Morrell, R.P. 1983. Intrusive rocks and plutonic belts of southeastern Alaska, U.S.A. *In* Circum-Pacific plutonic terranes. *Edited by* J.A. Roddick. Geological Society of America Memoir 159: pp. 171–193.

Brew, D.A., Ford, A.B., and Himmelberg, G.R. 1989. Evolution of the western part of the Coast plutonic- metamorphic complex, south-eastern Alaska, USA. *In* A summary in evolution of metamorphic belts. *Edited by* J.G. Daly, R.A. Cliff, and B.W.D. Yardley. Geological Society of London Special Publication 43. pp. 447–452.

Brown, E.H., and Dragovich, J.D. 2003. Tectonic elements and evolution of northwest Washington. Washington Division of Geology and Earth Resources, Geologic Map GM-52, 1 sheet, scale 1:625,000, with 12 p. text.

Brown, E.H., and Gehrels, G.E. 2007. Detrital zircon constraints on terrane ages and affinities and timing of orogenic events in the San Juan Islands and North Cascades, Washington. Canadian Journal of Earth Sciences, **44**(10): 1375–1396. doi:10.1139/e07-040.

Brown, E.H., and McClelland, W.C. 2000. Pluton emplacement by sheeting and vertical ballooning in part of the southeast Coast Plutonic Complex, British Columbia. Geological Society of America Bulletin, **112**: 708–719. doi:10.1130/0016-7606(2000)112<708:PEBSAV>2.0.CO;2.

Brown, E.H., and Walker, N.W. 1993. A magma-loading model for Barrovian metamorphism in the southeast Coast Plutonic Complex, British Columbia and Washington. Geological Society of America Bulletin, **105**: 479–500. doi:10.1130/0016-7606(1993)105<0479:AMLMFB>2.3.CO;2.

Brown, E.H., Bernardi, M.L., Christenson, B.W., Cruver, J.R., Haugerud, R.A., Rady, P.M., and Sondergaard, J.N. 1981. Metamorphic facies and tectonics in part of the Cascade Range and Puget Lowland of northwestern Washington. Geological Society of America Bulletin, **92**: 170–178. doi:10.1130/0016-7606(1981)92<170:MFATIP>2.0.CO;2.

Brown, E.H., Talbot, J.L., McClelland, W.C., Feltman, J.A., Lapen, T.J., Bennett, J.D., et al. 2000. Interplay of plutonism and regional deformation in an obliquely convergent arc, southern Coast belt, British Columbia. Tectonics, **19**: 493–511. doi:10.1029/1999TC001168.

Brown, K.L., Hart, W.K., and Stuck, R.J. 2018. Temporal and geochemical signatures in granitoids of northwestern Nevada: Evidence for the continuity of the Mesozoic magmatic arc through the western Great Basin. Lithosphere, **10**: 327–350. doi:10.1130/L694.1.

Brownlee, S.J., and Renne, P.R. 2010. Thermal history of the Ecstall pluton from $^{40}Ar/^{39}Ar$ geochronology and thermal modeling. Geochimica Cosmochimica Acta, **74**: 4357–4391. doi:10.1016/j.gca.2010.04.023.

Bundtzen, T.K., and Gilbert, W.G. 1983. Outline of geology and mineral resources of the upper Kuskokwim region, Alaska. *In* Proceedings of the 1982 Symposium on Western Alaska Geology and Resource Potential. Journal of the Alaska Geological Society. Vol. 3. pp. 101–119.

Burke, K. 2011. Plate tectonics, the Wilson cycle, and mantle plumes: Geodynamics from the top. Annual Reviews, Earth and Planetary Sciences, **39**: 1–29. doi:10.1146/annurev-earth-040809-152521.

Burke, K., and Torsvik, T.H. 2004. Derivation of large igneous provinces of the past 200 million years from long-term heterogeneities in the deep mantle. Earth and Planetary Science Letters, **227**: 531–538. doi:10.1016/j.epsl.2004.09.015.

Butler, R.F., Gehrels, G.E., Baldwin, S.L., and Davidson, C. 2002. Paleomagnetism and geochronology of the Ecstall pluton in the Coast Mountains of British Columbia: Evidence for local deformation rather than large-scale transport. Journal of Geophysical Research: Solid Earth, **107**: EPM 3-1–EPM 3-13. doi:10.1029/2001JB000270.

Champion, D.E., Howell, D.G., and Gromme, C.S. 1984. Paleomagnetic and geologic data indicating 2500 km of northward displacement for the Salinian and related terranes, California. Journal of Geophysical Research: Solid Earth, **89**: 7736–7752. doi:10.1029/JB089iB09p07736.

Chapman, A.D., Ducea, M.N., Kidder, S., and Petrescu, L. 2014. Geochemical constraints on the petrogenesis of the Salinian arc, central California: Implications for the origin of intermediate magmas. Lithos, **200–201**: 126–141. doi:10.1016/j.lithos.2014.04.011.

Clennett, E.J., Sigloch, K., Mihalynuk, M.G., Seton, M., Henderson, M.A., Hosseini, K., et al. 2020. A quantitative tomotectonic plate reconstruction of western North America and the eastern Pacific basin. Geochemistry, Geophysics, Geosystems, **21**: e2020GC009117. doi:10.1029/2020GC009117.

Clift, P.D., Draut, A.E., Kelemen, P.B., Blusztajn, J., and Greene, A. 2005. Stratigraphic and geochemical evolution of an oceanic arc upper crustal section: The Jurassic Talkeetna Volcanic Formation, south- central Alaska. Geological Society of America Bulletin, **117**: 902–925. doi:10.1130/B25638.1.

Cloos, M., and Housh, T.B. 2008. Collisional delamination: Implications for porphyry-type Cu-Au ore formation in New Guinea. *In* Ores and orogenesis: Circum-Pacific tectonics, geologic evolution, and ore deposits.

Edited by J.E. Spencer and S.R. Titley. Arizona Geological Society Digest. Vol. 22. pp. 235–244.

Cobbing, E.J. 1978. The Andean geosyncline in Peru, and its distinction from Alpine geosynclines. Journal of the Geological Society, **135**: 207–218. doi:10.1144/gsjgs.135.2.0207.

Cohen, H.A., and Lundberg, N. 1993. Detrital record of the Gravina arc, southeastern Alaska: petrology and provenance of Seymour Canal Formation sandstones. Geological Society of America Bulletin, **105**: 1400–1414. doi:10.1130/0016-7606(1993)105<1400:DROTGA>2.3.CO;2.

Colpron, M., Nelson, J.L., and Murphy, D.C. 2006. A tectonostratigraphic framework for the pericratonic terranes of the northern Canadian Cordillera. *In* Paleozoic evolution and metallogeny of Pericratonic terranes at the Ancient Pacific Margin of North America, Canadian and Alaskan Cordillera. *Edited by* M. Colpron and J.L. Nelson. Geological Association of Canada Special Paper 45. pp. 1–23.

Cook, R.D., Crawford, M.L., Omar, G.I., and Crawford, W.A. 1991. Magmatism and deformation, southern Revillagigedo Island, southeastern Alaska. Geological Society of America Bulletin, **103**: 829–841. doi:10.1130/0016-7606(1991)103<0829:MADSRI>2.3.CO;2.

Crafford, A.E.J. 2007. Geologic Map of Nevada. United States Geological Survey Data Series 249, scale 1:250,000, 1 CD-ROM, 46 p., 1 plate.

Crafford, A.E.J. 2008. Paleozoic tectonic domains of Nevada: An interpretive discussion to accompany the *Geologic Map of Nevada*. Geosphere, **4**: 260–291. doi:10.1130/GES00108.1.

Crawford, M.L., and Hollister, L.S. 1982. Contrast of metamorphic and structural histories across the Work Channel lineament, Coast Plutonic Complex, British Columbia. Journal of Geophysical Research, **87**: 3849–3860. doi:10.1029/JB087iB05p03849.

Crawford, M.L., Hollister, L.S., and Woodsworth, G.J. 1987. Crustal deformation and regional metamorphism across a terrane boundary, Coast Plutonic Complex, British Columbia. Tectonics, **6**: 343–361. doi:10.1029/TC006i003p00343.

Crickmay, C.H. 1925. The geology and paleontology of the Harrison Lake District, British Columbia, together with a general review of the Jurassic faunas and stratigraphy of western North America. Ph.D. thesis, Stanford University, Stanford, California. 140pp.

Criss, R.E., and Fleck, R.J. 1987. Petrogenesis, geochronology, and hydrothermal systems of the northern Idaho Batholith and adjacent areas based on $^{18}O/^{16}O$, D/H, $^{87}Sr/^{86}Sr$, K-Ar, and $^{40}Ar/^{39}Ar$ studies. United States Geological Survey Professional Paper 1436. pp. 95–137.

DeBari, S.M., and Coleman, R.G. 1989. Examination of the deep levels of an island arc: Evidence from the Tonsina ultramafic-mafic assemblage, Tonsina, Alaska. Journal of Geophysical Research: Solid Earth, **94**: 4373–4391. doi:10.1029/JB094iB04p04373.

de Boorder, H., Spakman, W., White, S.H., and Wortel, M.J.R. 1998. Late Cenozoic mineralization, orogenic collapse and slab detachment in the European Alpine belt. Earth and Planetary Science Letters, **164**: 569–575. doi:10.1016/S0012-821X(98)00247-7.

DeCelles, P.G. 2004. Late Jurassic to Eocene evolution of the Cordilleran thrust belt and foreland basin system, western USA. American Journal of Science, **304**: 105–168. doi:10.2475/ajs.304.2.105.

de Haller, A., Corfu, F., Fontboté, L., Schaltegger, U., Barra, F., Chiaradia, M., et al. 2006. Geology, geochronology, and Hf and Pb isotope data of the Raúl-Condestable iron oxide-copper-gold deposit, central coast of Peru. Economic Geology, **101**: 281–310. doi:10.2113/gsecon-geo.101.2.281.

Dickinson, W.R. 1970. Global Tectonics. Science, **168**: 1250–1259.

Dorsey, C. 2019. Detrital zircon geochronology of the Queen Charlotte Group, Haida Gwaii, British Columbia. M.Sc. thesis, University of Calgary, Calgary, Alta. 138pp. Available from http://hdl.handle.net/1880/109489.

Dorsey, M.S. 2018. Testing the correlation of rocks east and west of the Harrison Lake Shear Zone: Implications for the eastern boundary of the Insular Superterrane. M.Sc. thesis, University of Calgary, Calgary, Alta. 116pp. Available from http://hdl.handle.net/1880/109356.

Douglass, S.L., Webster, J.H., Burrell, P.D., Lanphere, M.L., and Brew, D.A. 1989. Major-element chemistry, radiometric ages, and locations of samples from the Petersburg and parts of the Port Alexander and Sumdum quadrangles, southeastern Alaska. U.S. Geological Survey, Open-File Report 89-527. 66pp.

Dragovich, J.D., Norman. D.K., Haugerud, R.A., and Miller, R.B. 1997. Geologic map and bedrock history of the Gilbert 7.5-minute Quadrangle, Chelan and Okanogan Counties, Washington. Washington Division of Geology and Earth Resources. Geologic Map GM-46. 67pp.

Ducea, M. 2001. The California arc: Thick granitic batholiths, eclogitic residues, lithospheric-scale thrusting, and magmatic flare-ups. GSA Today, **11**: 4–10. doi:10.1130/1052-5173(2001)011<0004:TCATGB>2.0.CO;2.

Du Bray, E.A. 2007. Time, space, and composition relations among northern Nevada intrusive rocks and their metallogenic implications. Geosphere, **3**: 381–405. doi:10.1130/GES00109.1.

Dusel-Bacon, C., Hopkins, M.J., Mortensen, J.K., Dashevsky, S.S., Bressler, J.R., and Day, W.C. 2006. Paleozoic tectonic and metallogenic evolution of the pericratonic rocks of east-central Alaska and adjacent Yukon. *In* Paleozoic evolution and metallogeny of Pericratonic terranes at the Ancient Pacific Margin of North America, Canadian and Alaskan Cordillera. *Edited by* M. Colpron and J.L. Nelson. Geological Association of Canada Special Paper 45. pp. 25–74.

Elder, W.P., and Saul, L.R. 1993. Paleogeographical implications of molluscan assemblages in the Upper Cretaceous Pigeon Point Formation, California. *In* Mesozoic Paleogeography of the Western United States—II. *Edited by* G. Dunne, and K. McDougall. Pacific Section, Society of Economic Paleontologists and Mineralogists, 71: 171–186.

Enkin, R.J., Baker, J., and Mustard, P.S. 2001. Paleomagnetism of the Upper Cretaceous Nanaimo Group, southwestern Canadian Cordillera. Canadian Journal of Earth Sciences, **38**(10): 1403–1422. doi:10.1139/e01-031.

Enkin, R.J., Mahoney, J.B., and Baker, J. 2006*a*. Paleomagnetic signature of the Silverquick/Powell Creek succession, south-central British Columbia: Reaffirmation of Late Cretaceous large-scale terrane translation. *In* Paleogeography of the North American Cordillera: evidence for and against large-scale displacements. *Edited by* J.W. Haggart, R.J. Enkin, and J.W.H. Monger. Geological Association of Canada Special Paper 46. pp. 201–220.

Enkin, R.J., Johnston, S.T., Larson, K.P., and Baker, J. 2006*b*. Paleomagnetism of the 70 Ma Carmacks Group at Solitary Mountain, Yukon, confirms and extends controversial results: Further evidence for the Baja British Columbia model. *In* Paleogeography of the North American Cordillera: evidence for and against large-scale displacements. *Edited by* J.W. Haggart, R.J. Enkin, and J.W.H. Monger, Geological Association of Canada Special Paper 46. pp. 221–232.

Erdmer, P., and Mortensen, J.K. 1993. A 1200-km-long Eocene metamorphic-plutonic belt in the northwestern Cordillera—Evidence from southwest Yukon. Geology, **21**: 1039–1042. doi:10.1130/0091-7613(1993)021<1039:AKLEMP>2.3.CO;2.

Fasulo, C.R. 2019. Sedimentary record of tectonic growth along a convergent margin: Insights from detrital zircon geochronology of Mesozoic sedimentary basins and modern rivers in south-central Alaska: unpublished M.S. thesis, Purdue University, West Lafayette, Indiana. 235pp.

Fleck, R.J. 1990. Neodymium, strontium, and trace-element evidence of crustal anatexis and magma mixing in the Idaho Batholith. *In* The nature & origin of Cordilleran magmatism. *Edited by* J.L. Anderson. Geological Society of America Memoir 174. pp. 359–373.

Fleck, R.J., and Criss, R.E. 1985. Strontium and oxygen isotopic variations in Mesozoic and Tertiary plutons of central Idaho. Contributions to Mineralogy and Petrology, **90**: 291–308. doi:10.1007/BF00378269.

Fleck, R.J., and Criss, R.E. 2007. Location, age, and tectonic significance of the Western Idaho suture zone. *In* Geological studies of the Salmon River suture zone and adjoining areas, west-central Idaho and eastern Oregon. *Edited by* M.A. Kuntz and L.W. Snee. United States Geological Survey Professional Paper 1738. pp. 15–50.

Friedman, R.M., and Armstrong, R.L. 1995. Jurassic and Cretaceous geochronology of the southern Coast belt, British Columbia, 49°–50°N. *In* Jurassic Magmatism and Tectonics of the North American Cordillera. *Edited by* D. Miller and C. Busby. Geological Society of America Special Paper 299. pp. 95–139.

Friedman, R.M., Monger, J.W.H., and Tipper, H.W. 1990. Age of the Bowen Island Group, southwestern Coast Mountains, British Columbia. Canadian Journal of Earth Sciences, **27**(11): 1456–1461. doi:10.1139/e90-154.

Friedman, R.M., Tyson, T.M., and Journeay, J.M. 1992. U–Pb age of the Mt. Mason pluton in the Cairn Needle area, southern Coast Belt, British Columbia. *In* Current Research, Part A. Geological Survey of Canada Paper 92-IA. pp. 261–266.

Fuentes, F., DeCelles, P.G., Constenius, K.N., and Gehrels, G.E. 2011. Evolution of the Cordilleran foreland basin system in northwestern Montana, U.S.A. Geological Society of America Bulletin, **123**: 507–533. doi:10.1130/B30204.1.

Gaschnig, R.M., Vervoort, J.D., Lewis, R.S., and McClelland, W.C. 2010. Migrating magmatism in the northern US Cordillera: In situ U–Pb geochronology of the Idaho batholith. Contributions to Mineralogy and Petrology, **159**: 863–883. doi:10.1007/s00410-009-0459-5.

Gehrels, G., Rusmore, M., Woodsworth, G., Crawford, M., Andronicos, C., Hollister, L., et al. 2009. U-Th-Pb geochronology of the Coast Mountains Batholith in north-coastal British Columbia: Constraints on age, petrogenesis, and tectonic evolution. Geological Society of America Bulletin, **121**: 1341–1361. doi:10.1130/B26404.1.

Gehrels, G.E. 2002. Detrital zircon geochronology of the Taku terrane, southeast Alaska. Canadian Journal of Earth Sciences, **39**(6): 921–931. doi:10.1139/e02-002.

Gibson, H.D., and Monger, J.W.H., 2014. The Cretaceous–Cenozoic Coast-Cascade orogen: The Chilliwack Valley–Harrison Lake connection. Geological Society of America Field Guide, Field trip 411. 45pp. Available from http://www.sfu.ca/~hdgibson/Research/Gibson&Monger_GSAFieldGuide_411_2014.pdf.

Giesler, D., Gehrels, G., Pecha, M., White, C., Yokelson, I., and McClelland, W.C. 2016. U–Pb and Hf isotopic analyses of detrital zircons from the Taku terrane, southeast Alaska. Canadian Journal of Earth Sciences, **53**(10): 979–992. doi:10.1139/cjes-2015-0240.

Giorgis, S., McClelland, W., Fayon, A., Singer, B.S., and Tikoff, B. 2008. Timing of deformation and exhumation in the western Idaho shear zone, McCall, Idaho. Geological Society of America Bulletin, **120**: 1119–1133. doi:10.1130/B26291.1.

Girardi, J.D., Patchett, P.J., Ducea, M.N., Gehrels, G.E., Cecil, M.R., Rusmore, M.E., et al. 2012. Elemental and isotopic evidence for granitoid genesis from deep-seated sources in the Coast Mountains batholith, British Columbia. Journal of Petrology, **53**: 1505–1536. doi:10.1093/petrology/egs024.

Gladwin, K., and Johnston, S.T. 2006. Mid-Cretaceous pinning of accreted terranes to miogeoclinal assemblages in the northern Cordillera: Irreconcilable with paleomagnetic data. *In* Paleogeography of the North American Cordillera: Evidence for and against Large-Scale Displacements. *Edited by* J.W. Haggart, R.J. Enkin, and J.W.H. Monger. Geological Association of Canada Special Paper 46. pp. 299–306.

Grand, S.P. 1994. Mantle shear structure beneath the Americas and surrounding oceans. Journal of Geophysical Research, **99**(11): 591–511. 621, doi:10.1029/94JB00042.

Granirer, J.L. 1985. Paleomagnetic evidence for northward transport of the Methow-Pasayten belt: unpublished M.S. thesis, Western Washington State University. 143pp.

Greene, A.R., Scoates, J.S., and Weis, D. 2008. Wrangellia flood basalts in Alaska: A record of plume-lithosphere interaction in a Late Triassic accreted oceanic plateau. Geochemistry Geophysics Geosystems, **9**: Q12004. doi:10.1029/2008GC002092.

Haeussler, P.J. 1992. Structural evolution of an arc-basin: The Gravina belt in central southeastern Alaska. Tectonics, **11**: 1245–1265. doi:10.1029/92TC01107.

Haggart, J.W. 2004. Geology, Queen Charlotte Islands, British Columbia. Geological Survey of Canada, Open File 4681, scale 1:250,000.

Hagstrum, J.T., McWilliams, M., Howell, D.G., and Grommé, S. 1985. Mesozoic paleomagnetism and northward translation of the Baja California Peninsula. Geological Society of America Bulletin, **96**: 1077–1090. doi:10.1130/0016-7606(1985)96<1077:MPANTO>2.0.CO;2.

Hampton, B.A., Ridgway, K.D.J., O'Neill, J.M., Gehrels, G.E., Schmidt, J., and Blodgett, R.B. 2007. Pre-, syn-, and post-collisional stratigraphic framework and provenance of Upper Triassic-Upper retaceous strata in the northwestern Talkeetna Mountains, Alaska. *In* Tectonic growth of a collisional continental margin: crustal evolution of south-central Alaska. *Edited by* K.D. Ridgway, J.M. Trop, J.M.G. Glen, and J.M. O'Neill. Geological Society of America Special Paper 431. pp. 401–438. doi:10.1130/2007.2431(16).

Hampton, B.A., Ridgway, K.D., O'Neill, J.M., and Gehrels, G.E. 2010. A detrital record of Mesozoic island arc accretion and exhumation in the North American Cordillera: U–Pb geochronology of the Kahiltna basin, southern Alaska. Tectonics, **29**(4). doi:10.1029/2009TC002544.

Hamza, V.M., and Vieira, F.P. 2012. Global distribution of the lithosphere-asthenosphere boundary: a new look. Solid Earth, **3**: 199–212. doi:10.5194/se-3-199-2012.

Hart, C.J.R., Goldfarb, R.J., Lewis, L.L., and Mair, J.L. 2004. The Northern Cordillera Mid-Cretaceous Plutonic Province: Ilmenite/magnetite-series granitoids and intrusion-related mineralization. Resource Geology, **54**: 253–280. doi:10.1111/j.1751-3928.2004.tb00206.x.

Haugerud, R.A., Mahoney, J.B., and Dragovitch, J.D. 1996. Geology of the Methow block: Northwest Geological Society, Fall Field Trip, Guidebook. Northwest Geological Society, Seattle, Washington. 37pp.

Herriott, T.M., Wartes, M.A., and Decker, P.L. 2017. Deep-water canyons and sequence-stratigraphic framework of the Upper Jurassic Naknek Formation, south-central Alaska. Alaska Division of Geological and Geophysical Surveys Report of Investigation, 2017-4. pp. 1–53. doi:10.14509/29707.

Herriott, T.M., Wartes, M.A., O'Sullivan, P.B., and Gillis, R.J. 2019. Detrital zircon maximum depositional dates for the Jurassic Chinitna and Naknek formations, Lower Cook Inlet, Alaska: a preliminary view. Alaska Division of Geological and Geophysical Surveys Report of Investigation, 2019-5. 11pp.

Hildebrand, R.S. 2009. Did westward subduction cause Cretaceous–Tertiary orogeny in the North American Cordillera? Geological Society of America Special Paper, **457**: 71. doi:10.1130/2009.2457.

Hildebrand, R.S. 2013. Mesozoic Assembly of the North American Cordillera: Geological Society of America Special Paper 495. 169pp. doi:10.1130/2013.2495.

Hildebrand, R.S. 2014. Geology, mantle tomography, and inclination corrected paleogeographic trajectories support westward subduction during Cretaceous orogenesis in the North American Cordillera. Geoscience Canada, **41**: 207–224. doi:10.12789/geocanj.2014.41.032.

Hildebrand, R.S. 2015. Dismemberment and northward migration of the Cordilleran orogen: Baja-BC resolved. GSA Today, **25**(11): 4–11. doi:10.1130/GSATG255A.1.

Hildebrand, R.S., and Whalen, J.B. 2014*a*. Arc and slab-failure magmatism in Cordilleran batholiths I— The Cretaceous Coastal batholith of Peru and its role in South American orogenesis and hemispheric subduction flip. Geoscience Canada, **41**: 255–282. doi:10.12789/geocanj.2014.41.047.

Hildebrand, R.S., and Whalen, J.B. 2014*b*. Arc and slab-failure magmatism in Cordilleran batholiths II— The Cretaceous Peninsular Ranges batholith of Southern and Baja California. Geoscience Canada, **41**: 399–458. doi:10.12789/geocanj.2014.41.059.

Hildebrand, R.S., and Whalen, J.B. 2017. The Tectonic Setting and Origin of Cretaceous Batholiths Within the North American Cordillera: The Case for Slab Failure Magmatism and Its Signifcance for Crustal Growth. Geological Society of America Special Paper 532. 113pp. doi:10.1130/SPE532.

Hildebrand, R.S., and Whalen, J.B. 2021. The mid-Cretaceous Peninsular Ranges orogeny: a new slant on Cordilleran tectonics? I: Mexico to Nevada. Canadian Journal of Earth Sciences. [This issue.] doi:10.1139/cjes-2020-0154.

Hildebrand, R.S., Whalen, J.B., and Bowring, S.A. 2018. Resolving the crustal composition paradox by 3.8 billion years of slab failure magmatism and collisional recycling of continental crust. Tectonophysics, **734–735**: 69–88. doi:10.1016/j.tecto.2018.04.001.

Himmelberg, G.R., and Loney, R.A. 1995. Characteristics and petrogenesis of Alaskan-type ultramafic- mafic intrusions, southeastern Alaska. U.S. Geological Survey Professional Paper 1564. 47pp.

Himmelberg, G.R., Haeussler, P.J., and Brew, D.A. 2004. Emplacement, rapid burial, and exhumation of 90-Ma plutons in southeastern Alaska. Canadian Journal of Earth Sciences, **41**(1): 87–102. doi:10.1139/e03-087.

Hollister, L.S., and Andronicos, C. 2000. The Central Gneiss Complex, Coast Mountains, British Columbia. *In* Tectonics of the Coast Mountains, SE Alaska and British Columbia. *Edited by* H.H. Stowell and W.C. McClelland. Geological Society of America Special Paper 343. pp. 45–59.

Hou, Z., Yang, Z., Lu, Y., Kemp, A., Zheng, Y., Li, Q., et al. 2015. A genetic linkage between subduction- and collision-related porphyry Cu deposits in continental collision zones. Geology, **43**: 247–250. doi:10.1130/G36362.1.

Hutchison, W.W. 1970. Metamorphic framework and plutonic styles in the Prince Rupert region of the central Coast Mountains, British Columbia. Canadian Journal of Earth Sciences, **7**(2): 376–405. doi:10.1139/e70-034.

Hyndman, D.W. 1983. The Idaho batholith and associated plutons, Idaho and western Montana, *In* Circum-Pacific plutonic terranes. *Edited by* J.A. Roddick. Geological Society of America Memoir 159. pp. 213–240.

Irving, E., Thorkelson, D.J., Wheadon, P.M., and Enkin, R.J. 1995. Paleomagnetism of the Spences Bridge Group and northward displacement of the Intermontane Belt, British Columbia: A second look. Journal of Geophysical Research, **100**: 6057–6071. doi:10.1029/94JB03012.

Irving, E., Wynne, P.J., Thorkelson, D.J., and Schiarizza, P. 1996. Large (1000–4000 km) northward movements of tectonic domains in the northern Cordillera, 83 to 45 Ma. Journal of Geophysical Research, **101**(17): 901–917 and 916. doi:10.1029/96JB01181.

James, E.W. 1992. Cretaceous metamorphism and plutonism in the Santa Cruz Mountains, Salinian block, California, and correlation with the southernmost Sierra Nevada. Geological Society of America Bulletin, **104**: 1326–1339. doi:10.1130/0016-7606(1992)104<1326:CMAPIT>2.3.CO;2.

Johnston, S.T. 2008. The Cordilleran ribbon continent of North America. Annual Review of Earth and Planetary Sciences, **36**: 495–530. doi:10.1146/annurev.earth.36.031207.124331.

Johnston, S.T., and Canil, D. 2007. Crustal architecture of SW Yukon, northern Cordillera: Implications for crustal growth in a convergent margin orogen. Tectonics, **26**. doi:10.1029/2006TC001950.

Journeay, J.M., and Friedman, R.M. 1993. The Coast belt thrust system: Evidence of Late Cretaceous shortening in southwest British Columbia. Tectonics, **12**: 756–775. doi:10.1029/92TC02773.

Kalbas, J.L., Ridgway, K.D., and Gehrels, G.E. 2007. Stratigraphy, depositional systems, and provenance of the Lower Cretaceous Kahiltna assemblage, western Alaska Range: Basin development in response to oblique collision. *In* Tectonic growth of a collisional continental margin: crustal evolution of south-central Alaska. *Edited by* K.D. Ridgway, J.M. Trop, J.M.G. Glen, and J.M. O'Neill. Geological Society of America Special Paper 431. pp. 307–343. doi:10.1130/2007.2431(13).

Kapp, P.A., and Gehrels, G.E. 1998. Detrital zircon constraints on the tectonic evolution of the Gravina belt, southeastern Alaska. Canadian Journal of Earth Sciences, **35**(3): 253–268. doi:10.1139/e97-110.

Kidder, S., Ducea, M., Gehrels, G., Patchett, P.J., and Vervoort, J. 2003. Tectonic and magmatic development of the Salinian Coast Ridge belt, California. Tectonics, **22**. doi:10.1029/2002TC001409.

Kiilsgaard, T.H., Lewis, R.S., and Bennett, E.H. 2001. Plutonic and hypabyssal rocks of the Hailey 1°x2° quadrangle, Idaho. United States Geological Survey Bulletin 2064-U. 18pp.

Kimbrough, D.L., Smith, D.P., Mahoney, J.B., Moore, T.E., Grove, M., Gastil, R.G., et al. 2001. Forearc-basin sedimentary response to rapid Late Cretaceous batholith emplacement in the Peninsular Ranges of southern and Baja California. Geology, **29**: 491–494. doi:10.1130/0091-7613(2001)029<0491:FBSRTR>2.0.CO;2.

Kimbrough, D.L., Abbott, P.L., Balch, D.C., Bartling, S.H., Grove, M., Mahoney, J.B., and Donohue, R.F. 2014. Upper Jurassic Peñasquitos Formation — Forearc basin western wall rock of the Peninsular Ranges batholith. *In* Peninsular Ranges Batholith, Baja California and southern California. *Edited by* D.M. Morton and F.K. Miller. Geological Society of America Memoir, 211. pp. 625–643. doi:10.1130/2014.1211(19).

Kistler, R.W., and Champion, D.E. 2001. Rb-Sr Whole-Rock and Mineral Ages, K–Ar, $^{40}Ar/^{39}Ar$, and U–Pb Mineral Ages, and Strontium, Lead, Neodymium, and Oxygen Isotopic Compositions for Granitic Rocks from the Salinian Composite Terrane, California. United States Geological Survey Open-File Report 01-453. 84pp.

Kleinspehn, K.L. 1985. Cretaceous sedimentation and tectonics, Tyaughton-Methow Basin, southwestern British Columbia. Canadian Journal of Earth Sciences, **22**(2): 154–174. doi:10.1139/e85-014.

Labrado, A., Pavlis, T.L., Amato, J.M., and Day, E.M. 2015. The tectonic significance of the Early Cretaceous forearc-metamorphic assemblage in south-central Alaska based on detrital zircon U–Pb dating of sedimentary protoliths. Canadian Journal of Earth Sciences, **52**(12): 1182–1190. doi:10.1139/cjes-2015-0046.

Lassiter, J.C., DePaolo, D.J., and Mahoney, J.J. 1995. Geochemistry of the Wrangellia flood basalt province: Implications for the role of continental and oceanic lithosphere in flood basalt genesis. Journal of Petrology, **36**: 983–1009. doi:10.1093/petrology/36.4.983.

Lee, C., and King, S.D. 2011. Dynamic buckling of subducting slabs reconciles geological and geophysical observations. Earth and Planetary Science Letters, **312**: 360–370. doi:10.1016/j.epsl.2011.10.033.

Loewy, S.L., Connelly, J.N., and Dalziel, I.W.D. 2004. An orphaned basement block: The Arequipa– Antofalla basement of the central Andean margin of South America. Geological Society of America Bulletin, **116**: 171–187. doi:10.1130/B25226.1.

Lowey, G.W. 1998. A new estimate of the amount of displacement on the Denali Fault system based on the occurrence of carbonate megaboulders in the Dezadeash Formation (Jura–Cretaceous), Yukon, and the Nutzotin Mountains sequence (Jura–Cretaceous), Alaska. Bulletin of Canadian Petroleum Geology, **46**: 379–386.

Lowey, G. 2019. Provenance analysis of the Dezadeash Formation (Jurassic–Cretaceous), Yukon, Canada: implications regarding a linkage between the Wrangellia composite terrane and the western margin of Laurasia. Canadian Journal of Earth Sciences, **56**(1): 77–100. doi:10.1139/cjes-2017-0244.

Lund, K., and Snee, L.W. 1988 Metamorphism, structural development, and age of continent–island arc juncture in west-central Idaho. *In* Metamorphism and Crustal Evolution of the Western United States, Rubey Volume 7. *Edited by* W.G. Ernst. Englewood Cliffs, New Jersey, Prentice Hall. pp. 296–331.

Lynch, G. 1992. Deformation of Early Cretaceous volcanic-arc assemblages, southern Coast Belt, British Columbia. Canadian Journal of Earth Sciences, **29**(12): 2706–2721. doi:10.1139/e92-214.

Lynch, G. 1995. Geochemical polarity of the Early Cretaceous Gambier Group, southern Coast Belt, British Columbia. Canadian Journal of Earth Sciences, **32**(6): 675–685. doi:10.1139/e95-058.

Ma, C., Foster, D.A., Mueller, P.A., and Dutrow, B.L. 2017. Magma-facilitated transpressional strain partitioning within the Sawtooth metamorphic complex, Idaho: A zone accommodating Cretaceous orogen-parallel translation in the Idaho batholith. Tectonics, **36**: 444–465. doi:10.1002/2016TC004264.

Mahar, M.A., Pavlis, T.L., Bowman, J.R., Conrad, W.K., and Goodell, P.C. 2019. Early Cretaceous ridge subduction beneath southern Alaska: Insights from zircon U–Pb geochronology, hafnium, and oxygen isotopic compositions of the Western Chugach tonalite-trondhjemite suite. GSA Bulletin, **131**: 521–546. doi:10.1130/B31918.1.

Mahoney, J.B., Friedman, R.M., and McKinley, S.D. 1995. Evolution of a Middle Jurassic volcanic arc: Stratigraphic, isotopic, and geochemical characteristics of the Harrison Lake Formation, southwestern British Columbia. Canadian Journal of Earth Sciences, **32**(10): 1759–1776. doi:10.1139/e95-137.

Mahoney, J.B., Gordee, S.M., Haggart, J.W., Friedman, R.M., Diakow, L.J., and Woodsworth, G.J. 2009. Magmatic evolution of the eastern Coast plutonic complex, Bella Coola region, west-central British Columbia. Geological Society of America Bulletin, **121**: 1362–1380. doi:10.1130/B26325.1.

Manduca, C.A., Silver, L.T., and Taylor, H.P., Jr. 1992. $^{87}Sr/^{86}Sr$ and $^{18}O/^{16}O$ isotopic systematics and geochemistry of granitoid plutons across a steeply-dipping boundary between contrasting lithospheric blocks in western Idaho. Contributions to Mineralogy and Petrology, **109**: 355–372. doi:10.1007/BF00283324.

Manduca, C.A., Kuntz, M.A., and Silver, L.T. 1993. Emplacement and deformation history of the western margin of the Idaho batholith near McCall, Idaho: Influence of a major terrane boundary. Geological Society of America Bulletin, **105**: 749–765. doi:10.1130/0016-7606(1993)105<0749:EADHOT>2.3.CO;2.

Manselle, P. 2019 Physical volcanology, sedimentology and geochemistry of the Mid-Cretaceous Chisana Formation, south-central Alaska: implications for models of Wrangellia composite terrane accretion. M.S. thesis, Kansas State University, Manhattan, Kansas. 105pp.

Mansfield, C.F. 1979. Upper Mesozoic subsea fan deposits in the southern Diablo Range, California: Record of the Sierra Nevada magmatic arc. Geological Society of America Bulletin, **90**: 1025–1046. doi:10.1130/0016-7606(1979)90<1025:UMSFDI>2.0.CO;2.

Manuszak, J.D., Ridgway, K.D., Trop, J.M., and Gehrels, G.E. 2007. Sedimentary record of the tectonic growth of a collisional continental margin: Upper Jurassic–Lower Cretaceous Nutzotin Mountains sequence, eastern Alaska Range, Alaska. *In* Tectonic Growth of a Collisional Continental `Margin: Crustal Evolution of South-Central Alaska. *Edited by* K.D. Ridgway, J.M. Trop, J.M.G. Glen, and J.M. O'Neill. Geological Society of America Special Paper 431. pp. 345–377. doi:10.1130/2007.2431(14).

Martin, A.J., Wyld, S.J., Wright, J.E., and Bradford, J.H. 2010. The Lower Cretaceous King Lear Formation, northwest Nevada: Implications for Mesozoic orogenesis in the western U.S. Cordillera. Geological Society of America Bulletin, **122**: 537–562. doi:10.1130/B26555.1.

Matthews, W.A., Guest, B., Coutts, D., Bain, H., and Hubbard, S. 2017. Detrital zircons from the Nanaimo basin, Vancouver Island, British Columbia: An independent test of Late Cretaceous to Cenozoic northward translation. Tectonics, **36**: 854–876. doi:10.1002/2017TC004531.

Mattinson, J.M. 1978. Age, origin, and thermal histories of some plutonic rocks from the Salinian block of California. Contributions to Mineralogy and Petrology, **67**: 233–245. doi:10.1007/BF00381451.

Mattinson, J.M. 1990. Petrogenesis and evolution of the Salinian magmatic arc. *In* The nature and origin of Cordilleran Magmatism. *Edited by* J.L. Anderson. Geological Society of America Memoir 174. pp. 237–250.

Matzel, J.E.P., Bowring, S.A., and Miller, R.B. 2006. Time scales of pluton construction at differing crustal levels: Examples from the Mount Stuart and Tenpeak intrusions, North Cascades, Washington. Geological Society of America Bulletin, **118**: 1412–1430. doi:10.1130/B25923.1.

May, S.R., Gray, G.G., Summa, L.I., Stewart, N.R., Gehrels, G.E., and Pecha, M.E. 2013. Detrital zircon geochronology from Cenomanian–Coniacian strata in the Bighorn Basin, Wyoming, U.S.A.: Implications for stratigraphic correlation and paleogeography. Rocky Mountain Geology, **48**: 41–61. doi:10.2113/gsrocky.48.1.41.

Mauel, D.J., Lawton, T.F., González-Léon, C., Iriondo, A., and Amato, J.M. 2011. Stratigraphy and age of Upper Jurassic strata in north-central Sonora, Mexico: southwestern Laurentian record of crustal extension and tectonic transition. Geosphere, **7**: 390–414. doi:10.1130/GES00600.1.

McClelland, W.C., Gehrels, G.E., and Saleeby, J.B. 1992. Upper Jurassic–Lower Cretaceous basinal strata along the Cordilleran margin: Implications for the accretionary history of the Alexander-Wrangellia- Peninsular terrane. Tectonics, **11**: 823–835. doi:10.1029/92TC00241.

Miller, R.B. 1985. The ophiolitic Ingalls Complex, north-central Cascade Mountains, Washington. Geological Society of America Bulletin, **96**: 27–42. doi:10.1130/0016-7606(1985)96<27:TOICNC>2.0.CO;2.

Miller, R.B., Gordon, S.M., Bowring, S.A., Doran, B.A., McLean, N.M., Michels, Z.D., et al. 2009. Linking deep and shallow crustal processes in an exhumed continental arc, North Cascades, Washington. *In* Volcanoes to vineyards: geologic field trips through the dynamic landscape of the Pacific Northwest. *Edited by* J.E. O'Connor, R.J. Dorsey and I.P. Madin. Geological Society of America Field Guide 15. pp. 373–406. doi:10.1130/2009.fld015(19).

Miller, R.B., DeBari, S.M., and Paterson, S.R. 2018. Construction, emplacement, and geochemical evolution of deep-crustal intrusions: Tenpeak and Dirtyface plutons, North Cascades, western North America. Geosphere, **14**: 1298–1323. doi:10.1130/GES01490.1.

Monger, J.W.H., and Brown, E.H. 2016. Tectonic evolution of the southern Coast-Cascade Orogen, northwestern Washington and southwestern British Columbia. *In* The geology of Washington and beyond: from Laurentia to Cascadia. *Edited by* E. Cheney. Chapter 10. pp. 101–130.

Monger, J.W.H., Price, R.A., and Tempelman-Kluit, D.J. 1982. Tectonic accretion and the origin of the two major metamorphic and plutonic welts in the Canadian Cordillera. Geology, **10**: 70–75. doi:10.1130/0091-7613(1982)10<70:TAATOO>2.0.CO;2.

Monger, J.W.H., van der Heyden, P., Journeay, J.M., Evenchick, C.A., and Mahoney, J.B. 1994. Jurassic-Cretaceous basins along the Canadian Coast Belt: Their bearing on pre-mid-Cretaceous sinistral displacements. Geology, **22**: 175–178. doi:10.1130/0091-7613(1994)022<0175:JCBATC>2.3.CO;2.

Montz, W.J., and Kruckenberg, S.C. 2017. Cretaceous partial melting, deformation, and exhumation of the Potters Pond migmatite domain, west-central Idaho. Lithosphere, **9**: 205–222. doi:10.1130/L555.1.

Mustard, P.S. 1994. The Upper Cretaceous Nanaimo Group, Georgia Basin. *In* Geology and geological hazards of the Vancouver Region, southwestern British Columbia. *Edited by* J.W.H. Monger. Geological Survey of Canada Bulletin 481. pp. 27–95.

Mustard, P.S., Parrish, R.R., and McNicoll, V. 1995. Provenance of the Upper Cretaceous Nanaimo Group, British Columbia: Evidence from U–Pb analyses of detrital zircons. *In* Stratigraphic development in foreland basins. *Edited by* S.L. Dorobek and G.M. Ross. SEPM Special Publication 52. pp. 112–127.

Olson, N.H., III. 2015. The geology, geochronology, and geochemistry of the Kaskanak Batholith, and other Late Cretaceous to Eocene Magmatism at the Pebble Porphyry Cu-Au-Mo Deposit, SW Alaska. M.S. thesis, Oregon State University, Corvallis, Oregon. 248pp.

Patzke, M. 2017. Characterizing the Hazard Creek complex of the Western Idaho Shear Zone: Analysis of a middle Cretaceous Idaho Arc. B.Sc. thesis, Trinity University, San Antonio, Texas. 54pp.

Pavlis, T.L., Amato, J.M., Trop, J.M., Ridgway, K.D., Roeske, S.M., and Gehrels, G.E. 2019. Subduction polarity in ancient arcs: A call to integrate geology and geophysics to decipher the Mesozoic tectonic history of the northern Cordillera of North America. GSA Today, **29**: 4–10. doi:10.1130/GSATG402A.1.

Pavlis, T.L., Amato, J.M., Trop, J.M., Ridgway, K.D., Roeske, S.M., and Gehrels, G.E. 2020. Subduction polarity in ancient arcs: A call to integrate geology and geophysics to decipher the Mesozoic tectonic history of the northern Cordillera of North America: Reply. GSA Today, **29**: e51–10. doi:10.1130/GSATG465Y.1.

Peryam, T.C., Lawton, T.F., Amato, J.M., González-León, C.M., and Mauel, D.J. 2012. Lower Cretaceous strata of the Sonora Bisbee Basin: A record of the tectonomagmatic evolution of northwestern Mexico. Geological Society of America Bulletin, **124**: 532–548. doi:10.1130/B30456.1.

Pitcher, W.S. 1993. The Nature and Origin of Granite. London, Blackie Academic, 321 pp. doi:10.1007/978-94-017-3393-9.

Plafker, G., Nokleberg, W.J., and Lull, J.S. 1989. Bedrock geology and tectonic evolution of the Wrangellia, Peninsular, and Chugach terranes along the Trans-Alaska Crustal Transect in the northern Chugach Mountains and southern Copper River Basin, Alaska. Journal of Geophysical Research, **94**: 4255–4295. doi:10.1029/JB094iB04p04255.

Rapp, R.P., Watson, E.B., and Miller, C.F. 1991. Partial melting of amphibolite/eclogite and the origin of Archaean trondhjemites and tonalites. Precambrian Research, **51**: 1–25. doi:10.1016/0301-9268(91)90092-O.

Redman, E. 1984. An unconformity associated with conglomeratic sediments in the Berners Bay area of southeastern Alaska. Alaska Division of Geological and Geophysical Surveys. Professional Report 86. pp. 1–4.

Richter, D.H., Lanphere, M.A., and Matson, N.A., Jr. 1975. Granitic plutonism and metamorphism, eastern Alaska Range, Alaska. Geological Society of America Bulletin, **86**: 819–829. doi:10.1130/0016-7606(1975)86<819:GPAMEA>2.0.CO;2.

Richter, D.H., Preller, C.C., Labay, K.A., and Shew, N.B. 2006. Geologic map of the Wrangell–Saint Elias Park and Preserve, Alaska. United States Geological Survey Scientific Investigations Map 2877, scale 1:350,000.

Ricketts, B.D. 2019. Cordilleran sedimentary basins of western Canada record 180 million years of terrane accretion. *In* The sedimentary basins of the United States and Canada. 2nd ed. *Edited by* A.D. Miall. Elsevier, Amsterdam, the Netherlands. pp. 445–475.

Rioux, M., Hacker, B., Mattinson, J., Kelemen, P., Blusztajn, J., and Gehrels, G. 2007. Magmatic development of an intra-oceanic arc: High-precision U–Pb zircon and whole-rock isotopic analyses from the accreted Talkeetna arc, south-central Alaska. Geological Society of America Bulletin, **119**: 1168–1184. doi:10.1130/B25964.1.

Roddick, J.A. (*Editor*). 1983. Geophysical review and composition of the Coast plutonic complex, south of latitude 55°. *In* Circum-Pacific plutonic terranes. Geological Society of America Memoir 159. pp. 195–211. doi:10.1130/MEM159-p195.

Roddick, J.A., and Hutchinson, W.W. 1974. Setting of the Coast Plutonic Complex, British Columbia. Pacific Geology, **8**: 91–108.

Ross, D.C. 1977. Pre-intrusive metasedimentary rocks of the Salinian block, California—A paleotectonic dilemma, *In* Paleozoic paleogeography of the western United States. *Edited by* J.H. Stewart, C.H. Stevens, and A.E. Fritsche. Los Angeles, California, Pacific Section, Society of Economic Paleontologists and Mineralogists, Pacific Coast Paleogeography Symposium 1. pp. 371–380.

Ross, D.C. 1978. The Salinian block—A Mesozoic granitic orphan in the California Coast Ranges. *In* Mesozoic Paleogeography of the Western United States. *Edited by* D.G. Howell, and K.A. McDougall, Los Angeles, California, Pacific Section, Society of Economic Paleontologists and Mineralogists, Pacific Coast Paleogeography Symposium 2. pp. 509–522.

Rubin, C.M., and Saleeby, J.B. 1987. The inner boundary zone of the Alexander terrane, southern SE Alaska—A newly discovered thrust belt. Geological Society of America Abstracts with Programs, **19**(455).

Rubin, C.M., and Saleeby, J.B. 1991. The Gravina sequence: Remnants of a mid-Mesozoic arc in southern-southeast Alaska. Journal of Geophysical Research, **96**(14): 551–514 and 568. doi:10.1029/91JB00591.

Rubin, C.M., and Saleeby, J.B. 2000. U–Pb geochronology of mid-Cretaceous and Tertiary plutons along the western edge of the Coast Mountains, Revillagigedo Island, and Portland Peninsula, southeast Alaska. *In* Tectonics of the Coast Mountains, SE Alaska and British Columbia. *Edited by* H.H. Stowell and W.C. McClelland. Geological Society of America Special Paper 343. pp. 145–157.

Rubin, C.M., Saleeby, J.B., Cowan, D.S., Brandon, M.T., and McGroder, M.F. 1990. Regionally extensive mid-Cretaceous west-vergent thrust system in the northwestern Cordillera: Implications for continent-margin tectonism. Geology, **18**: 276–280. doi:10.1130/0091-7613(1990)018<0276:REMCWV>2.3.CO;2.

Rusmore, M.E., and Woodsworth, G.J. 1991. Coast plutonic complex: A mid-Cretaceous contractional orogen. Geology, **19**: 941–944. doi:10.1130/0091-7613(1991)019<0941:CPCAMC>2.3.CO;2.

Rusmore, M.E., Woodsworth, G.J., and Gehrels, G.E. 2000. Structural history of the Sheemahant shear zone, southwest of Bella Coola, British Columbia, and implications for the Late Cretaceous evolution of the Coast orogen. *In* Tectonics of the Coast Mountains, SE Alaska and British Columbia. *Edited by* H.H. Stowell, and W.C. McClelland. Geological Society of America Special Paper 343. pp. 89–106.

Saleeby, J.B. 2000. Geochronologic investigations along the Alexander—Taku terrane boundary, southern Revillagigedo Island to Cape Fox areas, southeast Alaska. *In* Tectonics of the Coast Mountains, SE Alaska and British Columbia. *Edited by* H.H. Stowell and W.C. McClelland. Geological Society of America Special Paper 343. pp. 107–143.

Sauer, K.B., Gordon, S.M., Miller, R.B., Vervoort, J.D., and Fisher, C.M. 2017. Transfer of metasupracrustal rocks to midcrustal depths in the North Cascades continental magmatic arc, Skagit Gneiss Complex, Washington. Tectonics, **36**: 3254–3276. doi:10.1002/2017TC004728.

Schermer, E.R., Hoffnagle, E.A., Brown, E.H., Gehrels, G.E., and McClelland, W.C. 2018. U–Pb and Hf isotopic evidence for an Arctic origin of terranes in northwestern Washington. Geosphere, **14**: 835–826. doi:10.1130/GES01557.1.

Shea, E.K. 2014. Arc Magmatism at Different Crustal Levels, North Cascades, WA. Ph.D. thesis, Massachusetts Institute of Technology, Cambridge, Massachusetts. 555pp.

Sigloch, K. 2011. Mantle provinces under North America from multifrequency P-wave tomography. Geochemistry Geophysics Geosystems, **12**: Q02W08. doi:10.1029/2010GC003421.

Sigloch, K., and Mihalynuk, M.G. 2013. Intra-oceanic subduction shaped the assembly of Cordilleran North America. Nature, **496**: 50–56. doi:10.1038/nature12019.

Sigloch, K., and Mihalynuk, M.G. 2017. Mantle and geological evidence for a Late Jurassic–Cretaceous suture spanning North America. Geological Society of America Bulletin, **129**: 1489–1520. doi:10.1130/B31529.1.

Sigloch, K., and Mihalynuk, M.G. 2020. Comment on GSA Today article by Pavlis et al., 2019: "Subduction Polarity in Ancient Arcs: A Call to Integrate Geology and Geophysics to Decipher the Mesozoic Tectonic History of the Northern Cordillera of North America". GSA Today, **30**: e47. doi:10.1130/GSATG431C.1.

Singer, B.S., Jicha, B.R., Sawyer, D., Walaszczyk, I., Buchwaldt, R., and Mutterlose, J. 2021. Geochronology of late Albian–Cenomanian strata in the U.S. Western Interior. Geological Society of America Bulletin, **133**: 1665–1678. doi:10.1130/B35794.1.

Snee, L.W., Lund, K., Sutter, J.F., Balcer, D.E., and Evans, K.V. 1995. An $^{40}Ar/^{39}Ar$ chronicle of the tectonic development of the Salmon River suture zone, western Idaho. *In* Geology of the Blue Mountains Region of Oregon, Idaho, and Washington: Petrology and Tectonic Evolution of Pre-Tertiary Rocks of the Blue Mountains Region. *Edited by* T.L. Vallier and H.C. Brooks, United States. Geological Survey Professional Paper 1438, 359–414.

Snyder, D.C., and Hart, W.K. 2007. The White Mountain Granitoid Suite: Isotopic constraints on source reservoirs for Cretaceous magmatism within the Wrangellia Terrane. *In* Tectonic growth of a collisional continental margin: crustal evolution of south-central Alaska. *Edited by* K.D. Ridgway, J.M. Trop, J.M.G. Glen, and J.M. O'Neill. Geological Society of America Special Paper 431. pp. 379–399. doi:10.1130/2007.2431(15).

Solomon, M. 1990. Subduction, arc reversal, and the origin of porphyry copper-gold deposits in island arcs. Geology, **18**: 630–633. doi:10.1130/0091-7613(1990)018<0630:SARATO>2.3.CO;2.

Spencer, C.J., Murphy, J.B., Hoiland, C.W., Johnston, S.T., Mitchell, R.N., and Collins, W.J. 2019. Evidence for whole mantle convection driving Cordilleran tectonics. Geophysical Research Letters, **46**: 4239–4248. doi:10.1029/2019GL082313.

Stewart, J.H. 1970. Upper Precambrian and Lower Cambrian Strata in the Southern Great Basin, California and Nevada. United States Geological Survey Professional Paper 620. 206pp.

Stowell, H.H., and Crawford, M.L. 2000. Metamorphic history of the Coast Mountains orogen, western British Columbia and southeastern Alaska. *In* Tectonics of the Coast Mountains, SE Alaska and British Columbia. *Edited by* H.H. Stowell and W.C. McClelland. Geological Society of America Special Paper 343. pp. 257–284.

Stroup, C.N., Link, P.K., Janecke, S.U., Fanning, C.M., Yaxley, G.M., and Beranek, L.P. 2008. Eocene to Oligocene provenance and drainage in extensional basins of southwest Montana and east-central Idaho: Evidence from detrital zircon populations in the Renova Formation and equivalent strata. *In* Ores and orogenesis: Circum-Pacific tectonics, geologic evolution and ore deposits. *Edited by* J.E. Spencer and S.R. Titley. Arizona Geological Society Digest 22. pp. 529–546.

Surpless, K.D., Sickmann, Z.T., and Koplitz, T.A. 2014. East-derived strata in the Methow basin record rapid mid-Cretaceous uplift of the southern Coast Mountains batholith. Canadian Journal of Earth Sciences, **51**(4): 339–357. doi:10.1139/cjes-2013-0144.

Sutter, J.F., and Crawford, M.L. 1985. Timing of metamorphism and uplift in the vicinity of Prince Rupert, British Columbia and Ketchikan, Alaska. Geological Society of America Abstracts with Programs, Vol. **17**. 411pp.

Taubeneck, W.H. 1971. Idaho batholith and its southern extension. Geological Society of America Bulletin, **82**: 1899–1928. doi:10.1130/0016-7606(1971)82[1899:IBAISE]2.0.CO;2.

Templeman-Kluit, D.J. 1979. Transported cataclasite, ophiolite, and granodiorite in Yukon: evidence of arc-continent collision. Geological Survey of Canada Paper 79-14. 27pp.

Thorkelson, D.J. 1986. Volcanic stratigraphy and petrology of the mid-Cretaceous Spences Bridge Group near Kingsvale, southwestern British Columbia. M.S. thesis, University of British Columbia, Vancouver, B.C. 119pp.

Thorkelson, D.J., and Smith, A.D. 1989. Arc and intraplate volcanism in the Spences Bridge Group: Implications for Cretaceous tectonics in the Canadian Cordillera. Geology, **17**: 1093–1096. doi:10.1130/0091-7613(1989)017<1093:AAIVIT>2.3.CO;2.

Torsvik, T.H., Steinberger, B., Cocks, L.R.M., and Burke, K. 2008. Longitude: Linking Earth's ancient surface to its deep interior. Earth and Planetary Science Letters, **276**: 273–282. doi:10.1016/j.epsl.2008.09.026.

Trop, J.M., and Ridgway, K.D. 2007. Mesozoic and Cenozoic tectonic growth of southern Alaska: A sedimentary basin perspective. *In* Tectonic growth of a collisional continental margin: crustal evolution of south-central Alaska. *Edited by* K.D. Ridgway, J.M. Trop, J.M.G. Glen, and J.M. O'Neill. Geological Society of America Special Paper 431. pp. 55–94.

Trop, J.M., Ridgway, K.D., Manuszak, J.D., and Layer, P.W. 2002. Mesozoic sedimentary basin development on the allochthonous Wrangellia composite terrane, Wrangell Mountains basin, Alaska: A long-term record of terrane migration and arc construction. Geological Society of America Bulletin, **114**: 693–717. doi:10.1130/0016-7606(2002)114<0693:MSBDOT>2.0.CO;2.

Trop, J.M., Szuch, D.A., Rioux, M., and Blodgett, R.B. 2005. Sedimentology and provenance of the Upper Jurassic Naknek Formation, Talkeetna Mountains, Alaska: Bearings on the accretionary tectonic history of the Wrangellia composite terrane. Geological Society of America Bulletin, **117**: 570–588. doi:10.1130/B25575.1.

Trop, J.M., Benowitz, J.A., Koepp, D.Q., Sunderlin, D., Brueseke, M.E., Layer, P.W., and Fitzgerald, P.G. 2020. Stitch in the ditch: Nutzotin Mountains (Alaska) fluvial strata and a dike record ca. 117–114 Ma accretion of Wrangellia with western North America and initiation of the Totschunda fault. Geosphere, **16**: 82–110. doi:10.1130/GES02127.1.

Umhoefer, P.J., and Miller, R.B. 1996. Mid-Cretaceous thrusting in the southern Coast Belt, British Columbia and Washington, after strike-slip fault reconstruction. Tectonics, **15**: 545–565. doi:10.1029/95TC03498.

Unruh, D.M., Lund, K., Snee, L.W., and Kurtz, M.A. 2008. Uranium-lead zircon ages and Sr, Nd, and Pb isotope geochemistry of selected plutonic rocks from western Idaho. United States Geological Survey Open-File Report 2008–1142. 42pp.

Van Buer, N.J., and Miller, E.L. 2010. Sahwave batholith, NW Nevada: Cretaceous arc flare-up in a basinal terrane. Lithosphere, **2**: 423–446. doi:10.1130/L105.1.

Vetz, N.Q. 2011. Geochronologic asnd isotopic investigation of the Koipato Formation, northwestern Great Basin, Nevada. Implications for Late Permian-Early Triassic tectonics along the western U.S. Cordillera. M.S. thesis, Boise State University, Boise, Idaho. 147pp.

Walker, J.D., Martin, M.W., and Glazner, A.F. 2002. Late Paleozoic to Mesozoic development of the Mojave Desert and environs. *In* Geologic evolution of the Mojave Desert and southwestern basin and range. *Edited by* A.F. Glazner, J.D. Walker, and J.M. Bartley. Geological Society of America Memoir 195. pp. 1–18.

Wallace, C.A. 1987, Generalized geologic map of the Butte 1° x 2° quadrangle, Montana. United States Geological Survey, Miscellaneous Field Studies Map MF-1925, scale 1:250,000.

Wallace, C.A., Lidke, D.J., and Schmidt, R.G. 1990. Faults of the central part of the Lewis and Clark line and fragmentation of the Late Cretaceous foreland basin in west-central Montana. Geological Society of America Bulletin, **102**: 1021–1037. doi:10.1130/0016-7606(1990)102<1021:FOTCPO>2.3.CO;2.

Wetmore, P.H., and Ducea, M.N. 2011. Geochemical evidence of a near-surface history for source rocks of the central Coast Mountains Batholith, British Columbia. International Geology Review, **53**: 230–260. doi:10.1080/00206810903028219.

Whidden, K.J., Lund, S.P., Bottjer, D.J., Champion, D., and Howell, D.G. 1998. Paleomagnetic evidence the central block of Salinia (California) is not a far-traveled terrane. Tectonics, **17**: 329–343. doi:10.1029/97TC03021.

Whitmarsh, R.S. 1997. Geologic map of the Centennial Canyon 7.5' quadrangle, Inyo County, California. *In* Geologic Map of the Coso Range. Geological Society of America. doi:10.1130/1998-whitmarsh-coso.

Woodsworth, G.J., Loveridge, W.D., Parrish, R.R., and Sullivan, R.W. 1983. Uranium-lead dates from the Central Gneiss Complex and Ecstall pluton, Prince Rupert map area, British Columbia. Canadian Journal of Earth Sciences, **20**(9): 1475–1483. doi:10.1139/e83-133.

Wyld, S.J., and Wright, J.E. 2019. Jurassic backarc igneous province of the northern Great Basin: Evidence for slab break-off following arc collision. Geological Society of America Abstracts with Programs, **51**(5). doi:10.1130/abs/2019AM-340652.

Wyld, S.J., Rogers, J.W., and Copeland, P. 2003. Metamorphic evolution of the Luning-Fencemaker Fold-Thrust Belt, Nevada: illite crystallinity, metamorphic petrology, and $^{40}Ar/^{39}Ar$ geochronology. Journal of Geology, **111**: 17–38. doi:10.1086/344663.

Yokelson, I., Gehrels, G.E., Pecha, M., Giesler, D., White, C., and McClelland, W.C. 2015. U–Pb and Hf isotope analysis of detrital zircons from Mesozoic strata of the Gravina belt, southeast Alaska. Tectonics, **34**: 2052–2066. doi:10.1002/2015TC003955.

Zartman, R.E., Dyman, T.S., Tysdal, R.G., and Pearson, R.C. 1995. U–Pb ages of volcanogenic zircon from porcellanite beds in the Vaughn Member of the Mid-Cretaceous Blackleaf Formation, southwestern Montana. United States Geological Survey, Bulletin 2113-B, B1–16.

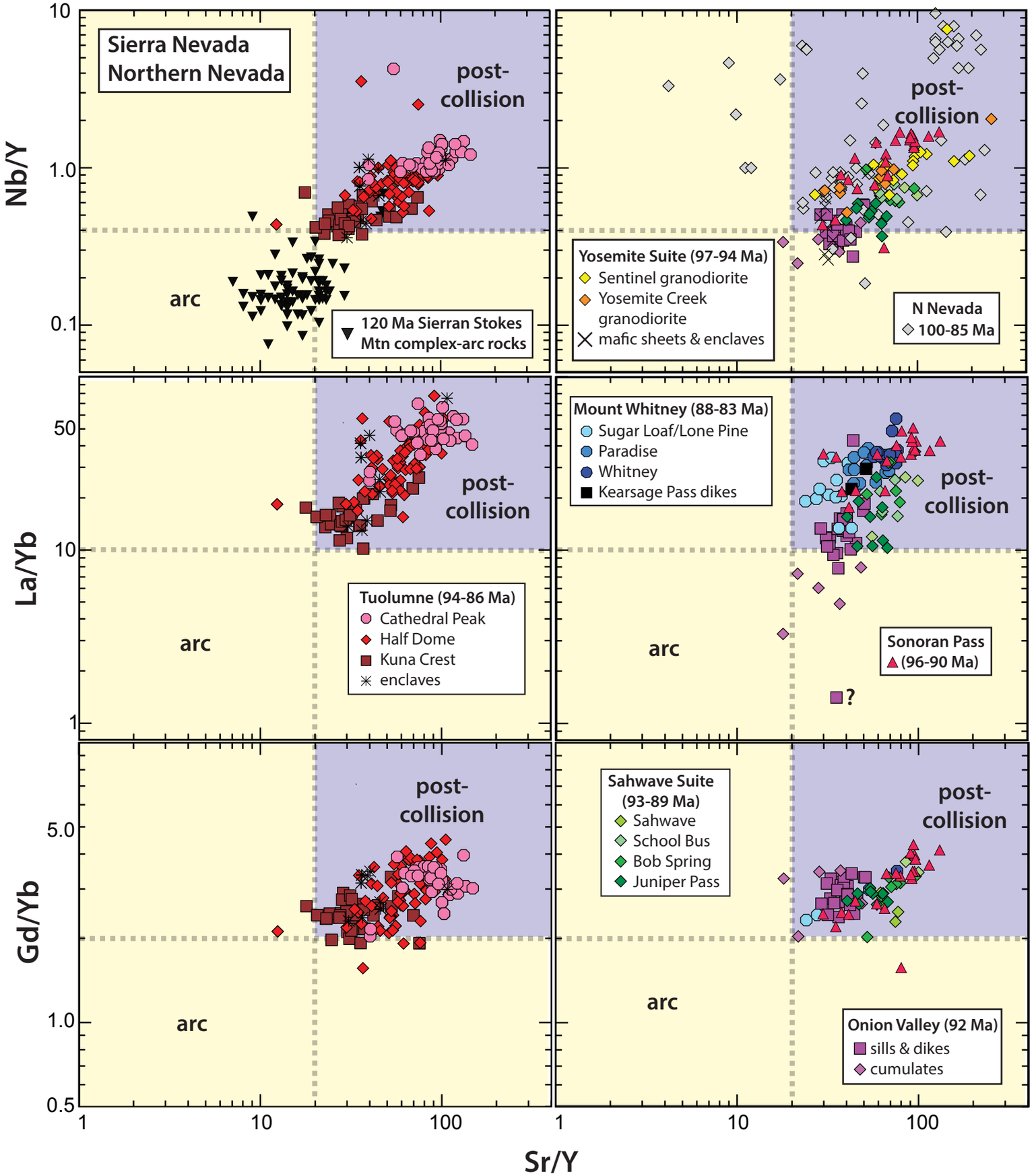

Supplemental Figure 1. Nb/Y, La/Yb, and Gd/Yb vs. Sr/Y discrimination diagrams for various Sierra Nevada and Nevadan plutonic suites, including pre-collisional 120 Ma Sierran Stokes Mountain complex arc rocks (Clemens-Knott, 1992), 100–84 Ma postcollisional Tuolumne intrusive suite (Memeti, 2009), Mount Whitney (Hirt, 2007), Sahwave intrusive suite of NW Nevada (Van Buer and Miller, 2010), Sonoran Pass intrusive suite (Alasino. 2019), and Onion Valley hornblende gabbro (Sisson et al., 1996) plus northern Nevada plutonic rocks (du Bray, 2007), illustrating that the pre–100 Ma arc rocks of the Stokes Mountain complex and the remaining plutonic units (100–80 Ma) are consistent with those of the Peninsular Ranges.

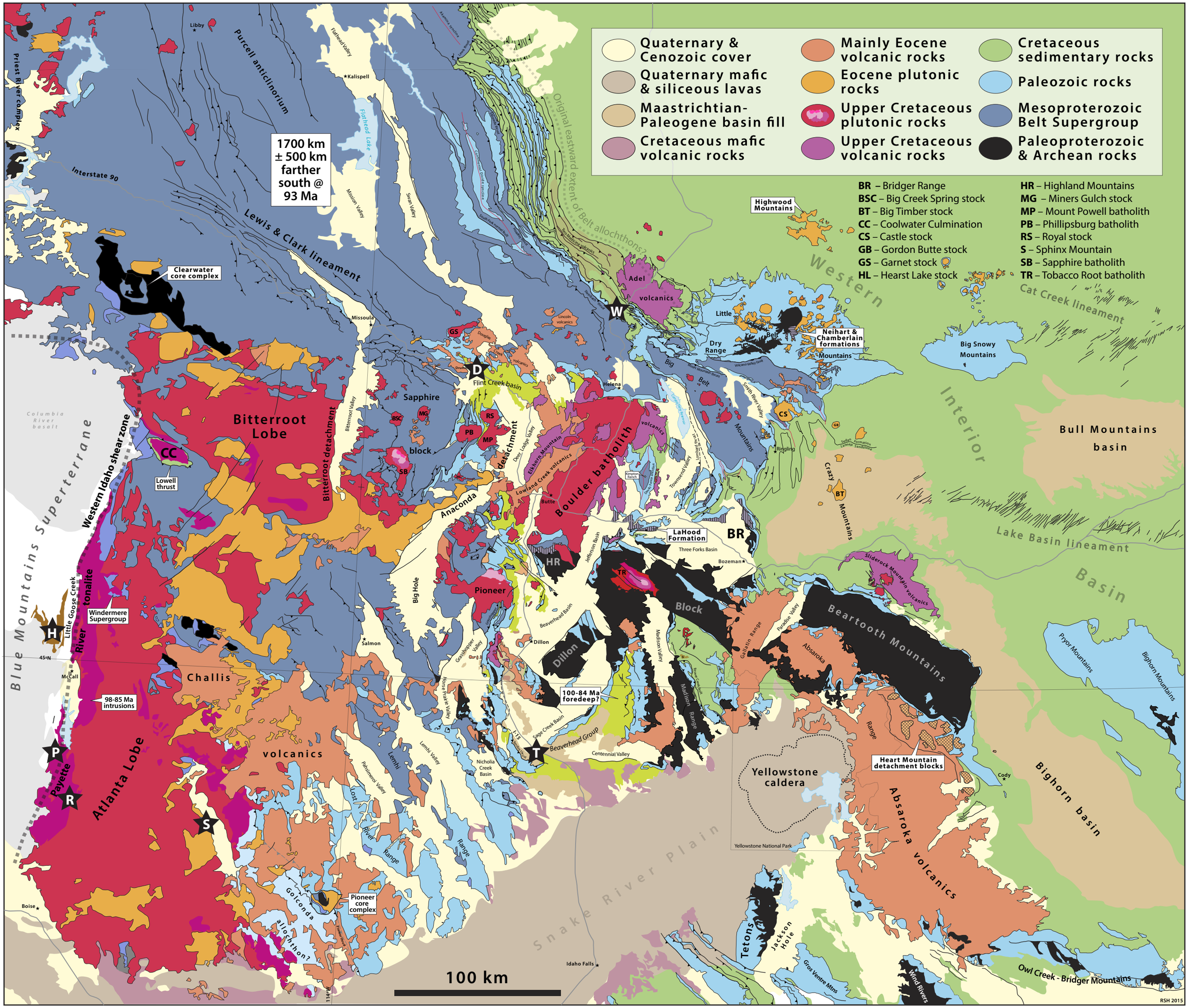

Supplemental Figure 2: Regional geological sketch map of the Helena salient, north-central U.S. Cordillera showing locations discussed in text. Modified from Hildebrand and Whalen (2017). H–Hazard Creek complex; P–Potter's Pond migmatite; S–Sawtooth Range; R–Rat Creek granodiorite; T–Tendoy thrust; W–Wolf Creek area; D–Drummond; lime green colour represents areas of 100-84 Ma foredeep deposits described in text; Owyhee Mountains are located 20-30 km southwest of the southwest corner of the map area.

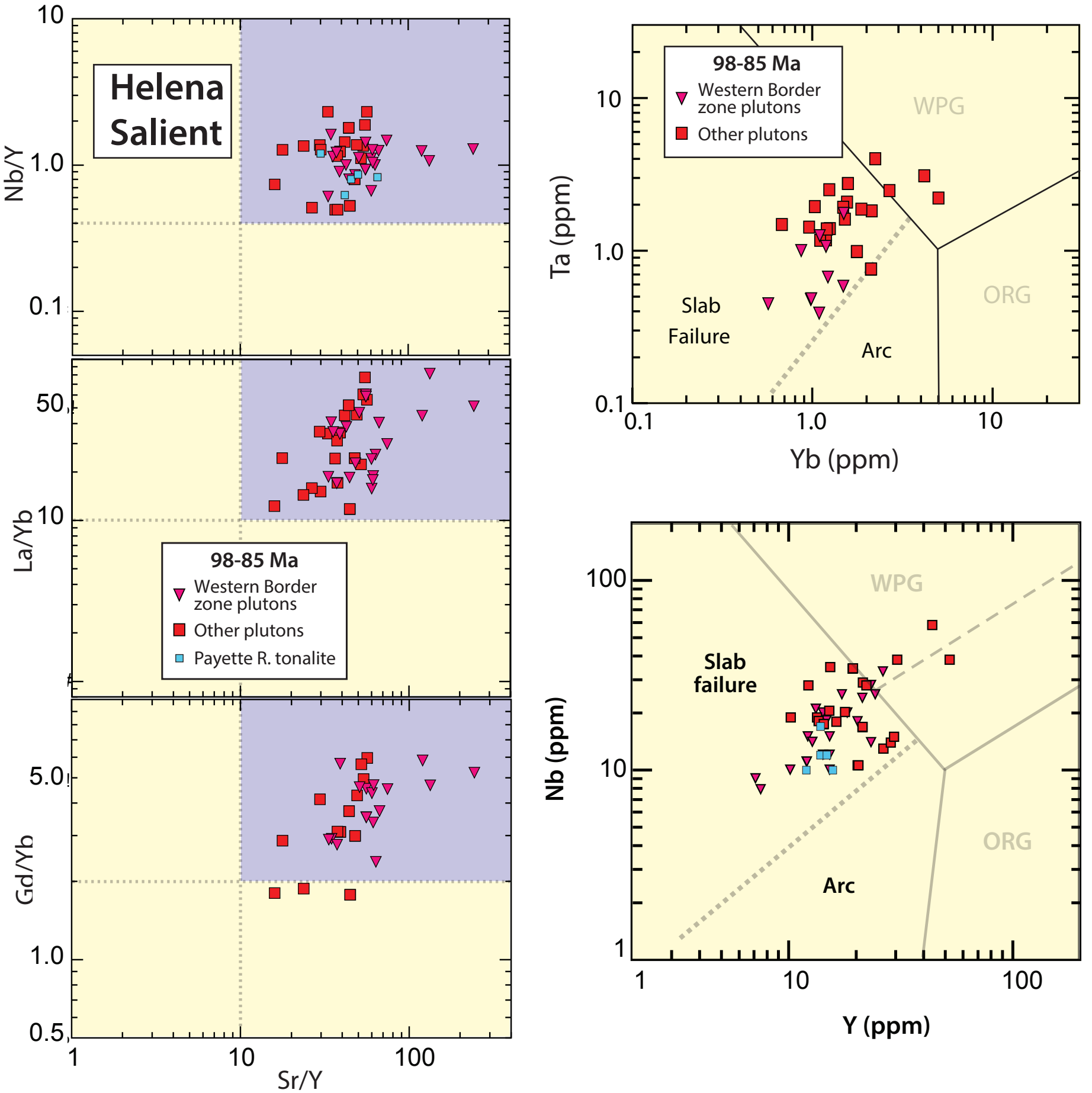

Supplemental Figure 3. Nb/Y, La/Yb, and Gd/Yb vs. Sr/Y and Ta vs. Yb and Nb vs. Y discrimination diagrams for 98–85 Ma plutons of the Peninsular Ranges orogen in the Helena salient. Based on these data and the postkinematic nature of plutonism, Hidebrand and Whalen (2017) interpreted the bodies to be slab failure features, not arc features. Data are from Manduca et al. (1993); Gaschnig (2015, personal commun.). WPG—within-plate granite; ORG-ocean-ridge granite.

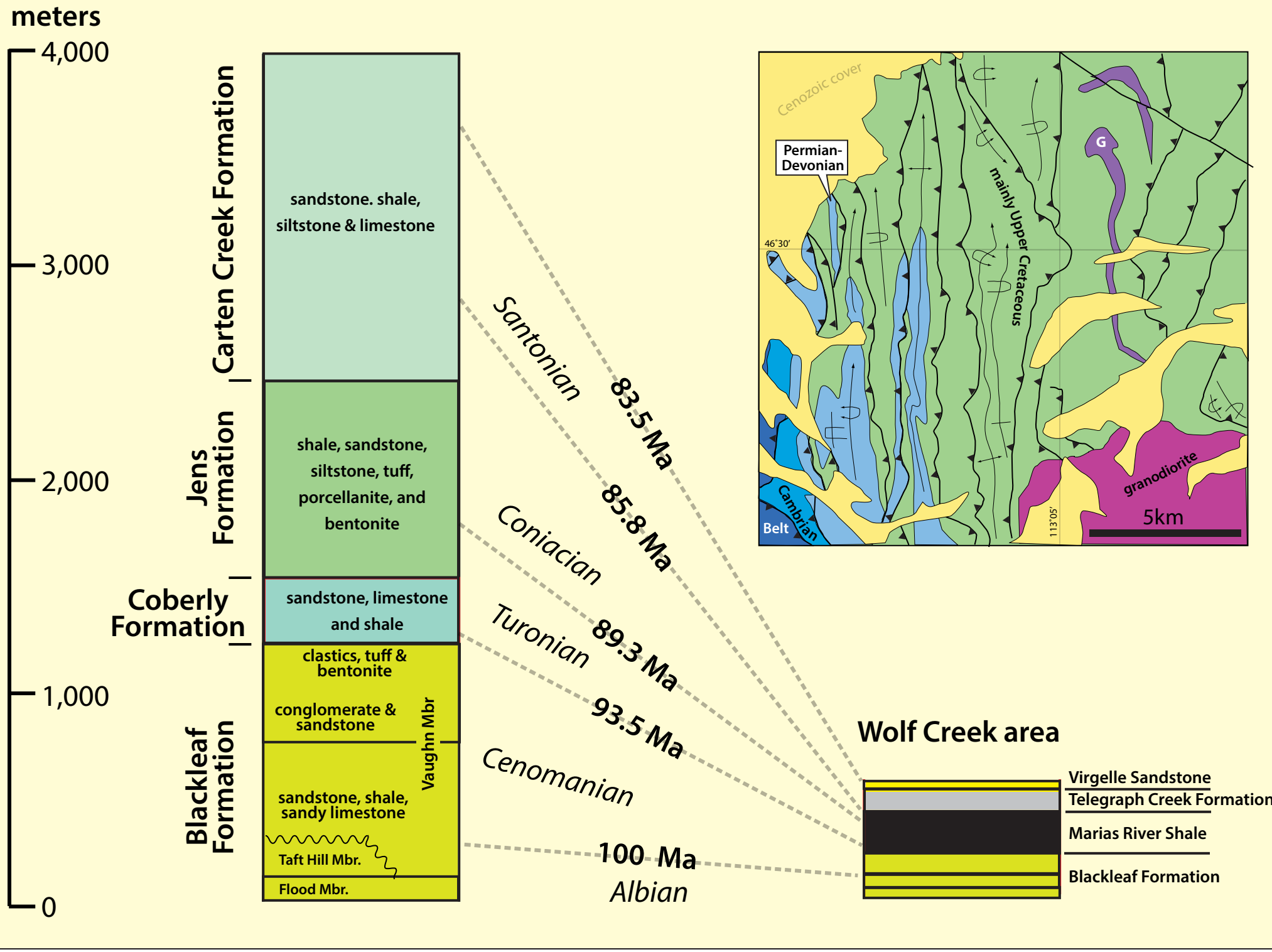

Supplemental Figure 4. Figure showing the thickness differences between the thick Upper Cretaceous sequence of sedimentary rocks exposed in a N-S band south of Drummond, Montana and those to the east within the Cordilleran thrust belt near Wolf Creek. We interpret the thick succession as part of the flexural foredeep of the Peninsular Ranges orogeny initiated at ~100 Ma when the Taft Hill member of the Blackleaf Formation was uplifted, eroded and then buried by sediments of the overlying Vaughn member. The inset map shows a portion of the thrust belt and its easterly vergent thrusts. Modified from Wallace et al. (1990) and Wallace (1987). G–gabbro.

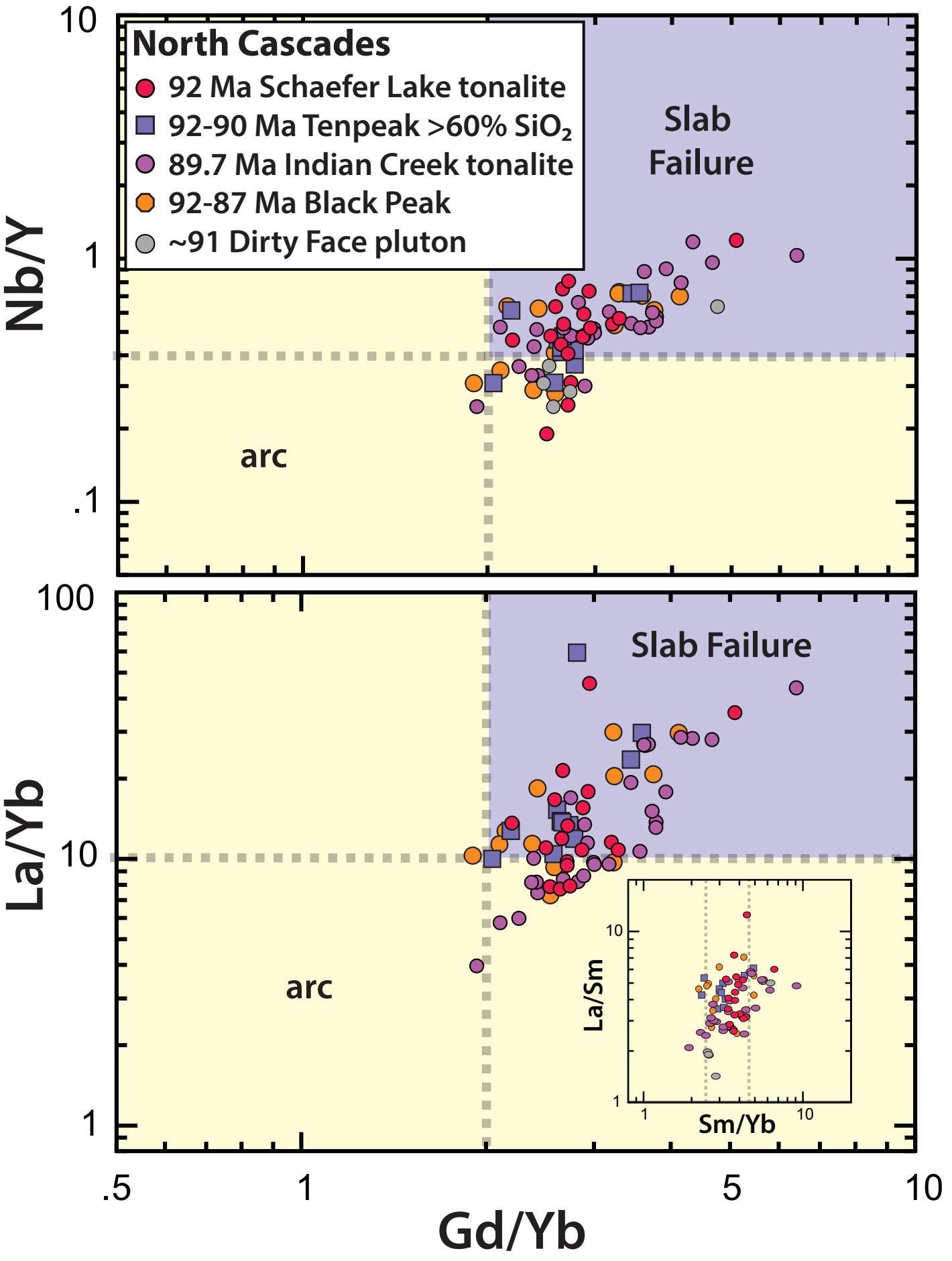

Supplemental Figure 5. Nb/Y and La/Yb vs. Gd/Yb and Ta vs. Yb and Nb vs. Y discrimination diagrams for the Northern Cascades <100 Ma plutonic rocks. Data are from Shea (2014) and Miller et al. (2018). WPG—within-plate granite; ORG—ocean-ridge granite

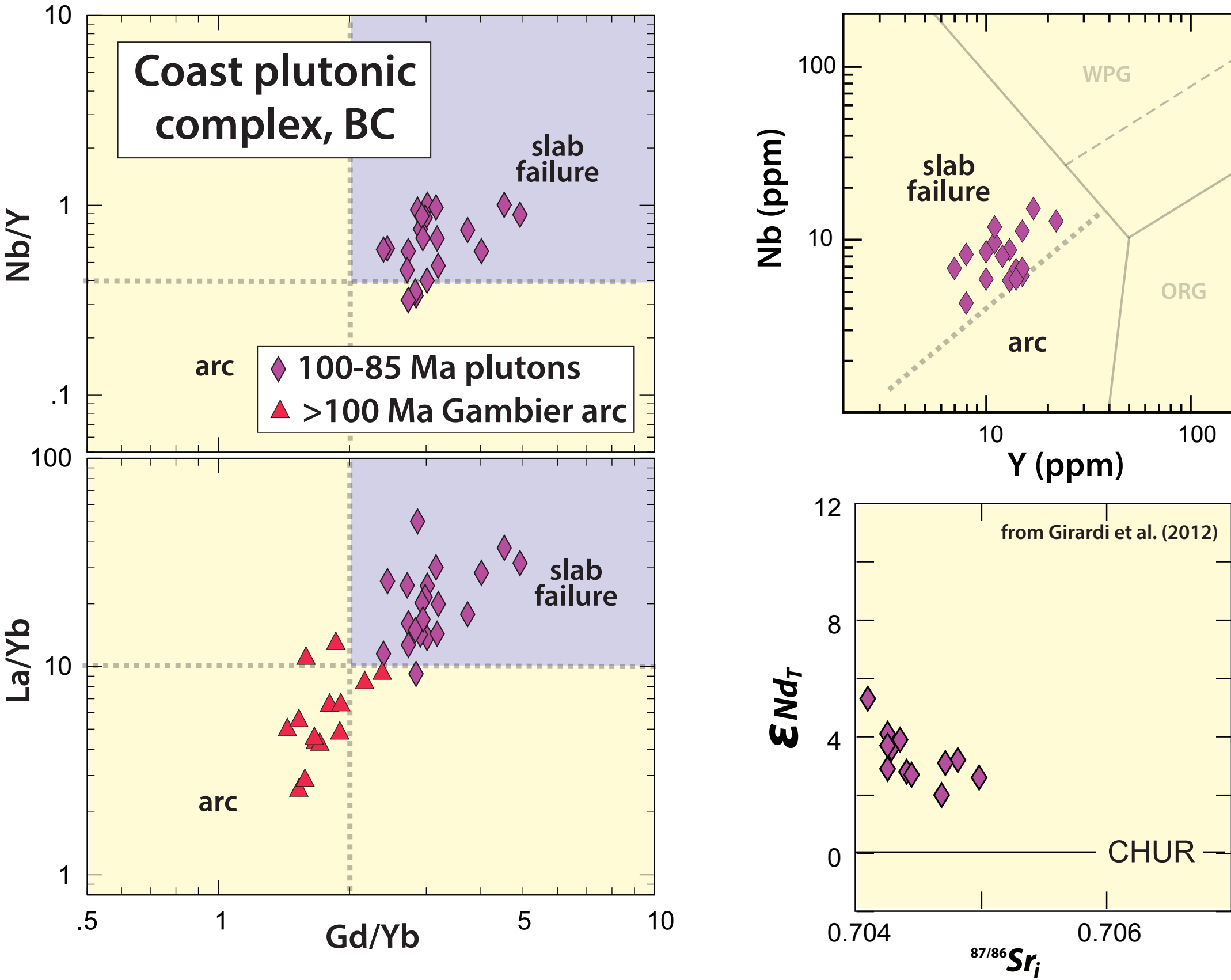

Supplemental Figure 6. Nb/Y and La/Yb vs. Gd/Yb, Ta vs. Yb, and Nb vs. Y discrimination diagrams modified from Hildebrand and Whalen (2017) for rocks of the Gambier Group, generally interpreted to represent remnants of a pre-100 Ma volcanic arc (Lynch, 1995), and 100–85 Ma post-collisional rocks of the Coast plutonic complex, British Columbia (BC). Plutonic data are from Crawford et al. (2005); Mahoney et al. (2009); Girardi et al. (2012). WPG—within-plate granite; ORG—ocean-ridge granite.

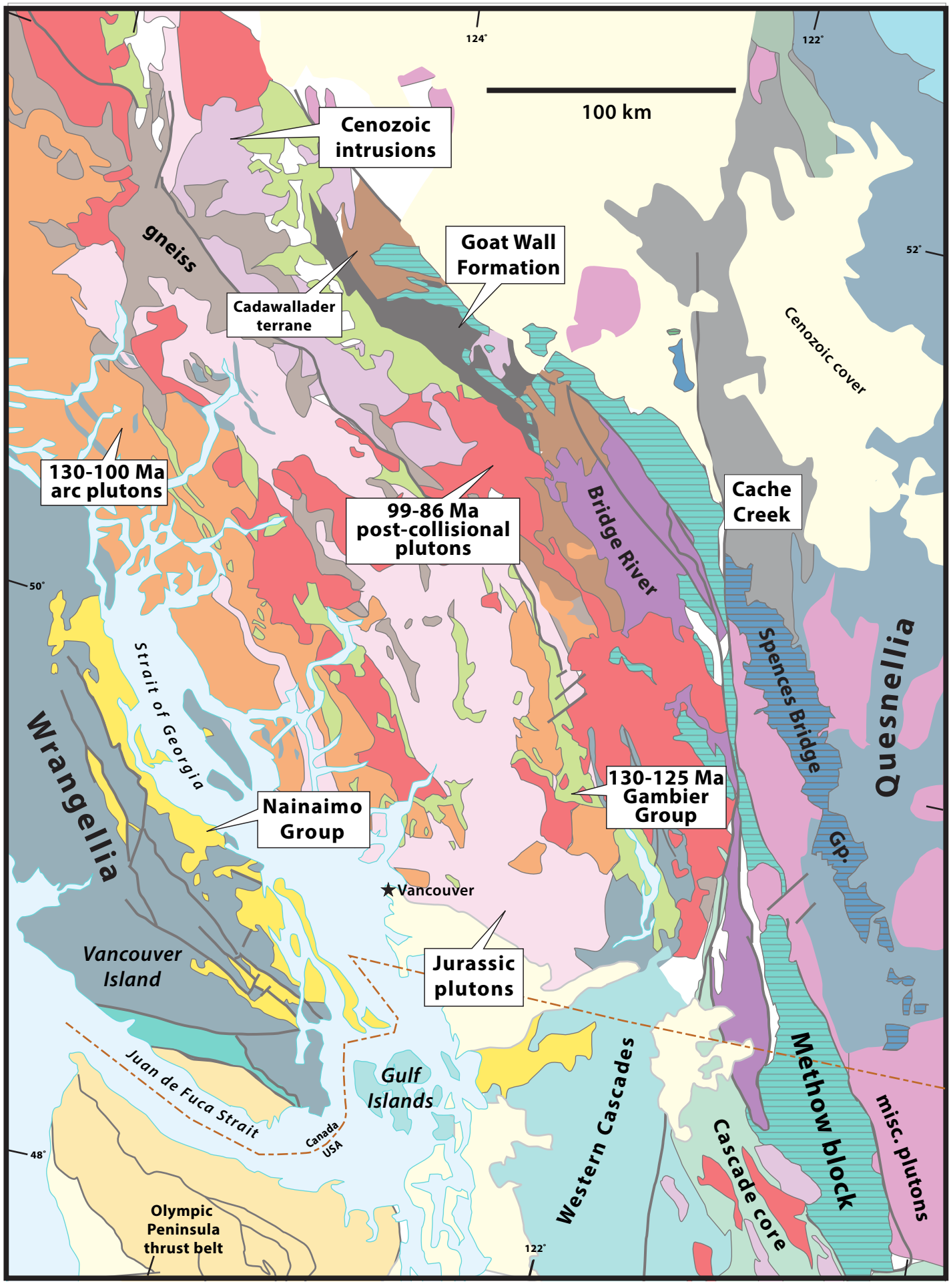

Supplemental Figure 7. Geological sketch map showing location of Spences Bridge Group, Methow block, and Nanaimo basin discussed in text. Geology modified from Wheeler and McFeeley (1991).

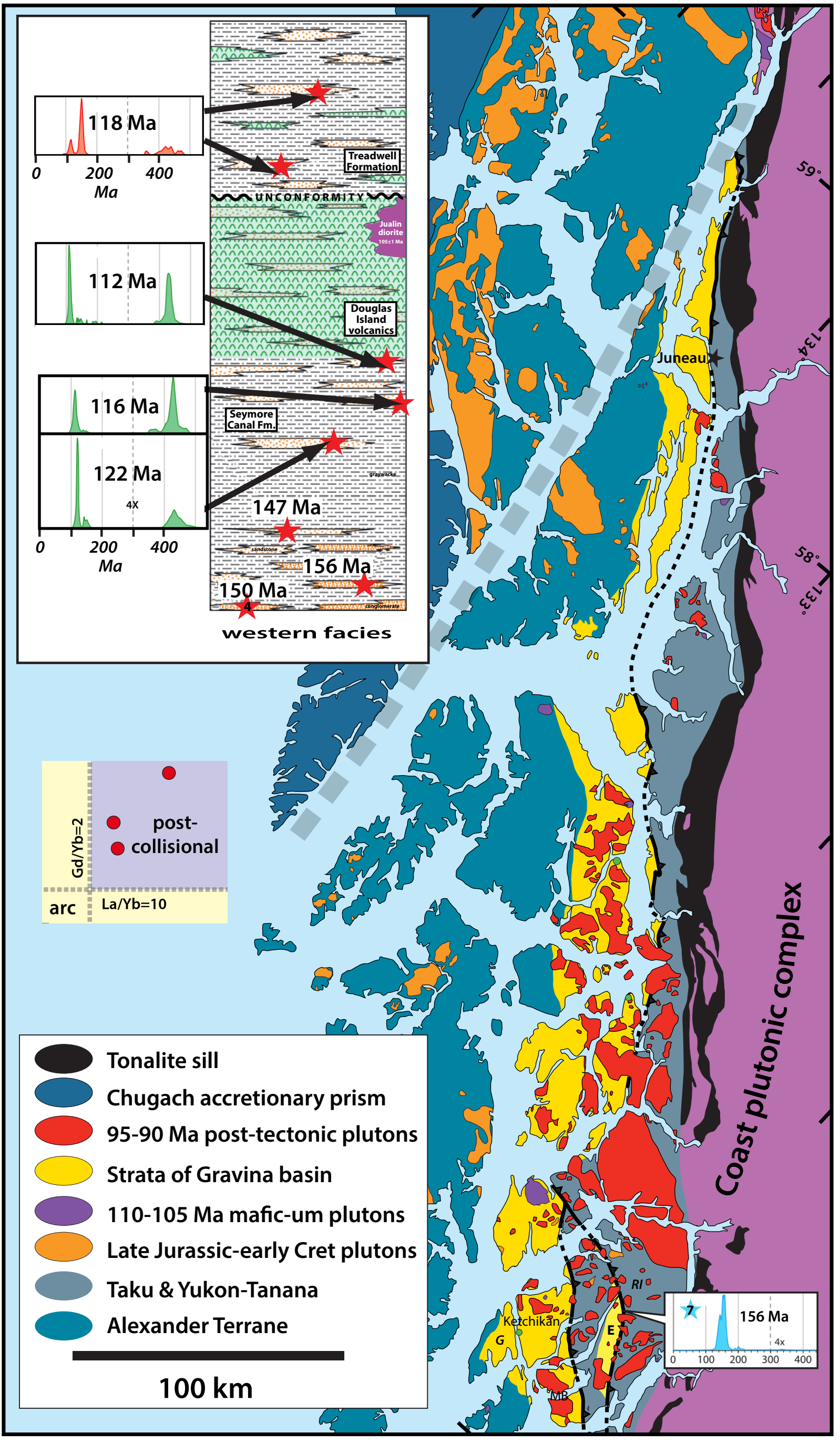

Supplemental Figure 8: Geological sketch map of rock units in part of Insular Alaska showing distribution of Gravina basin strata, post-collisional plutons, and various terranes (mainly after Gehrels and Berg (1992). Stratigraphic column of western facies of rocks from Gravina basin and detrital zircon data from Kapp and Gehrels (1998) and Yokelson et al. (2015); geochemistry of Moth Bay pluton (MB) from Cook et al. (1991). Note that rocks of the Treadwell Fm. are younger than 105 Ma as they unconformably overlie the Jualin diorite (Redman, 1984; Kapp and Gehrels, 1998). E–eastern facies of Gravina basin; *G–Gravina Island*; *RI–Revillagigedo Island*

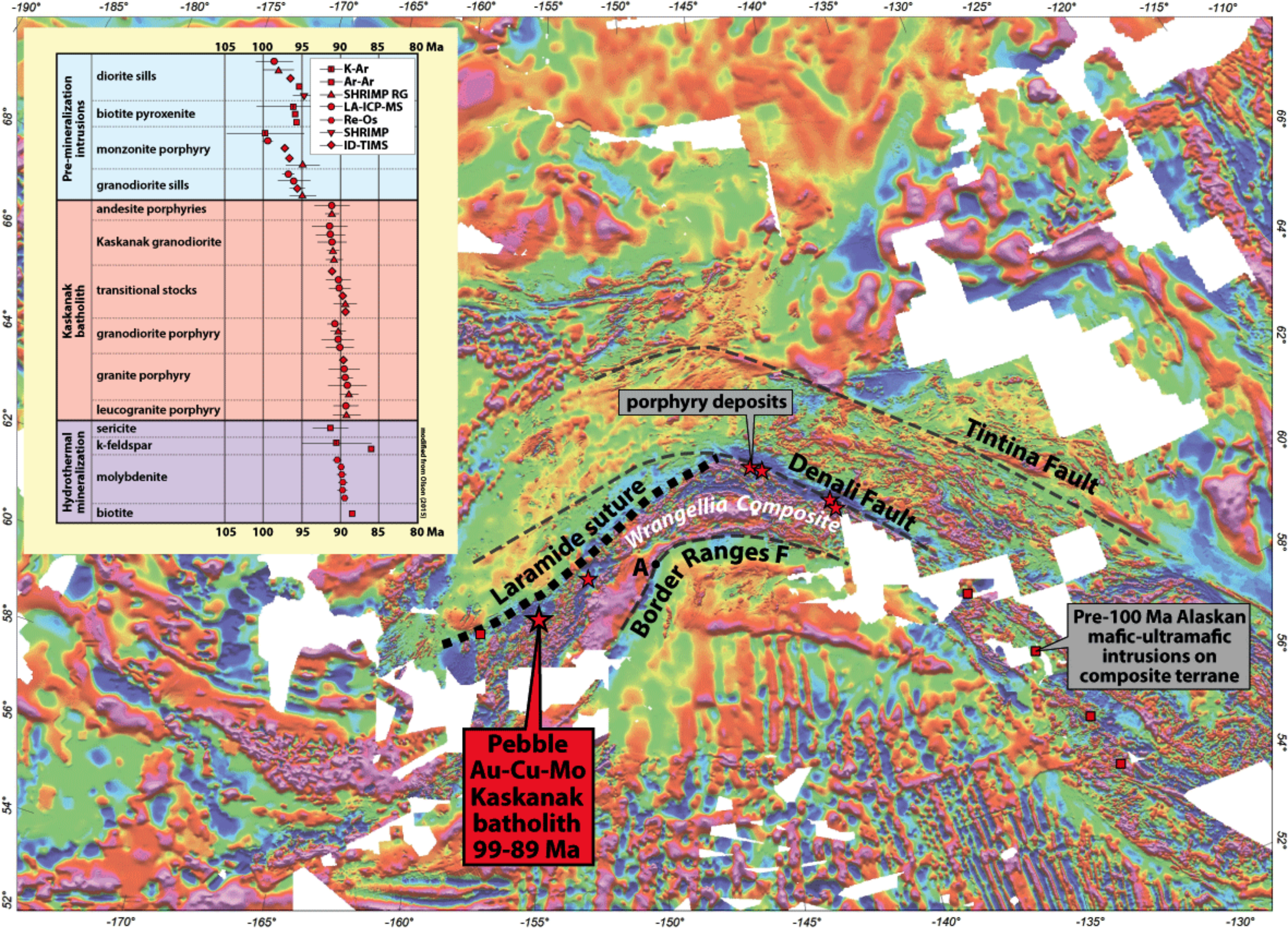

Supplemental File 9: Aeromagnetic map of southern Alaska, northwestern Canada, and adjacent seafloor of the Gulf of Alaska courtesy of Geological Survey of Canada, showing locations of pre-100 Ma Alaskan-type mafic-ultramafic intrusions emplaced into the Peninsular Ranges composite terrane and the location of porphyry deposits associated with 99-84 Ma post-collisional intrusions emplaced after closure of the seaway. A–Anchorage. Location of Laramide suture from Hults et al. (2013). Insert: Various ages from Pebble mine area of Kaskanax batholith from Olson (2015).

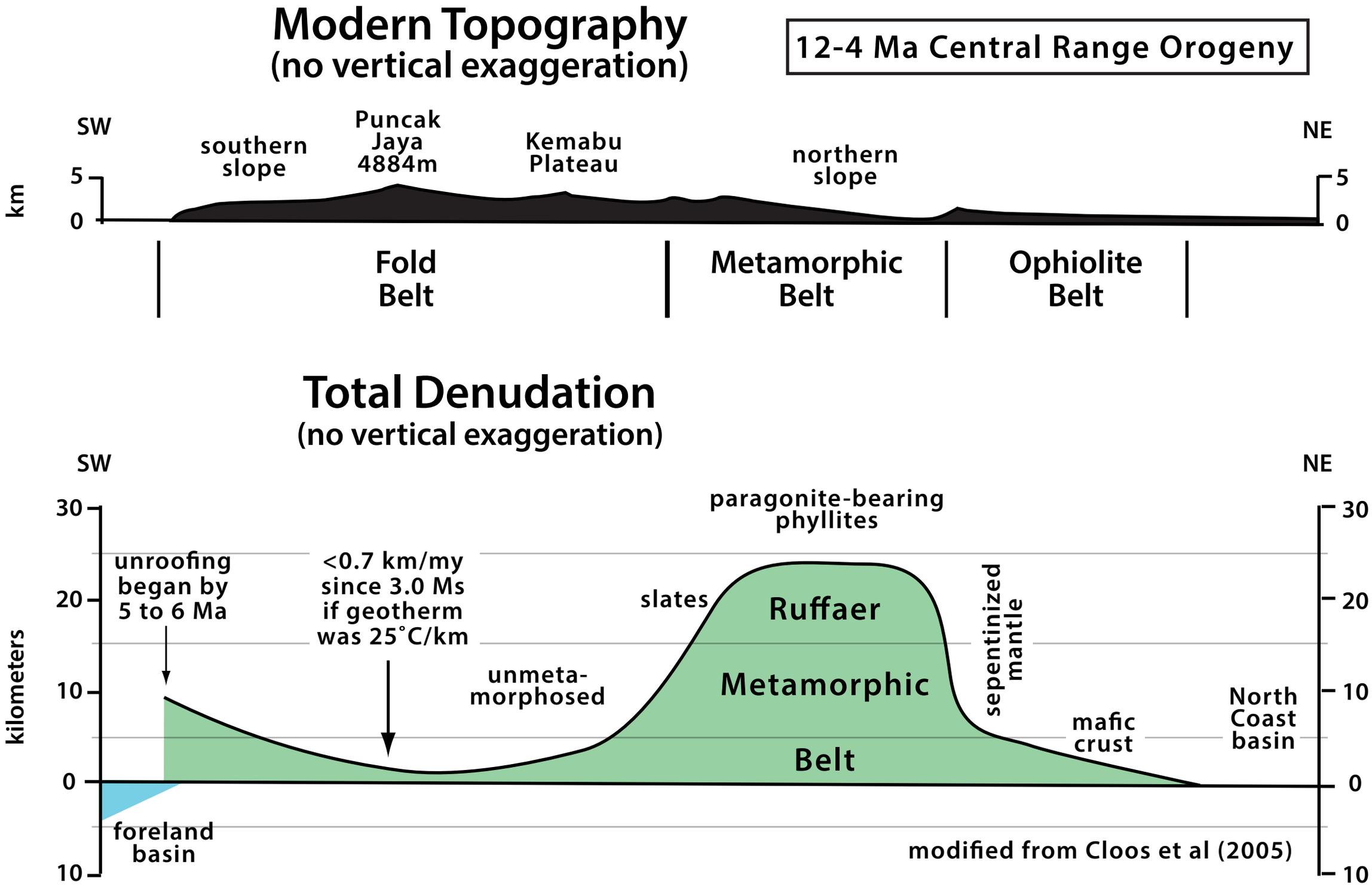

Supplemental Figure 10. Modern topography and differences in depth of denudation in the Central Range orogen of Papua, New Guinea, modified from Cloos et al. (2005), and illustrating ~25 km exhumation on the opposite side of the orogen from the foreland. Large rivers have transported most debris northward to the North Coast basin because the nearly 5 km high Central Range (Puncak Jaya) blocks drainage to the south. We see this as a more modern example of the post-collisional sedimentation in the back-arc region, such as the <100 Ma Valle, Great Valley, Nanaimo, and McHugh successions, caused by slab break off and consequent exhumation of the hinterland belt.

The mid-Cretaceous Peninsular Ranges orogeny: a new slant on Cordilleran tectonics? II: northern United States and Canada

HILDEBRAND, Robert S.,* 1401 N. Camino de Juan, Tucson, AZ 85745 USA
WHALEN, Joseph B., Geological Survey of Canada, 601 Booth Street, Ottawa, ON K1A 0E8, Canada

Supplemental Figure 1

Alasino, P.H., Ardill, K., Stanback, J., Paterson, S.R., Galindo, C., and Leopold, M. 2019. Magmatically folded and faulted schlieren zones formed by magma avalanching in the Sonora Pass Intrusive Suite, Sierra Nevada, California. Geosphere, **15**: 1677–1702, doi.org/10.1130/GES02070.1.

Clemens-Knott, D. 1992. Geologic and Isotopic Investigations of the Early Cretaceous Sierra Nevada Batholith, Tulare County, California, and the Ivrea Zone, Northwest Italian Alps: Examples of Interaction Between Mantle-Derived Magma and Continental Crust. Ph.D. thesis, California Institute of Technology, Pasadena, California, 389 p.

du Bray, E.A. 2007. Time, space, and composition relations among northern Nevada intrusive rocks and their metallogenic implications. Geosphere, **3**: 381–405. doi:10.1130/GES00109.1.

Hirt, W.H. 2007. Petrology of the Mount Whitney Intrusive Suite, eastern Sierra Nevada, California: Implications for the emplacement and differentiation of composite felsic intrusions. Geological Society of America Bulletin, **119**: 1185–1200. doi.org/10.1130/B26054.1.

Memeti, V. 2009. Growth of the Cretaceous Tuolumne Batholith and Synchronous Regional Tectonics, Sierra Nevada, CA: A Coupled System in a Continental Margin Arc Setting. Ph.D. thesis, University of Southern California, Los Angeles, California, 282 p.

Sisson, T.W., Grove, T.L., and Coleman, D.S. 1996. Hornblende gabbro sill complex at Onion Valley, California, and a mixing origin for the Sierra Nevada batholith. Contributions to Mineralogy and Petrology, **126**: 81–108, doi:10.1007/s004100050237.

Van Buer, N.J., and Miller, E.L. 2010. Sahwave batholith, NW Nevada: Cretaceous arc flare-up in a basinal terrane. Lithosphere, **2**: 423–446, doi:10.1130/L105.1.

Supplemental Figure 2

Hildebrand, R.S., Whalen, J.B. 2017. The Tectonic Setting and Origin of Cretaceous Batholiths Within the North American Cordillera: The Case for Slab Failure Magmatism and Its Signifcance for Crustal Growth. Geological Society of America Special Paper **532**, 113 p.

Supplemental Figure 3

Hildebrand, R.S., Whalen, J.B. 2017. The Tectonic Setting and Origin of Cretaceous Batholiths Within the North American Cordillera: The Case for Slab Failure Magmatism and Its Signifcance for Crustal Growth. Geological Society of America Special Paper **532**, 113 p.

Manduca, C.A., Kuntz, M.A., and Silver, L.T. 1993. Emplacement and deformation history of the western margin of the Idaho batholith near McCall, Idaho: Influence of a major terrane boundary. Geological Society of America Bulletin, **105**: 749–765, doi:10.1130/0016-7606(1993)105<0749:EADHOT>2.3.CO;2

Supplemental Figure 4

Wallace, C.A. 1987, Generalized geologic map of the Butte 1˚ x 2˚ quadrangle, Montana. United States Geological Survey, Miscellaneous Field Studies Map MF-1925, scale 1:250,000.

Wallace, C.A., Lidke, D.J., and Schmidt, R.G. 1990. Faults of the central part of the Lewis and Clark line and fragmentation of the Late Cretaceous foreland basin in west-central Montana. Geological Society of America Bulletin, **102**: 1021–1037, doi:10.1130/0016-7606(1990)102 <1021:FOTCPO>2.3.CO;2.

Supplemental Figure 5

Miller, R.B., DeBari, S.M., and Paterson, S.R. 2018. Construction, emplacement, and geochemical evolution of deep-crustal intrusions: Tenpeak and Dirtyface plutons, North Cascades, western North America. Geosphere, **14**, 1298–1323, doi:10.1130/GES01490.1.

Shea, E.K. 2014. Arc Magmatism at Different Crustal Levels, North Cascades, WA. Ph.D. thesis, Massachusetts Institute of Technology, Cambridge, Massachusetts, 555p.

Supplemental Figure 6

Crawford, M.L., Crawford, W.A., and Lindline, J. 2005. 105 million years of igneous activity, Wrangell, Alaska, to Prince Rupert, British Columbia. Canadian Journal of Earth Sciences, **42**: 1097–1116. doi: 10.1139/ e05-022.

Girardi, J.D., Patchett, P.J., Ducea, M.N., Gehrels, G.E., Cecil, M.R., Rusmore, M.E., Woodsworth, G.J., Pearson, D.M., Manthei, C., and Wetmore, P. 2012. Elemental and isotopic evidence for granitoid genesis from deep-seated sources in the Coast Mountains batholith, British Columbia. Journal of Petrology, **53**: 1505–1536, doi:10.1093/petrology/egs024.

Hildebrand, R.S., Whalen, J.B. 2017. The Tectonic Setting and Origin of Cretaceous Batholiths Within the North American Cordillera: The Case for Slab Failure Magmatism and Its Signifcance for Crustal Growth. Geological Society of America Special Paper **532**, 113 p.

Lynch, G. 1995. Geochemical polarity of the Early Cretaceous Gambier Group, southern Coast Belt, British Columbia. Canadian Journal of Earth Sciences, **32**: 675-685.

Mahoney, J.B., Gordee, S.M., Haggart, J.W., Friedman, R.M., Diakow, L.J., and Woodsworth, G.J. 2009. Magmatic evolution of the eastern Coast plutonic complex, Bella Coola region, west-central British Columbia. Geological Society of America Bulletin, **121**: 1362–1380, doi:10.1130/ B26325.1.

Supplemental Figure 7

Wheeler, J.O., and McFeely, P. 1991. Tectonic Assemblage Map of the Canadian Cordillera and Adjacent Parts of the United States of America. Geological Survey of Canada Map 1712A, 2 sheets, scale 1:2,000,000.

Supplemental Figure 8

Cook, R.D., Crawford, M.L., Omar, G.I., and Crawford, W.A. 1991. Magmatism and deformation, southern Revillagigedo Island, southeastern Alaska. Geological Society of America Bulletin, **103**: 829-841

Gehrels, G.E., and Berg, H.C. 1992. Geologic map of southeastern Alaska. U.S. Geological Survey Miscellaneous Investigations Map I-1867.

Kapp, P.A., and Gehrels, G.E. 1998. Detrital zircon constraints on the tectonic evolution of the Gravina belt, southeastern Alaska. Canadian Journal of Earth Sciences, **35**: 253–268. doi:10.1139/e97-110.

Redman, E., 1984. An unconformity associated with conglomeratic sediments in the Berners Bay area of southeastern Alaska. Alaska Division of Geological and Geophysical Surveys, Professional Report, **86**: 1–4.

Yokelson, I., Gehrels, G.E., Pecha, M., Giesler, D., White, C., and McClelland, W.C. 2015. U-Pb and Hf isotope analysis of detrital zircons from Mesozoic strata of the Gravina belt, southeast Alaska. Tectonics, **34**: 2052–2066, doi.org/10.1002/2015TC003955.

Supplemental Figure 9

Hults, C.P., Wilson, F.H., Donelick, R.A., and O'Sullivan, P.B. 2013. Two flysch belts having distinctly different provenance suggest no stratigraphic link between the Wrangellia composite terrane and the paleo-Alaskan margin. Lithosphere, 5: 575–594. doi:10.1130/L310.1.

Olson, N.H., III. 2015. The Geology, Geochronology, and Geochemistry of the Kaskanak Batholith, and other Late Cretaceous to Eocene Magmatism at the Pebble Porphyry Cu-Au-Mo Deposit, SW Alaska. M.S. thesis, Oregon State University, Corvallis, Oregon, 248p.

Supplemental Figure 10

Cloos, M., Sapiie, B., van Ufford, A.Q., Weiland, R.J., Warren, P.Q., and McMahon, T.P. 2005. Collisional Delamination in New Guinea: The Geotectonics of Subducting Slab Breakoff. Geological Society of America Special Paper 400, 51 p.

Canadian Journal of
Earth Sciences

Article

The mid-Cretaceous Peninsular Ranges orogeny: a new slant on Cordilleran tectonics? III: the orogenic foredeep

Robert S. Hildebrand[a], **Janok P. Bhattacharya**[b], **and Joseph B. Whalen**[c]

[a]1401 N. Camino de Juan, Tucson, AZ 85745, USA; [b]School of Geography and Earth Sciences, McMaster University, 1280 Main St. West, Hamilton, ON L8S 4L8, Canada; [c]Geological Survey of Canada, 601 Booth Street, Ottawa, ON K1A 0E8, Canada

Corresponding author: **Robert S. Hildebrand** (email: bob@roberthildebrand.com)

Abstract

The Cretaceous Western Interior Basin reflects the interplay between the North American craton and allochthonous terranes to the west. We divide the basinal stratigraphy into three successions, Aptian–Albian, Cenomanian–Turonian, and Santonian–Maastrichtian, each related to periods of deformation in the adjacent fold-thrust belt. Here we focus on the Cenomanian–Turonian succession, where progressive west to east uplift and fluvial incision of older Aptian–Albian sedimentary rocks (Cedar Mtn–San Pitch–Thermopolis–Skull Creek–Mannville) are interpreted as a migrating forebulge. Uplift was underway at 103 Ma in the west (Paddy–Blackleaf–Muddy sandstones) and propagated eastward throughout the trough by 99.5 Ma (Viking–Bow Island–Newcastle sandstones). The incised fluvial valleys were subsequently filled by swampy and shallow marine facies, then overlain by dark, marine *Neogastroplites*-bearing shale and associated bentonites of the 100–97.5 Ma Shell Creek–Mowry–Slater River–Goodrich–Shaftesbury–Westgate shales. The shales are characterized by a distinctive condensed horizon with abundant fish scales, teeth, and bones. They are interpreted as outer-trench slope deposits, with the overlying anoxic horizon representing a starved isochronous unit formed atop the slope deposits. The starved horizon is overlain by prodeltaic muddy clinoforms of easterly migrating clastic wedges (Trevor–Dunvegan–Frontier–Cintura–Mexcala) that can be traced 800 km atop the fish-scale hash and contain hinterland-derived 99–90 Ma detrital zircons. Although the Western Interior Basin has long been considered a retro-arc trough, the overall succession instead suggests that the Cretaceous–Turonian part represents a collisional foredeep created during the ~100 Ma collision between the arc-bearing Peninsular Ranges composite terrane and North America. The accretion brought tyrannosaurids, pachycephalosaurs, snakes, and marsupials to North America.

Key words: foredeep basin, dinosaur invasion, Cordillera, Peninsular Ranges orogeny, stratigraphy, Western Interior Basin

Introduction

Much of the western half of Cretaceous North America comprised a northerly trending couplet of distinct, yet intimately interrelated, tectonic entities: the Cordillera and the Western Interior Basin (Fig. 1). The mostly high-standing Cordillera consists of varied geological terranes, complexly mingled, mixed, rifted, and amalgamated, and mainly Phanerozoic; whereas to the east, the Cretaceous Western Interior Basin was generally a subdued, low-lying, asymmetric drainage trough, built on cratonic North America, and received sediment from Cordilleran uplands to the west, as well as more muted cratonic topography to the east (Roberts and Kirschbaum 1995; Carpenter 2014; Finzel 2014; Miall and Catuneanu 2019). From time to time, the trough was continuous from the Tethyan realm of the Gulf of Mexico to the Boreal realm of the Arctic Ocean (see Kauffman and Caldwell 1993), and so is commonly referred to as the Western Interior seaway.

Rocks of the Western Interior Basin unconformably overlie platformal siliciclastic and carbonate rocks of the west-facing Cambrian to Mesozoic platformal margin of North America. In contrast, rocks of the Cordilleran terranes are largely considered to be composite, allochthonous, and exotic to North America, although in some cases their provenance remains equivocal (Helwig 1974; Coney et al. 1980; Coney 1981; Monger et al. 1982; Hildebrand 2013). The boundary between the two geologic regions is represented by a linear belt of easterly vergent folds and thrusts of widely different ages, but collectively known as the Cordilleran fold-thrust belt, with an eastern limit that closely coincides with the cratonic hingeline (Stokes 1976; Aitken 1989).

During the mid-1960s while working in the fold-thrust belt of the Idaho–Wyoming border region, Armstrong and Oriel (1965) recognized that Mesozoic folds and thrust faults were progressively younger eastward, and as the deformation migrated, coarse detritus was deposited in front of the thrusts. In a related paper, Bally et al. (1966) used seismic data to demonstrate that the Canadian portion of the fold-thrust belt, along with high-grade gneiss and granitic plutons farther west, sat structurally upon the western edge of cratonic North America and that the progressively eastward-migrating thrust stack, not only loaded and depressed the subjacent

Fig. 1. Location of the Western Interior Basin in the proposed paleogeography of North America during the Cretaceous. Source map © 2013 Colorado Plateau Geosystems Inc.

lithosphere, but that it shed clastic detritus into an asymmetrical basin migrating eastward in front of the thrust wedge. Their synthesis implied, as they noted, that the structurally higher and more westerly thrust sheets formed prior to those to the east.

By 1969, in their zeal to explore and understand the landward implications of plate tectonics, early advocates used a Cenozoic Andean framework to interpret the strongly deformed Mesozoic rocks of the high-pressure, low-temperature Franciscan thrust complex, located in western California, with similar age sedimentary rocks of the Great Valley Group, plutons of the Sierran-Klamath batholith, and the Cordilleran fold-thrust belt as a two-sided orogen: bound on both sides by major, but opposed, structural elements that collectively reflected eastward subduction of the Pacific seafloor beneath North America from the Jurassic to the Eocene (Dickinson 1970; DeCelles 2004; Yonkee and Weil 2015; Pavlis et al. 2020).

This long-standing and generally accepted hypothesis has created problems for those working in the Western Interior Basin, as phases of thrusting, thought to range in age from the Jurassic to Eocene, were active intermittently, and so are difficult to link genetically to specific events farther west (e.g., Cant and Stockmal 1989; Price 1994; Liu et al. 2005; Plint et al. 2012; Pana and van der Pluijm 2015; Quinn et al. 2016).

Some workers (Ducea and Barton 2007; DeCelles et al. 2009; Ducea et al. 2015) tried to resolve the problems by developing a complex model where magmatic high-flux events in the arc were linked to retro-arc thrusting, which, in turn, led to increased sedimentation and subsidence within the Western Interior Basin. In this model, ~400 km of upper crustal sedimentary rocks were progressively detached from crystalline basement and transported eastward on thrusts, causing an equal length of middle to lower crust and subjacent lithospheric mantle to be underthrust beneath the hinterland and Sierran arc, where they hypothesized that the crust melted to provide more than 50% of Sierran arc magmatism.

However, there are several problems with this model. First, they provide no sound mechanism for how 400 km of buoyant cratonic lithosphere was thrust beneath the Sierra Nevada nor where the heat to melt it might have come from. Second, the underthrust lithosphere would still have had a dry lower crust and refractory, intact mantle root, typical of old cratons, which would have amplified the difficulty of generating melts. Third, given that the Sierran high-flux plutons have bulk compositions no more than 10%–12% different than bulk lower and middle crust (Ducea 2002), a mechanism must be found to melt nearly all of that crust, implying a paucity of dense restite to delaminate and sink into the mantle. Fourth, the lack of delamination, coupled with the underthrusting of such large volumes of material, creates severe room problems. Finally, the plutonic rocks of the high-flux events can have, where there is no old, enriched subcratonic lithospheric mantle, positive εNd_T and Sr_i <0.704 that rule out significant input of continental crust (Wetmore and Ducea 2009; Cecil et al. 2021), or, as in the case of the Sierran Crest magmatic suite of Coleman and Glazner (1998), have $\delta^{18}O_{zircon}$ values more typical of the mantle than continental crust (Lackey et al. 2008; Hildebrand et al. 2018).

Other models envisaged flexural loading and isostatic compensation caused by the accreted terranes, the thrust stack, and their eroded sediments as the main driver for subsidence in the basin (Price 1973; Beaumont 1981; Jordan 1981). Over the next couple of decades, models were invoked to better constrain the development of the basinal subsidence not only in terms of thrust load and lithospheric flexure (Stockmal et al. 1986; Stockmal and Beaumont 1987) but also by accounting for the shape of the orogen, the rifted margin, the shape of the basal detachment, and the way their interaction developed through time (e.g., Jamieson and Beaumont 1988; Beaumont et al. 1993). However, at times the basin subsided to extend eastward to the Dakotas and beyond, which is simply too far to be explained by isostatic loads in the Cordillera. As a result, some researchers invoked dynamic pressure variations in the asthenosphere above shallowly dipping oceanic lithosphere beneath the craton (Mitrovica et al. 1989; Gurnis 1992; Burgess and Moresi 1999; Liu et al. 2014; Li and Aschoff 2022). In every case, the models assumed the basin was in a retro-arc position above a persistently eastward-dipping slab of oceanic lithosphere beneath cratonic North America—but as dynamic topography is governed by transient variations in the mantle density and flow, it is difficult to interpret surface heights (topography) from mantle convection processes (Molnar et al. 2015), especially where the isostatic components are so poorly known that they cannot be removed to better isolate the dynamic contribution (Yang and Gurnis 2016). Additionally, slab break-off and migration of a broken slab beneath a continent as it moved laterally can also produce a downward pull on the surface, much in the way the Indian foredeep basin (Siwaliks) was apparently deepened when the torn and bent oceanic slab passed beneath

it (Husson et al. 2014). Overall, better geological constraints are necessary to understand the sources of the variations in surface topography.

In this paper, we examine the mid-Cretaceous stratigraphy of the Western Interior Basin, from the latest Albian into the Cenomanian–Turonian. We start with a brief overview of our tectono-sedimentary divisions for the basin to better integrate our results within the larger continuum of plate interactions that bear on its overall development. Then we describe mid-Cretaceous stratigraphic units throughout the basin to demonstrate their along-strike similarities in both lithology and timing. We end with a model that ties the stratigraphy within the Cenomanian–Turonian sector of the Western Interior Basin directly to interactions between the Peninsular Ranges composite terrane and the North American craton during the mid-Cretaceous Peninsular Ranges orogeny of Hildebrand and Whalen (2021*a*, 2021*b*).

Tectono-sedimentary subdivisions of the basinal stratigraphy

The bulk of the Western Interior Basin developed during the Cretaceous (Kauffman and Caldwell 1993); although some workers, most notably Royse (1993), along with DeCelles and colleagues (DeCelles and Currie 1996; DeCelles 2004; DeCelles and Coogan 2006; Fuentes et al. 2011), suggested that the basin initially formed during the Late Jurassic; but in either case, the Jurassic rocks were uplifted and eroded prior to the deposition of Cretaceous sediments as old as Aptian–Albian (see Heller et al. 1986). Within the southern Canadian sector of the basin, Pana et al. (2018*a*, 2019) presented the results of U-Pb dating of ash beds, along with biostratigraphy and sedimentology, from units as old as Lower Jurassic, which support the concept of one or more Jurassic foredeep basins. Within the US portion of the basin, remnant sedimentary rocks of the Upper Jurassic Morrison Formation are known to be 155–148 Ma (Kowallis et al. 1998, 2007) and could be equivalent to the youngest stratigraphic units of the Canadian Jurassic.

Regardless of the interpretation of the Jurassic stratigraphy, the Western Interior Basin is dominantly a Cretaceous basin (Fig. 2). Here we divide its Cretaceous rocks into three major intervals: Aptian–Albian (125–100.5 Ma), Cenomanian–Turonian (100.5–90 Ma), and Coniacian–Maastrichtian (90–66 Ma), each apparently related to recognized periods of shortening, uplift, and exhumation in the adjacent fold-thrust belt to the west. We use the terms Sevier (~124 Ma), Peninsular Ranges (~100 Ma), and Laramide to refer to the three orogenies, respectively, with the Laramide subdivided into an early thin-skin orthogonal phase (90–72 Ma) and a younger thick-skin transpressive phase (72–50 Ma) as per Hildebrand and Whalen (2017).

Unconformably overlying, and cutting downward into paleosols of the Jurassic Morrison Formation are incised paleovalleys filled with a regional pebble conglomerate (Yingling and Heller 1992; Currie 1998; Heller et al. 1986; Heller and Paola 1989), a regional gravelly conglomerate, that was traced eastward as far as the Black Hills of South Dakota, which

Fig. 2. Schematic west to east US cross section illustrating our tripartite divisions of the Cretaceous stratigraphy within the Western Interior Basin. Each succession is correlative with the named periods of shortening, uplift, and exhumation recognized in the adjacent fold-thrust belt. Modified from Weimer (1986).

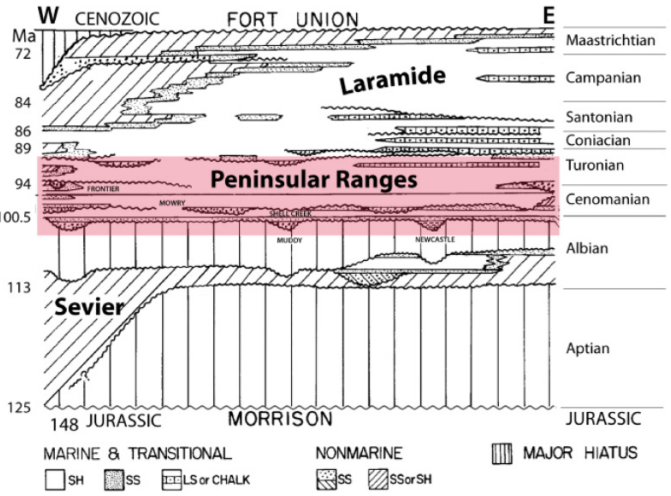

suggests that the regional surface sloped gently eastward (Heller et al. 2003). In Utah, the conglomerates are overlain by synorogenic sedimentary rocks of the Ruby Ranch Member of the Cedar Mountain Formation and the San Pitch Formation, which on the basis of detrital zircon populations, are interpreted to have been derived largely from thrust sheets located to the west, such as the Canyon Range thrust (Lawton et al. 2010), and interpreted, on the basis of $\delta^{18}O$ in dinosaur ingested water, to have been deposited in the arid lee of mountains to the west (Suarez et al. 2014). The onset of Early Cretaceous thrusting in the Great Basin segment is constrained to be ~124–120 Ma based on (i) detrital zircon peaks in sedimentary units beneath the Ruby Ranch Member (Greenhalgh 2006; Greenhalgh and Britt 2007; Britt et al. 2007; Mori 2009), (ii) a 119.4 ± 2.6 Ma U-Pb age of palustrine carbonate, and (iii) a good match between $\delta^{13}C_{org}$ excursions in early terrestrial foredeep sedimentary rocks and well-dated Albian features of the global carbon isotope chemostratigraphy (Ludvigson et al. 2010). More recent dating of detrital zircons in mudstone palaeosols from the lowermost member of the Cedar Mountain Formation, known as the Yellow Cat Member, produced a maximum depositional age (MDA) of 136.3 ± 1.3 Ma (Joeckel et al. 2020). However, most researchers consider the overlying, more continuous, and westward thickening Ruby Ranch Member to represent the earliest basinal fill related to Sevier thrusting in Utah (Kirkland et al. 2016).

Regional thrusting, originally assigned to the Sevier orogeny by Armstrong (1968), stopped during the mid-Albian at about 105 Ma, as documented by alluvial fan and fluvial sedimentary rocks of the Canyon Range wedge-top basin that unconformably overstep the Canyon Range thrust (Lawton et al. 2007). In the Wyoming sector of the belt the Ephraim Conglomerate, which was deposited unconformably upon Jurassic strata, is inferred on the basis of detrital zircon spectra

and conglomerate clast types to be debris shed from the oldest Paris thrust sheet. The Ephraim Conglomerate contains Aptian charophytes (Gentry et al. 2018; Heller et al. 1986). Additionally, apatite fission track ages of 117 ± 6 Ma and 111 ± 8 Ma collected along the Paris thrust attest to significant cooling at that time (Burtner and Nigrini 1994). In southern Canada, thrusts were shown to predate 108 Ma as they are cut by post-kinematic plutons of the Bayonne suite (Logan 2002; Larson et al. 2006). The sedimentary package in Canada starts with a basal Aptian pebbly conglomerate (Cadomin Formation), which sits unconformably upon Jurassic strata (Leckie and Cheel 1997; Leier and Gehrels 2011). The regional conglomerate unit is overlain by a thick package of siliciclastic strata contained within the Blairmore, Mannville, Luscar, and Bullhead groups (Hayes et al. 1994), which locally contain volcanic and plutonic clasts, and more elevated εNd (epsilon Nd) than rocks of the Cadomin Formation (Ross et al. 2005), consistent with uplift and erosion of young volcano-plutonic material to the west.

Throughout the basin, an unconformity within the uppermost Albian strata forms the base of a new cycle of sedimentation and co-genetic thrust activity to the west, during which movement on the thrust faults folded the earlier thrusts to form structural culminations, that are more or less coeval with part of the Cenomanian–Turonian succession of sedimentary rocks within the basin (Pujols et al. 2020; Yonkee and Weil 2015). These rocks are the main focus of this contribution.

More thrusts, active some 15 Myr later during the Santonian–Early Campanian, document another pulse of shortening (Yonkee and Weil 2015) and are unconformably overlain by large eastward-prograding, fluvial megafans deposited during the Campanian–Maastrichtian (DeCelles and Cavazza 1999). This thrusting marks what we term the early Laramide phase of deformation and related sedimentation (Hildebrand 2014; Hildebrand and Whalen 2017) when the shortening direction was approximately NE-SW. This early Laramide event involved some northward migration of the foredeep (Catuneanu et al. 2000), followed by contraction and local inversion of the Western Interior Basin during the Maastrichtian–Paleocene when the more localized thick-skin Laramide basins and uplifts (Dickinson et al. 1988) formed as shortening progressed to N-S (Gries 1983) and produced large-scale meridional migration of much of the Cordillera (Enkin 2006; Gladwin and Johnston 2006; Hildebrand 2014, 2015).

The mid-Cretaceous of the Western Interior Basin

During the early part of the late Albian, central to western North America (Fig. 3) was covered by an epeiric seaway that extended from the Gulf of Mexico to the Arctic Ocean, known as the Joli Fou-Skull Creek Sea (Porter et al. 1998; Cobban and Reeside 1952). By the latest Albian, a marine regression resulted in the southern margin of the basin migrating northward to Montana, Wyoming, north-central Colorado, and the western Dakotas (Roberts and Kirschbaum 1995). During this regression, incised valleys were cut into the older units progressively from west to east and subsequently filled with sinuous bodies of sandstone, such as occur in the dominantly non-marine Newcastle and Muddy sandstones. Later, as the Boreal Sea transgressed from west to east into northwestern Colorado and northeastern Utah, rocks of the Muddy/Newcastle were overlain by shales, siltstones, and bentonites of the Shell Creek and upper Thermopolis formations, which in turn were covered by shales of the siliceous Mowry Formation, a dominantly anoxic, condensed unit containing abundant disarticulated fish bones, teeth, and scales, as well as numerous bentonite beds (Walaszczyk and Cobban 2016). These units have equivalents to the north in Canada, and in both countries the condensed units holding abundant fish hash were abruptly overlain by eastward-prograding clastic wedges containing abundant 99–90 Ma detrital zircons derived from the orogenic hinterland to the west.

Fig. 3. Hypothesized paleogeography from Blakey (2014) for the Western Interior Basin or seaway from Late Albian to Middle Cenomanian. Source maps © 2014 Colorado Plateau Geosystems Inc.

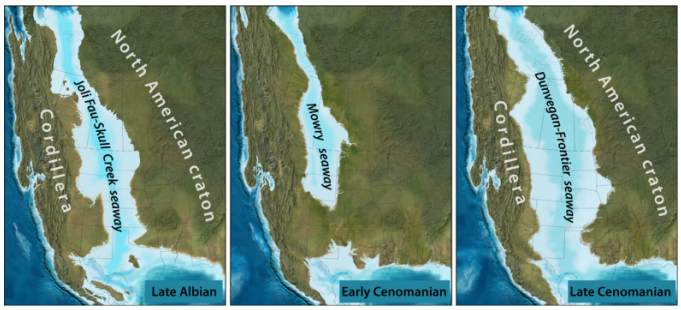

Thermopolis Formation

This succession of rocks, which largely predates rocks we are interested in, is widely known from Wyoming where it underlies the Muddy Sandstone and is commonly subdivided into several informal members (Fig. 4): Rusty beds, "lower" Thermopolis shale, middle silt, and "upper" Thermopolis shale. Although rocks of the formation occur in the Black Hills of South Dakota (Fig. 5), they are only about 5 m thick and so undivided (Eicher 1958). In the upper Thermopolis Shale, a bentonite bed collected below the base of the Muddy Sandstone yielded a $^{40}Ar/^{39}Ar$ sanidine age of 101.36 ± 0.11 Ma (Singer et al. 2021), which constrains the Muddy Sandstone and the Shell Creek Shale to be younger, whereas the underlying Thermopolis Shale is about 5 million years older (Fig. 4). In the Big Horn and Powder River basins (Fig. 5), "upper" Thermopolis Shale is a black, nearly silt-free shale 20–35 m thick containing scarce ironstone beds, a couple of bentonites near the top, and in only the Big Horn Basin, radiolarians in its upper layers (Eicher 1958). Some workers include the Muddy Sandstone and overlying Shell Creek Shale in the Thermopolis Shale, but as they are demonstrably younger and represent in part non-marine successions, we treat them

Fig. 4. Middle Cretaceous stratigraphic chart with $^{40}Ar/^{39}Ar$ sanadine ages after Singer et al. (2021) and additions in Canada from sources cited in text. Note the eastward younging of the Muddy and Newcastle sandstones.

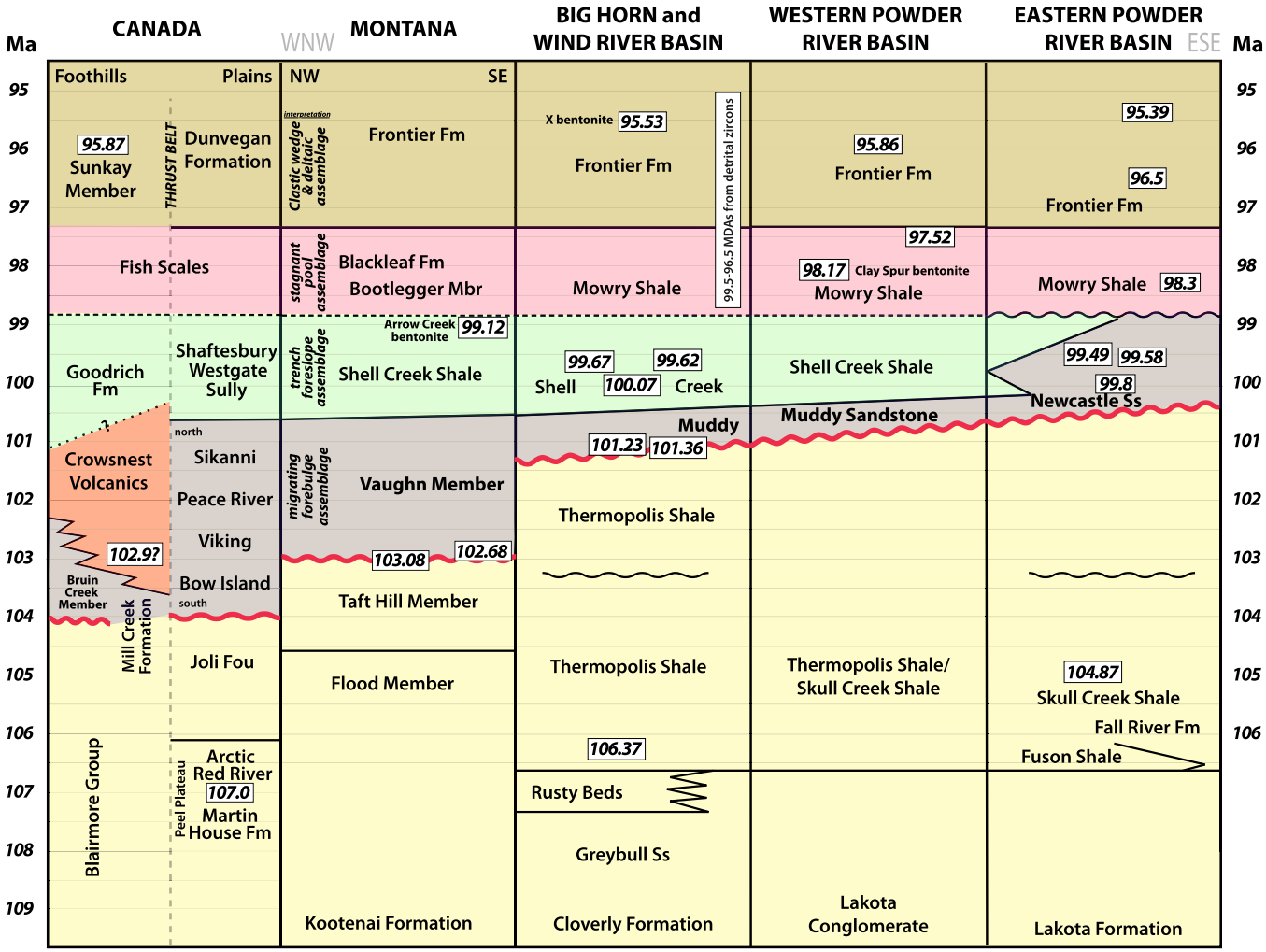

as separate units (see also Kirschbaum and Mercier 2013; Bremer 2016).

Muddy Sandstone

The Muddy Sandstone (Fig. 4) is known from much of Wyoming, but in the southwest is commonly termed the Dakota Sandstone. Eicher (1962) originally argued for separation of the Muddy Sandstone from adjacent units and for it to be given formational status. As this formation is a major petroleum reservoir, there is plenty of available data. Waring (1976) used it to show that in the northeast Powder River Basin of Wyoming (Fig. 5) and southeastern Montana the unit represented infilled channels of a dendritic river system. Whiteford (1962), Dresser (1974), and Curry (1962) studied rocks of the Muddy Formation in the Wind River Basin (Fig. 5) and found quartzose and chert-bearing sandstone, siltstones, silty shales, carbonaceous sandstones, conglomerates, rare bentonite, black and gray shale, and lignitic shale lying atop the Thermopolis Shale. In places, the Muddy Sandstone is up to 50 m thick, but more typically ranges from 3 to 13 m thick, and is overlain disconformably by the Shell Creek Shale (Curry 1962), which consists of shallow marine sedimentary rocks (Gustason 1988). Depending on location, the basal 1–10 m of the Muddy Sandstone consists of sandy or silty mudstone, muddy sandstone, lignite, and scarce bentonites, one of which was dated using $^{40}Ar/^{39}Ar$ by Singer et al. (2021) as 101.23 ± 0.09 Ma (Fig. 4). Plant remains such as leaves, amber, fusain, ferns, conifers, and dicots are abundant (Curry 1962). The basal succession shoals upwards to a non-marine sandy shoreline and (or) swampy section.

The middle sector of the formation comprises local, irregularly distributed bar, channel, and deltaic facies of a distributary river system, with some trough crossbedded sandstone filling channels as wide as several kilometers cut 30 m deep into the finer grained units below (Whiteford 1962). Dresser (1974) also reported facies diagnostic of a northeast-trending siliciclastic shoreline. Gustason (1988) documented that the middle parts of the formation contain foraminifera characteristic of the *Miliammina manitobensis* zone as do the overlying Shell Creek and Mowry shales, whereas the lower parts of the formation were more similar to the Skull Creek facies

Fig. 5. Sketch map of part of western North America after Reed et al. (2005) showing distribution of Cretaceous sedimentary rocks of the Western Interior Basin and geologic elements discussed in text. Not all geological units are shown.

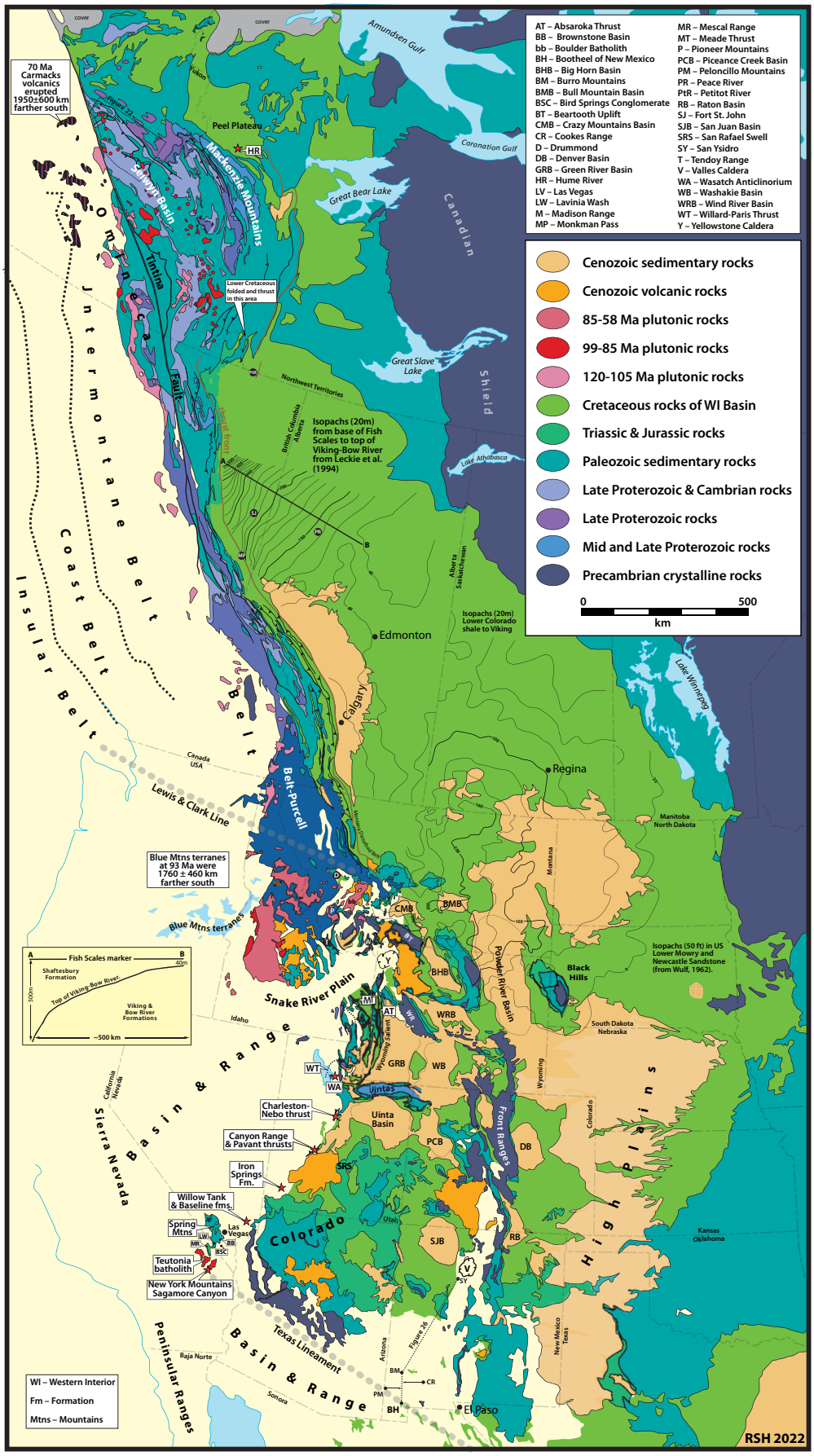

Fig. 6. Paleontological zonation of various formations described and discussed in text (from Walaszczyk and Cobban 2016).

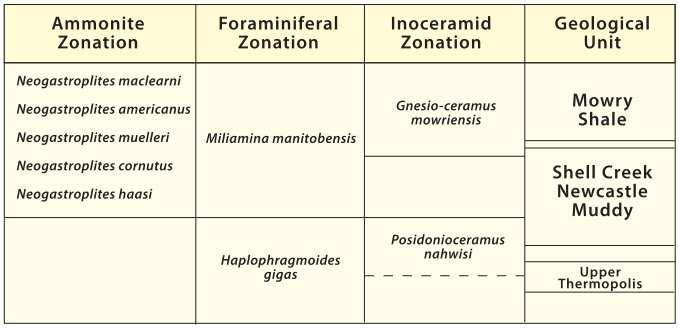

and contain the late Albian *Haplophragmoides gigas* biofacies (Fig. 6).

In the upper part of the unit, lagoonal, shallow marine sediments buried the sandy channels and covered the shoreline with shallow-water muds, detrital lignites, paleosols, fine sands with abundant ripple marks and mud cracks, with thin, burrowed tidal flat sands, and silts (Dresser 1974). According to Curry (1962), the uppermost shallow marine facies contains brachiopods.

Dolson et al. (1991) used published subsurface maps, more than 1000 core descriptions, a 900-well cross-section grid, and a computerized regional formation-top file of over 30 000 wells to reconstruct the Muddy Sandstone. Their earliest sedimentation, sheet sands that migrated westward, are several million years older than the Muddy and relate to the Kiowa-Skull Creek Sea (Singer et al. 2021). However, these studies recognized younger valley fill, alluvial plain channel fill, and transgressive marine units. They point out that valley incision and the development of at least 10 different drainage basins took place during a relative fall in sea level and that the incised valleys were filled by both fluvial and transgressive marine facies.

Newcastle Sandstone

The Newcastle Sandstone (Fig. 4), partly overlaps in age with, but is mostly slightly younger than, the Muddy Sandstone (Singer et al. 2021). Rocks of the formation are mainly of fluvial to neritic origin and were largely deposited in incised paleovalleys cut into Skull Creek Shale and oriented westerly, northwesterly, and northerly. Throughout its outcrop area of the western Dakotas, Wyoming, and southeastern Montana, the formation contains anastomosing sand bodies of a dendritic drainage system and generally ranges from 30 to 50 m thick (Stapp 1967; Finzel 2017). Examination of more than 9000 wireline logs and 23 drill cores over its outcrop area by LeFever and McCloskey (1995) documented a basal alluvial sandstone, incised during a subsequent lowstand, then overlain and infilled by a package consisting of a westward-deepening, marginal to offshore transgressive succession of sandstones, mudstones, and minor coal, similar to units of the upper Muddy Sandstone to the west. During the eastward-migrating transgression, the older fluvial and shoreline systems were reworked and deposited as shallow to marginal marine deposits. Recent age determinations show rocks of the formation (Fig. 4) to be Lower Cenomanian with $^{40}Ar/^{39}Ar$ sanidine ages of 99.49 ± 0.07 (lower), 99.58 ± 0.12 Ma (middle), and 99.8 ± 0.4 Ma (upper) for bentonites intercalated with sandstone, mudstones, and coal (Singer et al. 2021). Finzel (2017) reported six detrital zircons with ages ranging from 103 to 98 Ma, which probably represent zircons from ash beds eroded and redeposited within the fluvial unit as the Newcastle Sandstone is confined to the far eastern sector of the trough.

Shell Creek Shale

The Shell Creek Shale (Fig. 4) is the basal marine shale unit deposited during the rise and transgression of the Shell Creek-Mowry Sea (Kirschbaum and Roberts 2005). It was first given formational status separate from both the overlying Mowry and underlying Thermopolis Shale by Eicher (1962). Rocks of the Shell Creek Shale are dominated by fissile, dark-gray shale and thin bentonite beds that overlie either the Thermopolis Shale or the Muddy Sandstone in the Green River and Bighorn basins (Fig. 5), pinch out to the west, and can be traced intermittently to the Black Hills of South Dakota (Redden and DeWitt 2008). Locally, a thin, poorly sorted, granular to pebbly conglomerate and pebbly sandstone, containing crocodile and fish teeth, interpreted as a transgressive lag, occurs on top of the Muddy Sandstone (Bremer 2016). Curry (1962) pointed out that rocks of the Muddy Sandstone contained Boreal, but no Tethyan faunas, implying that the trough was not connected to the Gulf of Mexico at that time. Singer et al. (2021) dated three bentonite beds using $^{40}Ar/^{39}Ar$ on sanidine (100.07 ± 0.07 Ma, 99.67 ± 0.13 Ma, and 99.62 ± 0.07 Ma) in the Shell Creek Shale from outcrops in the Big Horn Basin of Wyoming and Montana (Figs. 4 and 5). They noted that the 99.62 Ma bentonite in the lower Shell Creek Shale is indistinguishable in age from the middle Newcastle Sandstone to the east (Fig. 4), and so their correlation constrains the location of the eastern shoreface during the Early Cenomanian.

Mowry Shale

The Mowry Shale (Fig. 4) is widespread in Wyoming, southern Montana, northern Utah and Colorado, and in the Black Hills of western South Dakota. It extends the width of the trough from the thrust belt, where it is called Aspen Shale, to the east side of the Black Hills. It was originally described at the northern end of the Bighorn Mountains of Wyoming by Darton (1904), who identified abundant fish scales, bones, and teeth. It was distinguished from shales above and below by its ridge-forming nature, attributed to the presence of abundant siliceous ash beds or porcellanites (Rubey 1929). The Mowry Shale overlies a variety of units including black Thermopolis Shale, Shell Creek Shale, and Muddy Sandstone, Dakota Formation, and (or) Newcastle Sandstone, depending on location, and is overlain by the Belle Fourche or Chalk Creek members of the Frontier Formation (Reeside and Cobban 1960; Kirschbaum and Roberts 2005; Lichtner et al. 2020).

In most locations, the Mowry Shale is a dark siliceous shale with abundant bentonite or porcellanite beds: Reeside and Cobban (1960) describe a section just under 60 m thick containing 55 bentonite beds with several beds extending for hundreds of kilometers (Kauffman 1977). Due to its high silica content, rocks of the formation tend to form ridges of silvery colored shale. In addition to the volcanic debris, the unit is rich in disarticulated fish remains, especially scales and teeth. It thickens westward from 60 to 72 m thick in the Black Hills, where it contains abundant bentonite beds (Cobban and Larson 1997) to about 200 m in western Wyoming. Singer et al. (2021) obtained $^{40}Ar/^{39}Ar$ sanidine ages of 98.17 ± 0.11 Ma and 97.52 ± 0.09 Ma for bentonites in the Mowry Shale of the western Powder River basin (Fig. 4). Hannon (2020) dated one bentonite from the Mowry Shale in the Black Hills by U-Pb inductively coupled plasma mass spectrometry (ICP-MS) on zircon to be 98.3 ± 1.1 Ma (Fig. 4).

Reeside and Cobban (1960) recognized five gastroplitine ammonite zones in the Mowry Shale of Wyoming, from oldest to youngest: *Neogastroplites haasi, Neogastroplites cornutus, Neogastroplites muelleri, Neogastroplites americanus,* and *Neogastroplites maclearni* (Fig. 6). These species of ammonite were apparently endemic to the early Cenomanian of the Mowry Sea (Cobban and Kennedy 1989). In the Black Hills of South Dakota, Cobban and Larson (1997) documented *Neogastroplites americanus and Metengonoceras aspenanum* in the upper part of the formation.

Within the Wind River Basin of Wyoming, Finn (2021) included the Shell Creek Shale as the lower member of the Mowry Shale and constructed isopach maps for the total thickness, as well as both the upper siliceous member and the lower Shell Creek Member. All three maps showed thinning to the east-southeast, with the thickness of the Mowry Shale decreasing from about 190 m thick in the western part of the basin to about 75 m in the extreme eastern sector of the basin.

Another succession rich in porcellanite that appears correlative with the Mowry Shale occurs just west of the Boulder batholith in the Flint Creek basin near Drummond, Montana (Fig. 5) and southward through the eastern Pioneer Range (Fig. 5) into the Snowcrest Range, Centennial Mountains, and Lima Peaks area (Tysdal et al. 1989; Vuke 1984; see also Hildebrand and Whalen 2021*b*). In the Madison (Fig. 5) and Gallatin ranges, 1 km of sedimentary rocks and abundant intercalated porcellanite beds of the Blackleaf/Mowry formations lie just east of the Tendoy thrust (Dyman and Nichols 1988; Wallace et al. 1990; Dyman et al. 2000). Detrital zircons collected from the Vaughn member of the Blackleaf Formation to the north near Drummond (Fig. 5) yielded a peak of 100 Ma (Stroup et al. (2008). Also, Zartman et al. (1995) dated three porcellanites from the middle of the Vaughn member of the Blackleaf as 97–95 Ma by U-Pb on zircon; whereas Dyman et al. (2000) used Ar-Ar laser fusion geochronometry to date a sample from the uppermost Vaughn of the Lima Peaks area as 99.78 Ma.

Although the above units are superficially similar to strata of the Blackleaf Formation to the east and northeast in the Montana Disturbed Belt (Fig. 5), on the basis of the available radiometric ages, they are several million years younger. These units, as well as rocks of the Blackleaf Formation to the east in the Disturbed Belt, were transported on thrust faults of potentially very different ages and so are difficult to restore palinspastically.

To the northeast of the Montana Disturbed Belt, Cobban et al. (1976) correlated rocks of the 100 m thick Bootlegger Member of the Blackleaf Formation (Fig. 4) with the Mowry Shale and suggested that it was a near-shore facies. The Bootlegger Formation consists of very fine interlaminated marine sandstone, siltstone, shale, bentonite, and pebbly lags of chert, including an uppermost sandy unit holding chert pebbles to 5 cm and abundant fish bones, overlain by the Floweree Member of the Marias River Shale, which contains no bentonites and only sparse fish debris. The Arrow Creek bentonite (Fig. 4), which occurs in the Shell Creek Shale directly below the Bootlegger Formation, was recently dated to be 99.12 ± 0.14 Ma (Singer et al. 2021). Arnott (1988) studied the Bootlegger Formation near Great Falls, Montana, and found it to contain five stacked successions comprising coarsening upward cycles grading upwards from low to moderate bioturbated offshore shelf mudstone to shoreface sandstone capped by a transgressive lag deposit of chert pebble conglomerate sitting on an erosional surface.

Outcrops of Mowry Shale continue to the south into northeastern Utah, where they consist of siliceous marine shales containing abundant disarticulated fish bones, scales, and shark teeth that overlie a nonmarine section of the Dakota Formation and underlie the Frontier Formation (Sprinkel et al. 2012). A U-Pb age from a bentonite in the middle Dakota Formation beneath the Mowry Shale was dated as 101.4 ± 0.4 Ma (Sprinkel et al. 2012), which constrains the maximum age of the Mowry Shale in northeastern Utah. Sprinkel (personal communication, 2022) now considers the Dakota there as Muddy Sandstone, with the dated bentonite just beneath it in Thermopolis Shale, consistent with the work of Singer et al. (2021) farther north (Fig. 4).

Anderson and Kowallis (2005) also examined a section of Mowry Shale in extreme northeastern Utah, but near its southwestern extent, and concluded that, although fish fossil debris occurs throughout the unit, they are particularly concentrated on bedding planes as a result of material trapped in bottom scours by storm currents on a gently sloping shelf starved of coarse sediment.

In a study of the paleoenvironments of the Mowry Shale, Byers and Larson (1979) used bentonite datum planes to demonstrate an eastward progradation of the shoreline over an east-dipping paleoslope, which they estimated at 0°0.3′. In their study, they found that the Mowry/Frontier contact is isochronous, but that Mowry facies are oblique to the contact with lower Mowry mudstones characterized as anoxic and lethal, with facies becoming richer in oxygen upwards, in what is overall a time transgressive succession from west to east, They found, as did others, that the thickest sections occurred in the thrust belt to the west. We turn now to some of those equivalent units.

Aspen and Sage Junction formations

The Aspen Shale and Sage Junction Formation are stratigraphic equivalents to the Mowry Shale that are exposed

Fig. 7. Wide-angle view looking north at an easterly dipping section of Frontier Formation near Willow Creek, Powder River Basin of Wyoming showing Mowry Shale with white bentonite on the left overlain by sandstones and shales of the Frontier Formation capped by Turonian sandstone of the Wall Creek Member (Zupanic 2017) along the ridgeline. The labeled bentonite occurs between the Mowry and Frontier formations and, although not dated at this locale, is likely the same as that dated as 97.52 ± 0.09 Ma by Singer et al. (2021).

in relatively thick sections in the fold-thrust belt of the Wyoming salient to the west (location AT on Fig. 5). In southwesternmost Wyoming and eastern Idaho, the Aspen Shale, which ranges in thickness from 200 to 600 m, is considered correlative with the Mowry Shale, and comprises shales containing *Neogastroplites cornutus* and *N. americanus*, abundant fish scales and porcellanites; overlies the shallow marine to nonmarine Bear River Formation, as well as nonmarine sandstones and conglomerates of the Kelvin Formation; and sits beneath the coal-bearing sandstones and shales of the Frontier Formation (Reeside and Cobban 1960). About 25 miles to the west, they describe a nearly 2 km-thick succession of sandstones, shales, porcellanites, bentonites, coal beds, and limestone that suggested to them a more shoreward facies of the Aspen Shale. When describing the two formations, Reeside and Cobban (1960, p. 11) wrote that "the conspicuous rocks of both the Mowry and Aspen shales are so similar to each other and so different from other rocks in the Cretaceous sequence that it is difficult not to believe them the product of one series of events".

West of the Green River basin in Wyoming, the Aspen Shale is exposed in the footwall successions below the much younger Absaroka thrust (Fig. 5), where it was described by M'Gonigle and Dover (1992) to consist of 245–370 m of dark and light-silvery weathering marine shale, siltstone, siliceous sandstone, and ridge-forming porcellanites. They reported that the unit contains abundant fish scales. A tuff in the Aspen Shale produced a U-Pb tuffzirc age of 98.8 ± 0.4 Ma (Gentry et al. 2018). Rocks of the formation are overlain by 300–430 m of largely non-marine shale, bentonitic shale, tuff, sandstone carbonaceous shale, coal, and planar to cross-bedded sandstone of the Chalk Creek Member of the Frontier Formation (M'Gonigle and Dover 1992).

The hanging wall of the Absaroka thrust fault (Fig. 5) contains a different, but equivalent, succession of rocks known as the Wayan and Sage Junction formations (Oriel and Platt 1980; M'Gonigle and Dover 1992). The Wayan Formation, about 1200 m thick, comprises variegated red, purple, and gray mudstone, siltstone, and sandstone with minor porcellenite, bentonite, and coal (Oriel and Platt 1980). The Wayan Formation is, on the basis of fauna, early Cenomanian and contains the burrowing dinosaur *Oryctodromeus* as well as flora similar to the dated flora of the 98 Ma Dakota Sandstone near Westwater, Utah (Krumenacker 2010; Barclay et al. 2015). Rubey, who had earlier defined and named the units, considered the Sage Junction Formation, which comprises slightly more than 1 km of gray siltstone and mudstone with sandstone, quartzite, and thin, but common interbeds of porcellanite throughout, except in the upper 80 m or so, to be the most probable equivalent of the Aspen Formation (Rubey 1973), but he wondered if the upper non-porcellanite facies could be a correlative of the Frontier Formation, as it contained more grit and conglomerate.

Frontier clastic wedge

The Frontier Formation (Fig. 4) of Wyoming, Utah, Montana, and Colorado is well known from both outcrops and drill holes in the eastern part of the thrust belt and even farther east in the Green River, Bighorn, and Powder River basins (Fig. 5), where it consists of southeastward prograding marine and non-marine sandstone, siltstone, shale, conglomerate, coal, and bentonite (Cobban and Reeside 1952; Merewether et al. 1984; Merewether and Cobban 1986). Within the thrust belt, the sections of Frontier are nonmarine, up to 2.1 km thick, and were transported eastward on younger thrust faults (Royse et al. 1975; Dyman and Tysdal 1998).

In the western Powder River basin of central Wyoming, rocks of the Frontier Formation (Fig. 4) constitute a Cenomanian to Turonian clastic wedge that prograded east and southeastward over the Mowry Shale, holding the 98.17 ± 0.11 Ma Clay Spur bentonite ($^{40}Ar/^{39}Ar$ sanidine age; Singer et al. 2021), and was studied in detail by Bhattacharya and Willis (2001). In western Wyoming and eastern Utah, thick

Fig. 8. Relatively immobile elements from 101.5 to 95 Ma bentonites (Hannon 2020) plotted on Nb vs. Y and Ta vs. Yb discrimination diagrams of Whalen and Hildebrand (2019) illustrating their probable slab failure origin.

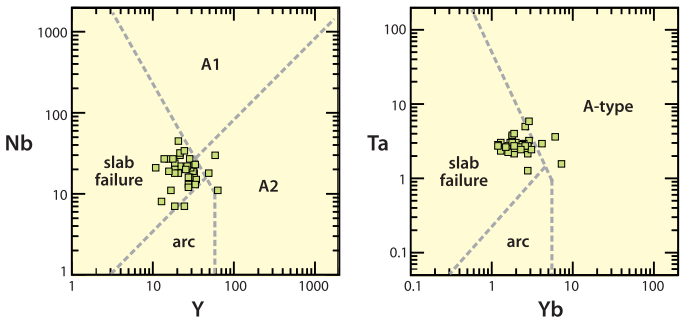

fluvial conglomeratic facies were interpreted to fill incised valleys, but in the eastern Powder River basin (Fig. 7) several hundred kilometers to the east, three unconformity-bound sandstone members are separated by marine shales (Hamlin 1996; Bhattacharya and Willis 2001). Within the basal Belle Fourche Member, Bhattacharya and Willis (2001) correlated six, meter-thick, bentonite beds through 50 outcrop sections and 550 well logs to produce a "grid of isochronous surfaces" spanning about 25 000 km^2 from which they were able to demonstrate several coarsening upward cycles grading from little to moderately bioturbated mudstone to sandstone capped by coarse-grained lag deposits sitting on disconformities. They used the overall lobate to elongate form of the sandstone bodies, radiating paleocurrent measurements, clinoforms, low to moderate shallow marine burrowing, and top-truncated beds to infer low-stand deltaic environments fed by river systems to the northwest for each of the main three bodies studied.

Hutsky et al. (2012) measured 26 outcropping sections of the Frontier Formation in the northeastern Bighorn Basin. They found tidal and wave-influenced fluvio-deltaic successions that prograded southeastward into a shallow marine environment with low accommodation space and sea-floor gradient. They also identified six bentonite beds, in addition to what they called the Clay Spur Bentonite, recently re-dated using $^{40}Ar/^{39}Ar$ sanidine to be 98.17 ± 0.11 Ma (Singer et al. 2021) at the base of the formation, in dark-gray laminated mudstone units, which they correlated through 26 measured sections. The X-Bentonite, located about 75 m above the base in their composite section, yielded an age of 95.53 ± 0.09 Ma (Ogg and Hinnov 2012).

Hannon (2020) collected several bentonites from the Frontier Formation in the Black Hills area and, in addition to dating them by U-Pb zircon methods, analyzed them for whole rock geochemistry as well as Sr and Nd isotopes (Hannon et al. 2019). Discrimination plots using relatively immobile high field strength trace elements point to a slab failure, not arc, origin (Fig. 8). Their isotopic results, $^{87/86}Si_i = 0.708$ and ENd_T ranging from −7 to −9.5. suggest interaction with subcratonic lithospheric mantle as hypothesized by Hildebrand et al. (2018) for post-collisional magmatism elsewhere. Five of his dated bentonites were collected from the Belle Fourche Member of the Frontier Formation, and dated by ICP-MS, with the Clay Spur at 97.19 ± 0.9 Ma and others at 96.87 ± 0.81 Ma, 96.8 ± 1.1 Ma, 96.5 ± 1.0 Ma, and 96.0 ± 1.3 Ma.

May et al. (2013*a*, 2013*b*) collected and studied detrital zircons from the Cenomanian–Coniacian sedimentary units in the northern Bighorn Basin and found detrital populations dominated by young peaks that approximate the age of the units, with the youngest peak ages in the Mowry Shale and Frontier Formation ranging in age mainly from 99.4 to 96.5 Ma (Fig. 9), which agree with the stratigraphic age, as there the Lower Mowry contains the ammonite *Neogastroplites cornutus*, which is considered by Reeside and Cobban (1960) to be an index fossil for the Mowry Shale. Whereas most, if not all, zircons within the Mowry Shale were derived from airfall eruptions into the basin, many of the zircons with ages <100 Ma in the Frontier clastic wedge were likely derived during uplift and exhumation of the hinterland belt as Hannon (2020) reported igneous clasts in the Frontier Formation. Painter et al. (2014) also examined detrital zircon suites from the Frontier and younger formations in Wyoming and found consistent peaks between 100 and 90 Ma in formations younger than the Dakota, whereas older formations were dominated by detrital zircon populations older than 100 Ma. Because rocks of the Frontier Formation contain abundant zircons derived from rocks <100 Ma (Fig. 9), we consider the Frontier clastic wedge to represent molasse shed during exhumation and uplift of the hinterland.

In northern Utah, major exhumation and cooling of the 125–115 Ma Willard-Paris thrust sheets (Fig. 5) also occurred at 105–95 Ma, which led to increased subsidence to the east and deposition of the 100–96 Ma Aspen and Frontier formations in the foreland basin and conglomeratic debris adjacent to the Paris thrust (Yonkee et al. 2019; Pujols et al. 2020). A thrust duplex of Paleoproterozoic crystalline rocks, known as the Farmington complex, seemingly sits on the Archean basement of the Wyoming—Grouse Creek block (Mueller et al. 2011; Yonkee et al. 2003). The band of Paleoproterozoic crystalline rocks likely continues northward into Idaho, where Paleoproterozoic crystalline basement occurs within the Cabin—Medicine Lake thrust system just east of the Idaho batholith (Skipp 1987) and the Tendoy thrust (Fig. 5) of southwestern Montana (Skipp and Hait 1977; DuBois 1982).

Farther north in the Montana sector of the thrust belt, Carrapa et al. (2019) studied exhumation and uplift using low-temperature thermochronology. Although they were focused on the geology of the younger Laramide orogeny, their zircon (U-Th)/He modeling results for several mountainous massifs in that sector showed that exhumation commenced at 100 Ma (Fig. 10) similar to areas farther south.

Mussentuchit Member and correlative units in Utah

To the south in central Utah (Fig. 11), the smectite-rich, 25–40 m thick Mussentuchit Member of the Cedar Mountain Formation appears to be bentonite-rich and temporally equivalent to the Mowry Shale, but is non-marine. There, a discontinuous, basal black-chert-pebble lag separates the Mussentu-

Fig. 9. Detrital zircon data (May et al. 2013*a*, 2013*b*) from several units within the Bighorn basin. The Graybull samples are from the older Aptian–Albian succession and have a strong similarity to samples from the Alleghanian foredeep as shown (Benyon et al. (2014). The sample from Newcastle Sandstone of the Black Hills is from Finzel (2017) and is similar to the Alleghanian and Graybull profiles, plus an ~100 Ma peak that presumably represents airfall reaching this far eastern location. Samples from the Muddy, Mowry, and Frontier are entirely dissimilar to the Greybull and Newcastle, except for the ~100 Ma airfall and hinterland detrital peaks, which suggest the difficulty of getting Appalachian Alleghanian detritus across the eastward-migrating bulge. Plotted with detritalPy (Sharman et al. 2018).

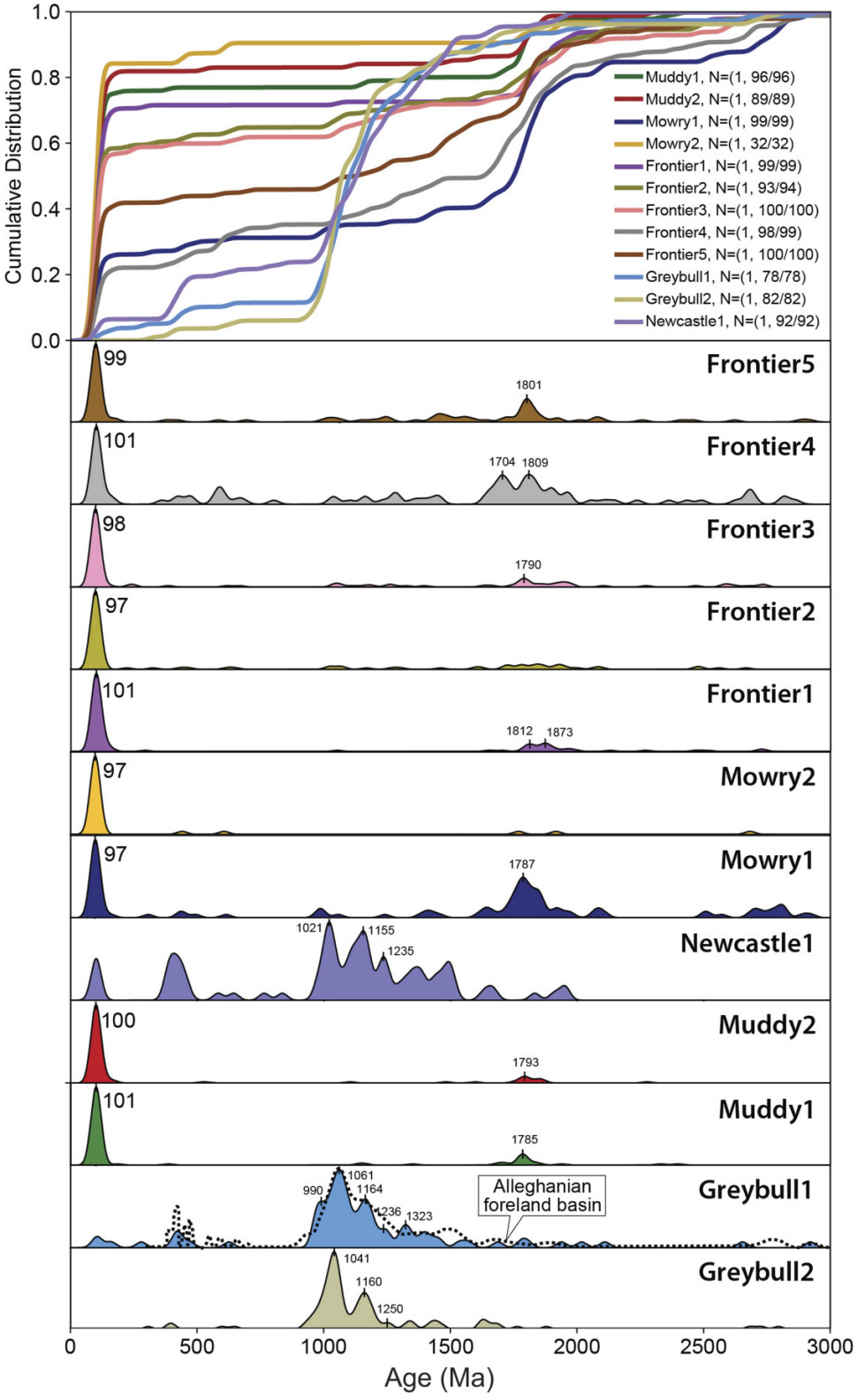

Fig. 10. Thermochronological models using zircon (U-Th)/He) from the Helena Salient area (Carrapa et al. 2019), indicating initial cooling and exhumation of several Precambrian-cored, mountain blocks starting at 100 Ma. (See Fig. 5 for locations of uplifted massifs.) Those authors suggest that the observed cooling/exhumation was tectonically driven as opposed to magmatic cooling. (See original work for modeling techniques and error propagation.)

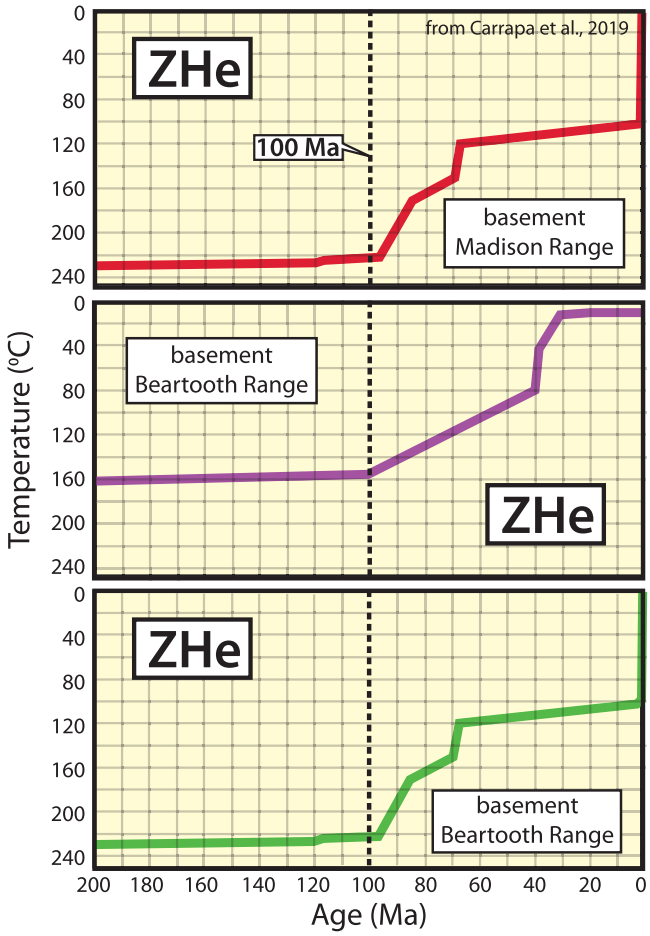

chit from the underlying Ruby Ranch Member of the Cedar Mountain Formation, interpreted to represent debris shed eastward from the ~120 Ma Sevier orogeny (Lawton et al. 2010; Hunt et al. 2011). Rocks of the Mussentuchit Member are overlain by shales of the Naturita/Dakota Formation, but to the east where the Naturita was eroded, rocks of the member are overlain by the Tununk Member of the Mancos Shale, also with a basal pebble lag (Kirkland and Madsen 2007). The Mussentuchit Member is best known along the western side of the San Rafael Swell (Figs. 5 and 11) where it overlies a distinctive cobbly conglomerate up to 5 m thick holding quartzite clasts (Doelling and Kuehne 2013). The member is dominated by gray, silty mudstone and muddy siltstone high in organic carbon from fossil plant material with local beds of lignite, all deposited on a broad coastal plain (Kirkland et al. 2016). Tucker et al. (2020) also reported variably preserved shell hash.

Several bentonites within the Mussentuchit Member on the San Rafael Swell were dated by $^{40}Ar/^{39}Ar$ to be 98.2–96.7 Ma, but generally have high analytical errors and do not match their stratigraphic order (Garrison et al. 2007). For this reason, we prefer to use the average of four bentonite ages, likely from the same bed, and with a weighted mean age of 98.39 ± 0.07 Ma (Cifelli et al. 1997) consistent with ages from the Mowry Shale (Fig. 4). Tucker et al. (2020) collected detrital zircons from volcaniclastic rocks in the member and argued that it was deposited no earlier than 96–94 Ma, an interpretation which conflicts with the $^{40}Ar/^{39}Ar$ sanidine ages from bentonite beds, and their own age from the lower Mussentuchit of 102.1 Ma, as determined by averaging seven different methods of determining the MDA.

Kirkland et al. (2016, p. 160) point out that dinosaur eggshells are common in the Mussentuchit Member and that vertebrate fauna from the member "is the oldest dinosaur fauna with representatives of each family characteristic of the remainder of the Late Cretaceous in North America" as documented by Cifelli et al. (1997). Researchers have recognized at least 22 species of mammals, albanerpetonids, salamanders, adocid turtles, the oldest North American snakes, marsupials, bird teeth, and a wealth of dinosaur teeth representing brachiosaurids and a diverse group of meat-eating dinosaurs, such as velociraptors and North America's oldest tyrannosaurids (Cifelli et al. 1997, 1999; Kirkland et al. 1997, 1999, 2016; Kirkland and Madsen 2007). Scientists also note that several dinosaurs collected from rocks of the Mussentuchit Member, such as the tyrannosaurids and pachycephalosaurs, as well as other vertebrates such as snakes, anocid turtles, and the world's most primitive marsupials, have Asian affinities and are hypothesized to have immigrated to North America over a polar land bridge (Cifelli et al. 1997; Gardner and Cifelli 1999; Kirkland et al. 2016; Avrahami et al. 2018). Their arrival may have led to extinction of native North American dinosaur clades, such as Sauropods, which went extinct at about the same time (Kirkland et al. 1997, 1999). Cifelli et al. (1997) suggested that perhaps the accretion of Wrangellia to southern Alaska might have brought the Asian family groups to North America at ~100 Ma.

Other formations of the same age within the basin also contain new fauna. The first discovery of both trace and body fossils of a burrowing and denning dinosaur, *Oryctodromeus*, occur in the Blackleaf Formation of Montana (Varricchio et al. 2007), which also hosts a similar dinosaur fauna as the Mussentuchit Member (Ullmann et al. 2012).

Mid-Cretaceous thrust-related stratigraphy of southwest Utah, Nevada, and California

To the west of the San Rafael swell, in the Sanpete and San Pitch mountains (Fig. 11), rocks of the Cedar Mountain Formation and overlying Indianola Group represent the foredeep stratigraphy in the thrust belt of the Pavant Valley, and Canyon Ranges, where coarse conglomeratic facies, known as the Canyon Range Conglomerate, overstep the Pavant thrust (Figs. 5 and 11) and lie unconformably upon the Canyon Range culmination (Spieker 1946; Sprinkel 1994; Schwans 1995; Sprinkel et al. 1999; Lawton et al. 2007).

Fig. 11. Stratigraphic units with ages in Ma for some lower to mid-Cretaceous stratigraphic successions in Utah and southern Nevada. Data from sources cited in text. MDA–maximum depositional age from detrital zircons; Fm—formation. Broad gray line is approximate location of cratonic hingeline. Thrust symbols provide approximate locations of important thrust faults mentioned in text with ages in Ma.

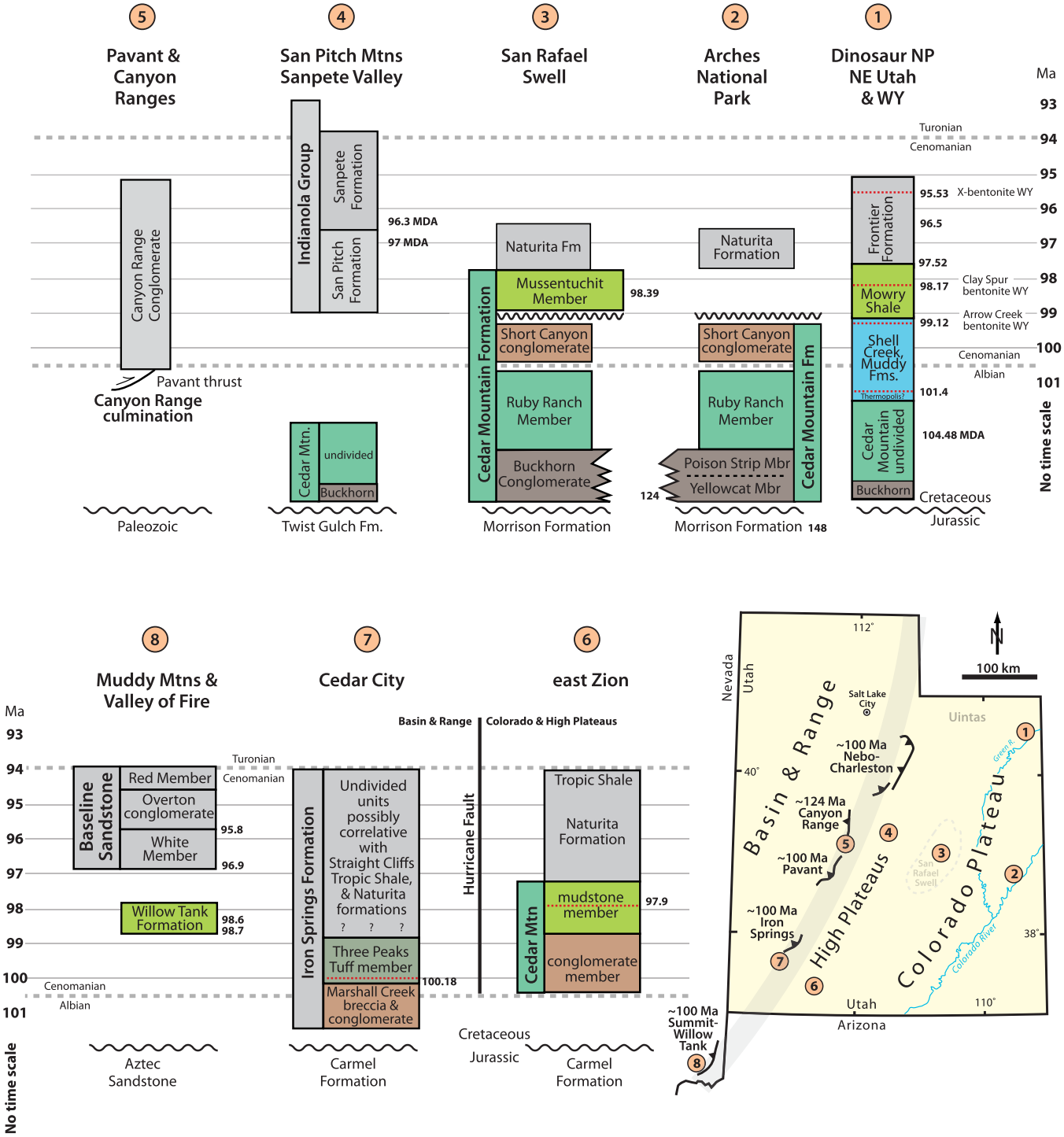

The Pavant thrust fault and Canyon Range culmination are one segment of the mid-Cretaceous thrust belt of the US Cordillera (Sevier of Armstrong 1968). It occurs in central Utah as well as western Wyoming where it is known as the Wyoming salient (Fig. 5). Thrust faults of the Pavant–Charleston–Nebo thrust system transported Neoproterozoic metasedimentary rocks, Paleoproterozoic crystalline basement of the Santaquin complex (Nelson et al. 2002), and a Phanerozoic sedimentary succession, eastward, and led to the development of a large nearly recumbent anticline. The Pavant sector of the thrust system deformed and elevated the Canyon Range thrust into an antiformal culmination during its emplacement (DeCelles and Coogan 2006). Early work by Christiansen (1952) and more recent work by Lawton et al.

(2007) demonstrated that the Canyon Range Conglomerate was deposited atop the Pavant thrust after thrusting contemporaneously with exhumation. Zircon (U/Th)/He ages from the Pavant–Nebo thrust sheets document exhumation and uplift of the thrust sheets between 102 and 96 Ma (Pujols et al. 2020). Using detrital zircon (U/Th)/He ages, they also found that the exhumation was concurrent with sediment dispersal eastward into the Cenomanian Dakota Formation, the temporally equivalent foredeep stratigraphic unit. Thus, the Pavant–Charleston–Nebo thrust system was active at about ~100 Ma and the Canyon Range Conglomerate is best interpreted as post-thrusting molasse.

Farther south in Utah, around and in Zion National Park (Fig. 11), a conglomeratic unit and an overlying smectitic mudstone unit were assigned to the Cedar Mountain Formation by Biek and Hylland (2007) and Hylland (2010). They obtained a single crystal $^{40}Ar/^{39}Ar$ sanidine age of 97.9 ± 0.5 Ma from an ash bed in the mudstone member, so correlated it with the Mussentuchit Member of the Cedar Mountain Formation of the western San Rafael Swell.

To the west, rocks related to the mid-Cretaceous thrust belt of the US Cordillera (Armstrong 1968), are known in the Cenomanian–Turonian Iron Springs Formation (Figs. 5 and 11), which consists of 800–1000 m of nonmarine conglomerate, sandstone, debris-flow breccia, mudstone, and limestone, with minor bentonite beds deposited on a fluvial N-NE sloping braidplain (Fillmore 1991). Zircons from a dacitic tuff intercalated with coarse talus breccias, conglomerates, and sandstones of the formation were recently dated by both laser ablation-inductively coupled plasma-mass spectrometry and chemical abrasion-thermal ionization mass spectrometry to be 100.18 ± 0.04 Ma (Quick et al. 2020).

In the Muddy Mountains east and northeast of Las Vegas (Fig. 11), Bohannon (1983) mapped and described rocks of the Willow Tank Formation and the White Member of Baseline Sandstone (Fig. 5), which he argued were both deposited during thrusting and overlain by the Red Member and Overton Conglomerate Member of the Baseline Sandstone. He reported that swamp and lake deposits of the Willow Tank Formation lie upon a gravel-covered unconformity on the Aztec Sandstone with up to 10 m of paleotopography on the basal contact (Reese 1989), and that the non-marine shallow-water deposits pass upwards into fluvial quartz arenite, minor conglomerate, and local talus breccias, which are tectonically overlain by the Summit-Willow Tank thrust in the southern part of the North Muddy Mountains. To the south, in the Valley of Fire, the Red Member and Overton Conglomerate interfinger and overstep the Summit-Willow Tank thrust fault. Bohannon (1983) also reported that the Muddy Mountain thrust, located west of the Summit-Willow Tank thrust, overrode at least part of the Overton Conglomerate. Carpenter (1989) documented a reverse clast stratigraphy within the Red and Overton Conglomerate members and noted that carbonate blocks up to 20 m within the Overton Member indicate deposition on alluvial fans close to the thrust front.

Bonde (2008) and Bonde et al. (2008, 2012) reported extensively on the fauna preserved within the Willow Tank Formation and noted the presence of tyrannosaurids, iguanodonts, turtles, and fossil dinosaur eggshells. Those fauna closely match fauna of the Mussentuchit Member of the Cedar Mountain Formation in central Utah, whereas fauna from the Aptian Newark Canyon Formation farther north in the Central Nevada thrust belt (Di Fiori et al. 2020) are closely allied with those of the Ruby Ranch Member of the Cedar Mountain Formation (Bonde et al. 2015), which support the concept of an Asian faunal influx into North America at about 100 Ma (Cifelli et al. (1997).

Decades ago, two K/Ar ages were determined on biotite from tuff beds in the Willow Tank Formation and yielded 98.6 and 98.4 Ma (Fleck 1970); whereas K/Ar analyses from biotite in the Baseline Sandstone produced ages of 95.8 and 93.1 Ma. More recently, Troyer et al. (2006) dated zircons from three ash beds of the Willow Tank Formation by SHRIMP RG U-Pb to be 101.6 ± 1 Ma to 99.9 ± 2 Ma; whereas Pape et al. (2011) reported that sanidine crystals collected from epiclastic units near the base and top of the Willow Tank Formation produced ages of 98.68 and 98.56 Ma, respectively.

On the western flank of Las Vegas valley, a conglomerate unit within Brownstone Basin (Fig. 5) sits structurally beneath the Red Spring thrust and contains cobbles and pebbles apparently derived from the Wheeler Pass thrust plate to the west (Axen 1987), as well as detrital zircons as young as 103–102 Ma (Wells 2016). Rocks within the Wheeler Pass thrust sheet itself, where exposed in the Spring Mountains (Fig. 5), contain evidence for exhumation during the Late Jurassic (Giallorenzo 2013), which perhaps reflects the Nevadan event; however, zircon (U–Th)/He thermochronology from the thrust sheet, where exposed in the Nopah Range to the southwest, shows that exhumation started there at ~100 Ma (Giallorenzo 2013).

In the southern Spring Mountains just southwest of Las Vegas (Page et al. 2005), non-marine sedimentary and volcaniclastic rocks of the Lavinia Wash sequence (Fig. 5), interpreted as synorogenic deposits by Carr (1980), lie structurally below the Contact thrust plate. A rhyolitic boulder in conglomerate of the Lavinia Wash sequence was dated at 98.0 Ma, and plagioclase from an ignimbrite in the sequence yielded a $^{40}Ar/^{39}Ar$ age of 99.0 ± 0.4 Ma (Fleck and Carr 1990).

In the Mescal Range to the southwest, a succession of 100.5 ± 2 Ma basaltic lavas and epiclastic rocks overlain by plagioclase porphyritic ignimbrites and lavas known as the Delfonte volcanics was detached, folded, and transported eastward on thrust faults (Fleck et al. 1994; Walker et al. 1995) prior to the emplacement of the 98–90 Ma Teutonia batholith (Fig. 5).

The thrust belt continues southward into the New York Mountains of California (Burchfiel and Davis 1977). There, highly strained metavolcanic rocks range in age from 98.4 to 97.6 Ma, whereas associated metasedimentary rocks of Sagamore Canyon (Fig. 5) have MDAs of 98 Ma (Wells 2016). The age of thrusting is constrained because the faults deform the volcanic rocks, but are cut by 90.4 ± 0.8 Ma Mid Hills monzogranite, which is one of several plutons of the 98–90 Ma Teutonia batholith (Beckerman et al. 1982; Miller et al. 2007; Haxel and Miller 2007; Wells 2016).

Sevier Foredeep in Canada

In the Canadian Cordillera, the Cretaceous of the Western Interior Basin contains Aptian to Albian clastic wedges equivalent to those in the western United States, and they are interpreted as a foredeep succession related to the Sevier orogeny, which started at 124–120 Ma (Currie 2002; Hildebrand 2013, 2014). These rocks, which sit unconformably upon Jurassic rocks, commonly have a basal conglomerate, the Cadomin Formation (Leckie and Cheel 1997; Leier and Gehrels 2011), much like the Buckhorn, Cloverly, Lakota, and Kootenai conglomerates, which unconformably overlie the Jurassic Morrison Formation and lateral equivalents of the US sector (Heller et al. 1986; Heller and Paola 1989). In Utah, the conglomerates are overlain by the dominantly non-marine Cedar Mountain and San Pitch formations (Lawton et al. 2010; Kirkland et al. 2016). In Canada, the basal conglomerates and sandstones do not extend as far east as their US counterparts, but instead were deposited by northward flowing rivers between alluvial fans on the west and escarpments to the east (Hayes et al. 1994). The clastic units grade upwards into finer-grained fluvial to marginal-marine, commonly deltaic, sandstones and shales of the Blairmore Group and farther to the east, northward flowing fluvial systems of the Mannville Group and restricted-marine Swan River Formation (Cycle 2 of Leckie and Smith 1992). The top of the succession throughout most of the basin is marked by an unconformity (Hayes et al. 1994).

Using mismatches in geology and robust paleomagnetism of Cordilleran rocks, Hildebrand (2013, 2014, 2015) argued that the western hinterland of the US Sevier belt is now located within the Canadian Cordillera, where it is known as the Omineca Belt (Monger et al. 1982). Scads of plutons (Fig. 5) ranging in age from 118–105 Ma intrude the Omineca belt (Hart et al. 2004) and are interpreted to represent post-collisional slab failure plutons emplaced into the upper-plate hinterland (Hildebrand and Whalen 2017). Middle Albian clastic rocks in the Canadian foreland contain a significant 108 Ma detrital zircon peak that Ross et al. (2005) suggested was formed from exhumation and weathering of plutons to the west. The slightly younger Hulcross Formation (Fig. 12), dominated by siltstone, shale, and sandstone, contains abundant bentonite and tonstein layers (Gibson 1992) and may represent extrusive phases of the post-collisional magmatism.

Joli Fou Seaway in Canada

Rocks of the successions in the Sevier foredeep in Canada are unconformably overlain by rocks of the Fort St. John and Colorado groups (Fig. 12), which Leckie and Smith (1992) termed Cycle 3. Overall, this succession is dominated by shale and represents a major transgression that allowed the Boreal and Tethyan oceans to flood the craton (Fig. 3) and form a continuous seaway known in Canada as the Joli Fou Sea and in the United States as the Kiowa-Skull Creek Sea (Leckie and Reinson 1993). Deposition of mudrocks in the seaway was interrupted by a period of relative drop in sea level within the basin, which led to the incision of fluvial channels and development of swamps and paleosol complexes found in the upper Boulder Creek Formation, the Paddy Member of the Peace River Formation, and farther east, the Viking, Bow Island, and Newcastle formations. These fluvial, non-marine units are in turn overlain by marine shales of the Shaftesbury and Westgate formations of the Canadian Plains and equivalents in the Foothills of Alberta, British Columbia, and the Northwest Territories (Fig. 12), which represent a second major basin-wide transgression, as once again the seaway grew to connect the Gulf of Mexico with the Boreal Sea (Leckie and Smith 1992; Leckie and Reinson 1993; Schröeder-Adams et al. 1996).

One of the major differences between the Canadian and US sectors of the trough is the much greater amount of latest Cretaceous–early Cenozoic shortening in the fold-thrust belt of Canada, which has destroyed, or at least masked, the western part of the basin there as exemplified by the isopach maps of Leckie et al. (1990, 1994) and Reinson et al. (1994). Thus, rocks of many formations, such as the Viking and Bow Island formations, generally considered temporally correlative with the Muddy and Newcastle sandstones of the US sector, are difficult to directly link with their American counterparts, despite overall similarities.

Boulder Creek–Paddy–Viking–Bow Island strata

Deposition of mud within the Joli Fou Seaway was interrupted by a relative drop of sea level, but instead of progressing from east to west as expected for a westward paleoslope, it appears to have passed from west to east similar to the relations documented in the western US where the more westerly units of the Muddy Sandstone are older than rocks of the lithologically similar Newcastle Sandstone located farther east (Fig. 4). We interpret the similarities in both US and Canadian successions to reflect the passing of a flexural bulge from west to east across the continental margin, such that the cratonic margin was uplifted, eroded, and locally incised, then pulled down below sea level again as it rode along the relatively starved outer slope towards the trench.

Although geochronology is sparse and proposed lithologic correlations require thorough testing, the Viking Formation appears to be correlative with the Muddy Formation of Wyoming. In Canada, a number of formations also appear more or less correlative, although not all workers agree (Reinson et al. 1994). According to their analysis, the Viking Formation, the Bow Island, the Paddy Member of the Peace River Formation, the Walton Creek Member of the Boulder Creek Formation, the Newcastle Sandstone of Manitoba, and the Crowsnest volcanics (Fig. 12) are all considered to be more or less broadly correlative, except that the volcanics occur above, rather than below, the sequence boundary common to the other units. More recent work, summarized by Roca et al. (2008), divided rocks of the late Albian–early Cenomanian into alloformations on the basis of regional unconformities as well as transgressive surfaces and found a southeastward spatial and temporal migration of uplift and erosion followed by subsidence and sedimentation, represented by the Walton Creek and Paddy successions in the west to the Joli Fou

Fig. 12. Stratigraphic correlation diagram for the relevant part of the Western Interior Basin in Canada. Largely from Bloch et al. (1993, 1999) and Schröder-Adams et al. (1996) with modifications from Stott (1982), Leckie et al. (1989), and Leckie and Reinson (1993).

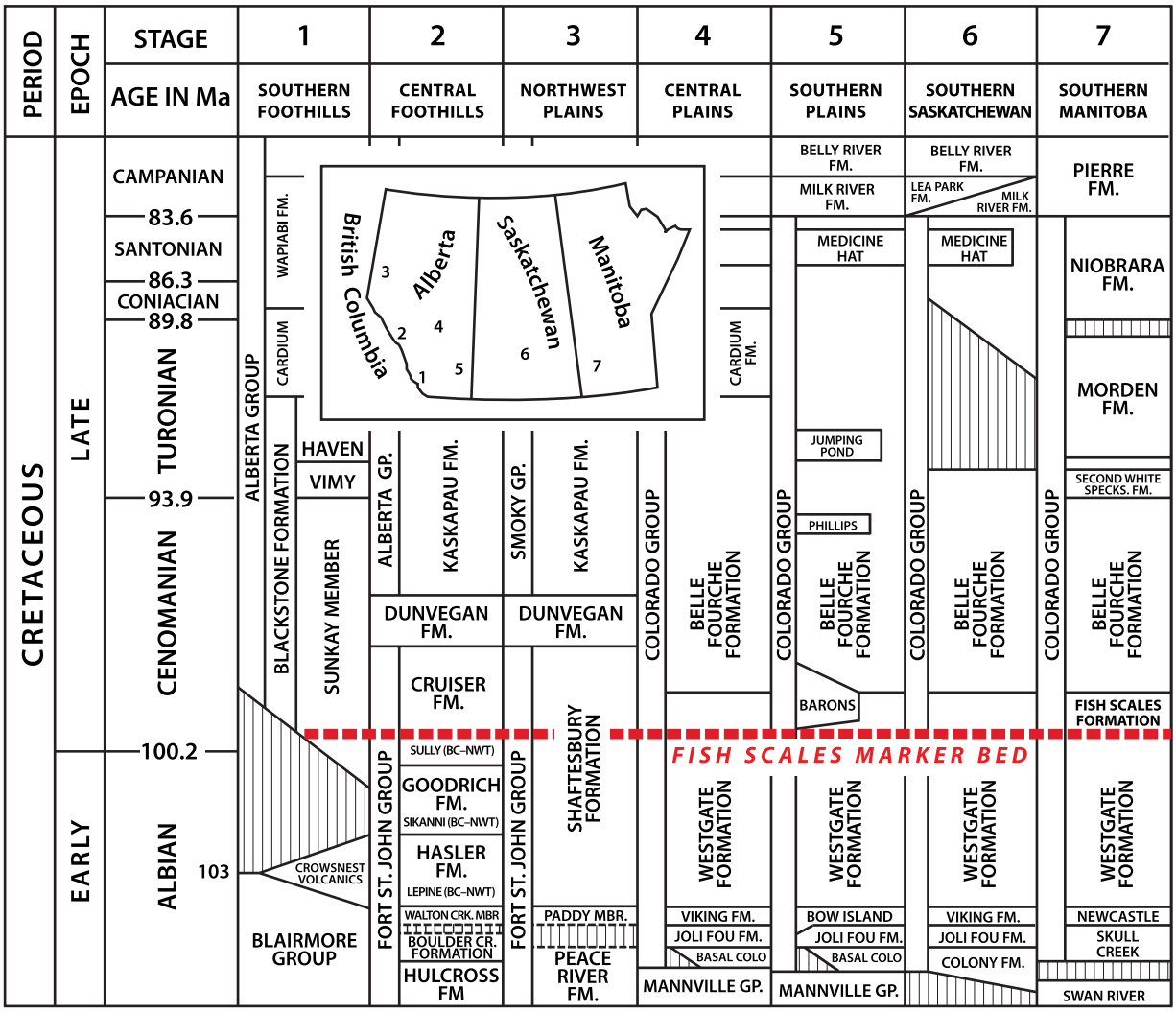

Formation and to the Viking Formation in the southeast (see their Fig. 28).

The initial drying of the trough seems to have started in the west with the upwards passage of the lower Boulder Creek rocks, which were dominated by marginal marine shoreface to foreshore sandstone and conglomerate, into strata of the mainly non-marine Walton Creek Member (Fig. 12), which contains channelized fluvial conglomerates and sandstones, coal seams, and abundant paleosols, including silica-rich forms known as ganisters (Leckie et al. 1989; Gibson 1992).

In northwestern Alberta and northeastern British Columbia, the Paddy Member of the Peace River Formation (Fig. 12) correlates with the Boulder Creek Formation and occurs in the area of the Peace River Arch, which subsided during the Albian (Leckie et al. 1990; Reinson et al. 1994; Roca et al. 2008; Plint et al. 2018). The eastward-thinning Paddy Member is lithologically variable and comprises a variety of fluvial channel, coastal plain, estuarine, and barrier island facies, that unconformably overlie and fill channels incised into the Caddie Member of the Peace River Formation and are overlain by marine mudstone of the Shaftesbury Formation, which contains the well-known Mowry equivalent Fish Scales unit (Fig. 12). Leckie et al. (1990), used data from 4500 wire logs plus 60 drill cores and local outcrops, to suggest that much of the Paddy Member consisted of debris deposited in a single broad shallow valley, tens of kilometers wide and hundreds long cut into previously deposited sediments. They also suggested that the incision of channels in the Paddy Member coincided with development of a paleosol complex in the Walton Creek Member in the Foothills at Monkman Pass (Fig. 5). To the north, the depositional edge of the Paddy Member occurs along a northeast trending line, which marks the northern limit of a sandy barrier island complex at least 350 km long and a northward facies change to interbedded marine siliciclastic rocks (Leckie et al. 1990; Plint et al. 2018). Other studies (Leckie and Singh 1991; Leckie and Reinson 1993) found that the top of the underlying Cadotte Member was incised by paleovalleys up

to 15 m deep, then onlapped and filled with rocks of the Paddy Member. A sample stratigraphic section is shown in Fig. 13 and described in detail by Leckie and Singh (1991). The section shares many similarities with those of the Muddy and Newcastle in the western United States, as well as the Bow River and Viking in Canada.

More recently, Plint et al. (2018) divided the Paddy Member into nine allomembers on the basis of flooding surfaces, and when traced to the west into alluvial facies, the surfaces seem to coincide with the base of alluvial or lacustrine mudstones that cap paleosol horizons, or with conglomerate and pebbly sandstone units that fill paleovalleys. The basal six allomembers are wedge shaped and onlap progressively eastward onto the eroded substrate, which formed a broad subaerial ridge that they suggest has characteristics of a forebulge, whereas three younger allomembers are sheetlike bodies that do not onlap, show little variation in thickness over ~300 km, blanket the ridge, and merge eastward and southeastward with deltaic rocks of the marine Pelican/Viking formations (Plint et al. 2018). A multigrain U-Pb discordia from zircons in a thin tuff layer in the Hulcross Formation, which lies beneath the Boulder Creek Formation (Fig. 12), gave an age of about 102.5 ± 2.5 Ma (Yanagi et al. 1988).

The uppermost Albian Viking Formation (Fig. 12) is a shale-encased sandstone unit that occurs in south-central Alberta and Saskatchewan and is correlated with the Bow Island Formation of southwestern Alberta, the Newcastle Sandstone in Manitoba, and parts of the Peace River Formation in northwestern Alberta (Stelck and Koke 1987; Leckie et al. 1994). The formation is 15–35 m thick over most of the Alberta plains, but it is thicker in southern Alberta where it merges with rocks of the Bow Island Formation. It overlies the shales of the Joli Fou Formation, in places gradationally, but in others, especially to the west and northwest, as well as in Saskatchewan, unconformably (Leckie et al. 1994). The formation is capped by conglomerate of a transgressive pebbly lag, which in turn, is overlain by black mudstones with thin lenses of very fine-grained sandstone of the Westgate Formation.

On the basis of more than 500 well logs and 153 cores, Boreen and Walker (1991) divided the rocks of the Viking Formation of the Alberta plains into five allomembers separated by four bounding discontinuities. Rocks of the Viking Formation sit disconformably on a pebbly lag atop Joli Fou shales, and the oldest two allomembers are composed of sheet-like, marine, upward-coarsening sequences of bioturbated mudstones and sandstones with several intercalated bentonites, all deposited beneath fairweather wave base (Drljepan 2018; Boreen and Walker 1991). A relative drop in sea level allowed non-marine rivers to cut channels 11–33 m deep in the older rocks during a lowstand in the middle of Viking deposition (Reinson et al. 1994). The channels are reminiscent of the incised valley systems cut during Muddy-Newcastle time in the western United States and, like those channels, were filled with finer grained, marginal marine sediments during the subsequent transgression. K-Ar dating of sanidine and biotite from bentonites collected from drill core in the Viking Formation east of Calgary (Tizzard and Lerbekmo 1975) yielded ages ranging from 105 to 94 Ma, but one 30 cm bed is widely traceable and interpreted to be about 100 Ma.

The stratigraphic equivalent to the Viking Formation in the southwestern Alberta Plains is known as the Bow Island Formation (Fig. 12), which Vorobieva (2000) divided into three informal members with the upper member assigned to the *Miliammina manitobensis* Zone with lesser fauna of the *Haplophragmoides gigas* Zone (Fig. 6), similar to shales above the Viking Formation (Tizzard and Lerbekmo 1975), the Paddy Member (Stelck and Leckie 1990), the Shell Creek Shale of the western United States (Eicher 1962), and more northerly locations, such as Sikanni Sandstone of northwestern British Columbia (Stelck 1975), and the Arctic Red Formation of the Peel Plateau (Thomson et al. 2011). Langenberg et al. (2000) reported the Bow Island Formation as dominantly marine, comprising immature sandstones, bentonite beds, and chert-pebble conglomerates, some amalgamated to 25 m thick, with the middle Bow Island Formation containing well-developed paleosols representing subaerial exposure as recorded in the middle of the Viking. They also reported that the rocks of the Bow Island Formation interfinger with rocks of the Bruin Creek Member of the Mill Creek Formation, which in turn are intercalated with volcanics of the Crowsnest Formation in the fold-thrust belt (Fig. 12).

Crowsnest Formation

Westward into the Foothills from the Alberta Plains, the typical upper Albian to lower Cenomanian marine and nonmarine units of the trough are generally represented in the fold-thrust belt of the southern Canadian Rockies by volcaniclastic to epiclastic strata of the Crowsnest Formation. Rocks of this formation commonly sit on, and interfinger with, a conspicuous conglomerate at the top of the Bruin Creek Member of the Mill Creek Formation (Blairmore Group; Fig. 12) and comprise up to 488 m of volcaniclastic and epiclastic sandstone consisting largely of sanidine, melanite garnet, and clinopyroxene crystal fragments, as well as conglomerate, breccia, and debris flows containing igneous clasts, some to 10 m in diameter (Peterson et al. 1997; Leckie and Burden 2001).

Rocks of the Bruin Creek Member overlie strata of the Blairmore Group in sharp, irregular basal contact with overlying westerly derived, coarse-grained, trough cross-bedded sandstone and (or) a laterally discontinuous volcanic-clast conglomerate (McDougall-Segur horizon) in beds 30 m thick and 3 km wide that Leckie and Burden (2001) considered to be lateral equivalents of the Crowsnest Formation. The volcanic clast conglomerates, locally auriferous (Leckie and Craw 1995), contain a variety of plutonic and volcanic clasts, dated by K-Ar to range from 173 to 113 Ma, with fewer chert and quartzite clasts (Norris et al. 1965). Leckie and Burden (2001) also report that the upper contact of the Crowsnest Formation is sharp with up to 37 m of relief beneath either 1–2.5 m of fine-grained sandstone or, more typically, black marine shale of the Blackstone Formation (Fig. 12).

Although Norris et al. (1965) considered many of the exposures of the Crowsnest Formation to contain primary volcanic rocks, Peterson et al. (1997) interpreted most of the

Fig. 13. Composite section illustrating relations of the Paddy Member of the Peace River Formation and its interpretation (modified from Leckie and Singh 1991). Note the emergent nature that led to the deposition and incision of the Cadotte Formation followed by the resubmergence and filling of the incised channels by estuarine and shallow marine sediments. The Walton Creek, Viking, and Bow Island formations in Canada, as well as the Muddy and Newcastle sandstones in the United States, have similar stratigraphic units and relations.

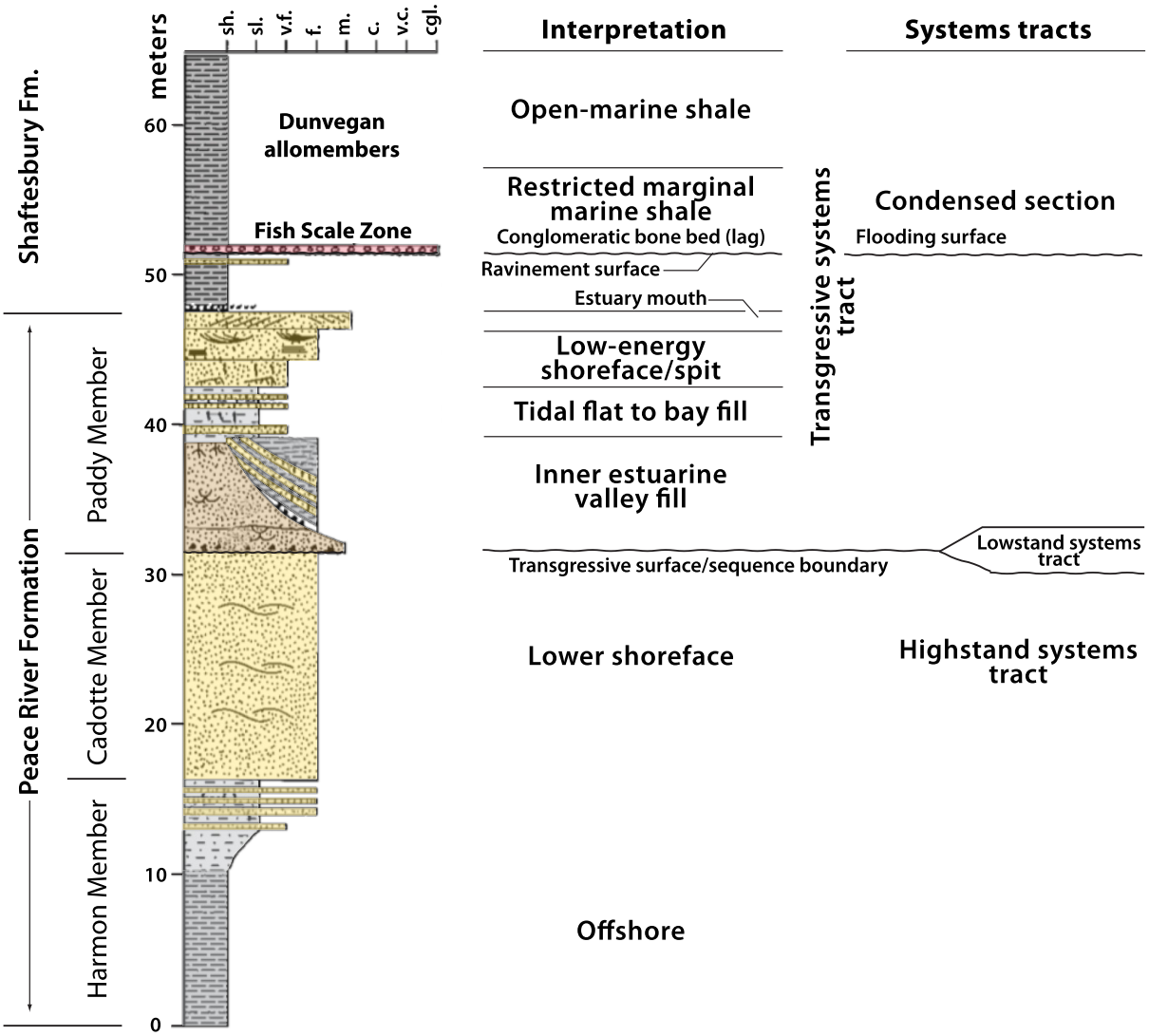

rocks to be epiclastic. They reported that some plane-bedded sandstones comprise grains of sanidine, garnet, and clinopyroxene, but that definitive evidence for a primary pyroclastic origin is lacking. A more recent study (Adair and Burwash 1996) used evidence such as plastically deformed volcanic fragments, charred wood, bedforms, and baked margins of clasts to indicate that many of the rocks in the formation were primary volcanic rocks, which originated as pyroclastic flows from collapsing eruption columns. Regardless of their origin, angular blocks and fragments include porphyritic analcime phonolites, analcite phonolite, trachyandesite, and trachyte (Peterson et al. 1997).

The age of the Crowsnest Formation has generally been considered to be close to 100 Ma on the basis of the paleontology above and below the formation, as well as a single sanidine $^{40}Ar/^{39}Ar$ age of 102 ± 0.5 Ma generated by Obradovich and reported in Leckie and Burden (2001), who found poorly preserved palynomorphs that they considered to possibly be Cenomanian. More recently, Pana et al. (2018*b*) analyzed U-Pb isotopes from melanite garnet xenocrysts in the lower Crowsnest Formation using isotope dilution–thermal ionization mass spectrometry, then averaged two analyses for a final result of 102.9 ± 1.1 Ma. They also dated titanite (U-Pb) from an alkaline sill also within the thrust belt, but located a few kilometers to the west and produced a crystallization age of 102.4 ± 0.5 Ma, within error of the age obtained from the xenocrystic melanite garnets in the Crowsnest Formation. Adair (1986, p. 141) noted that "melanite garnets identical

Fig. 14. Trace element discrimination plots (Hildebrand and Whalen 2017; Whalen and Hildebrand 2019) illustrating that rocks of the alkaline Crowsnest volcanics (Bowerman et al. 2006) plot in the slab failure fields as do 101.5–95 Ma bentonites from Wyoming (Bremer 2016), andesite clasts from the Frontier Formation of north-central Wyoming (Khandaker 1991), and for comparison, analyses from 8.5 to 0.2 Ma post-collisional magmatic rocks (55%–70% SiO_2) of Tuscany Province, Italy (from Peccerillo 2005), and late- to post-kinematic alkaline plutons of the Paleozoic Scandian orogeny in the Scottish Northern Highlands terrane (from Archibald et al. 2022).

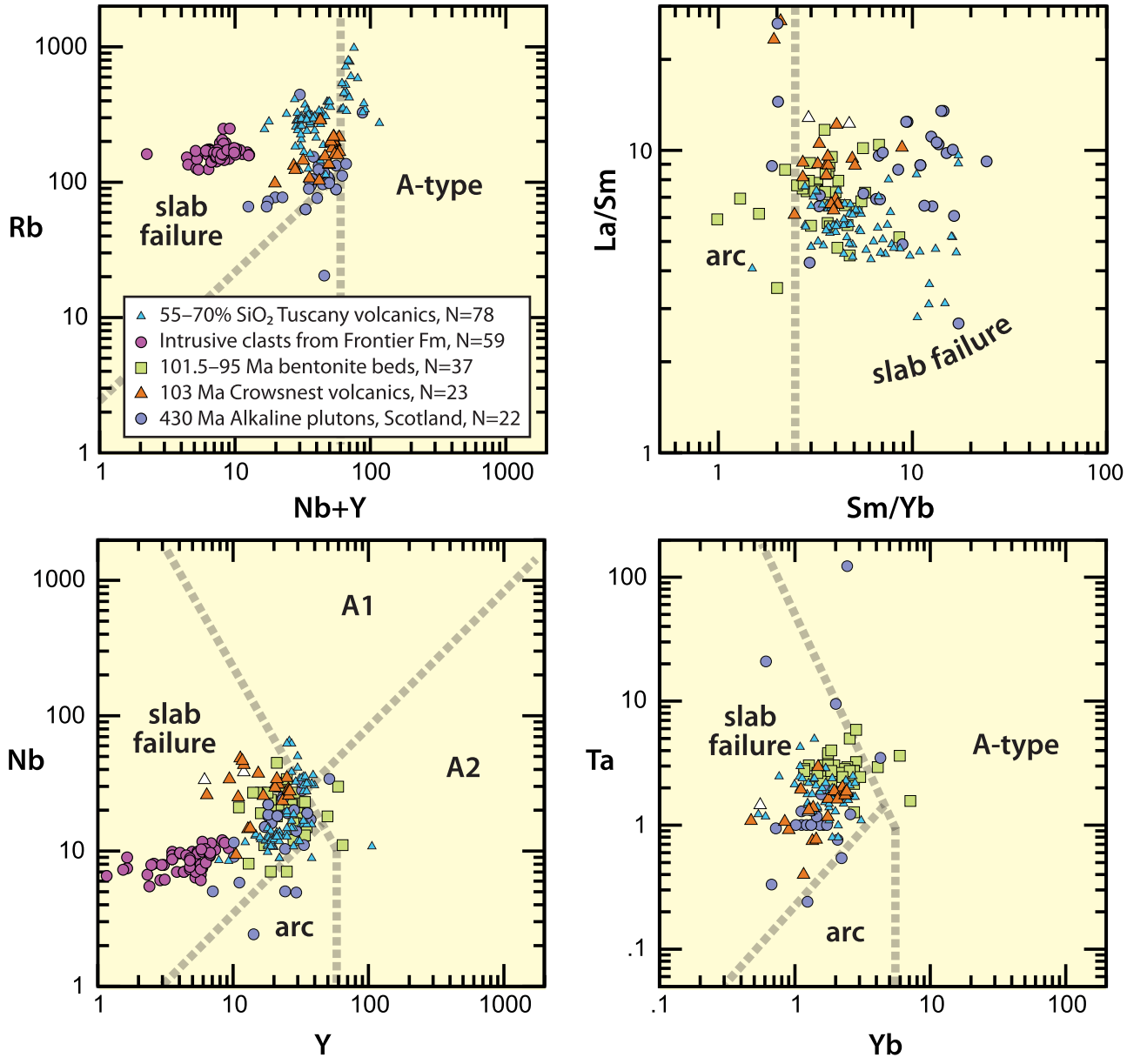

to those of the Crowsnest Formation are found consistently in the fine-grained sands and shales of the Viking Formation from the oil fields northwest of Calgary", which as discussed earlier, are interpreted to interfinger with rocks of the basal Crowsnest Formation. Ross et al. (2005) dated detrital zircons from the Bruin Creek Member and found nine zircons with ages between 107 and 102 Ma.

Geochemically, the rocks are high-K alkaline, do not contain normative nepheline or quartz, are depleted in high-field strength elements, lack Eu anomalies, are enriched in light rare earth elements and have flat heavy rare earth element profiles (Peterson et al. 1997; Bowerman et al. 2006). Initial $^{87}Sr/^{86}Sr$ values range from 0.704 to 0.706, and eNd_T ranges from −7 to −16 (Bowerman et al. 2006). We plotted geochemical data from the Crowsnest Formation on our discrimination diagrams, and most samples plot in the slab failure field (Fig. 14). The elevated initial $^{87}Sr/^{86}Sr$ and negative eNd_T values suggest interaction with subcratonic lithospheric mantle, not asthenosphere (Hildebrand et al. 2018).

Fig. 15. Sketch map showing the known localities of the endemic ammonite *Neogastroplites* spp. in the foothills belt of the Canadian Rockies and the Liard Plateau region (from Stott 1982). mp–Monkman Pass.

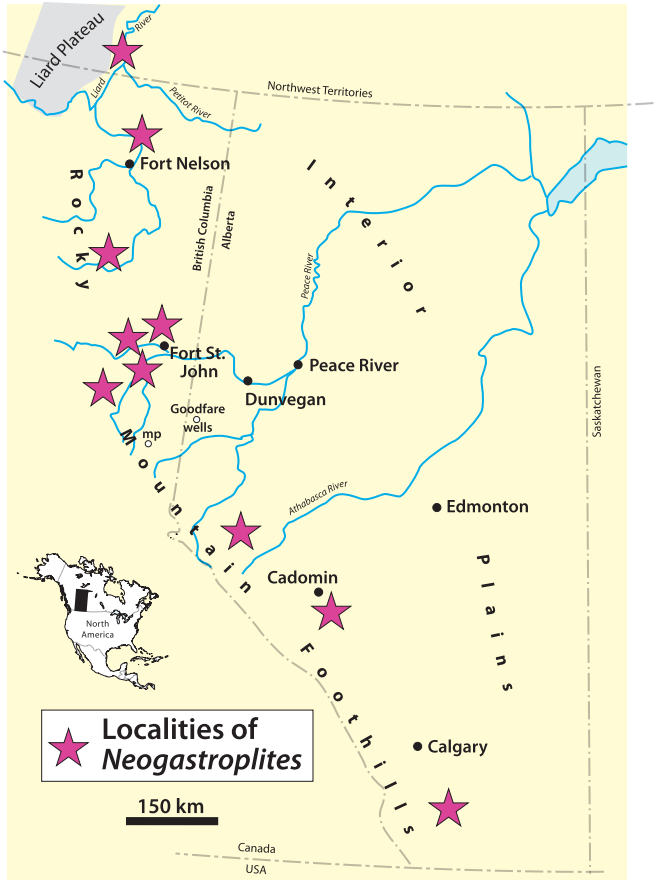

Fig. 16. Close-up view of block from Fish Scales Marker Bed exposed along Petitot River (Fig. 15) showing abundant fish scales on bedding surface. Rock hammer for scale.

Shaftesbury Formation and Fish Scales Marker Bed

The Fish Scale Marker Bed of the Shaftesbury Formation is widely recognized throughout the Western Interior Basin in Canada (Fig. 12). On the basis of lithology and the occurrence of *Neogastroplites* spp., most researchers correlate it with the Mowry Shale. The unit is typically radioactive and has the hallmarks of a condensed section (Leckie et al. 1992; Schröeder-Adams et al. 1996; Roca et al. 2008). Near Peace River, Alberta (Figs. 5 and 15), where it is well exposed in outcrop, Leckie et al. (1992) recognized three units within the Shaftesbury Formation: (1) a 13 m basal bioturbated shale unit devoid of fish remains, but with abundant foraminifera and dinoflagellates representing pelagic sedimentation in an offshore marine setting with a well-oxygenated water column; (2) a 1.5 m section of conglomerate, sandstone, siltstone, black shale, and bentonite holding abundant fish remains, sparse dinoflagellates, but no benthic foraminifera; and (3) an upper shale unit, 11 m thick, with some fish remains, minor foraminifera but only at the top, and moderate quantities of dinoflagellates.

The thin middle part of the formation represents the Fish Scale Marker Bed and according to Leckie et al. (1992), from which this section is adapted, is composite, with four distinct subdivisions. The lowermost 30 cm is in sharp contact with underlying shales and comprises finely interbedded non-burrowed shale, lenticular-graded or parallel-laminated siltstone, and very fine ripple-laminated lenses of sandstone with abundant fish scales, teeth, and probable coprolites, mostly within coarse siltstone and sandstone laminae. This unit is interpreted to represent distal storm deposits or density flows starved of sand, which apparently also carried some of the fish bones into the area. The fine laminations indicate no bioturbation and anoxic bottom conditions. This unit is overlain by 8 cm of phosphatic, fish-hash conglomerate containing fragments of scales and teeth to 1 cm (Fig. 16), scarce vertebrae of marine reptiles to 5 cm, and a conspicuous scarcity of extra-formational clasts. Leckie et al. (1992) interpret this unit as a lag deposit separating shallow water sediments below from deeper water deposits above (see Fig. 13).

Overlying the fish-hash conglomerate is just over 1 m of black shale holding abundant fish remains and a 20 cm bentonite bed. Tiny wisps of coarse siltstone and fine sandstone are interbedded with the shale, and the unit is not bioturbated. Fish debris, including scales, teeth, and their aggregates, likely coprolites, are concentrated in the silty and sandy laminae. The upper unit comprises 11 m of blocky weathering shale with only faint laminations and no bioturbation. Progressively decreasing amounts of fish debris upwards through the section suggested to Leckie et al. (1992) that the upper shale might represent an increase in a rate of sedimentation and so represent a progradational event, which was confirmed by overlying clinoforms that downlap onto the Fish Scale Marker Bed as shown in regional wireline cross sections (Bhattacharya 1994; Plint 2000; Plint et al. 2009).

In the Foothills of Alberta, the Hasler, Goodrich, and Cruiser formations are the equivalents of the Shaftesbury

Fig. 17. Outcrop in bank along Petitot River (Fig. 15) showing Fish Scales marker unit in the Sully Formation. The Fish Scales unit marks the transition from east-derived sediment below to west-derived sediment above. The Sully Formation is a stratigraphic equivalent of the Shaftesbury Formation in northwestern British Columbia and southwestern Northwest Territories (Stott 1982).

Formation (Fig. 12), whereas in the subsurface of the plains the muddy to silty Westgate Formation is correlative with the lower Shaftesbury (Bloch et al. 1993, 1999). In northeastern British Columbia and the southwesternmost corner of the Northwest Territories, the Lepine, Sikanni, and Sully formations are the correlative units (Fig. 17). Stott (1982), in his extensive overview of the stratigraphy of the Fort St. John Group in the Foothills of British Columbia and the northwestern Plains, compiled and reported many occurrences of *Neogastroplites* in the Shaftesbury Formation and all its equivalents in British Columbia and the Northwest Territories (Fig. 15). The ammonites undoubtably occurred in the basin to the east, but as the data come dominantly from drill holes there, they are not recognized. All of these correlative formations lie at least in part within the *Miliammina manitobensis* foraminiferal zone (Fig. 6).

The Fish Scales marker occurs in the central Foothills within the Cruiser Formation (Fig. 9), comprising ~300 m of thinly bedded and non-bioturbated marine shale, siltstone, and bentonite with sandy beds containing abundant fish scales near its base (Stelck 1962). He recorded the ammonites, *Neogastroplites americanus* and *Neogastroplites mclearni,* from the fish scale units and noted the correlation with the Mowry Shale. A second Fish Scale horizon occurs about 68 m higher in the section and thin bentonite beds about 15–20 cm thick increase in number throughout the upper portion of the formation (Stelck 1962).

In northeastern British Columbia and in the Liard River area of the Northwest Territories, Stott (1982) documented the occurrence of the Fish Scales unit in the Sully Formation (Fig. 12), which is a dark gray to black marine shale, 100–200 m thick, that is from west to east, sits on successively older sandstones of the Sikanni Formation, which contains *N. cornutus* and *N. muelleri*. Deposition on progressively older units to the east suggests that the older rocks dipped westward. The Fish Scale unit contains a silty argillaceous mudstone with abundant fish scales and bone fragments, along with associated bentonite beds, overlain by a gradational succession of sandstone and shale, where the contact is placed at the lower downlap surface of the overlying Dunvegan Formation (Fig. 17).

Dunvegan Formation

Lying stratigraphically above the Shaftesbury, Sully, and equivalent formations are rocks of the Dunvegan Formation (Fig. 12). Bhattacharya (1989) collected data from about 500 well logs and 130 cores to create isopach maps and detailed facies interpretations of the rocks, which form a southeastward prograding clastic wedge atop the Fish Scales Marker Bed (Bhattacharya and Walker 1991*a*, 1991*b*; Plint 2000; Plint et al. 2009).

The Shaftesbury shale unit above the Fish Scales Marker Bed is considered by Battacharya (1994) to be the basal unit of the southeasterly prograding Dunvegan clastic wedge because the bioturbated and rippled silty mudstones, generally lacking in fish parts, indicate deposition in brackish, prodeltaic, shallow-water conditions caused by southeastward progradation of the deltaic depositional system. Bhattacharya and Walker (1991*a*) subdivided the Dunvegan (Fig. 18) into seven allomembers separated from one another by transgressive, marine flooding surfaces that represent progradational cycles beginning with basal marine mudstones passing upwards through interbedded mudstones, siltstones, and sandstones into shallow, marine shoreline sandstones topped by non-marine facies such as coals and paleosols. The non-marine units thicken to the northwest. The southern continuation of the Dunvegan is the Blackstone Formation (Fig. 12), but most of the unit is truncated or obscured at the thrust belt to the west, so only the eastern muddy facies are preserved within the basin as documented by Plint (2000) and Plint et al. (2009), who, using more than 2300 well logs and >60 outcrop sections, traced the Fish Scales Member over 950 km southeast to the Blackstone Formation. They

Fig. 18. Regional cross section of Dunvegan Alloformation illustrating its wedge-shaped form and that its various allomembers (labeled G to C) downlap onto the planar surface of the Fish Scales unit (modified from Bhattacharya 1994). Correlation lines are interpreted to be chronostratigraphically significant surfaces. Location of section A to B is shown in the inset. Note that in the north facies trend more or less northerly, but to the south they are truncated by much younger Upper Cretaceous–Paleocene deformation in the Laramide fold-thrust belt (Fig. 5).

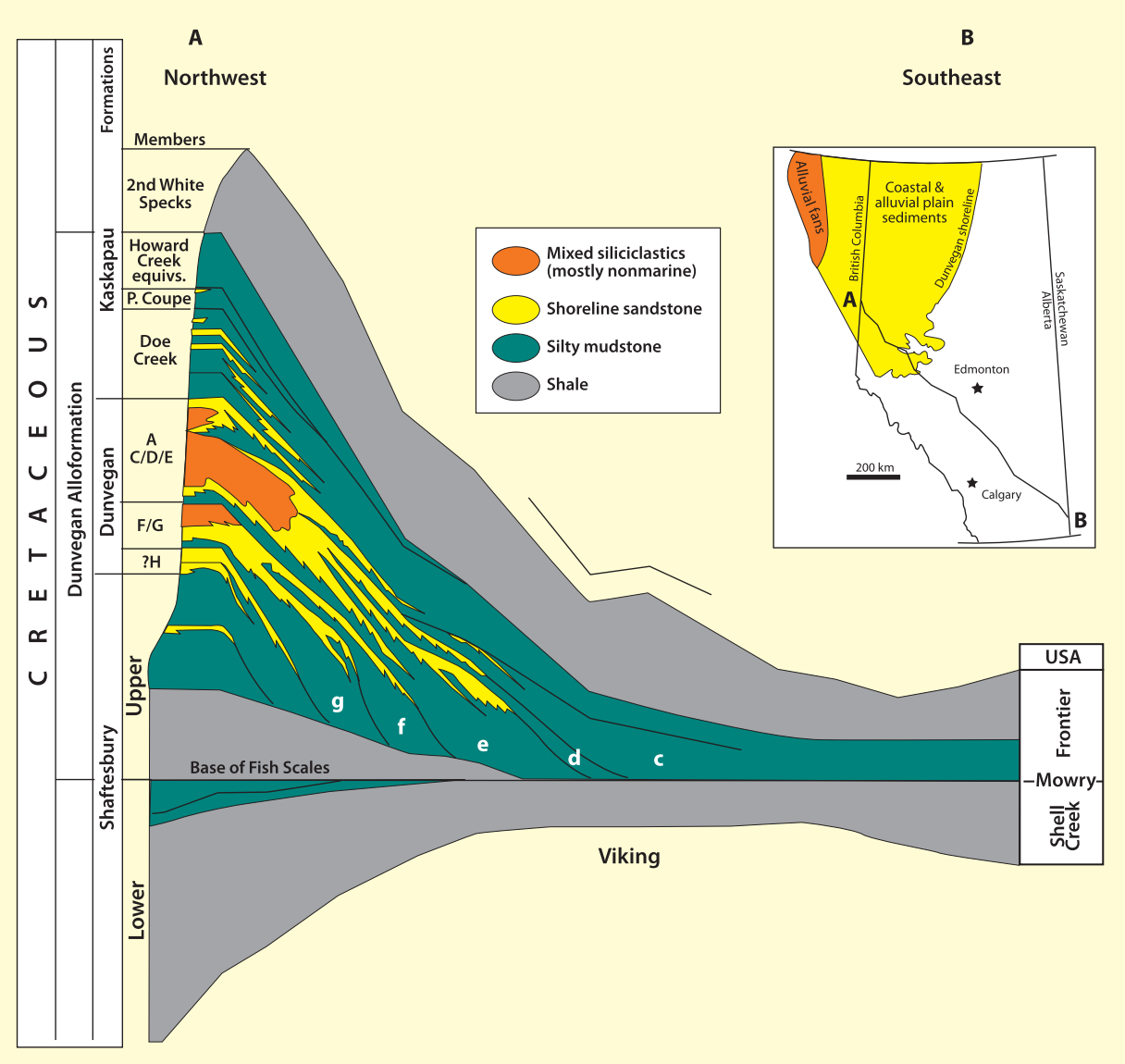

also documented that individual clinoforms of the prodelta mud-wedge in the Dunvegan Formation range from 80 km in the lower few allomembers; but progressively in the upper section they found progradational distances to be ~150, ~220, and ~250 km, with the upper allomembers, extending as 10–20 m thick tabular sheets for 400 km for allomember C and 800 km for allomember A at the Montana border (Fig. 19). Hay and Plint (2020) showed that the upper two allomembers of the formation preserved evidence of progressive drowning and had smaller and more linear delta-front sandstone bodies upsection, which suggested to them that more open-marine conditions were established over that interval.

Far to the east in Manitoba, rocks of the Belle Fourche Member of the Ashville Formation (also called Belle Fourche Formation), considered correlative with rocks atop the Fish Scale unit to the west (Fig. 12), are dominantly dark shales lacking in benthic foraminifera (Schröeder-Adams et al. 2001). They report that basal beds are not bioturbated and contain a 1-cm-thick bed of fish teeth, scales, and other debris, that coarsens upwards into bioturbated sandstones, shell beds, and additional bonebeds, some with vertebrate fossils. Apparently, the water column of the basin was stratified, with anoxia reaching into the photic zone as far east as its exposed margin in southern Canada, and remained starved for some time after deposition of the Fish Scales

Fig. 19. Diagram illustrating the geometry and shape of allomembers of the Dunvegan Formation (Plint et al. 2009) on a line from Fort St. John in the northwest to the US–Canada border in the SE. The top of the condensed Fish Scales unit is a downlap surface and represents a southeastward surface upon which successive younger clinoforms were deposited farther to the southeast. Plint et al. (2009) point out that the Fish Scales unit is a basin-wide deposit and marks the shutdown of deposition in the basin. Vertical exaggeration is about 1600.

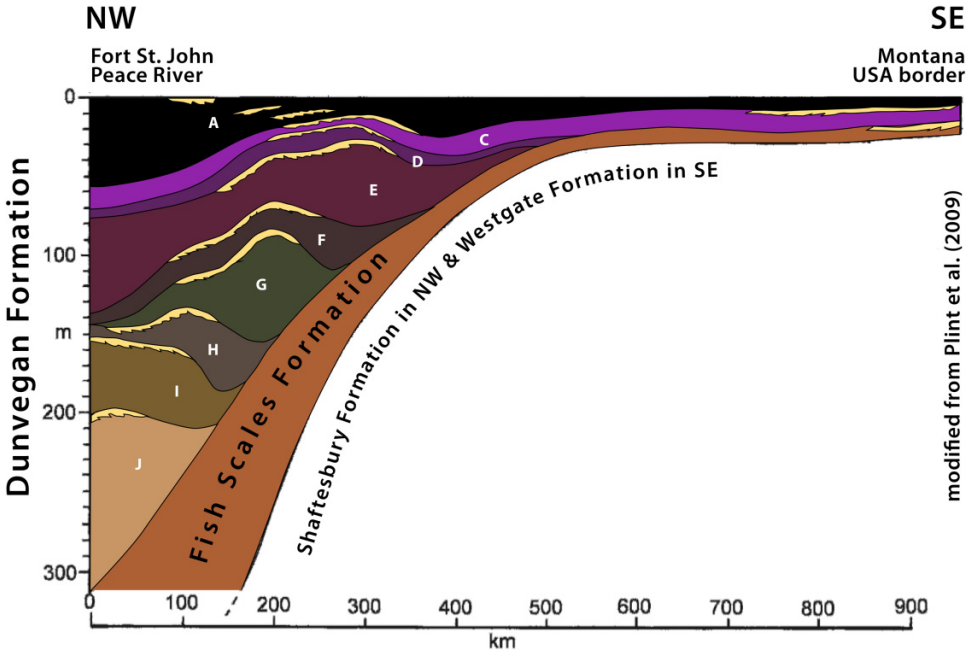

horizon, while clastic wedges prograded eastward across the basin.

Although bentonite beds are directly associated with the Fish Scales horizon and have been collected for dating, they remain unpublished; however, Plint (personal communication, 2021) reported the radiometric age as consistent with ages determined by Singer et al. (2021) for the Mowry Formation. A bentonite bed located to the south within dark marine mudstone of the Sunkay Member of the Blackstone Formation (Figs. 4 and 12), which was traced northward 350 km to the upper allomembers of the Dunvegan Formation (Tyagi et al. 2007), was dated by U-Pb on zircon to be 95.87 ± 0.10 Ma (Barker et al. 2011).

Buechmann (2013) studied detrital zircons in units above and below the Fish Scales Marker Bed (Fig. 20) and discovered a shift in provenance from dominantly Precambrian zircons (93%) below the bed in the Viking Formation to Paleozoic and Cretaceous in the Dunvegan Formation above the Fish Scale Marker. He interpreted the bulk of debris within the Viking Formation to have been derived from sources in the Canadian Shield with lesser quantities of Paleozoic rocks, perhaps largely cannibalized from incised paleovalleys cut into older rocks by pre-Viking erosion. Detrital zircons from the Dunvegan Formation (Fig. 20) are dominated by Mesozoic grains (69%) with prominent age peaks at 100, 101, and 102 Ma, which we infer to represent detritus shed from the rising hinterland to the west.

Peel Plateau—Great Bear Plain

Northeast and north of the Mackenzie Mountains, along the Hume River (Fig. 5) a sedimentary succession, about 2 km thick, sits unconformably upon a basement of Devonian sedimentary rocks and comprises a basal 20 m thick Albian transgressive sandstone, the Martin House Formation (Fig. 21), overlain by as many as 1000 m of Albian bioturbated, marine mudstones of the Arctic Red Formation, which contains a bentonite dated by U-Pb zircon as 107.0 ± 1.9 Ma (Thomson et al. 2011). Because strata of the Martin House Formation lie directly on Paleozoic basement, instead of Lower Cretaceous sedimentary rocks, field relationships are more straightforward than farther south.

Hadlari et al. (2014) indicate that the sandstones of the basal transgressive Martin House Formation are marginal marine and fine upwards, as well as westward, into offshore mudstones of the Arctic Red Formation, which reflect a westward-deepening basin. The Albian succession is capped by a pisolitic ironstone facies, holding rare wood fragments, unconformably overlain by mudstone and bentonite beds of the Cenomanian Slater River Formation, which is up to 500 m thick with a base composed of black carbonaceous shale and rare coal seams overlain by a 10 cm condensed section of nonbioturbated and radioactive mudstone with fish teeth, bones, and other organic material, but no foraminifera (Thomson et al. 2011). Gray mudstones with few foraminifera dominate the remainder of the Slater River Formation, but minor rippled sandstone beds occur towards the top, and the entire succession grades upwards through a transgressive peb-

Fig. 20. Detrital zircons of five samples from the Viking and Dunvegan formations collected and analyzed by Buechmann (2013) replotted as cumulative distribution and KDE (kernel density estimator) plots. The Viking is interpreted to be derived from the Canadian shield with lesser quantities of recycled zircons from the fold-thrust belt, whereas the zircons in the Dunvegan Formation were almost exclusively derived from the collisional hinterland to the west as reflected by the 100 Ma peaks. Curve labeled Great Bear Lake on plot of Viking 2 is from Hadlari et al. (2012) and illustrates zircons in Cambrian strata derived from the Wopmay orogen just south of Great Bear Lake. Plotted with detritalPy (Sharman et al. 2018).

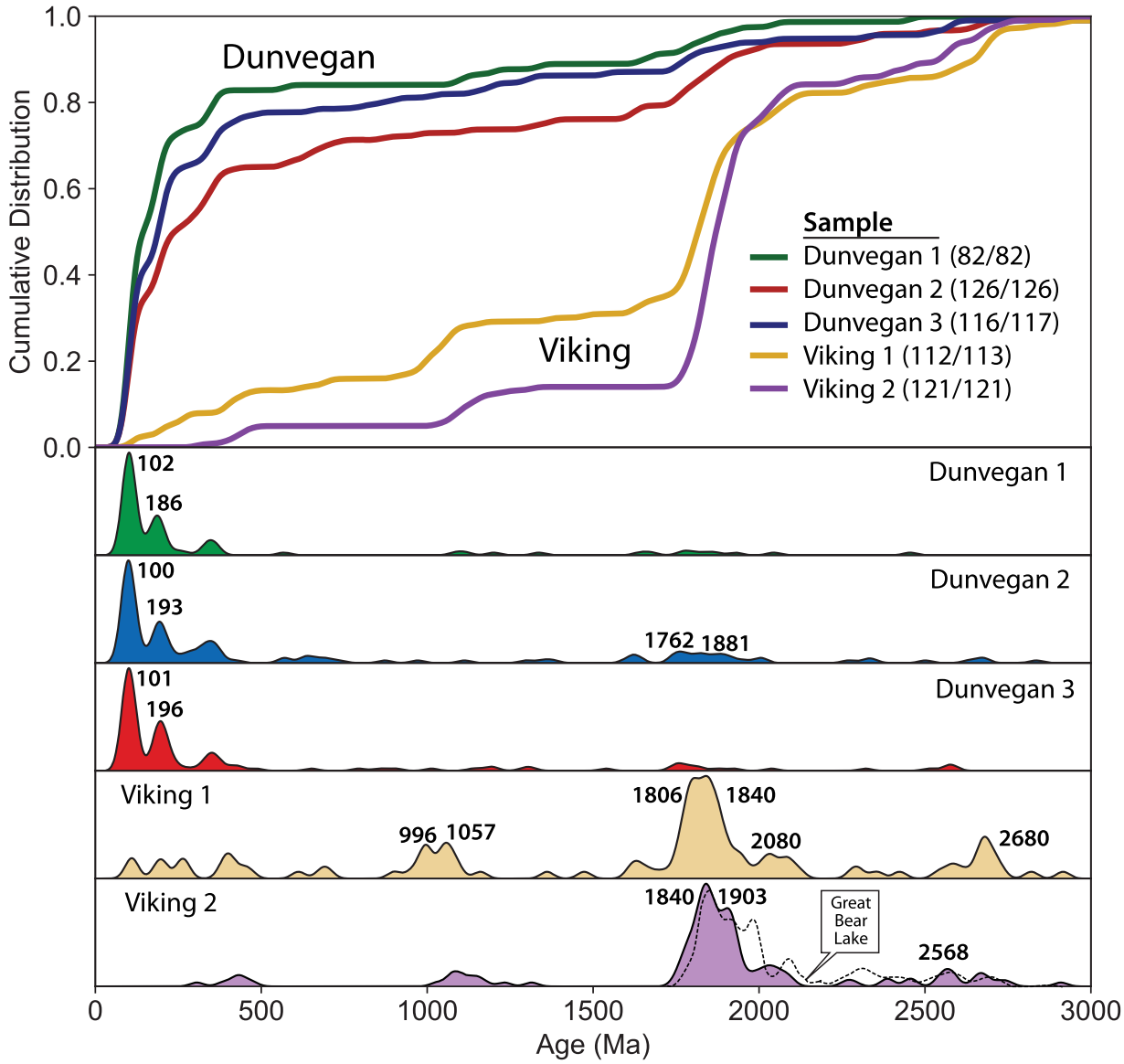

bly lag into 700 m of siliciclastic parasequences representing an easterly prograding clastic wedge of the Trevor Formation (Hadlari et al. 2014).

Ages of detrital zircons (Fig. 21) collected from the basal Martin House Formation are consistent with an easterly source in the Orosirian Wopmay orogen, whereas zircons from the Trevor Formation have a broader age range, similar to the Neoproterozoic to Mississippian rocks known in the Mackenzie Mountains, but also with a prominent, near-syndepositional peak at 93 Ma, similar in age to post-deformational plutons of the Selwyn Basin (Mair et al. 2006; Hadlari et al. 2014; Rasmussen 2013; Hildebrand and Whalen 2017).

Hadlari et al. (2014) interpreted the entire succession to have been deposited in an easterly migrating foredeep with the westerly prograding Albian sequence deposited on the eastern slope of the basin with sediment derived from the Shield to the east, whereas the Cenomanian section prograded towards the east and contains debris from the Mackenzie Mountains thrust belt and post-collisional plutons of Selwyn Basin (Fig. 22). In a general sense, we agree with this interpretation, except that we consider that the Albian section formed part of a Lower Cretaceous passive margin on the east side of the basin rather than in the younger foredeep trough. We note that the pisolitic ironstone beds at the top of the Albian succession are readily interpreted as soil horizons

Fig. 21. Stratigraphic section at Hume River (HR on Fig. 5) for mid-Cretaceous sedimentary rocks of the Peel Plateau, located just north of the Mackenzie Mountains showing the age probability curves of detrital zircons from pre-and post-Fish Scales units (modified from Hadlari et al. 2014). We interpret the Martin House and Arctic Red Formations as part of the west-facing passive margin of the 140–100 Ma seaway and were derived from the east. As the margin was pulled down into the west-dipping subduction zone, rocks of the margin were subaerially exposed on the peripheral bulge where a ferruginous paleosol complex developed. After passing over the bulge the region was resubmerged on the outer slope to the trench where the starved and anoxic Fish Scales unit of the Slater River Formation was deposited. Rocks of the overlying Trevor Formation were derived from the west and contain young detritus from post-collisional plutons in the hinterland.

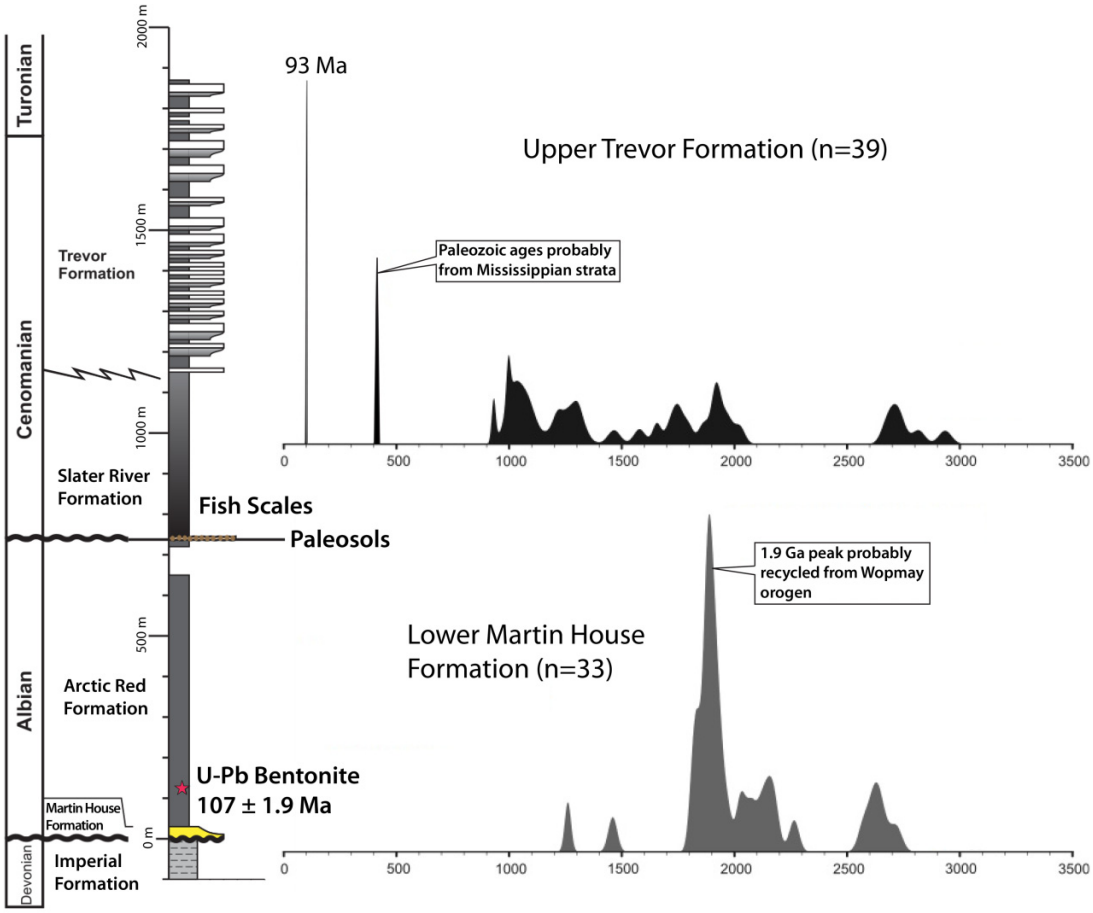

(Thomson et al. 2011) and that the unconformably overlying strata are recognized throughout the Western Interior Basin, where, as we have seen, they are known as the "fish debris marker" (Thomson et al. 2011), or Fish Scales Formation.

Whereas in a foredeep scenario, the easterly progradation of thrusts should result in a progressively deepening flexural basin to the east, the opposite occurred as the margin was uplifted, exposed, and eroded, before being buried by a condensed, anoxic interval. In our conception, the Albian succession was exposed when the passive margin rode over the outer swell (Jacobi 1981). The exposure generated the pisolitic soil horizons, which were investigated and described in detail by Thomson et al. (2011). Afterwards, the region subsided to form a restricted marginal marine to marshy environment that progressively deepened and is represented by the thin radioactive condensed horizon containing fish hash but no foraminifera, which Thomson et al. (2011, p. 281) interpreted to represent "an offshore marine environment … where sediment input to the system is minimal". The lack of sediment influx and inhospitable conditions for benthic life suggest to us that the area lay on the outer trench-slope, where sediment-starved conditions are typical. The overlying westerly derived siliciclastic rocks of the Trevor Formation represent orogenic debris shed from the hinterland.

Strata in Mexico, Arizona and New Mexico

A more complete geological record is preserved in northern Mexico and the southwestern United States (Fig. 23), where a pene-contemporaneous basin known as the Bisbee–Arperos seaway, or trough (see Martini et al. 2014) is well-exposed, relatively undeformed, and unconformably overlies pre-Nevadan Jurassic and Tithonian sedimentary and volcanic rocks of the Peñasquitos and Cucurpe formations, both deformed between about 145 and 139 Ma (Mauel et al. 2011; Kimbrough et al. 2014; Hildebrand and Whalen 2014, 2021*a*).

Fig. 22. Sketch map of part of the Selwyn Basin showing stratigraphic units, thrust faults, and 99–93 Ma plutons that postdate the thrust faults. Location of area shown on Fig. 5. From Murphy (1997).

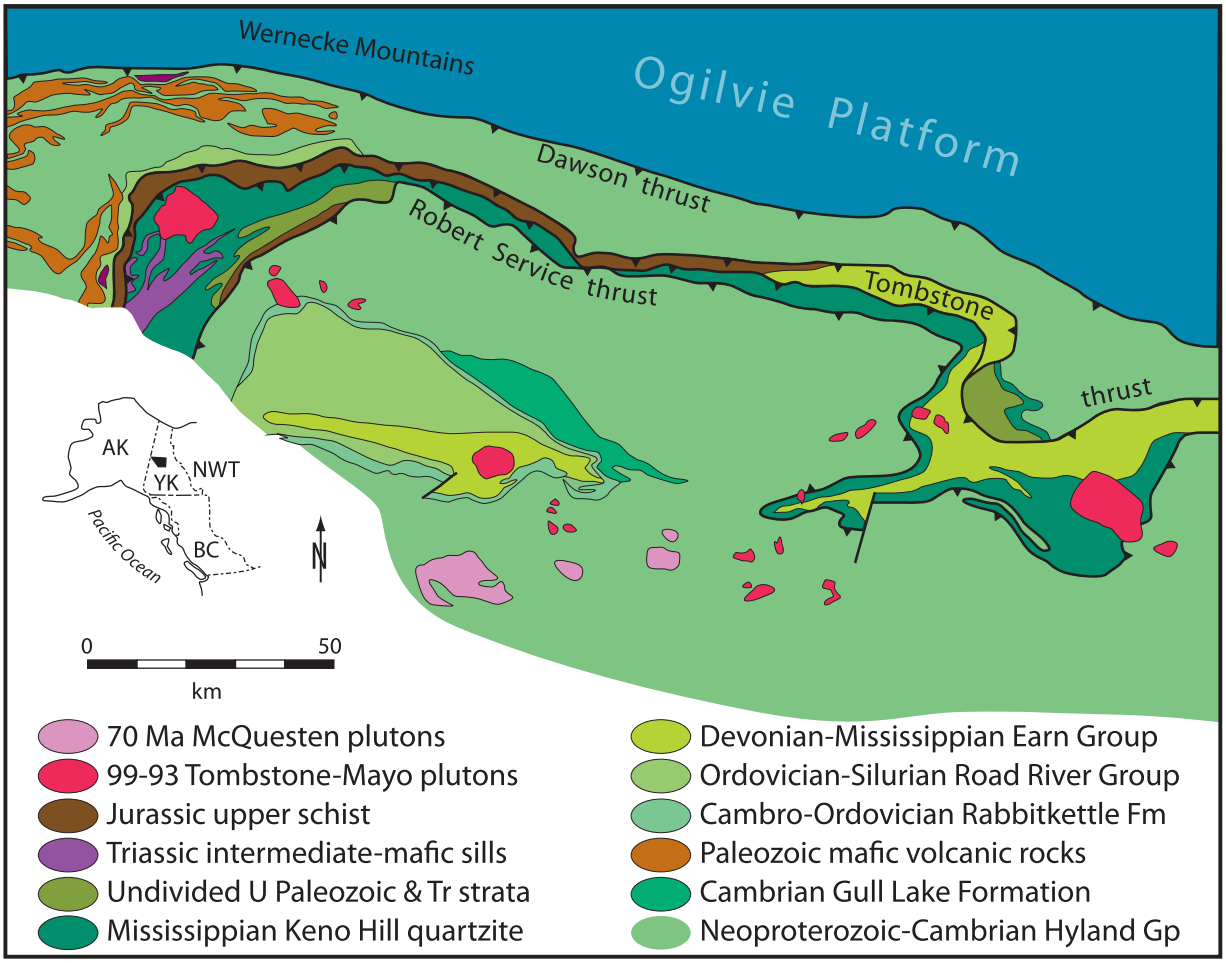

These units constrain the age of the pre-collisional seaway to be younger than about 140 Ma.

The eastern side of the trough is characterized by a west-facing Lower Cretaceous continental margin capped by a widespread carbonate platform/ramp, known as the Guerrero–Morelos platform in central-southern Mexico or Mural Formation of the Sonoran platform in Arizona and Sonora (Lawton et al. 2020*a*). During the late Albian, upward growth of the west-facing carbonate platform stopped, as marked by a disconformity atop massive bioclastic carbonate overlain by a few meters of well-laminated beds of detrital carbonate, breccia, condensed horizons rich in Late Albian faunal debris (Fig. 24), and capped by a thin interval of hemipelagic shale, itself passing up section into the extensive Cenomanian Mexcala flysch (Monod et al. 2000; Lawton et al. 2020*b*). U-Pb analyses of detrital zircons from the Mexcala flysch in central Mexico, just east of the suture (Lawton et al. 2015), yielded large age peaks at 97 and 95 Ma (Fig. 25).

To the north in the Bisbee Basin, the dominantly Albian Mural Limestone of the west-facing carbonate (Sonoran) platform/ramp (Fig. 23) was buried by at least 1500 m of westerly derived Cenomanian and Turonian fluvial and shallow marine siliciclastic rocks termed the Cintura Formation in Sonora and southeastern Arizona and in southwestern New Mexico, the Mojado Formation (Warzeski 1987; Jacques-Ayala 1995; González-León et al. 2008). Both are interpreted to have been deposited in a flexural foredeep by fluvial systems (Mack 1987; González-Léon and Jacques-Ayala 1988; Lawton et al. 2020*b*). The southwesternmost exposures of the Cintura Formation are in excess of 2000 m thick and are overlain gradationally by latest Albian–early Cenomanian fluvio-deltaic sandstone with sparse pebbles of quartzite and limestone and overthrust from the southwest by plutonic rocks (Jacques-Ayala 1992; Lawton et al. 2020*b*). In Sonora, the Cintura Formation is overlain by conglomerate and intercalated andesite of the Cocóspera Formation, the latter of which yielded a $^{40}Ar/^{39}Ar$ age of 93.3 ± 0.7 Ma (González-León et al. 2011). Lawton et al. (2020*b*) demonstrated the coeval nature of the west-facing, passive margin sequence of North America with the Alisitos arc of the Guerrero Superterrane to the west, established the temporal correlation between the Mojado and Cintura formations by U-Pb studies of detrital zircons and ash beds, inferred steep subsidence curves in the Sonora sector of the basin at ~100 Ma, and confirmed the consanguineous

Fig. 23. Sketch map illustrating key geological units of the Peninsular Ranges orogeny and Aptian–Albian volcano-sedimentary rocks of the Alisitos—Santiago Peak arc, various subterranes of the Guerrero superterrane, and Albian carbonate platforms, mostly located west of the younger Laramide suture and its related fold-and-thrust belt. The Peninsular Ranges batholith continues the length of Baja California, as indicated by a conspicuous aeromagnetic anomaly (Langenheim et al. 2014), but the batholith is buried by younger volcanic rocks south of the state line. Red dots represent drilled and dated core from La Posta plutons (Duque-Trujillo et al. 2015). Rocks of similar age and lithology to those of the Peninsular Ranges batholith crop out in Zihuatanejo (Centeno-García et al. 2011). Westward-facing Albian carbonate banks of the Sonora and Guerrero–Morelos platforms were pulled westward beneath rocks of the Guerrero superterrane at 100 Ma during closure of the Bisbee–Arperos seaway. We follow Hildebrand and Whalen (2014) and include the Cortes and Caborca terranes in Guerrero superterrane as they were thrust over the Sonoran shelf at ~100 Ma (Pubellier et al. 1995). Co–Concordia; MP–Mineral de Pozos; RG–Rio Grande; TT–Teloloapan thrust.

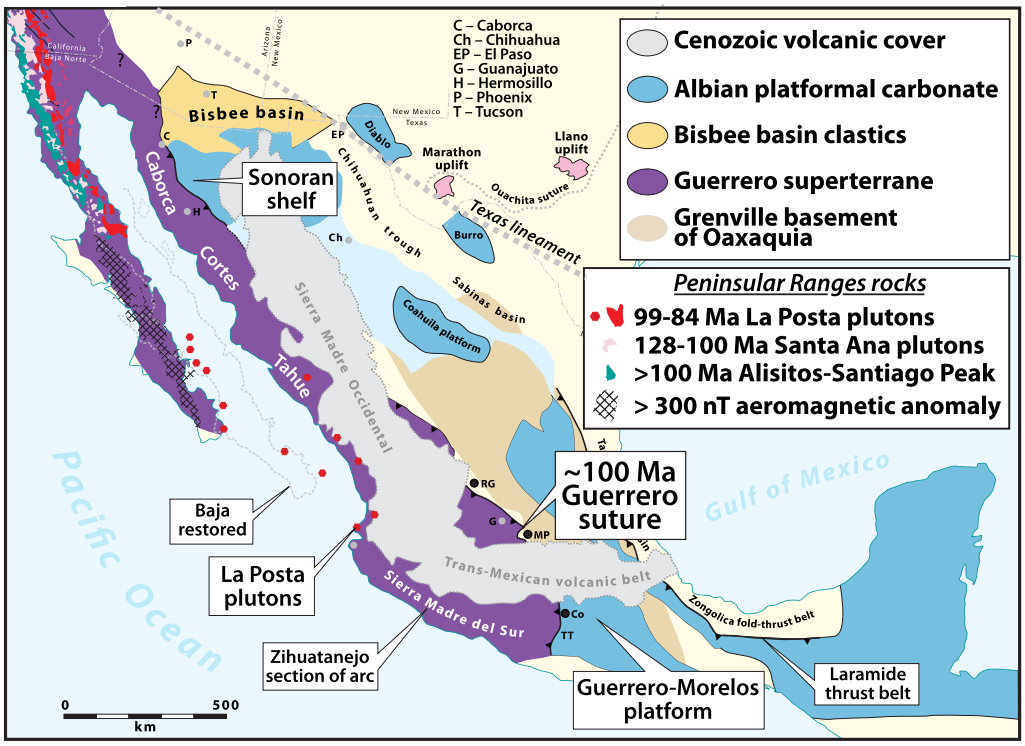

nature of the fluvial to marine foredeep system as far to the east as El Paso, Texas, and northeast to the Dakota Formation of the southeastern Colorado Plateau and Western Interior Basin (Fig. 26).

The lack of an Albian foredeep succession and related fold-thrust belt in southern Arizona and Mexico suggest that the Sevier collision, and thus, the Sevier colliding block, did not impact North America at this latitude. Likewise, the lack of similar features, discussed previously, on the Peel Plateau in northern Canada, constrain the northern extent of the incoming Sevier block and hence its overall length to about 2000 km.

The Peninsular Ranges orogeny

Hildebrand and Whalen (2021*a*, 2021*b*) expanded their earlier tectono-magmatic synthesis of the southwestern United States and Mexico (Hildebrand and Whalen 2014) to include the mid-Cretaceous geology of the Cordillera from southern Mexico to Alaska, which they interpreted to represent the closing of an oceanic trough, or basin, by westerly subduction at about 100 Ma, an event they termed the Peninsular Ranges orogeny. What follows is only a brief synopsis as the development of the orogen along the length of North America was described and discussed in the two most recent papers cited above.

The basin, or trough, was an ocean that formed after the Late Jurassic—Early Cretaceous Nevadan orogeny and associated post-collisional magmatism, when a long, linear sliver rifted from the western margin of the tectonic collage of previously accreted terranes then attached to the westernmost margin of North America. As originally suggested for the general case by Wilson (1968), the basin opened more or less along the Jurassic suture such that fragments of the collision ended up on both sides of the ocean basin (the subsequently named Wilson cycle). The trough was open for ~40 million years and during the Early Cretaceous a west-facing, passive-margin, sedimentary prism was deposited on its eastern margin (cratonic North America) whereas a well-developed, dominantly marine arc developed on the western fragment, or ribbon

Fig. 24. Detailed cross section of the uppermost few meters of the west-facing Guerrero–Morelos carbonate platform showing the rapid transition from carbonate shelf to orogenic deposits near Concordia, Estado de Guerrero. Hoffman (2012) presents an excellent overview of the process of platform foundering at the beginning of orogenesis. The figure is modified from Monod et al. (2000). (For location of Concordia, see Fig. 23.)

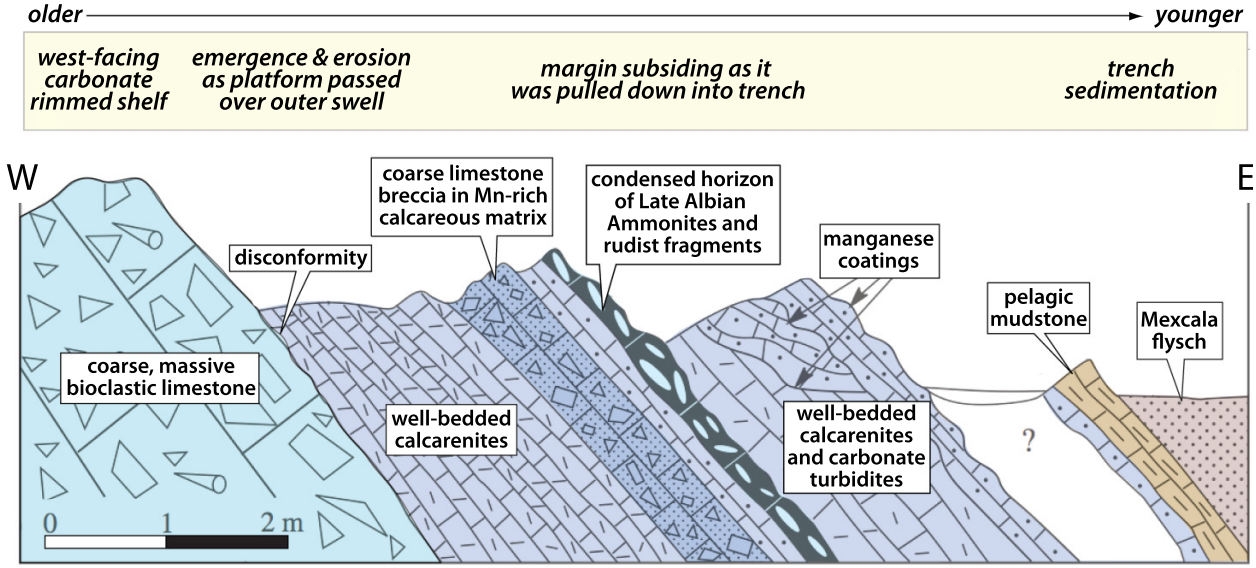

Fig. 25. Detrital zircon populations from four turbidite samples collected in central Mexico east of the suture between the Guerrero Superterrane and North America illustrating the dominant post-100 Ma peaks (from Lawton et al. 2015). (See Fig. 23 for locations: MP–Mineral de Pozos and RG–Rio Grande.) Plotted with detritalPy; Sharman et al. (2018).

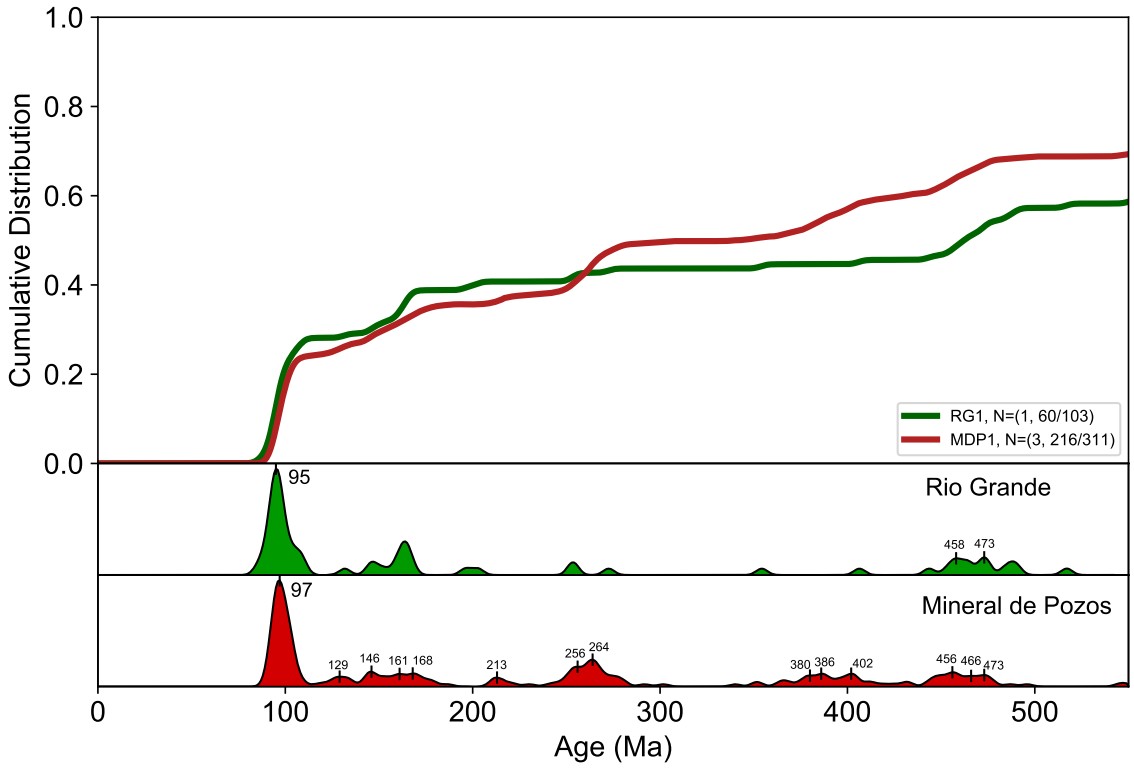

(Coney et al. 1980; Campa and Coney 1983; Tardy et al. 1994; Dickinson and Lawton 2001; Centeno-Garcia et al. 1993, 2008, 2011). The arc, known in southern California and Peninsular Mexico as the Alisitos–Santiago Peak arc, was active from about 130 Ma until ~100 Ma (Hildebrand and Whalen 2014).

As described above, platformal-carbonate rocks of the westerly facing passive margin in Mexico are disconformably over-

Fig. 26. Stratigraphic correlations from Bootheel area of southwestern New Mexico (Fig. 5) northeast to eastern Colorado Plateau at San Ysidro, illustrating detrital zircon maximum depositional ages, and tuff ages of Mojado Formation and stratigraphic equivalents modified from Lawton et al. (2020*b*). The Mojado Formation is the more easterly correlative of the Cintura Formation in Arizona and Sonora, which is the clastic wedge that sits atop the west-facing Mural carbonate platform of the Bisbee Basin. Location of sections and line are shown in Fig. 5.

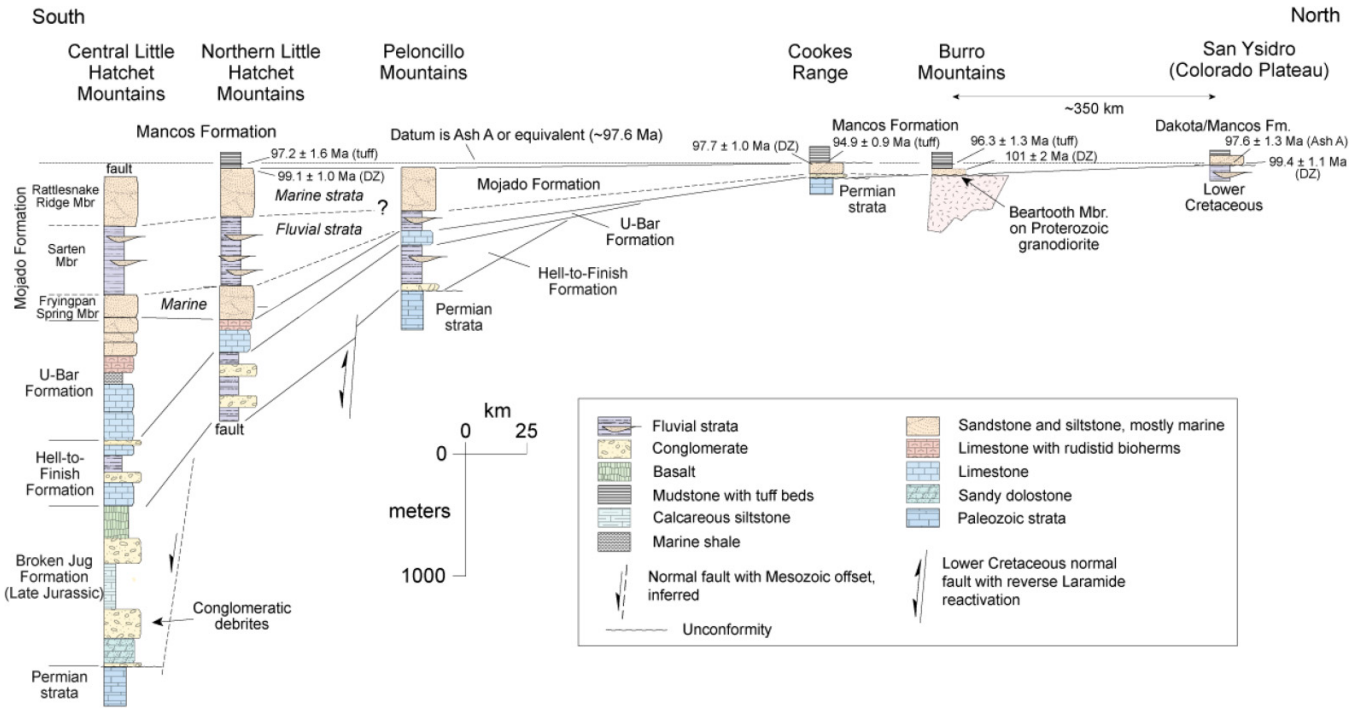

lain by a few meters of transported carbonate and condensed horizons rich in Late Albian faunal debris (Fig. 24) capped by hemipelagic shale and Cenomanian Mexcala flysch containing 97–95 Ma detrital zircons (Fig. 25) similar in age to those of the Frontier and Dunvegan formations to the north. The disconformity, as well as the rapid tectonic subsidence and burial of the carbonate platform by hemipelite and orogenic flysch, is readily explained by a collision, during which transport of a platform over the outer swell to a trench, where it was eroded (Jacobi 1981). Then, as the platform was pulled into the trench, it was covered by a thin veneer of hemipelagic mud deposited on the starved outer-trench slope, only to be overwhelmed by trench-fill turbidites upon arrival in the trench axis (see Sinclair 1997; Hoffman 2012; Sabbatino et al. 2021). These rocks were detached and scraped off their cratonic basement, accreted to the upper plate as part of the accretionary prism, and then transported eastwards over the craton.

The post-100 Ma detrital zircons in the orogenic flysch were most plausibly derived from the suite of 99–86 Ma La Posta plutons (Fig. 23), which were emplaced into the collisional hinterland located west of the foredeep (Hildebrand and Whalen 2014). The plutons postdate ~100 Ma deformation of the Alisitos–Santiago Peak arc and its basement of Guerrero superterrane, as well as the drowning and burial of the west-facing upper Albian carbonate platform perched on the western margin of North America (Hildebrand and Whalen 2014). The La Posta plutons intrude as far west as the Santiago Peak–Alisitos arc, but predominantly outcrop just to the east of it (Fig. 23), and have long been recognized to differ in age, trace element and isotope content, opaque mineralogy, depth of emplacement, and crustal thickness from the Alisitis-Santiago Peak arc rocks (Gastil et al. 1975, 1990; Silver et al. 1979; Gromet and Silver 1987; Silver and Chappell 1988; Kimbrough et al. 2001; Tulloch and Kimbrough 2003). We compiled modern geochemical data from both the Alisitos–Santiago Peak arc rocks and the post-100 Ma La Posta plutons and found consistent major and minor geochemical differences between the two suites (Hildebrand and Whalen 2014). For example, most rocks of the La Posta plutonic suite contained 60%–70% SiO_2 whereas the arc suite displayed a continuous range from basalt to rhyolite. Relative to the arc rocks, members of the La Posta suite are generally more enriched in incompatible elements, Na, and Nb, but are depleted in Y and Yb. We exploited the differences between the pre- and post-collisional suites to develop several discrimination diagrams (Fig. 27) that distinguish arc from failed slab rocks, and then tested them using Cenozoic suites (Hildebrand et al. 2018), before applying the discriminants to other Cordilleran batholiths in western North America, where we found similar rocks and relations northward through the Cordillera to Alaska (Hildebrand and Whalen 2017; Whalen and Hildebrand 2019; Hildebrand and Whalen 2021*a*, 2021*b*). More recently, these discrimi-

Fig. 27. Volcanic and plutonic samples with SiO_2 > 60% from the Peninsular Ranges batholith plotted on five discrimination diagrams modified from Hildebrand and Whalen (2014, 2017) and Whalen and Hildebrand (2019). Santiago Peak–Alisitos arc rocks are 130–100 Ma, whereas the post-collisional La Posta suite is 100–86 Ma. The Nb vs. Y and Ta vs. Yb discrimination diagrams were modified from Pearce et al. (1984) by addition of fields for post-collisional and arc plutons based empirically on samples from the Peninsular Ranges batholith. Alisitos volcanic arc data are from Morris et al. (2019).

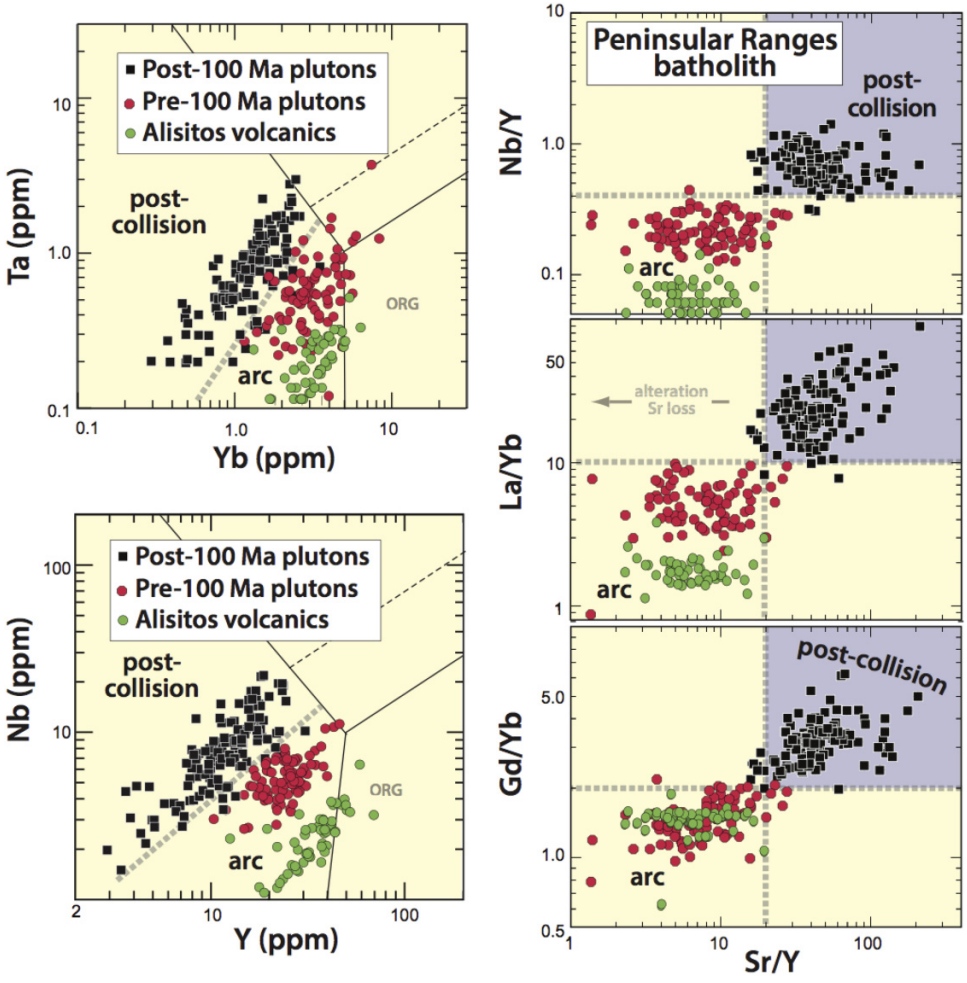

nation diagrams have been applied elsewhere to discriminate arc from failed slab rocks (e.g., Archibald and Murphy 2021; Dostal and Jutras 2021; Gianni and Navarrete 2022).

Understanding the age of collision is important not only for resolving the origin of plutons in the hinterland (Hildebrand and Whalen 2017) but also because the debris eroded from them during uplift and exhumation can be used to demonstrate that specific depocenters or even entire basins can be properly recognized as post-collisional. For example, Kimbrough et al. (2001) demonstrated that the La Posta plutons of Peninsular and Southern California closely postdated a period of contractional deformation, were deep-seated, and emplaced during rapid uplift/exhumation on the basis of debris, including 99–92 Ma zircons, shed rapidly westward from the rising hinterland into what they assumed was a forearc basin represented by rocks of the Valle Group. However, as we demonstrated, subduction was westward beneath the Alisitos–Santiago Peak arc, and so the Valle Group was deposited west of the thickened collision zone and not in a pre-collisional forearc setting. In fact, similarly preserved fragments along strike, such as the Valle and eastern Great Valley groups, the Hornbrook of the eastern Klamaths, the Ochoco Group of Oregon, the Cascade River schist, lower Nanaimo Group, Queen Charlotte Group, and the McHugh complex—all of which contain abundant 100–90 Ma detrital zircons—combine to suggest that the westerly basin, or sea, was continuous from the Baja Peninsula to Alaska and was partially filled after the collision in a retro-collisional setting, not in a forearc (Hildebrand and Whalen 2021*a*, 2021*b*).

In another case, researchers working in central Mexico argued that the Arperos sector of the basin closed during the lower Cretaceous (Martini et al. 2013) rather than at about 100 Ma as we suggested (Hildebrand and Whalen 2014). They cited a location in the complex thrust stack of the Sierra de Guanajuato (Fig. 23) where a ~50 m-thick Aptian–Albian carbonate unit, known as the La Perlita Formation, unconformably overlies a basal conglomerate deposited on greenschist-grade, isoclinally folded, Tithonian–

Berriasian metasedimentary rocks (Chiodi et al. 1988; Quintero-Legorreta 1992; Martini et al. 2011), so inferred that the rocks of the La Perlita Formation were deposited after collision. However, elsewhere in the Sierra they noted several thrust sheets carrying younger volcanic and related epiclastic successions such as the westerly derived Teloloapan and Arperos formations and the easterly derived, siliciclastic Cuestecita Formation, which all have the youngest detrital zircon peaks ranging mainly from 133 to 116 Ma, consistent with ages of the Alisitos–Santiago Peak arc built on Guerrero superterrane (Talavera-Mendoza et al. 2007; Martini et al. 2011), as well as upper Aptian–upper Albian platform facies to the east on the North American side of the basin (Lawton et al. 2004). These observations suggest that the Tithonian–Berriasian successions in the Sierra de Guanajuato are correlative with the more northerly Cucurpe and Peñasquitos successions, both deformed between about 145 and 139 Ma (Mauel et al. 2011; Kimbrough et al. 2014; Hildebrand and Whalen 2014, 2021*a*), and *then* overlain by rocks of the Bisbee–Arperos basin, much in the way the older deformed successions of the Sierra de Guanajuato were overlain by conglomeratic and carbonate rocks of the Albian La Perlita Formation. Thus, we see no conflict between areas, and the stratigraphy constrains the age of the seaway to be younger than about 140 Ma with terminal collision at about 100 Ma. This is consistent with the geology farther south in the Zihuatanejo area (Fig. 23), where 250 m of Albian carbonate of the Ixtapa Formation was uplifted, eroded, and unconformably overlain by 2–10 m of carbonate-clast conglomerate and breccia capped by >2000 m of molasse: red volcaniclastic sandstone, conglomerate, and shale, containing samples with detrital zircon peaks of 123, 109, 106, 99, 97, and 94 Ma (Martini et al. 2010; Martini and Ferrari 2011; Centeno-Garcia et al. 2011), which represent both pre-collisional arc and post-collisional plutons of the La Posta suite.

Although dismembered and translated during younger tectonic events, the rocks and their temporal relations as found in the southwestern North American sector (Fig. 28) are readily recognized and correlated northward along the entire Cordillera from southern Mexico to Alaska and constitute the Peninsular Ranges orogeny (Hildebrand and Whalen 2021*a*, 2021*b*). The continent-long parallelism between the structural axis of the orogen, coupled with the post-collisional basin to the west of the collision zone, suggests to us that rocks within the mid-Cretaceous succession of the Western Interior Basin were not deposited in a retro-arc foreland basin developed above an easterly dipping oceanic slab (Dickinson 1970), but instead may have formed as a collisional foredeep related to westerly subduction and collision of the Peninsular Ranges composite terrane with North America during the ~100 Ma Peninsular Ranges orogeny (Fig. 28). With the timing of the collision to the west reasonably well-constrained, along with numerous dated bentonite beds and detailed studies of detrital zircons from many stratigraphic units within the Western Interior basin, it seemed timely to ask: How does the stratigraphy, sedimentology, and volcanism of the basin fit with the mid-Cretaceous geology of the Peninsular Ranges orogeny?

Discussion

During our study of the Cenomanian–Turonian stratigraphy of the Western Interior Basin, we recognized three distinct sectors of the basin: central, northern, and southern. The northern sector is represented by the succession on the Peel Plateau of Boreal Canada; the southern sector extends from southern Mexico to southern Arizona; and the central sector lies between the two.

In northern Canada and Arizona–Mexico, we interpret foredeep sediments of the Peninsular Ranges orogeny to sit disconformably atop Cretaceous passive margin sedimentary successions, which themselves sit unconformably upon cratonic North America basement (Hildebrand and Whalen 2021*a*, 2021*b*). In both regions, relations are straightforward: a west-facing marine platform was uplifted, eroded, and then promptly submerged, creating a succession that we interpret to reflect the migration of a forebulge (see Crampton and Allen 1995). In Mexico and southern Arizona, the platform was capped by Albian carbonate as it was located in a warm, southerly climate, whereas in the northern Canadian Peel Plateau, the margin was muddy, as befits its northern Boreal connection and location during the Cenomanian–Turonian (Kauffman and Caldwell 1993; Kent and Irving 2010).

In the successions of southern Mexico, the top of the carbonate platform was disconformably overlain by 2 m of channelized calcarenites and calcareous turbidites, themselves overlain by a condensed horizon containing an abundance of closely packed Late Albian ammonites and rudist fragments covered by an Mn-rich, dark-red to black, shaley coating (Monod et al. 2000), likely formed in an anoxic environment (Fig. 24). The carbonates were covered by less than a meter of pelagic mudstone then buried by Cenomanian Mexcala flysch, which contains 97–95 Ma detrital zircons derived from post-collisional La Posta plutons (Lawton et al. 2015) emplaced into the orogenic hinterland farther west. Although Mendoza and Suástegui (2000) considered that the carbonate succession represents an upper-plate patch reef, it constitutes part of an extensive thrust panel of upper Aptian–Albian platformal carbonate, so we interpreted (Hildebrand and Whalen 2021*a*) the overall sedimentary succession above the disconformity, which consists of (1) shallow- to deep-water carbonate deposition on the margin; (2) hemipelagic mud; and (3) deep water siliciclastic turbidites, to represent superposition of lateral facies changes as the migrating margin was pulled downwards into the trench. Overall, it constitutes a typical lower-plate foreland basin sequence (Sinclair 1997).

On the Peel Plateau of Boreal Canada (Fig. 5), a west-facing mid- to upper-Albian marine siliciclastic margin (Fig. 21) was uplifted and sufficiently exposed to develop a paleosol complex comprising pisoidal ironstones containing sparse wood fragments, then submerged and buried initially by black carbonaceous shale with thin, but rare, coal beds, overlain by a 10 cm thick condensed section of radioactive, dark-black mudrock containing fish teeth, bone and organic material, but no benthic foraminifera, passing upwards into the Lower Cenomanian Fish Scales marker, also devoid of foraminifera (Thomson et al. 2011). Overlying Cenomanian–Turonian oro-

Fig. 28. Similarities along strike within the Peninsular Ranges orogen, from Mexico to Alaska, of major sedimentological, magmatic, and tectonic packages arranged from west to east, along with their age constraints, where known. Note the coeval nature of most units along strike, which are comparable to the along-strike stratigraphic continuity found in units of the Western Interior Basin over the same N-S distance. Modified from Hildebrand and Whalen (2021*a*).

West → East

North ↑ South

Location	Western retroarc debris 99-83 Ma	Arc terrane 130-100 Ma	Syn-arc basin 140-100 Ma	Age of Collision	Post-collision plutonism 99-84 Ma
Mainland Alaska	McHugh complex	133-98 Ma Chisana	Kahiltna	103-97 Ma	94-88 Ma Tok-Tetlin Gardiner Crk. ?
Insular Alaska	Queen Charlotte Group	Muir-Chichagof suite & Gravina	Gravina	105-95 Ma	95-90 Ma Moth Bay & many others
Coast Plutonic belt, BC	Nainaimo Group	Gambier Group Firvale & Desire plutonic suites	Gambier Group	101-97 Ma	Ecstall & many others 99-85 Ma
Cascades	Cascade River Skagit gneiss ?	Chiwaukum schist	Nooksack	108-96 Ma	Many plutons 96-89 Ma
Idaho & Montana	Ochoco Basin (Oregon)	Little Goose Hazard Creek 120-108 Ma	unknown	100-91 Ma	Atlanta lobe Payette-Rat Cr. 98-84 Ma
Nevada/UT	unknown	King Lear 125-123 Ma	Newark Canyon ?	101-96 Ma	Many plutons 98-84 Ma
Sierra Nevada	Eastern Great Valley Group	western arc terrane & Cinko Lake arc	Cinko Lake trough	103-98 Ma	Sierran Crest 99-84 Ma
Mojave Desert	unknown	Delfonte volcanics 100.5±2 Ma	not recognized	100.5-98 Ma	Teutonia & others 98-85 Ma
Peninsular Ranges Mexico & USA	Valle Gp	128-100 Ma Santiago Peak & Alisitos	Bisbee-Arperos trough	103-98 Ma	La Posta 99-84 Ma

genic deposits of the Trevor Formation, which were derived from the west and contain abundant detrital zircons between 100 and 90 Ma (Hadlari et al. 2014), presumably derived from 99 to 93 Ma post-deformational plutons to the southwest in the Selwyn basin (Figs. 5 and 22). This sector represents a siliciclastic, more northerly version of a typical foreland basin (Sinclair 1997).

Between the Arizona–Mexican and northern Canadian sectors, the western part of North America was earlier affected by the Sevier orogeny (Fig. 29), which involved 124–105 Ma thrusting and development of a foredeep trough (Lawton et al. 2010; Yonkee and Weil 2015; DeCelles and Coogan 2006), so the overall stratigraphic succession is different there. Nevertheless, the relations within the sector are similar to those both north and south in that pre-existing Albian sedimentary rocks were uplifted and exposed just prior to 100 Ma, subaerially exposed, after which they were incised by fluvial systems; then rapidly buried by neritic successions, commonly deposited in paleovalleys eroded in mid-Cretaceous sandstone. These successions fine upwards into mudstone and a condensed, anoxic section containing abundant faunal debris, overlain the length of the basin by Cenomanian

Fig. 29. Cartoon view of western North America just before ~124 Ma collision illustrating arrival of the Sevier upper plate. Its collision with North America was followed at ~100 Ma by the arrival of another ribbon, this one carrying the Santiago Peak–Alisitos arc, during the Peninsular Ranges orogeny.

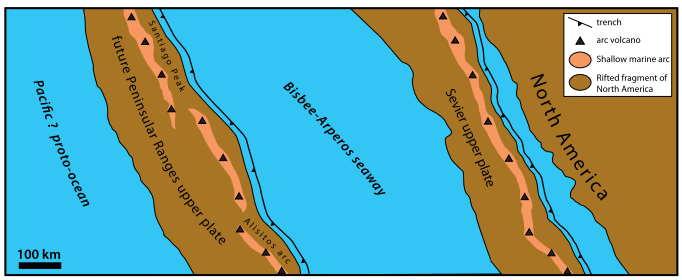

clastic wedges, such as the Dunvegan, Frontier, and Mexcala, which contain 97–93 Ma detrital zircons (Figs. 7, 20, 21, and 25).

In all three sectors, the post-unconformity, neritic succession fines upward into mudstones that, in turn, pass upwards into a condensed anoxic section termed either the Fish Scales Formation or the Mowry Shale, each of which contains abundant fish scales, teeth, and disarticulated bones. In most sectors, the condensed section is accompanied by abundant bentonite beds and an endemic gastroplitine ammonite fauna, which collectively provide excellent age control. Nearly everywhere in the basin atop the condensed, bentonite-rich zone, there are easterly prograding clastic wedges, such as the Trevor, Dunvegan, Frontier, Cintura, and Mexcala units, each of which contains abundant detrital zircons with ages between 99 and 90 Ma, indicating that the wedges represent post-collisional molasse.

The overall sequence sitting atop a regional, eastward-migrating disconformity of (1) shallow-water sediments fining progressively upwards into (2) condensed hemipelagite, overlain by (3) orogenic debris derived from the rising hinterland is typical of the sedimentation in active collisional foredeeps (Crampton and Allen 1995: Sinclair 1997; DeCelles 2012; Sabbatino et al. 2020, 2021). Although the overall mid-Cretaceous stratigraphy is convincing and fits the timing known from the Peninsular Ranges orogeny (Hildebrand and Whalen 2021*a*, 2021*b*), the following additional points support our stratigraphic argument that the overall Cenomanian–Turonian succession within the basin better fits a collisional foredeep setting than the more widely accepted retro-arc basin scenario.

First, sedimentation within the basin was remarkably consistent, both across and along its length, as well as temporally, which collectively requires a plate-scale explanation, not one related to displacement, loading, and flexure on individual thrust faults. This problem is especially acute because researchers have demonstrated that thrust timing, shortening, and hence loading, in the fold-thrust belt varied along strike (Price and Sears 2000; DeCelles and Coogan 2006).

Second, the width of the basin is simply too large, some 1500 km, to be explained by lithospheric flexure generated by a thrust load to the west or to rise of sea level (Beaumont et al. 1993). This led some workers to speculate that a slab of cold oceanic lithosphere dipped eastward beneath the craton, which, along with sea level rise, pulled the surface downward to create a basin that could be as wide as 1500 km (Mitrovica et al. 1989). How a shallowly dipping slab can exist when cratonic lithosphere is thick remains unresolved. Also, arc magmatism appears to have ceased at 100 Ma (Hildebrand and Whalen 2021*a*, 2021*b*) coincident with drowning of the North American passive margin and its burial by orogenic clastics.

The eastward migration of the peripheral bulge from near the thrust front to the Dakotas, some 650 km to the east, is too broad to be caused by loading of thrust faults in the fold-thrust belt, especially given that sedimentation in the basin was sparse at that time. Following passage of the bulge, this area of the basin was closer to the thrust belt, yet received only limited sedimentary input, which is inconsistent with thickening, loading, exhumation, and emergence in the thrust belt to the west.

Where the westerly derived clastic wedges have been studied in great detail, such as the distal regions of the Dunvegan clastic wedge, individual prodeltaic clinoforms are documented to have prograded across the anoxic Fish Scales unit for up to 800 km, demonstrating the essentially featureless, low gradient, and isochronous nature of the Fish Scales–Mowry horizon (Bhattacharya 1994; Plint et al. 2009). A similar result was found by Byers and Larson (1979), who used bentonite datum planes to document that the Frontier–Mowry contact was isochronous and dipped very gently eastward over the width of the basin. It is difficult to reconcile these observations with a retro-arc setting where the basin was caused by a thick thrust stack located to the west, as in that case the basinal floor should dip westward towards the load, not eastward as observed. This observation is better understood to represent the rebound of the collisional hinterland once slab break-off freed the cratonic lip from the oceanic slab pulling it down.

Where not extremely altered, trace element geochemistry of the Upper Cretaceous bentonites suggests that they are not arc magmas, but instead, post-collisional slab break-off magmas (Fig. 14). Compositions of volcanic rocks of the Crowsnest Formation also support a break-off origin, as early post-collisional magmatism is commonly alkaline.

All these relations are better explained by attempted westward subduction of the North American craton, which led to the entire western edge of the craton dipping to the west as it was pulled into the trench. After the forebulge on the margin was uplifted and subsided beneath the wave base, the basin floor dipped westward, but very gently. By deposition of the Fish Scales unit, the floor of the basin was reversed again to dip ever so slightly eastward, the opposite direction from that expected for loading by thrust sheets to the west. It appears that exhumation in the hinterland was not fully underway until deposition of the Frontier and related clastic wedges.

If correct, then the Mowry–Fish Scales succession records the syn- to early post-collisional time interval, and because it is isochronous and occurs both across and over the length of the entire basin, it is unlikely that the basin was the product of dynamic topography, other than some initial subsidence related to the vertical sinking of the detached slab. It is more likely that, because the basin sits almost entirely east of the North American cratonic hingeline, the effective elastic thickness of the North American craton, which is a measure of its flexural rigidity (Turcotte 1979; Flück et al. 2003), was likely in excess of 100 km, perhaps even 150–200 km (Tesauro et al. 2015), consistent with other Precambrian cratons (Zuber et al. 1989; Hansen et al. 2009). This is because the thermal regime primarily controls the flexural rigidity, except perhaps close to the hingeline, where there may have been some local ductile necking during creation of the older passive margin. Other potential modifications, such as heating from extension and magmatism within the United States and Mexican Basin and Range, as well as those of the Rio Grande Rift, are all much younger than the age of the ~100 Ma Peninsular Ranges orogeny (Fig. 30), so it is reasonable to infer a typical cratonic thickness for the area. If elastic thickness is ~125 km, typical for Precambrian cratonic lithosphere, Flück et al. (2003) calculated that the flexural wavelength would be nearly 1100 km and would increase propor-

Fig. 30. Effective elastic thickness (*Te*) of the lithosphere in kilometers for two different models of North America modified from Tesauro et al. (2015). We suggest that during the Cretaceous the region east of the US hingeline had a thicker, more typical cratonic *Te* than at present. The thickness was likely much diminished during the Cenozoic by extension and magmatism.

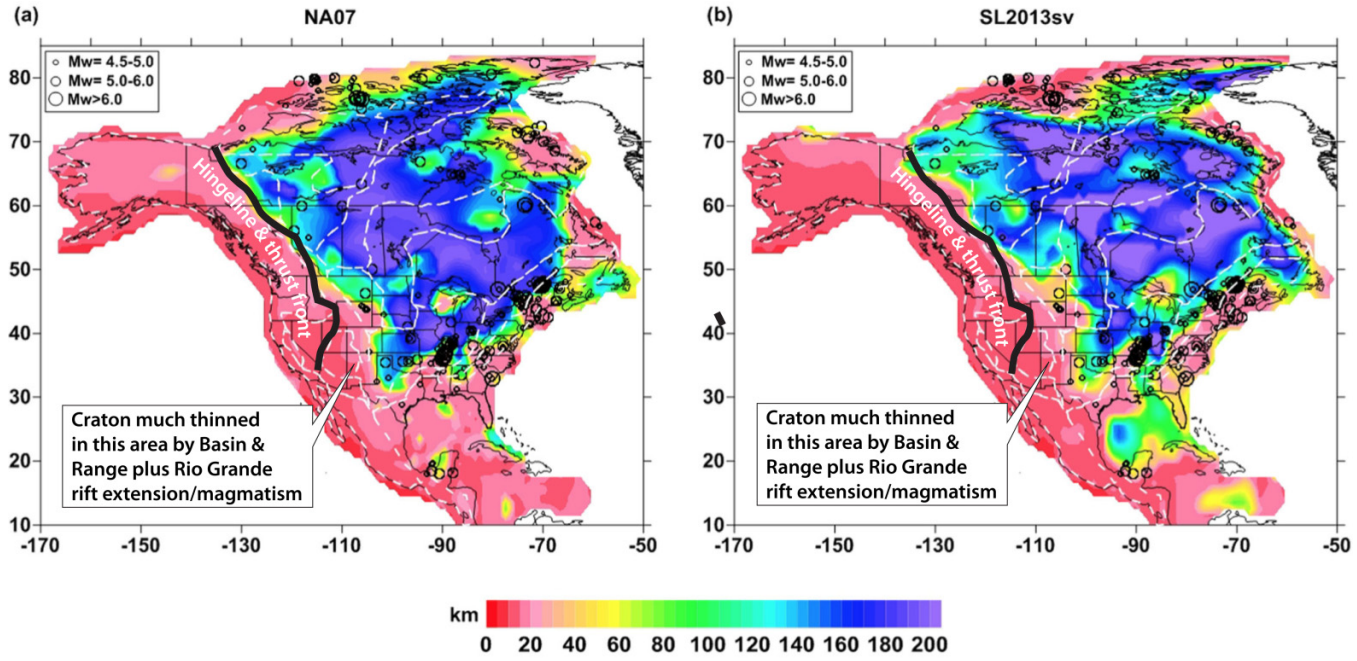

tionally with a thicker elastic thickness. This calculation is consistent with the distance from the thrust belt to the Black Hills, which is about 600 km, approximately half the flexural wavelength. Therefore, we favor flexural bending of the cratonic lithosphere as it entered the trench, augmented by local isostatic subsidence along the western margin caused by the bulk of the thrust stack and related post-collisional sediments sitting on the lithosphere.

The downward flexure of the cratonic or oceanic lithosphere into a trench is accompanied by the generation and migration of an adjacent peripheral bulge, or lithospheric upwarp, located seaward of the trench (Section 3–17: Turcotte and Schubert 1982). The uplift causes stratigraphic condensation and commonly a forebulge unconformity. Within the Western Interior Basin, where temporal constraints are documented, such as the Wyoming–Dakota transect of the basin (Fig. 4), exposure and incision of the sedimentary succession due to relative sea level fall occurred earlier to the west in Wyoming than in South Dakota, which is the reverse of that expected for a basin that shoaled to the east. Our preferred explanation is that the eastward migration and passage of the peripheral bulge progressively elevated a sector of the basin above sea level (such that it could be eroded), only for it to rapidly subside below sea level rather promptly after passage (Crampton and Allen 1995). The sector that rode up and over the bulge then lay on the outer slope to the trench, which is, in many places, a region characterized by low sedimentation rates of mostly pelagic sediment (see Harris 2011; Heirtzler 1974 for an example). Within the US sector of the Western Interior Basin, the emergent Muddy and Newcastle sandstones likely relate to the passage of the peripheral bulge (Fig. 31), whereas the overlying and partly coeval Shell Creek Shale consists of shale, fine sandstone, siltstone, and bentonites deposited on the outer slope to the trench, located some distance to the west. As the flexural bulge migrated eastward into the craton, its wavelength likely increased proportionately with a thicker elastic thickness as it encountered older, thicker, and more rigid cratonic lithosphere (Flück et al. 2003), causing it to progressively widen and decrease in amplitude, dampening its topographic and stratigraphic expression and rendering it more difficult to recognize.

Within the shaley units that sit atop the neritic-facies rocks deposited on the western flank of the migrating flexural bulge, the presence of bentonites might reflect ash erupted from an arc approaching from the west, but in the case of the upper Shell Creek and the Mowry shales, the bentonites have compositions more consistent with post-collisional slab failure magmas than arc magmas, as do volcanic rocks of the Crowsnest Formation in Canada (Fig. 14). The volcanics and associated sills are the only known magmatic rocks other than bentonites within the predominantly sedimentary succession, and so without an extensive data set of ages along strike we cannot tell if break-off was diachronous as we expect, or merely leaked magmas locally. In either case, the age of the unit relative to the basinal bentonites could be documented more precisely by obtaining high-quality $^{40}Ar/^{39}Ar$ sanidine ages from the volcanic rocks.

Within the Canadian sector of the Western Interior Basin, reliable radiometric ages from bentonites are scarce (Fig. 4). However, the lithological similarities between the Canadian and US sectors and their successions attest to similar origins.

Fig. 31. Idealized eastward migrating peripheral bulges in Canada and the United States.

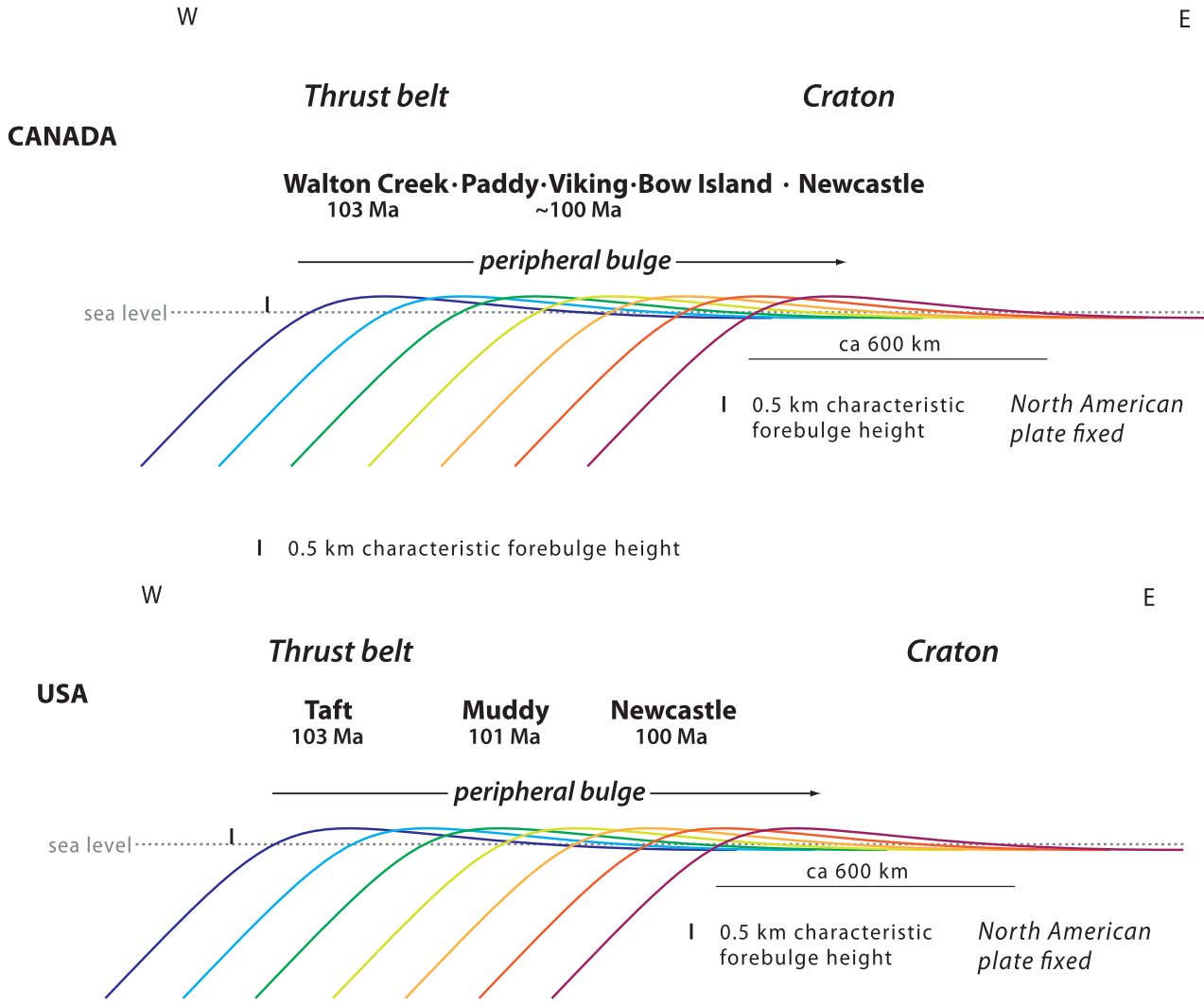

For example, basinal rock packages within the Fort St. John and Colorado Groups (Fig. 31), such as the Walton Creek, Paddy, Viking, and Bow Island successions, all exhibit erosion, soil horizons, fluvial incision, and deposition of neritic facies prior to re-submergence and deposition of overlying shales, including the Fish Scales unit, prior to being overwhelmed by westerly derived clastic wedges, such as the Dunvegan or Frontier with their abundant post-100 Ma detrital zircons.

Isopachs of the lower part of the Shaftesbury Formation, that is, the post Viking–Bow Island and pre-Fish Scales shale unit (Fig. 5), yield insight into potential processes. First, note the approximately logarithmic westward slope over the western 500 km of isopachs, which range from over 500 m in the west to about 40 m in the east. As the Fish Scales unit is essentially isochronous, the thickness of the basal shale under it should reflect the slope of the surface beneath it and provide a minimum for the available accommodation space. The logarithmic nature of the thickness variations suggests the bending, and likely rollback of the subjacent basement, as the oceanic lithosphere steepened and was pulled downward into the trench to the west. It is difficult to relate the bending to isostatic load as there was no commensurate deposit of coarse clastic debris that might signify the emergence of a thrust stack to the west. Instead, the area was exposed subaerially during the immediately underlying Viking–Bow River interval, but rapidly subsided, a scenario consistent with the eastward migration of a peripheral bulge through the area (see also Roca et al. 2008; Fig. 28). The migration could be tested and refined by systematically dating bentonites within the Viking–Bow River interval of the basin by $^{40}Ar/^{39}Ar$ to ascertain if the outer swell migrated eastward at about the same rate as that in the United States. (See Sabbatino et al. 2020, 2021, for a well-dated example from the Apennine collisional orogen.) Nevertheless, on the basis of the foregoing, we consider that the foredeep to the Peninsular Ranges orogeny displays the effects of the passage of the peripheral bulge along its entire length from southern Mexico to northern Canada and affected both pre-existing carbonate and clastic margins as well as older orogenic deposits related to the Sevier orogeny in the central sector of North America.

In our collisional model, slab break-off must have occurred rather widely by upper Shell Creek time as the number of bentonites increases up section into the Mowry, where they dominate the succession. The starved nature of the Mowry–Fish Scales may represent the time when break-off was underway, but that exhumation of the hinterland had not started, or at least was still insufficiently emergent to flood the basin with sediment.

Models designed to observe surface deformation resulting from slab break-off indicate that after break-off, the detached part of the slab sinks vertically into the mantle, which creates flow within the viscous mantle that pulls the overlying lithosphere downward (Buiter et al. 2002; Chatelain et al. 1992). As the lithospheric slab sinks farther, the suction and downward pull are reduced. Presumably, this would delay surface uplift and exhumation such that sediment flux into the basin would be dramatically retarded and reduced. This process could create the somewhat short-lived sediment-starved sequence with a high flux of ash and an anoxic hypolimnion as observed for the Fish Scales–Mowry succession. This is consistent with the model of Plint et al. (2009), who argued that the basin-wide Fish Scales Formation was a downlap surface and represents a sedimentological hiatus of up to 2 Myr. It was during this hiatus that the slope of the basin was reversed from west dipping to east dipping, such that eventually the first prodeltaic muds of the Dunvegan and Frontier clastic wedges began to prograde eastward over the Mowry and Fish Scale units on the shallowly dipping basin floor.

Although we are attracted to the concept of additional subsidence due to slab break-off, it might only represent one component, or may not even be necessary to explain the lack of coarse detritus. A modern example of an accretionary prism in front of a starved and underfilled oceanic trough, but one in which the slab apparently has not failed yet, occurs in the Timor Trough, the 3 km deep trench south of the island of Timor, which represents an uplifted portion of the accretionary prism between Australia and the Banda arc. There, as noted by Harris (2011), the island of Timor is quite dry, with only a 4-month rainy season which provides the bulk of the 1.3 m annual precipitation. Due to the long dry period, and the consequent lack of vegetation, the amount of clastic sediment transported from the mountains to the coast as cobbly to pebbly debris by braided streams is huge: about 60% of the annual discharge of the Ganges/Brahmaputra River system of the Indian subcontinent (Cecil et al. 2003). As documented by DSDP 262, none of the coarse sediment reaches the adjacent Timor trough to the south, where only pelagic nanooze was found to overlie the Australian carbonate platform (Heirtzler 1974). Apparently, the coarse debris is trapped in submarine piggy-back thrust basins on Timor and unable to escape southward into the trench (Harris, personal communication, 2021). As southern North America was located near 30° N latitude during the mid-Cretaceous (Kent and Irving 2010), its western margin would have been relatively dry, perhaps with seasonal rainfall not very different than today. Thus, in the case of western North America, the combination of topography, seasonal climate, lack of vegetation, coupled with break-off-induced subsidence might have led to an especially starved basin.

One of the more interesting outcomes from our study of the Peninsular Ranges orogeny is the recognition that a new terrestrial faunal assemblage with Asian affinities (tyrannosaurids, hadrosaurids, pachycephalosaurs, snakes, anocid turtles, and marsupials) arrived in North America at about 100 Ma, the time of accretion of the Peninsular Ranges composite terrane, which suggests that the two events might be related. Cifelli et al. (1997) indicate that the new fauna are the oldest dinosaur fauna with representatives of each family characteristic of the remainder of the Late Cretaceous in North America. The bulk of the fauna was initially discovered in the Mussentuchit Member of the Cedar Mountain Formation of central Utah, where the unit was deposited along the terrestrial southern margin of the Mowry Sea (Fig. 3), which allowed newly arrived fauna to migrate into eastern North America. Similar faunal assemblages were found west of the seaway in the Blackleaf Formation of Montana and the Willow Tank Formation of southern Nevada as discussed previously. Some paleontologists (Cifelli et al. 1997; Kirkland et al. 1997, 1999) suggested that the introduction of the new taxa wiped out the previous inhabitants to dominate North America for the remainder of the Cretaceous. As the Canada Basin was still open at 100 Ma (Grantz et al. 2011), it is unlikely that there was a direct Asian–North American connection as sometimes hypothesized (Kirkland and Madsen 2007; Samson 2009); instead, it is more likely that the fauna arrived on the Peninsular Ranges composite terrane and spread throughout eastern North America following the collision. Overall, the paleontological findings support our collisional model for the 100 Ma Peninsular Ranges orogeny.

Summary

1. The tripartite succession of mid-Cretaceous stratigraphic units within the Western Interior Basin lies disconformably upon older rocks and is readily interpreted in terms of a collisional foredeep between the North American craton and the Peninsular Ranges composite terrane (Fig. 32). Upper Albian sediments were derived from the east, whereas Cenomanian–Turonian clastic wedges were westerly derived.
2. The earliest sign of collision was the eastward migration of the peripheral bulge from west to east along the western edge of cratonic North America (T1 and T2: Fig. 32) just before it was pulled down into the trench. Rocks in the western United States related to the uplift, erosion, and re-submergence of the margin during migration of the bulge were the Muddy and Newcastle sandstones, which range in age from 101 to 99.5 Ma. Equivalent strata in the Canadian sector include the Bruin Creek, Bow Island, Viking, Peace River, and Sikanni successions, but radiometric dating is scarce.
3. Thin, but westward-thickening, units of dark shale, such as the Shell Creek Shale in the United States and the Sully, Westgate, and Shaftesbury in Canada, were deposited on the starved outer slope of the trench between about 100 and 99 Ma (T3: Fig. 32). Bentonite beds are more common up section.

Fig. 32. Our model for development of the mid-Cretaceous Western Interior Basin as a collisional foredeep.

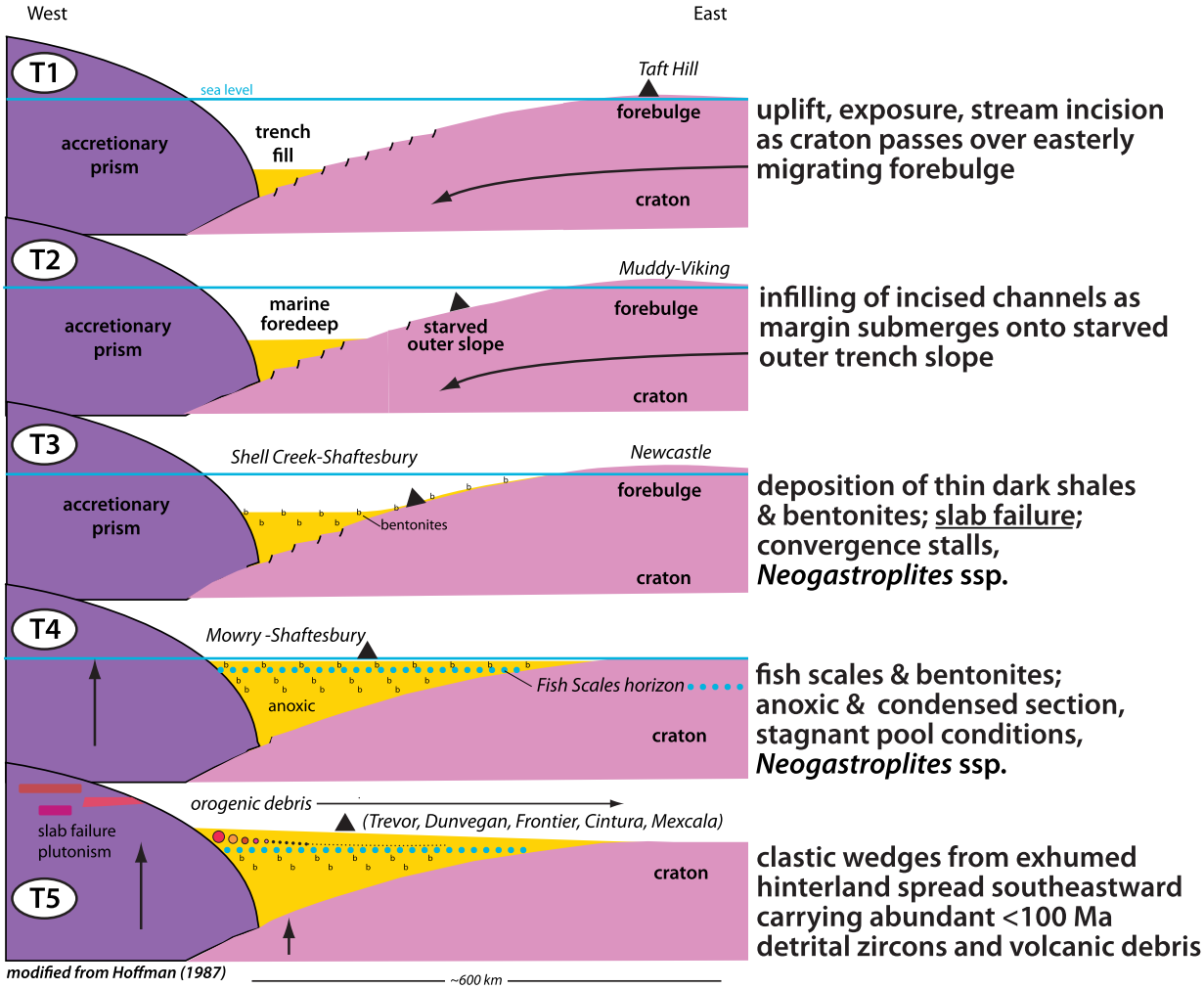

4. The dark shales are overlain by a condensed and anoxic, black-shale section, rich in fish debris and numerous beds of bentonite and porcellanite, known as the Mowry Shale in the United States and the Fish Scales Formation in Canada (T4: Fig. 32). In the United States, these rocks were deposited between about 99 and 97.5 Ma. The Shell Creek–Mowry–Fish Scales units contain five species of endemic ammonites (*Neogastroplites* ssp.), which reflect its restricted nature.
5. Bentonites deposited in marine environments are commonly altered, and their origin is difficult to decipher. However by using relatively immobile high-field strength and rare earth elements, those effects are minimized. We found that the intercalated bentonites have trace element compositions more typical of the failed slab, not arc, magmatism. This suggests that slab failure took place just before, or during, deposition of the Mowry–Fish Scales units, consistent with slightly older ages for the alkaline Crowsnest volcanics in the southern Canadian foothills.
6. Starting at about 97.5 Ma, the Mowry–Fish Scales unit was overlain by westerly derived, and easterly to southeasterly prograding, clastic wedges (T5: Fig. 32), which contained igneous clasts and abundant detrital zircons younger than 100 Ma derived from post-collisional magmatic rocks in the hinterland. These delta-front wedges included, from north to south, the Trevor, Dunvegan, Frontier, Cintura–Mojado, and Mexcala successions (Fig. 33).
7. Single delta-face clinoforms 10 m thick at the base of the clastic wedges can be traced for 800 km sitting directly on the Fish Scales unit, which, along with the evidence outlined above, indicates that the Mowry–Fish Scales represents an isochronous unit deposited on a very gently dipping eastward slope and that its upper surface might represent ~2 Myr of non-deposition. This precludes extensive thickening, uplift, and subaerial emergence of the thrust stack to the west during deposition of the Mowry–Fish Scales succession.
8. The Mowry–Fish Scales succession records the syn- to post-collisional time interval and represents the reversal of slope from westerly to easterly within the basin.
9. The presence of the Mowry–Fish Scales units over the entire width and length of the basin rules out generation by dynamic topography caused by a gently eastward-dipping slab, as there was no broadening of the basin

Fig. 33. Approximate locations of five deltas that transported material from the hinterland of the Peninsular Ranges orogen into the trough on the basis of stratigraphy and detrital zircon suites during the Middle to Late Cenomanian.

at that time. Instead, it is more likely that, because the basin sat almost entirely east of the hingeline, it was probably built on Precambrian cratonic lithosphere with an effective elastic thickness (*Te*) of more than 100 km (and perhaps even 150 km), the basin had a long wavelength and so was broad and shallow, with a narrow westernmost isostatic sector loaded by thrusts and coarse sediment.

10. Recognizing that the Cenomanian to Turonian sedimentary succession within the Western Interior Basin can be interpreted as a collisional foredeep, developed during the Peninsular Ranges orogeny, is consistent with the presence of a westerly facing passive margin setting atop North America, both in the south, where the platform was capped by a carbonate bank, and farther north in Canada, where it was a clastic margin.
11. The seemingly pene-contemporaneous break-off of the lower North American plate from northernmost Canada to southern Mexico suggests that the plate boundaries were not irregular with large and identifiable promontories, but fundamentally linear. Within the limits of the geochronology, which for the North American Cordillera are at reconnaissance level compared to the Alpine and Apennine belts, there was no obvious lateral migration of subsidence and uplift as seen in collision zones where lateral migration of slab detachment has been recognized, such as the Apennines (van der Meulen et al. 1998, 1999). Thus, it appears that break-off may have occurred rapidly over thousands of kilometers. More detailed studies, especially dating and improving the correlation of regionally abundant bentonite beds may refine this concept considerably.
12. The accretion of the Peninsular Ranges composite terrane at ~100 Ma was more likely to have led to arrival of vertebrates from Asia and their subsequent dispersal throughout North America, than their arrival by an unrecognized polar route.

Acknowledgements

This work relies heavily on the exquisite geochronology of Brad Singer, as well as detailed work by countless sedimentologists and petroleum geologists over many decades. Although our knowledge of the Cordillera is only at a reconnaissance level by Alpine standards, we are nevertheless amazed that we could discover a previously unrecognized Cretaceous orogenic belt and hope that our success, or lack of it, depending on one's viewpoint, will suggest new avenues to explore and ideas to test.

We received insightful and supportive comments on early drafts of the manuscript by Bob Hatcher, Paul Hoffman, and Paul Link. Late night discussions on Cordilleran tectonics throughout the pandemic with Basil Tikoff were always interesting and informative. Suggestions during discussion with Josh Bonde helped expand our understanding of the 100 Ma faunal introduction. Reviews by Tim Lawton and an anonymous reviewer were very useful, as were detailed editorial comments by Brendan Murphy. As usual, this study relied entirely on personal funding.

Article information

History dates

Received: 10 August 2022
Accepted: 19 September 2022
Accepted manuscript online: 27 September 2022
Version of record online: 23 December 2022

Copyright

Data availability

All data are in cited publications and associated online files.

Author information

Author ORCIDs

Robert S. Hildebrand https://orcid.org/0000-0001-5870-1342

Author contributions

Conceptualization: RSH
Formal analysis: RSH, JBW
Investigation: RSH, JPB
Methodology: RSH, JPB, JBW
Project administration: RSH
Writing – original draft: RSH
Writing – review & editing: RSH, JPB, JBW
Validation: JPB
Data curation, Resources: JBW

Competing interests

The authors declare there are no competing interests

References

Adair, R., and Burwash, R.A. 1996. Evidence for pyroclastic emplacement of the Crowsnest Formation, Canadian Journal of Earth Sciences, **33**: 715–728. doi:10.1139/e96-055.

Adair, R.N. 1986. The pyroclastic rocks of the Crowsnest Formation, Alberta. M.S. thesis, University of Alberta, Edmonton, AB, 196p.

Aitken, J.D. 1989. The Sauk Sequence — Cambrian to Lower Ordovician miogeocline and platform Western Canada Sedimentary Basin: a case history. *Edited by* B.D. Ricketts Canadian Society of Petroleum Geologists, Calgary. pp. 105–119.

Anderson, A.D., and Kowallis, B.J. 2005. Storm deposited fish debris in the Cretaceous Mowry Shale near Vernal, Utah. *In* Uinta Mountain Geology. *Edited by* C.M. Dehler, J.L. Pederson, D.A. Sprinkel and B.J. Kowallis Utah Geological Association Publication 33, pp. 125–130.

Archibald, D.B., and Murphy, J.B. 2021. A slab failure origin for the Donegal composite batholith, Ireland, as indicated by trace-element geochemistry, *In* Pannotia to Pangaea: Neoproterozoic and Paleozoic orogenic cycles in the circum-Atlantic region. *Edited by* J.B. Murphy, R.A. Strachan and C. Quesada. Geological Society of London, Special Publication 503, pp. 347–370. doi:10.1144/SP503.

Archibald, D.B., Murphy, J.B., Fowler, M., Strachan, R.A., and Hildebrand, R.S. 2022. Testing petrogenetic models for contemporaneous mafic and felsic-intermediate magmatism within the 'Newer Granite' suite of the Scottish and Irish Caledonides. *In* New developments in the Appalachian-Caledonian-Variscan orogen. *Edited by* Y.D. Kuiper, J.B. Murphy, R.D. Nance, R.A. Strachan and M.D. Thompson. Geological Society of America Special Paper 554. The Geological Society of America, Boulder, CO. pp. 375–400. doi:10.1130/2021.2554(15).

Armstrong, F.C., and Oriel, S.S. 1965. Tectonic development of Idaho-Wyoming thrust belt. American Association of Petroleum Geologists Bulletin, **49**: 1847–1866.

Armstrong, R.L. 1968. Sevier orogenic belt in Nevada and Utah. Geological Society of America Bulletin, **79:** 429–458. doi:10.1130/0016-7606(1968)79[429:SOBINA]2.0.CO;2.

Arnott, R.W.C. 1988. Regressive-transgressive couplets of the Bootlegger Sandstone (Cretaceous), north-central Montana – the possible influence of the Sweetgrass Arch, sequences, stratigraphy, sedimentology: surface and subsurface. *Edited by* D.P. James and D.A. Leckie. Canadian Society of Petroleum Geologists Memoir 15. Canadian Society of Petroleum Geologists, Calgary, AB. pp. 255–260.

Avrahami, H.M., Gates, T.A., Heckert, A.B., Makovicky, P.J., and Zanno, L.E. 2018. A new microvertebrate assemblage from the Mussentuchit Member, Cedar Mountain Formation: insights into the paleobiodiversity and paleobiogeography of early Late Cretaceous ecosystems in western North America. PeerJ, **6**: e5883. doi:10.7717/peerj.5883.

Axen, G.J. 1987. The keystone and red spring thrust faults in the La Madre Mountain area, eastern Spring Mountains, Nevada. *In* Centennial field guide. *Edited by* M.L. Hill. Geological Society of America, North American Geology, Vol. 1. pp. 57–60.

Bally, A.W., Gordy, P.L., and Stewart, G.A. 1966. Structure, seismic data, and orogenic evolution of southern Canadian Rocky Mountains. Bulletin of Canadian Petroleum Geology, **14:** 337–381.

Barclay, R.S., Rioux, M., Meyer, L.B., Bowring, S.A., Johnson, K.R., and Miller, I.M. 2015. High precision U–Pb zircon geochronology for Cenomanian Dakota Formation floras in Utah. Cretaceous Research, **52**: 213–237. doi:10.1016/j.cretres.2014.08.006.

Barker, I., Moser, D., Kamo, S., and Plint, A.G. 2011. High-precision TIMS U-Pb zircon dating of two transcontinental bentonites: Cenomanian stage, western Canada foreland basin. Canadian Journal of Earth Sciences, **48**: 543–556. doi:10.1139/E10-042.

Beaumont, C. 1981. Foreland basins. Geophysical Journal International, **65**: 291–329. doi:10.1111/j.1365-246X.1981.tb02715.x.

Beaumont, C., Quinlan, G., and Stockmal, G.S. 1993. The evolution of the Western Interior Basin: causes, consequences and unsolved problems. *In* Evolution of the Western Interior Basin. *Edited by* W.G. Caldwell and E.G. Kauffman. Geological Association of Canada, Special Paper 39. Geological Association of Canada, St. John's, NL. pp. 97–117.

Beckerman, G.M., Robinson, J.P., and Anderson, J.L. 1982. The Teutonia batholith: a large intrusive complex of Jurassic and Cretaceous age in the eastern Mojave Desert, California. *In* Mesozoic–Cenozoic tectonic evolution of the Colorado River region, California, Arizona, and Nevada. *Edited by* E.G. Frost and D.L. Martin. Cordilleran Publishers, San Diego, CA. pp. 205–220.

Benyon, C., Leier, A., Leckie, D.A., Webb, A., Hubbard, S.M., and Gehrels, G. 2014. Provenance of the Cretaceous Athabasca Oil Sands, Canada: implications for continental-scale sediment transport. Journal of Sedimentary Research, **84**: 136–143, doi:10.2110/jsr.2014.16.

Bhattacharya, J.P. 1989. Allostratigraphy and river- and wave-dominated depositional systems of the Upper Cretaceous Dunvegan Formation, Alberta. Unpublished Ph.D. dissertation, McMaster University, Hamilton, ON, 588p.

Bhattacharya, J.P. 1994. Chapter 22 – Cretaceous Dunvegan Formation of the western Canada sedimentary basin. *In* Geological Atlas of the Western Canadian sedimentary basin. *Compiled by* G.D. Mossop and I. Shetson. Canadian Society of Petroleum Geologists and Alberta Research Council, Calgary, AB. pp. 365–373.

Bhattacharya, J.P., and Walker, R.G. 1991a. Allostratigraphic subdivisions of the Upper Cretaceous Dunvegan, Shaftesbury, and Kaskapau formations in the northwestern Alberta subsurface. Bulletin of Canadian Petroleum Geology, **39**: 145–164.

Bhattacharya, J.P., and Walker, R.G. 1991b. River- and wave-dominated depositional systems of the Upper Cretaceous Dunvegan Formation, northwestern Alberta. Bulletin of Canadian Petroleum Geology, **39**: 165–191.

Bhattacharya, J.P., and Willis, B.J. 2001. Lowstand deltas in the Frontier Formation, Powder River Basin, Wyoming: implications for sequence stratigraphic models. American Association of Petroleum Geologists Bulletin, **85**: 261–294.

Biek, R.F., and Hylland, M.D. 2007. Geologic map of the Cogswell Point Quadrangle, Washington, Kane, and Iron counties, Utah. Utah Geological Survey Map 221, two plates, scale 1:24,000. Utah Geological Survey, Salt Lake City, UT.

Blakey, R.C. 2014. Paleogeography and paleotectonics of the Western Interior Seaway, Jurassic-Cretaceous of North America. AAPG Search and Discovery Article 30392.

Bloch, J., Schröder-Adams, C., Leckie, D.A., McIntyre, D.J., Craig, J., and Staniland, M. 1993. Revised stratigraphy of the Lower Colorado Group (Albian to Turonian), Western Canada. Bulletin of Canadian Petroleum Geology, **41**: 325–348.

Bloch, J.D., Schröder-Adams, C.J., Leckie, D.A., Craig, J., and McIntyre, D.J. 1999. Sedimentology, micropaleontology, geochemistry and hydrocarbon potential of shale from the Cretaceous Lower Colorado Group in western Canada. Geological Survey of Canada Bulletin **531**: 185p.

Bohannon, R.G. 1983. Mesozoic and Cenozoic tectonic development of the Muddy, North Muddy, and northern Black Mountains, Clark County, Nevada. *In* Tectonic and stratigraphic studies in the Eastern Great Basin. *Edited by* D.M. Miller, V.R. Todd and K.A. Howard. Geological Society of America Memoir 157. Geological Society of America, Boulder, CO. pp. 125–148. doi:10.1130/MEM157-p125.

Bonde, J. W., Varricchio, D.J., Jackson, F.D., Loope, D.B., and Shirk., A.M. 2008. Dinosaurs and dunes! Sedimentology and paleontology of the Mesozoic in the Valley of Fire State Park. *In* Field guide to plutons, volcanoes, faults, reefs, dinosaurs, and possible glaciation in selected areas of Arizona, California, and Nevada. *Edited by* E.M. Duebendorfer

and E.I. Smith. Geological Society of America Field Guide 11. Geological Society of America, Boulder, CO. pp. 249–262.

Bonde, J.W. 2008. Paleoecology and taphonomy of the Willow Tank Formation (Albian), Southern Nevada. M.Sc. thesis, Montana State University Bozeman, MT, 96p.

Bonde, J.W., Hilton, R.P., Jackson, F.D., and Druschke, P.A. 2015. Fauna of the Newark Canyon Formation (Lower Cretaceous), east-central Nevada. *In* Geological Society of Nevada Symposium. Geological Society of Nevada, Reno, NV. pp. 139–150.

Bonde, J.W., Varricchio, D.J., Bryant, G., and Jackson, F.D. 2012. Mesozoic vertebrate paleontology of Valley of Fire State Park, Clark County, Nevada. *In* Field Guide for the 71st Annual Meeting of the Society of Vertebrate Paleontology. *Edited by* J.W. Bonde and A.R.C. Milner. Nevada State Museum Paleontological Paper Number 1. Nevada Department of Tourism and Cultural Affairs. Division of Museums and History, Carson City, NV. pp. 108–126.

Boreen, T., and Walker, R.G. 1991. Definition of allomembers and their facies assemblages in the Viking Formation, Willesden Green area, Alberta. Bulletin of Canadian Petroleum Geology, **38**: 123–144.

Bowerman, M., Christianson, A., Creaser, R.A., and Luth, R.W. 2006. A petrological and geochemical study of the volcanic rocks of the Crowsnest Formation, southwestern Alberta, and of the Howell Creek suite, British Columbia. Canadian Journal of Earth Sciences, **43**: 1621–1637. doi:10.1139/e06-037.

Bremer, J.M. 2016. Stratigraphy and sedimentology of the Cretaceous Mowry Shale in the northern Bighorn Basin of Wyoming: implications for unconventional resource exploration and development, M.S. thesis, University of Nebraska, Lincoln, NE. 55p.

Britt, B.B., Burton, D., Greenhalgh, B.W., Kowallis, B.J., Christiansen, E., and Chure, D.J. 2007. Detrital zircon ages for the basal Cedar Mountain Formation (Early Cretaceous) near Moab, and Dinosaur National Monument, Utah. Geological Society of America Abstracts with Programs, **39**(5): 16.

Buechmann, D.L. 2013. Provenance, detrital zircon U-Pb geochronology, and tectonic significance of middle Cretaceous sandstones from the Alberta foreland basin. MS thesis, University of Houston, Houston, TX. 87p.

Buiter, S.J.H., Govers, R., and Wortel, M.J.R. 2002. Two-dimensional simulations of surface deformation caused by slab detachment. Tectonophysics, **354**: 195–210. doi:10.1016/S0040-1951(02)00336-0.

Burchfiel, B.C., and Davis, G.A. 1977. Geology of the Sagamore Canyon-Slaughterhouse Spring area. New York Mountains, California. Geological Society of America Bulletin. **88**: 1623–1640. doi:10.1130/0016-7606(1977)88⟨1623:GOTSCS⟩2.0.CO;2.

Burgess, P.M., and Moresi, L. 1999. Modelling rates and distribution of subsidence due to dynamic topography over subducting slabs: Is it possible to identify dynamic topography from ancient strata? Basin Research, **11**: 305–314. doi:10.1046/j.1365-2117.1999.00102.x.

Burtner, R.L., and Nigrini, A. 1994. Thermochronology of the Idaho-Wyoming thrust belt during the Sevier orogeny. American Association of Petroleum Geologists Bulletin. **78**: 1613–1636.

Byers, C.W., and Larson, D.W. 1979. Paleoenvironments of Mowry Shale (Lower Cretaceous), western and central Wyoming. American Association of Petroleum Geologists Bulletin, **63**: 354–375.

Campa, M.F., and Coney, P.J. 1983. Tectono-stratigraphic terranes and mineral resource distributions in Mexico. Canadian Journal of Earth Sciences, **20**: 1040–1051. doi:10.1139/e83-094.

Cant, D.J., and Stockmal, G.S. 1989. The Alberta foreland basin: relationship between stratigraphy and Cordilleran terrane-accretion events. Canadian Journal of Earth Sciences, **26**: 1964–1975. doi:10.1139/e89-166.

Carpenter, D.G. 1989. Geology of the North Muddy Mountains, Clark county, Nevada and regional structural synthesis: fold-thrust and basin-range in southern Nevada, southwest Utah and northwest Arizona. MS Thesis Oregon State University, Corvallis, OR. 139p.

Carpenter, K. 2014. Where the sea meets the land—the unresolved Dakota problem in Utah. *In* Geology of Utah's far south. *Edited by* J.S. MacLean, R.F. Biek and J.E. Huntoon. Utah Geological Association Publication 43. Utah Geological Association, Salt Lake City, UT. pp. 357–372.

Carr, M.D. 1980. Upper Jurassic to Lower Cretaceous (?) synorogenic sedimentary rocks in the southern Spring Mountains. Geology, **8**: 385–389. doi:10.1130/0091-7613(1980)8⟨385:UJTLCS⟩2.0.CO;2.

Carrapa, B., DeCelles, P.G., and Romero, M. 2019. Early inception of the Laramide orogeny in southwestern Montana and northern Wyoming: implications for models of flat-slab subduction. Journal of Geophysical Research, Solid Earth, **124**: 2102–2123. doi:10.1029/2018JB016888.

Catuneanu, O., Sweet, A.R., and Miall, A.D. 2000. Reciprocal stratigraphy of the Campanian–Paleocene western interior of North America. Sedimentary Geology, **134**: 235–255. doi:10.1016/S0037-0738(00)00045-2.

Cecil, C.B., Dulong, F.T., Harris, R.A., Cobb, J.C., Gluskoter, H.G., and Nuroho, H. 2003. Observations on climate and sediment discharge in selected tropical rivers, Indonesia. *In* Climate controls on stratigraphy. *Edited by* C.B. Cecil and T. Edgar. Society of Sedimentary Geology, Special Publication 77. Society of Sedimentary Geology, Tulsa, OK. pp. 29–50.

Cecil, M.R., Gehrels, G.E., Rusmore, M.E., Woodsworth, G.J., Stowell, H.H., Yokelson, I.N. et al. 2021. Mantle control on magmatic flare-ups in the southern Coast Mountains batholith, British Columbia. Geosphere. **17**: 2027–2041. doi:10.1130 /GES02361.1.

Centeno-García, E., Busby, C., Busby, M., and Gehrels, G. 2011. Evolution of the Guerrero composite terrane along the Mexican margin, from extensional fringing arc to contractional continental arc. Geological Society of America Bulletin, **123**: 1776–1797. doi:10.1130/B30057.1.

Centeno-García, E., Guerrero-Suastegui, M., and Talavera-Mendoza, O. 2008. The Guerrero composite terrane of western Mexico: collision and subsequent rifting in a supra-subduction zone. *In* Formation and applications of the sedimentary record in arc collision zones. *Edited by* A.E. Draut, P.D. Clift and D.W. Scholl. Geological Society of America Special Paper 436. Geological Society of America, Boulder, CO. pp. 279–308. doi:10.1130/2008.2436(13).

Centeno-García, E., Ruíz, J., Coney, P.J., Patchett, P.J., and Ortega-Gutiérrez, F. 1993. Geology of the Guerrero terrane and its role in the tectonic evolution of the southern North America Cordillera from new geochemical data. Geology, **21**: 419–422. doi:10.1130/0091-7613(1993)021%3c0419:GTOMIR%3e2.3.CO;2.

Chatelain, J., Molnar, P., Prévot, R., and Sacks, B. 1992. Detachment of part of the downgoing slab and uplift of the New Hebrides (Vanuatu) islands. Geophysical Research Letters, **19**: 1507–1510. doi:10.1029/92GL01389.

Chiodi, M., Monod, O., Busnardo, R., Gaspard, D., Sánchez, A., and Yta, M. 1988. Une descordance anté-Albienne daté par una faune d'Ammonites et de Brachiopods de type Téthysien au Mexique central. Geobios, **21**: 125–135. doi:10.1016/S0016-6995(88)80014-7.

Christiansen, F.N. 1952. Structure and stratigraphy of the Canyon Range, central Utah. Geological Society of America Bulletin, **63**: 717–740.

Cifelli, R.L., Kirkland, J.I., Weil, A., Deinos, A.R., and Kowallis, B.J. 1997. High-precision $^{40}Ar/^{39}Ar$ geochronology and the advent of North America's Late Cretaceous terrestrial fauna. Proceedings of the National Academy of Sciences of the United States of America, **94**: 11163–11167. doi:10.1073/pnas.94.21.11163.

Cifelli, R.L., Nydam, R.L., Gardner, J.D., Weil, A., Eaton, J.G., Kirkland, J.I., and Madsen, S.K. 1999. Medial Cretaceous vertebrates from the Cedar Mountain Formation, Emery County, Utah: the Mussentuchit local fauna. *In* Vertebrate paleontology in Utah. *Edited by* D.D. Gillette. Utah Geological Survey Miscellaneous Publication 99-1. Utah Geological Survey, Salt Lake City, UT. pp. 219–242.

Cobban, W.A., and Kennedy, W.J. 1989. The ammonite *Metengonoceras* Hyatt, 1903, from the Mowry Shale (Cretaceous) of Montana and Wyoming. United States Geological Survey Bulletin 1787-L, 22p.

Cobban, W.A., and Larson, N.L. 1997. Marine upper Cretaceous rocks and their ammonite record along the northern flank of the Black Hills uplift, Montana, Wyoming, and South Dakota. Rocky Mountain Geology, **32**: 27–35.

Cobban, W.A., and Reeside, J.B. 1952. Correlation of the Cretaceous formations of the Western Interior of the United States. Geological Society of America Bulletin, **63**: 1011–1044. doi:10.1130/0016-7606(1952)63%5b1011:COTCFO%5d2.0.CO;2.

Cobban, W.A., Erdmann, C.E., Lemke, R.W., and Maughan, E.K. 1976. Type sections and stratigraphy of the members of the Blackleaf and Marias River formations (Cretaceous) of the Sweetgrass Arch, Montana. U.S. Geological Survey Professional Paper 974. U.S. Geological Survey, Reston, VA. 71p. doi:10.3133/pp974.

Coleman, D.S., and Glazner, A.F. 1998. The Sierra Crest magmatic event: rapid formation of juvenile crust during the Late Cretaceous in California. *In* Integrated earth and environmental evolution of the southwestern United States: The Clarence A. Hall Jr. volume. *Edited by* W.G. Ernst and C.A. Nelson. Bellwether Publishing for the Geological Society of America, Columbia, MD. pp. 253–272.

Coney, P.J. 1981. Accretionary tectonics in western North America. *In* Relations of tectonics to ore deposits in the southern Cordillera. *Edited by* W.R. Dickinson and W.D. Payne. Arizona Geological Society Digest, **14**: 23–37.

Coney, P.J., Jones, D.L., and Monger, J.W.H. 1980. Cordilleran suspect terranes. Nature, **288**: 329–333. doi:10.1038/288329a0.

Crampton, S.L., and Allen, P.A. 1995. Recognition of flexural forebulge unconformities in the geologic record. American Association of Petroleum Geologists Bulletin, **79**: 1495–1514.

Currie, B.S. 1998. Upper Jurassic–Lower Cretaceous Morrison and Cedar Mountain formations, NE Utah–NW Colorado: relationships between nonmarine deposition and early Cordilleran foreland-basin development. Journal of Sedimentary Research, **68**: 632–652. doi:10.2110 /jsr.68.632.

Currie, B.S. 2002. Structural configuration of the Early Cretaceous Cordilleran foreland-basin system and Sevier thrust belt, Utah and Colorado. The Journal of Geology, **110**: 697–718. doi:10.1086/342626.

Curry, W.H., III. 1962. Depositional environments in central Wyoming during the early Cretaceous. *In* Symposium on Early Cretaceous rocks of Wyoming and adjacent areas: 17th Annual Field Conference Guidebook. Wyoming Geological Association, Casper, WY. pp. 118–123.

Darton, N.H. 1904. Comparison of the stratigraphy of the Black Hills, Bighorn Mountains, and Rocky Mountain Front Range. Geological Society of America Bulletin, **15**: 379–448.

DeCelles, P.G. 2004. Late Jurassic to Eocene evolution of the Cordilleran thrust belt and foreland basin system, western USA. American Journal of Science, **304**: 105–168. doi:10.2475/ajs.304.2.105.

DeCelles, P.G. 2012. Foreland basin systems revisited: variations in response to tectonic settings. *In* Tectonics of sedimentary basins: recent advances. *Edited by* C. Busby, A. Azor and A. Pérez. Blackwell Publishing Ltd., Chichester, UK, pp. 405–426.

DeCelles, P.G., and Cavazza, W. 1999. A comparison of fluvial megafans in the Cordilleran (Late Cretaceous) and modern Himalayan foreland basin systems. Geological Society of America Bulletin, **111**: 1315–1334. doi:10.1130/0016-7606(1999)111⟨1315:ACOFMI⟩2.3.CO;2.

DeCelles, P.G., and Coogan, J.C. 2006. Regional structure and kinematic history of the Sevier fold-and-thrust belt, central Utah. Geological Society of America Bulletin, **118**: 841–864. doi:10.1130/B25759.1.

DeCelles, P.G., and Currie, B.S. 1996. Long-term sediment accumulation in the middle Jurassic–early Eocene Cordilleran retroarc foreland basin system. Geology, **24**: 591–594. doi:10.1130/0091-7613(1996)024⟨0591:LTSAIT⟩2.3.CO;2.

DeCelles, P.G., Ducea, M.N., Kapp, P., and Zandt, G. 2009. Cyclicity in Cordilleran orogenic systems. Nature Geoscience, **2**: 251–257. doi:10.1038/ngeo469.

Di Fiori, R.V., Long, S.P., Fetrow, A.C., Snell, K.E., Bonde, J.W., and Vervoort, J. 2020. Syn-contractional deposition of the Cretaceous Newark Canyon Formation, Diamond Mountains, Nevada: implications for strain partitioning within the U.S. Cordillera. Geosphere, **16**: 546–566. doi:10.1130/GES02168.1.

Dickinson, W.R. 1970. Global tectonics. Science, **168**: 1250–1259. doi:10.1126/science.168.3936.1250.

Dickinson, W.R., and Lawton, T.F. 2001. Carboniferous to Cretaceous assembly and fragmentation of Mexico. Geological Society of America Bulletin, **113**: 1142–1160. doi:10.1130/0016-7606(2001)113⟨1142:CTCAAF⟩2.0.CO;2.

Dickinson, W.R., Klute, M.A., Hayes, M.J., Janecke, S.U., Lundin, E.R., McKittrick, M.A., and Olivares, M.D. 1988. Paleogeographic and paleotectonic setting of Laramide sedimentary basins in the central Rocky Mountain region. Geological Society of America Bulletin, **100**: 1023–1039. doi:10.1130/0016-7606(1988)100⟨1023:PAPSOL⟩2.3.CO;2.

Doelling, H.H., and Kuehne, P.A. 2013. Geologic map of the Short Canyon quadrangle, Emery County, Utah. Utah Geological Survey Map 255DM, two plates, scale 1:24,000.Utah Geological Survey, Salt Lake City, UT. 31p.

Dolson, J.C., Muller, D., Evetts, M.J., and Stein, J.A. 1991. Regional paleotopographic trends and production, Muddy Sandstone (Lower Cretaceous), central and northern Rocky Mountains. American Association of Petroleum Geologists Bulletin, **75**: 409–435.

Dostal, J., and Jutras, P. 2021. Tectonic and petrogenetic settings of the Eocene Challis-Kamloops volcanic belt of western Canada and the northwestern United States. International Geology Review. **64**(18): 2565–2583. doi:10.1080/00206814.2021.1992800.

Dresser, H.W. 1974. Muddy sandstone–Wind River basin. Earth Science Bulletin, **7**: 5–70.

Drljepan, M. 2018. Allostratigraphy of the Viking and Joli Fou formations, the Lower Colorado Group (Upper Albian), central Alberta and Saskatchewan, Western Canada foreland basin. Ph.D. dissertation, The University of Western Ontario, London, ON. 221p.

DuBois, D.P. 1982. Tectonic framework of basement thrust terrane, northern Tendoy Range, southwest Montana. *In* Geologic studies of the Cordilleran thrust belt. *Edited by* R.B. Powers. Rocky Mountain Association of Geologists. Denver, CO. pp. 145–158.

Ducea, M.N. 2002. Constraints on the bulk composition and root foundering rates of continental arcs: a California arc perspective. Journal of Geophysical Research. **107**: 2304. doi:10.1029/2001JB000 643.

Ducea, M.N., and Barton, M.D. 2007. Igniting flare-up events in Cordilleran arcs. Geology, **35**: 1047–1050. doi:10.1130/G23898A.1.

Ducea, M.N., Paterson, S.R., and DeCelles, P.G. 2015. High-volume magmatic events in subduction systems. Elements. **11**: 99–104. doi:10.2113/gselements.11.2.99.

Duque-Trujillo, J., Ferrari, L., Orozco-Esquivel, T., López-Martínez, M., Lonsdale, P. Bryan, S.E., et al. 2015. Timing of rifting in the southern Gulf of California and its conjugate margins: insights from the plutonic record. Geological Society of America Bulletin, **127**: 702–736. doi:10.1130/B31008.1.

Dyman, T.S., and Nichols, D.J. 1988. Stratigraphy of mid-Cretaceous Blackleaf and lower part of the Frontier formations in parts of Beaverhead and Madison counties, Montana. United States Geological Survey Bulletin 1773. United States Geological Survey, Denver, CO. 31p.

Dyman, T.S., and Tysdal, R.G. 1998. Stratigraphy and depositional environment of nonmarine facies of Frontier Formation, eastern Pioneer Mountains, southwestern Montana. The Mountain Geologist. **35**: 115–125.

Dyman, T.S., Porter, K.W., Tysdal, R.G., Cobban, W.A., and Obradovich, J.D. 2000. Late Albian Blackleaf and Thermopolis-Muddy sequence in southwestern Montana and correlation with time-equivalent strata in west-central Montana. *In* Montana Geological Society 50th Anniversary Symposium, **Volume I**: Montana Geological Society, Billings, MT. pp. 65–81.

Eicher, D.L. 1958. The Thermopolis Shale in eastern Wyoming. *In* Powder River Basin of Wyoming; 13th Annual Field Conference guidebook. Wyoming Geological Association, Casper, WY. pp. 79–83.

Eicher, D.L. 1962. Biostratigraphy of the Thermopolis, Muddy, and Shell Creek formations. *In* 17th Annual Field Conference Guidebook. Wyoming Geological Association, Casper, WY. pp. 72–93.

Enkin, R.J. 2006. Paleomagnetism and the case for Baja British Columbia. *In* Paleogeography of the North American Cordillera: Evidence for and against large-scale displacements. *Edited by* J.W. Haggart, R.J. Enkin and J.W.H. Monger. Geological Association of Canada Special Paper 46. Geological Association of Canada, St. John's, NL. pp. 233–254.

Fillmore, R.P. 1991. Tectonic influence on sedimentation in the southern Sevier foreland Iron Springs Formation (Upper Cretaceous), southwestern Utah. *In* Stratigraphy, depositional environments, and sedimentary tectonics of the western margin, Cretaceous Western Interior Seaway. *Edited by* J.D. Nations and J.G. Eaton. Geological Society of America Special Paper 260. Geological Society of America, Boulder, CO. pp. 9–25.

Finn, T.M. 2021. Stratigraphic cross sections of the Mowry Shale and associated strata in the Wind River Basin, Wyoming. United States Geological Survey, Scientific Investigations Map 3476. United States Geological Survey, Denver, CO. 14p.

Finzel, E.S. 2014. Detrital zircons from Cretaceous midcontinent strata reveal an Appalachian Mountains-Cordilleran foreland basin connection. Lithosphere, **6:** 378–382. doi:10.1130/L400.1.

Finzel, E.S. 2017. Detrital zircon microtextures and U-Pb geochronology of Upper Jurassic to Paleocene strata in the distal North Ameri-

can Cordillera foreland basin. Tectonics, **36**: 1295–1316. doi:10.1002/2017TC004549.1295.

Fleck, R.J. 1970. Tectonic style, magnitude, and age of deformation in the Sevier orogenic belt in southern Nevada and eastern California. Geological Society of America Bulletin, **81**: 1705–1720. doi:10.1130/0016-7606(1970)81[1705:TSMAAO]2.0.CO;2.

Fleck, R.J., and Carr, M.D. 1990. The age of the Keystone thrust: laser-fusion $^{40}Ar/^{39}Ar$ dating of foreland basin deposits, southern Spring Mountains, Nevada. Tectonics **9**: 467–476. doi:10.1029/TC009i003p00467.

Fleck, R.J., Mattinson, J.M., Busby, C.J., Carr, M.D., Davis, G.A., and Burchfiel, B.C. 1994. Isotopic complexities and the age of the Delfonte volcanic rocks, eastern Mescal Range, southeastern California: stratigraphic and tectonics implications. Geological Society of America Bulletin, **106**: 1242–1253. doi:10.1130/0016-7606(1994)106⟨1242:ICATAO⟩2.3.CO;2.

Flück, P., Hyndman, R.D., and Lowe, C. 2003. Effective elastic thickness *Te* of the lithosphere in western Canada. Journal of Geophysical Research, **108**: 2430. doi:10.1029/2002JB002201.

Fuentes, F., DeCelles, P.G., Constenius, K.N., and Gehrels, G.E. 2011. Evolution of the Cordilleran foreland basin system in northwestern Montana, USA. Geological Society of America Bulletin, **123**: 507–533. doi:10.1130/B30204.1.

Gardner, J.D., and Cifelli, R.L. 1999. A primitive snake from the mid-Cretaceous of Utah, USA—the geologically oldest snake from the New World. Special Papers in Palaeontology, **60**: 87–100.

Garrison, J.R., Brinkman, D., Nichols, D.J., Layer, P., Burge, D., and Thayn, D. 2007. A multidisciplinary study of the Lower Cretaceous Cedar Mountain Formation, Mussentuchit Wash, Utah: a determination of the paleoenvironment and paleoecology of the *Eolambia caroljonesa* dinosaur quarry. Cretaceous Research, **28**: 461–494. doi:10.1016/j.cretres.2006.07.007.

Gastil, R.G., Diamond, J., Knaack, C., Walawender, M., Marshall, M., Boyles, C., et al. 1990. The problem of the magnetite/ilmenite boundary in Southern and Baja California. *In* The nature and origin of Cordilleran magmatism. *Edited by* J.L. Anderson. Geological Society of America Memoir 174. Geological Society of America, Boulder, CO. pp. 19–32. doi:10.1130/MEM174-p19.

Gastil, R.G., Phillips, R.P., and Allison, E.C. 1975. Reconnaissance geology of the state of Baja California: Geological Society of America Memoir 140. Geological Society of America, Boulder, CO. 201p. doi:10.1130/MEM140-p1.

Gentry, A., Yonkee, W.A., Wells, M.L., and Balgord, E.A. 2018. Resolving the history of early fault slip and foreland basin evolution along the Wyoming salient of the Sevier fold-and-thrust belt: integrating detrital zircon geochronology, provenance modeling, and subsidence analysis. *In* Tectonics, sedimentary basins, and provenance: A celebration of William R. Dickinson's career. *Edited by* R.V. Ingersoll, T.F. Lawton and S.A. Graham. Geological Society of America Special Paper 540. Geological Society of America, Boulder, CO. pp. 509–545. doi:10.1130/2018.2540(23).

Giallorenzo, M. 2013. Application of (U-Th)/He and $^{40}Ar/^{39}Ar$ thermochronology to the age of thrust faulting in the Sevier orogenic belt. Unpublished Ph.D. dissertation. University of Nevada, Las Vegas, NV. 281p.

Gianni, G.M., and Navarrete, C.R. 2022. Catastrophic slab loss in southwestern Pangea preserved in the mantle and igneous record. Nature Communication, **13**, 698. doi:10.1038/s41467-022-28290-z.

Gibson, D.W. 1992. Stratigraphy and sedimentology of the Lower Cretaceous Hulcross and Boulder Creek formations, northeastern British Columbia. Geological Survey of Canada Bulletin 440. Geological Survey of Canada, Ottawa, ON. 105p.

Gladwin, K., and Johnston, S.T. 2006. Mid-Cretaceous pinning of accreted terranes to miogeoclinal assemblages in the northern Cordillera: irreconcilable with paleomagnetic data. *In* Paleogeography of the North American Cordillera: Evidence for and against Large-Scale Displacements. *Edited by* J.W. Haggart, R.J. Enkin and J.W.H. Monger. Geological Association of Canada Special Paper 46. Geological Association of Canada, St. John's, NL. pp. 299–306.

González-Léon, C., and Jacques-Ayala, C. 1988. Estratigrafía de las rocas cretácicas del área de Cerro de Oro, Sonora central. Boletín de Departmento de Universidad Sonora, **5**: 1–23.

González-León, C., Solari, L., Solé, J., Ducea, M.N., Lawton, T.F., Bernal, J.P., et al. Stratigraphy, geochronology, and geochemistry of the Laramide magmatic arc in north-central Sonora, Mexico. Geosphere, **7**: 1392–1418. doi:10.1130/GES00679.1.

González-León, C.M., Scott, R.W., Löser, H., Lawton, T.F., Robert, E., and Valencia, V.A. 2008. Upper Aptian–Lower Albian Mural Formation: stratigraphy, biostratigraphy and depositional cycles on the Sonoran shelf, northern México. Cretaceous Research, **29**: 249–266. doi:10.1016/j.cretres.2007.06.001.

Grantz, A., Hart, P.E., and Childers, V.A. 2011. Geology and tectonic development of the Amerasia and Canada basins, Arctic Ocean, *In* Arctic petroleum geology. *Edited by* A.M. Spencer, A.F. Embry, D.L. Gautier, A.V. Stoupakova and K. Sorensen. Geological Society of London Memoir 35. Geological Society, London. pp. 771–799. doi:10.1144/M35.50.Memoirs35.

Greenhalgh, B.W. 2006. A stratigraphic and geochronologic analysis of the Morrison Formation/Cedar Mountain Formation boundary, Utah. MS thesis, Brigham Young University, Provo, UT. 61p.

Greenhalgh, B.W., and Britt, B.B. 2007. Stratigraphy and sedimentology of the Morrison–Cedar Mountain Formation boundary, east-central Utah. *In* Central Utah—Diverse geology of a diverse landscape. *Edited by* G.C. Willis, M.D. Hylland, D.L. Clark and T.C. Chidsey, Jr. Utah Geological Association Publication 36. Utah Geological Association, Salt Lake City, UT. pp. 81–100.

Gries, R. 1983. North-south compression of Rocky Mountain foreland structures. *In* Mountain foreland basins and uplifts. *Edited by* J.D. Lowell, R. Gries and R. Denver. Rocky Mountain Association of Geologists, Denver, CO. pp. 9–32.

Gromet, L.P., and Silver, L.T. 1987. REE variations across the Peninsular Ranges batholith: implications for batholithic petrogenesis and crustal growth in magmatic arcs. Journal of Petrology, **28**: 75–125. doi:10.1093/petrology/28.1.75.

Gurnis, M. 1992. Rapid continental subsidence following the initiation and evolution of subduction. Science, **255**: 1556–1558. doi:10.1126/science.255.5051.1556.

Gustason, E.R. 1988. Depositional and tectonic history of the lower Cretaceous Muddy Sandstone, Lazy B Field, Powder River Basin, Wyoming. *In* Eastern Powder River Basin - Black Hills. Wyoming Geological Association, 39th Annual Field Conference Guidebook. Wyoming Geological Association, Casper, WY. pp. 129–146.

Hadlari, T., Davis, W.J., Dewing, K., Heaman, L.M., Lemieux, Y., Ootes, L., et al. 2012. Two detrital zircon signatures for the Cambrian passive margin of northern Laurentia highlighted by new U-Pb results from northern Canada. Geological Society of America Bulletin. **124**: 1155–1168. doi:10.1130/B30530.1.

Hadlari, T., Maclean, B.C., Galloway, J.M., Sweet, A.R., White, J.M., Thomson, D., et al. 2014. The flexural margin, the foredeep, and the orogenic margin of a northern Cordilleran foreland basin: Cretaceous tectonostratigraphy and detrital zircon provenance, northwestern Canada. Marine and Petroleum Geology, **57**: 173–186. doi:10.1016/j.marpetgeo.2014.05.019.

Hamlin, H. S. 1996. Frontier Formation stratigraphy on the Moxa arch, Green River Basin, Wyoming. The Mountain Geologist, **33**: 35–44.

Hannon, J.S. 2020. Reconstructing the generation, evolution, and migration of arc magmatism using the whole-rock geochemistry of bentonites: a case study from the Cretaceous Idaho-Farallon arc system. Ph.D. Dissertation, University of Cincinnati, Cincinnati, OH. 189p.

Hannon, J.S., Huff, W.D., and Sturmer, D.M. 2019. Geochemical relationships in Cretaceous bentonites as inferred from linear discriminant analysis: Sedimentary Geology, **390**: 1–14. doi:10.1016/j.sedgeo.2019.07.001.

Hansen, S.E., Nyblade, A.A., and Julia, J. 2009. Estimates of crustal and lithospheric thicknesses in sub-Saharan Africa from S-wave receiver functions. South African Journal of Geology, **112**: 229–240. doi:10.2113/gssajg.112.3-4.229.

Harris, R. 2011. The nature of the Banda arc–continent collision in the Timor region. *In* Arc continent collision. *Edited by* D. Brown and P.D. Ryan. Frontiers in earth sciences, Springer Verlag, Berlin, pp. 163–211.

Hart, C.J.R., Goldfarb, R.J., Lewis, L.L., and Mair, J.L. 2004. The northern Cordillera mid-Cretaceous plutonic province: ilmenite/magnetite-series granitoids and intrusion-related mineralisation. Resource Geology, **54**: 253–280. doi:10.1111/j.1751-3928.2004.tb00206.x.

Haxel, G.B., and Miller, D.M. 2007. Mesozoic rocks. *In* Geology and mineral resources of the East Mojave National Scenic Area, San Bernardino County, California. *Edited by* T.G. Theodore. United States Geological Survey Bulletin, 2160. United States Geological Survey, Denver, CO. pp.59–66.

Hay, M.J., and Plint, A.G. 2020. High-frequency sequences within a retrogradational deltaic succession: upper Cenomanian Dunvegan Formation, Western Canada foreland basin. Depositional Record, **6**: 524–551. doi:10.1002/dep2.114.

Hayes, B.J.R., Christopher, J.E., Rosenthal, L., Los, G., McKercher, B., Minken, D., et al. 1994. Chapter 19 – Cretaceous Mannville Group of the Western Sedimentary basin. *In* Geological atlas of the western Canadian sedimentary basin. *Compiled by* G.D. Mossop and I. Shetson. Canadian Society of Petroleum Geologists and Alberta Research Council, Calgary, AB. pp.317–334.

Heirtzler, J.R. 1974. Site 262. *In* initial reports of the Deep-Sea Drilling Project; Fremantle, Australia to Fremantle, Australia; November-December 1972: site reports. Initial Reports of the Deep-Sea Drilling Project. **27**: 193–278.

Heller, P.L., and Paola, C. 1989. The paradox of lower Cretaceous gravels and the initiation of thrusting in the Sevier orogenic belt, United States Western Interior. Geological Society of America Bulletin, **101**: 864–875. doi:10.1130/0016-7606(1989)101⟨0864:TPOLCG⟩2.3.CO;2.

Heller, P.L., Bowler, S.S., Chambers, H.P., Coogan, J.C., Hagen, E.S., Shuster, M.W., et al. 1986. Time of initial thrusting in the Sevier orogenic belt, Idaho-Wyoming and Utah. Geology, **14**: 388–391. doi:10.1130/0091-7613(1986)14⟨388:TOITIT⟩2.0.CO;2.

Heller, P.L., Ducker, K., and McMillan, M.E. 2003. Post-Paleozoic alluvial gravel transport as evidence of continental tilting in the U.S. Cordillera. Geological Society of America Bulletin, **115**: 1122–1132. doi:10.1130/B25219.1.

Helwig, J. 1974. Eugeosynclinal basement and a collage concept of orogenic belts. *In* Modern and ancient geosynclinal sedimentation. *Edited by* R.H. Dott, Jr. and R.H. Shaver. SEPM Special Publication 19. SEPM, Tulsa, OK. pp. 359–376.

Hildebrand, R.S. 2013. Mesozoic assembly of the North American Cordillera. Geological Society of America Special Paper 495. Geological Society of America, Boulder, CO. 169p. doi:10.1130/2013.2495.

Hildebrand, R.S. 2014. Geology, mantle tomography, and inclination corrected paleogeographic trajectories support westward subduction during Cretaceous orogenesis in the North American Cordillera. Geoscience Canada, **41**: 207–224. doi:10.12789/geocanj.2014.41.032.

Hildebrand, R.S. 2015. Dismemberment and northward migration of the Cordilleran orogen: Baja-BC resolved. GSA Today, **25**: 4–11. doi:10.1130/GSATG255A.1.

Hildebrand, R.S., and Whalen, J.B. 2014. Arc and slab-failure magmatism in Cordilleran batholiths II—The Cretaceous Peninsular Ranges batholith of Southern and Baja California. Geoscience Canada, **41**: 399–458. doi:10.12789/geocanj.2014.41.059.

Hildebrand, R.S., and Whalen, J.B. 2017. The tectonic setting and origin of Cretaceous batholiths within the North American Cordillera: the case for slab failure magmatism and its significance for crustal growth. Geological Society of America Special Paper 532. Geological Society of America, Boulder, CO. 113p.

Hildebrand, R.S., and Whalen, J.B. 2021a. The mid-Cretaceous Peninsular Ranges orogeny: a new slant on Cordilleran tectonics? I: Mexico to Nevada. Canadian Journal of Earth Sciences, **58**: 670–696. doi:10.1139/cjes-2020-0154.

Hildebrand, R.S., and Whalen, J.B. 2021b. The mid-Cretaceous Peninsular Ranges orogeny: a new slant on Cordilleran tectonics? II: northern United States and Canada. Canadian Journal of Earth Sciences, **58**: 697–719. doi:10.1139/cjes-2021-0006.

Hildebrand, R.S., Whalen, J.B., and Bowring, S.A. 2018. Resolving the crustal composition paradox by 3.8 billion years of slab failure magmatism and collisional recycling of continental crust. Tectonophysics, **734-735**: 69–88. doi:10.1016/j.tecto.2018.04.001.

Hoffman, P.F. 2012. The Tooth of time: how do passive margins become active? Geoscience Canada, **39**: 67–73.

Hunt, G.J., Lawton, T.F., and Kirkland, J.I. 2011. Detrital zircon U-Pb geochronological provenance of lower Cretaceous strata, foreland basin, Utah. *In* Sevier thrust belt—northern and central Utah and adjacent areas. *Edited by* D.A. Sprinkel, W.A. Yonkee and T.C. Chidsey. Utah Geological Association Publication 40. Utah Geological Association, Salt Lake City, UT. pp. 193–211.

Husson, L., Bernet, M., Guillot, S., Huyghe, P., Mugnier, J-L., Replumaz, A., et al. 2014. Dynamic ups and downs of the Himalaya. Geology, **42**: 839–842. doi:10.1130/G36049.1.

Hutsky, A.J., Fielding, C.R., Hurd, T.J., and Kittinger Clark, C. 2012. Sedimentology and stratigraphy of the upper Cretaceous (Cenomanian) Frontier Formation, northeast Bighorn Basin, Wyoming, USA. The Mountain Geologist, **49**: 77–98.

Hylland, M.D. 2010. Geologic map of the Clear Creek Mountain Quadrangle, Kane County, Utah. Utah Geological Survey Map 245, two plates, scale 1:24,000. Utah Geological Survey, Salt Lake City, UT.

Jacobi, R.D. 1981. Peripheral bulge – a causal mechanism for the lower/middle Ordovician unconformity along the western margin of the northern Appalachians. Earth and Planetary Science Letters, **56**: 245–251. doi:10.1016/0012-821X(81)90131-X.

Jacques-Ayala, C. 1992. Stratigraphy of the lower Cretaceous Cintura Formation, Sierra el Chanate, northwestern Sonora, Mexico. Universidad Nacional Autónoma de México, Instituto de Geologia Revista, **10**: 129–136.

Jacques-Ayala, C. 1995. Paleogeography and provenance of the lower Cretaceous Bisbee Group in the Caborca-Santa Ana area, northwestern Sonora. *In* Studies on the Mesozoic of Sonora and adjacent areas. *Edited by* C. Jacques-Ayala, C.M. González-León and J. Roldán-Quintana. Geological Society of America Special Paper 301. Geological Society of America, Boulder, CO. pp. 79–98. doi:10.1130/0-8137-2301-9.79.

Jamieson, R.A., and Beaumont, C. 1988. Orogeny and metamorphism: a model for deformation and pressure-temperature-time paths with applications to the central and southern Appalachians. Tectonics, **7**: 417–445. doi:10.1029/TC007i003p00417.

Joeckel, R.M., Ludvigson, G.A., Möller, A., Hotton, C.L., Suarez, M.B., Suarez, C.A., et al. 2020. Chronostratigraphy and terrestrial palaeoclimatology of Berriasian–Hauterivian strata of the Cedar Mountain Formation, Utah, USA. *In* Cretaceous climate events and short-term sea-level changes. *Edited by* M. Wagreich, M. B. Hart, B. Sames and I.O. Yilmaz. Geological Society of London, Special Publication 498. Geological Society of London, London. doi:10.1144/SP498-2018-133.SP49875.

Jordan, T.E. 1981. Thrust loads and foreland basin evolution, Cretaceous, western United States. AAPG Bulletin, **65**: 2506–2520.

Kauffman, E.G. 1977. Geological and biological overview: Western Interior Cretaceous basin. The Mountain Geologist, **14**: 75–99.

Kauffman, E.G., and Caldwell, W.G.E. 1993. The Western Interior basin in space and time. *In* Evolution of the Western Interior Basin. *Edited by* W.G.E. Caldwell and E.G. Kauffman. Geological Association of Canada Special Paper 39. Geological Association of Canada, St. John's, NL. pp. 1–30.

Kent, D.V., and Irving, E. 2010. Influence of inclination error in sedimentary rocks on the Triassic and Jurassic apparent pole wander path for North America and implications for Cordilleran tectonics. Journal of Geophysical Research, **115**: doi:10.1029/2009JB007205.

Khandaker, N.I. 1991. Tectonosedimentologic significance of the upper Cretaceous Frontier Formation, north-central Wyoming. Ph.D. dissertation. Iowa State University, Ames, IA, 251p.

Kimbrough, D.L., Abbott, P.L., Balch, D.C., Bartling, S.H., Grove, M., Mahoney, J.B., and Donohue, R.F. 2014. Upper Jurassic Peñasquitos Formation—forearc basin western wall rock of the Peninsular Ranges batholith. *In* Peninsular Ranges batholith, Baja California and Southern California. *Edited by* D.M. Morton and F.K. Miller. Geological Society of America Memoir 211. Geological Society of America, Boulder, CO. pp. 625–643. doi:10.1130/2014.1211(19).

Kimbrough, D.L., Smith, D.P., Mahoney, J.B., Moore, T.E., Grove, M., Gastil, R.G., et al. 2001. Forearc-basin sedimentary response to rapid late Cretaceous batholith emplacement in the Peninsular Ranges of southern and Baja California. Geology, **29**: 491–494. doi:10.1130/0091-7613(2001)029%3c0491:FBSRTR%3e2.0.CO;2.

Kirkland, J.I., and Madsen, S.K. 2007. The lower Cretaceous Cedar Mountain Formation, eastern Utah:—the view up an always interesting learning curve. *In* Field guide to geological excursions in southern Utah. *Edited by* W.R. Lund. Geological Society of America Rocky Mountain Section 2007 Annual Meeting, Grand Junction Geological Society,

and Utah Geological Association Publication 35, Salt Lake City, UT, pp. 1–108. Compact disc.

Kirkland, J.I., Britt, B.B., Burge, D.L., Carpenter, K., Cifelli, R., DeCourten, F., et al. 1997. Lower to middle Cretaceous dinosaur faunas of the central Colorado Plateau—a key to understanding 35 million years of tectonics, sedimentology, evolution, and biogeography. Brigham Young University Geology Studies, **42 (pt. II)**: 69–103.

Kirkland, J.I., Cifelli, R., Britt, B.B., Burge, D.L., DeCourten, F., Eaton, J., and Parrish, J.M. 1999. Distribution of vertebrate faunas in the Cedar Mountain Formation, east-central Utah. *In* Vertebrate paleontology in Utah. *Edited by* D.D. Gillette. Utah Geological Survey Miscellaneous Publication 99-1. Utah Geological Survey, Salt Lake City, UT. pp. 201–217.

Kirkland, J.I., Suarez, M., Suarez, C., and Hunt-Foster, R. 2016. The Lower Cretaceous in east-central Utah—the Cedar Mountain Formation and its bounding strata. Geology of the Intermountain West, **3**: 101–228. doi:10.31711/giw.v3.pp101-228.

Kirschbaum, M.A., and Mercier, T.J. 2013. Controls on the deposition and preservation of the Cretaceous Mowry Shale and Frontier Formation and equivalents, Rocky Mountain region, Colorado, Utah, and Wyoming. AAPG Bulletin, **97**: 899–921. doi:10.1306/10011212090.

Kirschbaum, M.A., and Roberts, L.N.R. 2005. Stratigraphic framework of the Cretaceous Mowry Shale, Frontier Formation and adjacent units, southwestern Wyoming province, Wyoming, Colorado, and Utah. *In* Petroleum systems and geologic assessment of oil and gas in the southwestern Wyoming province: Wyoming, Colorado, and Utah. U.S. Geological Survey Digital Data Series DDS–69–D. Denver, CO. 31p.

Kowallis, B.J., Britt, B.B., Greenhalgh, B.W., and Spinkel, D.A. 2007. New U-Pb zircon ages from an ash bed in the Brushy Basin Member of the Morrison Formation near Hanksville, Utah. *In* Central Utah—Diverse geology of a diverse landscape. *Edited by* G.C. Willis, M.D. Hylland, D.L. Clark and T.C. Chidsey, Jr. Utah Geological Association Publication 36. Utah Geological Association, Salt Lake City. pp. 75–80.

Kowallis, B.J., Christiansen, E.H., Deino, A.L., Peterson, F., Turner, C.E., Kunk, M.J., and Obradovich, J.D. 1998. The age of the Morrison Formation. Modern Geology, **22**: 235–260.

Krumenacker, L.J. 2010. Chronostratigraphy and paleontology of the mid-Cretaceous Wayan Formation of eastern Idaho, with a description of the first *Oryctodromeus* specimens from Idaho. Unpublished MSc thesis, Brigham Young University, Provo, UT. 88p.

Lackey, J.S., Valley, J.W., Chen, J.H., and Stockli, D.F. 2008. Dynamic magma systems, crustal recycling, and alteration in the central Sierra Nevada batholith: the oxygen isotope record. Journal of Petrology, **49**: 1397–1426. doi:10.1093/petrology/egn030.

Langenberg, C.W., Hein, F.J., Bieber, K., Losert, J., Berhane, H., and Cotterill, D.K. 2000. Regional geology of the upper Blairmore Group and Bow Island Formation: a subsurface study in southwestern Alberta. Alberta Energy and Utilities Board, Alberta Geological Survey, Earth Sciences Report 2000-6. Alberta Geological Survey, Edmonton, AB. 68p.

Langenheim, V.E., Jachens, R.C., and Aiken, C. 2014. Geophysical framework of the Peninsular Ranges batholith—implications for tectonic evolution and neotectonics. *In* Peninsular Ranges batholith, Baja California and Southern California. *Edited by* D.M. Morton and F.K. Miller. Geological Society of America Memoir 211. Geological Society of America, Boulder, CO. pp. 1–20. doi:10.1130/2014.1211(01).

Larson, K.P., Price, R.A., and Archibald, D.A. 2006. Tectonic implications of $^{40}Ar/^{39}Ar$ muscovite dates from the Mt. Haley stock and Lussier River stock, near Fort Steele, British Columbia. Canadian Journal of Earth Sciences, **43**: 1673–1684. doi:10.1139/e06-048.

Lawton, T.F., Amato, J.M., Machin, S.E.K., Gilbert, J.C., and Lucas, S.G. 2020b. Transition from Late Jurassic rifting to middle Cretaceous dynamic foreland, southwestern U.S. and northwestern Mexico. Geological Society of America Bulletin, **132**: 2489–2516. doi:10.1130/B35433.1.

Lawton, T.F., González-León, C.M., Lucas, S.G., and Scott, R.W. 2004. Stratigraphy and sedimentology of the Upper Aptian–Upper Albian Mural limestone (Bisbee Group) in northern Sonora, Cretaceous Research, **25**: 43–60. doi:10.1016/j.cretres.2003.09.003.

Lawton, T.F., Hunt, G.J., and Gehrels, G.E. 2010. Detrital zircon record of thrust belt unroofing in Lower Cretaceous synorogenic conglomerates, central Utah. Geology, **38**: 463–466. doi:10.1130/G30684.1.

Lawton, T.F., Pindell, J., Beltran-Triviño, A., Juárez-Arriaga, E., Molina-Garza, R., and Stockli, D. 2015. Late Cretaceous-Paleogene foreland sediment-dispersal systems in northern and eastern Mexico: Interpretations from preliminary detrital-zircon analysis. AAPG Search and Discovery Article #30423. American Association of Petroleum Geologists, Tulsa, OK.

Lawton, T.F., Sierra-Rojas, M.I., and Martens, U. 2020a. Stratigraphic correlation chart of Carboniferous–Paleogene rocks of Mexico, adjacent southwestern United States, Central America, and Colombia. *In* Southern and Central Mexico: Basement Framework, Tectonic Evolution, and Provenance of Mesozoic–Cenozoic Basins. *Edited by* U. Martens and R.S. Molina Garza. Geological Society of America Special Paper 546. Geological Society of America, Boulder, CO. pp. 115–142. doi:10.1130/2020.2546(05).

Lawton, T.F., Sprinkel, D.A., and Waanders, G.L. 2007. The Cretaceous Canyon Range Conglomerate, central Utah—stratigraphy, structure and significance. *In* Central Utah—diverse geology of a dynamic landscape. *Edited by* G.C. Willis, M.D. Hylland, D.L. Clark and T.C. Chidsey, Jr. Utah Geological Association Publication 36. Utah Geological Association, Salt Lake City, UT. pp.101–122.

Leckie, D.A., and Burden, E.T. 2001. Stratigraphy, sedimentology and palynology of the Cretaceous (Albian) Beaver Mines, Mill Creek and Crowsnest formations (Blairmore Group) of southwestern Alberta. Geological Survey of Canada Bulletin **563**: 103p.

Leckie, D.A., and Cheel, R.J. 1997. Sedimentology and depositional history of Lower Cretaceous coarse-grained clastics, southwest Alberta and southeast British Columbia. Bulletin of Canadian Petroleum Geology, **45**: 1–24.

Leckie, D.A., and Craw, D. 1995. Westerly derived early Cretaceous gold paleoplacers in the Western Canada foreland basin, southwestern Alberta: tectonic and economic implications. Canadian Journal of Earth Sciences, **32**: 1079–1092. doi:10.1139/e95-090.

Leckie, D.A., and Reinson, G.E. 1993. Effects of middle to late Albian sea-level fluctuations in the Cretaceous interior seaway, Western Canada. *In* Evolution of the Western Interior Basin. *Edited by* W.G.E. Caldwell and E.G. Kauffman. Geological Association of Canada, Special Paper 39. Geological Association of Canada, St. John's, NL. pp. 151–175.

Leckie, D.A., and Singh, C. 1991. Estuarine deposits of the Albian Paddy Member (Peace River Formation) and lowermost Shaftesbury Formation, Alberta, Canada. Journal of Sedimentary Petrology, **61**: 825–849.

Leckie, D.A., and Smith, D.G. 1992. Regional setting, evolution, and depositional cycles of the western Canada foreland basin. *In* Foreland basins and fold belts. *Edited by* R.W. MacQueen and D.A. Leckie. American Association of Petroleum Geologists Memoir 55. American Association of Petroleum, Tulsa, OK. pp. 9–46.

Leckie, D.A., Bhattacharya, J.P., Bloch, J., Gilboy, C.F., and Norris, B. 1994. Chapter 20 – Cretaceous Colorado/Alberta Group of the western Canada sedimentary basin. *In* Geological atlas of the western Canadian sedimentary basin. *Compiled by* G.D. Mossop and I. Shetson. Canadian Society of Petroleum Geologists and Alberta Research Council, Calgary, AB. pp. 335–352.

Leckie, D.A., Fox, C., and Tornacai, C. 1989. Multiple paleosols of the Late Albian Boulder Creek Formation, British Columbia, Canada. Sedimentology, **36**: 307–323. doi:10.1111/j.1365-3091.1989.tb00609.x.

Leckie, D.A., Singh, C., Bloch, J., Wilson, M., and Wall, J.H. 1992. An anoxic event at the Albian-Cenomanian boundary: the Fish Scale marker bed, northern Alberta, Canada. Palaeogeography, Palaeoclimatology, Palaeoecology, **92**: 139–166. doi:10.1016/0031-0182(92)90139-V.

Leckie, D.A., Staniland, M.R., and Hayes, B.J. 1990. Regional maps of the Albian Peace River and lower Shaftesbury formations on the Peace River arch, northwestern Alberta and northeastern British Columbia. Bulletin of Canadian Petroleum Geology, **38A**: 176–189.

LeFever, R.D., and McCloskey, G.G. 1995. Depositional history of the Newcastle Formation (Lower Cretaceous), Williston Basin, north Dakota, south Dakota and eastern Montana. *In* Seventh International Williston Basin Symposium, July 23, 1995. *Edited by* L.D.V. Hunter and R.A. Schalla. Montana Geological Society, Billings, MT. pp. 411–416.

Leier, A.L., and Gehrels, G.E. 2011. Continental-scale detrital zircon provenance signatures in Lower Cretaceous strata, western North America. Geology, **39**: 399–402. doi:10.1130/G31762.1.

Li, Z., and Aschoff, J. 2022. Constraining the effects of dynamic topography on the development of Late Cretaceous Cordilleran foreland

basin, western United States. Geological Society of America Bulletin. **134**(1-2): 446–462. doi:10.1130/B35838.1.134446.

Lichtner, D.T., Toner, R.N., Wrage, J.M., and Lynds, R.M. 2020. Upper Cretaceous strata in the Powder River Basin: formation tops database, structure and thickness contour maps, and associated well data. Wyoming Geological Survey Open File Report 2020-9. Wyoming Geological Survey, Casper, WY. 50p.

Liu, S., Nummedal, D., and Gurnis, M. 2014. Dynamic versus flexural controls of late Cretaceous Western Interior Basin, USA. Earth and Planetary Science Letters, **389**: 221–229. doi:10.1016/j.epsl.2014.01.006.

Liu, S., Nummedal, D., Yin, P., and Luo, H. 2005. Linkage of Sevier thrusting episodes and Late Cretaceous foreland basin megasequences across southern Wyoming (USA). Basin Research, **17**: 487–506. doi:10.1111/j.1365-2117.2005.00277.x.

Logan, J. 2002. Intrusion-related mineral occurrences of the Cretaceous Bayonne magmatic belt, southeast British Columbia. British Columbia Geological Survey, Geoscience Map 2001-1, scale 1:500,000. British Columbia Geological Survey, Victoria, BC.

Ludvigson, G.A., Joeckel, R.M., González, L.A., Gulbranson, E.L., Rasbury, E.T., Hunt, G.J., et al. 2010. Correlation of Aptian–Albian carbon isotope excursions in continental strata of the Cretaceous foreland basin, eastern Utah, U.S.A. Journal of Sedimentary Research, **80**: 955–974. doi:10.2110/jsr.2010.086.

M'Gonigle, J.W., and Dover, J.H. 1992. Geologic map of the Kemmerer 30′ × 60′ quadrangle, Lincoln, Uinta, and Sweetwater counties, Wyoming. United States Geological Survey Geologic Investigations Map I-2079, scale 1:100,000. United States Geological Survey, Denver, CO.

Mack, G.H. 1987. Mid-Cretaceous (Late Albian) change from rift to retroarc foreland basin in southwestern New Mexico. Geological Society of America Bulletin, **98**: 507–514. doi:10.1130/0016-7606(1987)98⟨507:MLACFR⟩2.0.CO;2.

Mair, J.L., Hart, C.J.R., and Stephens, J.R. 2006. Deformation history of the northwestern Selwyn basin, Yukon, Canada: implications for orogen evolution and mid-Cretaceous magmatism. Geological Society of America Bulletin, **118**: 304–323. doi:10.1130/B25763.1.

Martini, M., and Ferrari, L. 2011. Style and chronology of the Late Cretaceous shortening in the Zihuatanejo area (south-western Mexico): implications for the timing of the Mexican Laramide deformation. Geosphere, **7**: 1469–1479. doi:10.1130/GES00743.1.

Martini, M., Ferrari, L., López-Martínez, M., and Valencia, V. 2010. Stratigraphic redefinition of the Zihuatanejo area, southwestern Mexico. Revista Mexicana de Ciencias Geológicas, **27**: 412–430.

Martini, M., Mori, L., Solari, L., and Centeno-García, E. 2011. Sandstone provenance of the Arperos basin (Sierra de Guanajuato, central Mexico): Late Jurassic–Early Cretaceous back-arc spreading as the foundation of the Guerrero terrane. The Journal of Geology, **119**: 597–617. doi:10.1086/661989.

Martini, M., Solari, L., and Camprubí, A. 2013. Kinematics of the Guerrero terrane accretion in the Sierra de Guanajuato, central Mexico: new insights for the structural evolution of arc–continent collisional zones. International Geology Review, **55**: 574–589. doi:10.1080/00206814.2012.729361.

Martini, M., Solari, L., and Lopez-Martínez, M. 2014. Correlating the Arperos basin from Guanajuato, central Mexico, to Santo Tomás, southern Mexico: implications for the paleogeography and origin of the Guerrero terrane. Geosphere, **10**: 1385–1401. doi:10.1130/GES01055.1.

Mauel, D.J., Lawton, T.F., González-Léon, C., Iriondo, A., and Amato, J.M. 2011. Stratigraphy and age of upper Jurassic strata in north-central Sonora, Mexico: southwestern Laurentian record of crustal extension and tectonic transition. Geosphere, **7**: 390–414. doi:10.1130/GES00600.1.

May, S.R., Gray, G.G., Summa, L.I., Stewart, N.R., Gehrels, G.E., and Pecha, M.E. 2013a. Detrital zircon geochronology from Cenomanian–Coniacian strata in the Bighorn Basin, Wyoming, U.S.A.: implications for stratigraphic correlation and paleogeography. Rocky Mountain Geology, **48**: 41–61. doi:10.2113/gsrocky.48.1.41.

May, S.R., Gray, G.G., Summa, L.L., Stewart, N.R., Gehrels, G.E., and Pecha, M.E. 2013b. Detrital zircon geochronology from the Bighorn Basin, Wyoming, USA: implications for tectonostratigraphic evolution and paleogeography. Geological Society of America Bulletin, **125**: 1403–1422. doi:10.1130/B30824.1.

Mendoza, O.T., and Suastegui, M.G. 2000. Geochemistry and isotopic composition of the Guerrero terrane (western Mexico): implications for the tectono-magmatic evolution of southwestern North America during the late Mesozoic. Journal of South American Earth Sciences, **13**: 297–324. doi:10.1016/S0895-9811(00)00026-2.

Merewether, E.A., and Cobban, W.A. 1986. Evidence of mid-Cretaceous tectonism in the Frontier Formation, Natrona county, Wyoming. Earth Science Bulletin, **1**: 142–152.

Merewether, E.A., Blackmon, P.D., and Webb, J.C. 1984. The mid-Cretaceous Frontier Formation near the Moxa Arch, southwestern Wyoming. United States Geological Survey Professional Paper 1290. United States Geological Survey, Denver, CO. 29p.

Miall, A.D., and Catuneanu, O. 2019. The Western Interior Basin. *In* The sedimentary basins of the United States and Canada. *Edited by* A.D. Miall. Amsterdam, The Netherlands, Elsevier, pp. 401–443.

Miller, D.M., Miller, R.J., Nielson, J.E., Wilshire, H.G., Howard, K.A., and Stone, P. 2007. Geologic map of the East Mojave National Scenic Area, California. *In* Geology and mineral resources of the East Mojave National Scenic Area, San Bernardino County, California. *Edited by* T.G. Theodore. United States Geological Survey Bulletin 2160, Scale 1:125,000. United States Geological Survey, Denver, CO.

Mitrovica, J.X., Beaumont, C., and Jarvis, G.T. 1989. Tilting of continental interiors by the dynamical effects of subduction. Tectonics, **8**: 1079–1094. doi:10.1029/TC008i005p01079.

Molnar, P., England, P. C., and Jones, C.H. 2015. Mantle dynamics, isostasy, and the support of high terrain. Journal of Geophysical Research, Solid Earth, **120**: 1932–1957. doi:10.1002/2014JB011724.

Monger, J.W.H., Price, R.A., and Templeman-Kluitt, D. 1982. Tectonic accretion and the origin of two metamorphic and plutonic welts in the Canadian Cordillera. Geology, **10**: 70–75. doi:10.1130/0091-7613(1982)10⟨70:TAATOO⟩2.0.CO;2.

Monod, O., Busnardo, R., and Guerrero-Suastegui, M. 2000. Late Albian ammonites from the carbonate cover of the Teloloapan arc volcanic rocks (Guerrero State, Mexico). Journal of South American Earth Sciences, **13**: 377–388. doi:10.1016/S0895-9811(00)00030-4.

Mori, H. 2009. Dinosaurian faunas of the Cedar Mountain Formation with detrital zircon ages for three stratigraphic sections and the relationship between the degree of abrasion and U-Pb LA-ICP-MS ages of detrital zircons. M.S. thesis, Brigham Young University, Provo, UT. 102p.

Morris, R.A., DeBari, S.M., Busby, C., Medynski, S., and Jicha, B.R. 2019. Building arc crust: plutonic to volcanic connections in an extensional oceanic arc, the southern Alisitos arc, Baja California. Journal of Petrology, **60**: 1195–1228. doi:10.1093/petrology/egz029.

Mueller, P.A., Wooden, J.L., Mogk, D.W., and Foster, D.A. 2011. Paleoproterozoic evolution of the Farmington zone: implications for terrane accretion in southwestern Laurentia. Lithosphere, **3**: 401–408. doi:10.1130/L161.1.

Murphy, D.C. 1997. Geology of the McQuesten River region, northern McQuesten and Mayo map area, Yukon Territory, (115P/14, 15, 16; 105 M/13, 14). Exploration and Geological Services Division, Yukon, Indian and Northern Affairs Canada, Bulletin 6. Yukon, Indian and Northern Affairs Canada, Whitehorse, YT. 122p.

Nelson, S., Harris, R., Dorais, M., Heizler, M., Constenius, K., and Barnett, D. 2002. Basement complexes in the Wasatch fault, Utah, provide new limits on crustal accretion. Geology, **30**: 831–834. doi:10.1130/0091-7613(2002)030⟨0831:BCITWF⟩2.0.CO;2.

Norris, D.K., Stevens, R.D., and Wanless, R.K. 1965. K-Ar age of igneous pebbles in the McDougall-Segur conglomerate, southeastern Canadian Cordillera. Geological Survey of Canada, Paper 65-26. Geological Survey of Canada, Ottawa, ON. 11p.

Ogg, J.G., and Hinnov, L.A. 2012. Cretaceous. *In* The geologic time scale 2012. *Edited by* F.M. Gradstein, J.G. Ogg, M. Schmitz and G. Ogg. Elsevier, Amsterdam. pp. 793–853. doi:10.1016/B978-0-444-59425-9.00027-5.

Oriel, S.S., and Platt, L.B. 1980. Geologic map of the Preston 1° x 2° quadrangle, southeast Idaho and western Wyoming. United States Geological Survey, Geologic Investigations Map I-1127, scale 1:250,000. United States Geological Survey, Denver, CO.

Page, W.R., Lundstrom, S.C., Harris, A.G., Langenheim, V.E., Workman, J.B. Mahan, S.A., et al. 2005. Geologic and geophysical maps of the Las Vegas 30° x 60° Quadrangle, Clark and Nye Counties, Nevada,

and Inyo County, California. United States Geological Survey Scientific Investigations Map 2814, scale 1:100,000. United States Geological Survey, Denver, CO.

Painter, C.S., Carrapa, B., DeCelles, P.G., Gehrels, G.F., and Thomson, S.N. 2014. Exhumation of the North American Cordillera revealed by multi-dating of Upper Jurassic–Upper Cretaceous foreland basin deposits. Geological Society of America Bulletin, **126**: 1439–1464. doi:10.1130/B30999.1.

Pana, D.I., and van der Pluijm, B.A. 2015. Orogenic pulses in the Alberta Rocky Mountains: radiometric dating of major faults and comparison with the regional tectono-stratigraphic record. Geological Society of America Bulletin, **127**: 480–502. doi:10.1130/B31069.1.

Pana, D.I., Poulton, T.P., and DuFrane, S.A. 2019. U-Pb detrital zircon dating supports early Jurassic initiation of the Cordilleran foreland basin in southwestern Canada. Geological Society of America Bulletin, **131**: 318–334. doi:10.1130/B31862.1.

Pana, D.I., Poulton, T.P., and Heaman, L.M. 2018a. U-Pb zircon ages of volcanic ashes integrated with ammonite biostratigraphy, Fernie Formation (Jurassic), Western Canada, with implications for Cordilleran-foreland basin connections and comments on the Jurassic time scale. Bulletin of Canadian Petroleum Geology, **66:** 595–622.

Pana, D.I., Rukhlov, A.S., Heaman, L.M., and Hamilton, M. 2018b. Geochronology of selected igneous rocks in the Alberta Rocky Mountains, with an overview of the age constraints on the host formations. Alberta Energy Regulator/Alberta Geological Survey Open-File Report 2018-03. Alberta Geological Survey, Edmonton, AB. 67p.

Pape, D.E., Spell, T.L., Bonde, J.W., Fish, B., and Rowland, S.M. 2011. $^{40}Ar/^{39}Ar$ isotopic dates for the fossiliferous Willow Tank Formation (Cretaceous) in Valley of Fire State Park, Nevada. Geological Society of America Abstracts with Programs, **43**(5): 586.

Pavlis, T.L., Amato, J.M., Trop, J.M., Ridgway, K.D., Roeske, S.M., and Gehrels, G.E. 2020. Subduction polarity in ancient arcs: a call to integrate geology and geophysics to decipher the Mesozoic tectonic history of the northern Cordillera of North America. GSA Today, **29**: 4–10. doi:10.1130/GSATG465Y.1.

Pearce, J.A., Harris, N.B.W., and Tindle, A.G. 1984. Trace element discrimination diagrams for the tectonic interpretation of granitic rocks. Journal of Petrology, **25**: 956–983. doi:10.1093/petrology/25.4.956.

Peccerillo, A. 2005. Plio-Quaternary volcanism in Italy: Petrology, Geochemistry, Geodynamics. New York, Springer-Verlag, 365p with CD-ROM.

Peterson, T.D., Currie, K.L., Ghent, E.D., Bégin, N.J., and Beiersdorfer, R.E. 1997. Petrology and economic geology of the Crowsnest volcanics, Alberta. *In* Exploring for minerals in Alberta. *Edited by* R.W. MacQueen. Geological Survey of Canada Geoscience Contributions, Canada-Alberta agreement on mineral development (1992–1995). Geological Survey of Canada Bulletin 500. Geological Survey of Canada, Ottawa, ON. pp. 163–184.

Plint, A.G. 2000. Sequence stratigraphy and paleogeography of a Cenomanian deltaic complex: the Dunvegan and lower Kaskapau formations in subsurface and outcrop, Alberta and British Columbia, Canada. Bulletin of Canadian Petroleum Geology, **48**: 43–79. doi:10.2113/48.1.43.

Plint, A.G., Krawetz, J.R., Buckley, R.A., Vannelli, K.M., and Walaszczyk, I. 2018. Tectonic, eustatic and climatic controls on marginal-marine sedimentation across a flexural depocentre: Paddy Member of Peace River Formation (Late Albian), western Canada foreland basin. Depositional Record, **4**: 4–58. doi:10.1002/dep2.37.

Plint, A.G., Tyagi, A., Hay, M.J., Varban, B.L., Zhang, H., and Roca, X. 2009. Clinoforms, paleobathymetry, and mud dispersal across the Western Canada Cretaceous foreland basin: evidence from the Cenomanian Dunvegan Formation and contiguous strata. Journal of Sedimentary Research, **79**: 144–161. doi:10.2110/jsr.2009.020.

Plint, A.G., Tyagi, A., McCausland, P. J. A., Krawetz, J.R., Zhang, H., Roca, X., et al. 2012. Dynamic relationship between subsidence, sedimentation, and unconformities in mid-Cretaceous, shallow-marine strata of the Western Canada foreland basin: links to Cordilleran tectonics, chapter 24. *In* Tectonics of sedimentary basins: Recent advances. *Edited by* C. Busby and A. Azor. Blackwell Publishing, Oxford, UK. pp. 480–507.

Porter, K.W., Dyman, T.S., Cobban, W.A., and Reinson, G.E. 1998. Post-Manville/Kootenai Lower Cretaceous rocks and reservoirs, north-central Montana, southern Alberta and Saskatchewan. *In* Eighth International Williston Basin Symposium. *Edited by* J.E. Christopher et al. Saskatchewan Geological Society Special Publication 13. Saskatchewan Geological Society, Regina, SK. pp.123–127.

Price, R.A. 1973. Large scale gravitational flow of supracrustal rocks, southern Canadian Rockies. *In* Gravity and tectonics. *Edited by* K.A. De Jong and K. Scholten. John Wiley, New York, pp. 491–502.

Price, R.A. 1994. Chapter 2: Cordilleran tectonics and the evolution of the Western Canada sedimentary basin. *In* Geological atlas of the western Canada sedimentary basin. *Edited by* G. Mossop and I. Shetsen. Canadian Society of Petroleum Geologists and Alberta Research Council, Calgary, AB. pp. 13–24.

Price, R.A., and Sears, J.W. 2000. A preliminary palinspastic map of the Mesoproterozoic Belt-Purcell Supergroup, Canada and USA: implications for the tectonic setting and structural evolution of the Purcell anticlinorium and the Sullivan deposit. *In* The geological environment of the Sullivan deposit, British Columbia. *Edited by* J.W. Lydon, T. Höy, J.F. Slack and M.E. Knapp. Geological Association of Canada Special Publication 1. Geological Association of Canada, St. John's, NL. pp. 61–81.

Pubellier, M., Rangin, C., Rascon, B., Chorowicz, J., and Bellon, H. 1995. Cenomanian thrust tectonics in the Sahuaripa region, Sonora: implications about northwestern Mexico megashears. *In* Studies on the Mesozoic of Sonora and adjacent areas. *Edited by* C. Jacques-Ayala, C.M. González-León and J. Roldán-Quintana. Geological Society of America Special Paper 301. Geological Society of America, Boulder, CO. pp.111–120. doi:10.1130/0-8137-2301-9.111.

Pujols, E.J., Stockli, D.F., Constenius, K.N., and Horton, B.K. 2020. Thermo-chronological and geochronological constraints on late Cretaceous unroofing and proximal sedimentation in the Sevier orogenic belt, Tectonics, **39**: e2019TC005794. doi:10.1029/2019TC005794.

Quick, J.D., Hogan, J.P., Wizevich, M., Obrist-Farner, J., and Crowley, J.L. 2020. Timing of deformation along the Iron Springs thrust, southern Sevier fold-and-thrust belt, Utah: evidence for an extensive thrusting event in the mid-Cretaceous. Rocky Mountain Geology, **55**: 75–89. doi:10.24872/rmgjournal.55.2.75.

Quinn, G.M., Hubbard, S.M., van Drecht, R., Guest, B., Matthews, W.A., and Hadlari, T. 2016. Record of orogenic cyclicity in the Alberta foreland basin, Canadian Cordillera. Lithosphere, **8**: 317–332. doi:10.1130/L531.1.

Quintero-Legorreta, O. 1992. Geología de la región de Comanja, estados de Guanajuato y Jalisco. Universidad Nacional Autónoma de México, Instituto de Geología. **10**: 6–25.

Rasmussen, K.L. 2013. The timing, composition and petrogenesis of syn- to post-accretionary magmatism in the northern Cordilleran miogeocline, eastern Yukon and southwestern Northwest Territories. Ph.D. dissertation. University of British Columbia, Vancouver, BC. 788p.

Redden, J.A., and DeWitt, E. 2008. Maps showing geology, structure, and geophysics of the central Black Hills, South Dakota. United States Geological Survey, Scientific Investigations Map 2777, scale 1:100,000.

Reed, J.C., Jr., Wheeler, J.O., and Tucholke, B.E. 2005. Geologic map of North America. Decade of North American Geology Continental Scale Map 001, scale 1:5,000,000. Geological Society of America, Boulder, CO

Reese, J.A. 1989. Initial deposition in the Sevier foreland basin of southern Nevada; conglomerates of the Cretaceous Willow Tank Formation, Clark county, Nevada. M.S. Thesis, University of Nevada, Las Vegas, NV, 145p.

Reeside, J.B., Jr., and Cobban, W.A. 1960. Studies of the Mowry Shale (Cretaceous) and contemporary formations in the United States and Canada. United States Geological Survey Professional Paper 355. United States Geological Survey, Denver, CO. 126p.

Reinson, G.E., Warters, G.E., Cox, J., and Price, P.R. 1994. Chapter 21 – Cretaceous Viking Formation of the western Canada sedimentary basin. *In* Geological atlas of the western Canada sedimentary basin. G.D. Mossop and I. Shetsen. Canadian Society of Petroleum Geologists and Alberta Research Council, Calgary, AB. pp. 353–363.

Roberts, L.N.R., and Kirschbaum, M.A. 1995. Paleogeography of the Late Cretaceous of the Western Interior of middle North America: Coal distribution and sediment accumulation. U.S. Geological Survey Professional Paper 1561. U.S. Geological Survey, Denver, CO. 115p.

Roca, X., Rylaarsdam, J.R., Zhang, H., Varban, B.L., Sisulak, C.F., Bastedo, K., and Plint, A.G. 2008. Regional allostratigraphic correlation of Up-

per Albian to Lower Cenomanian foreland basin strata in the Rocky Mountain foothills and adjacent subsurface of Alberta and British Columbia: a genetic framework for a lower Colorado allogroup. Bulletin of Canadian Petroleum Geology, **56**: 259–299. doi:10.2113/gscpgbull.56.4.259.

Ross, G.M., Patchett, R.J., Hamilton, M., Heaman, L., DeCelles, P.G., Rosenberg, E., and Giovanni, M.K. 2005. Evolution of the Cordilleran orogen (southwestern Alberta, Canada) inferred from detrital mineral geochronology, geochemistry, and Nd isotopes in the foreland basin. Geological Society of America Bulletin, **117**: 747–763. doi:10.1130/B25564.1.

Royse, F., Jr. 1993. An overview of the geologic structure of the thrust belt in Wyoming, northern Utah, and eastern Idaho. *In* Geology of Wyoming. *Edited by* A.W. Snoke, J.R. Steidtmann and S.M. Roberts. Geological Survey of Wyoming Memoir 5. Geological Survey of Wyoming, Laramie, WY. pp. 272–311.

Royse, F., Jr., Warner, M.A., and Reese, D.L. 1975. Thrust-belt structural geometry and related stratigraphic problems, Wyoming-Idaho-northern Utah. *In* Deep drilling frontiers of the central Rocky Mountains. Rocky Mountain Association of Geologists Symposium 1975. Rocky Mountain Association of Geologists, Denver, CO. pp. 41–54.

Rubey, W.M. 1929. Origin of the siliceous Mowry shale of the Black Hills region. *In* Shorter contributions to general geology, 1928. United States Geological Survey Professional Paper 154-D. United States Geological Survey, Denver, CO. pp. 153–170.

Rubey, W.M. 1973. New Cretaceous formations in the western Wyoming thrust belt. United States Geological Survey Bulletin 1372-I, United States Geological Survey, Denver, CO. 35p.

Sabbatino, M., Tavani, S., Vitale, S., Orgacta, K., Corradetti, A., Consorti, L., et al. 2021. Forebulge migration in the foreland basin system of the central-southern Apennine fold-thrust belt (Italy): new high-resolution Sr-isotope dating constraints. Basin Research, **33**: 2817. doi:10.1111/bre.12587.

Sabbatino, M., Vitale, S., Tavani, S., Consorti, L., Corradetti, A., Cipriani, A., et al. 2020. Constraining the onset of flexural subsidence and peripheral bulge extension in the Miocene foreland of the southern Apennines (Italy) by Sr-isotope stratigraphy. Sedimentary Geology, **401**: 105634. doi:10.1016/j.sedgeo.2020.105634.

Samson, S.D. 2009. Dinosaur odyssey: Fossil threads in the web of life. University of California Press, Berkeley, CA. 332p.

Schröder-Adams, C.J., Cumbaa, S.L., Bloch, J., Leckie, D.A., Craig, J., Seif El-Dein, S.A., et al. 2001. Late Cretaceous (Cenomanian to Campanian) paleoenvironmental history of the eastern Canadian margin of the Western Interior seaway: bonebeds and anoxic events. Palaeogeography, Palaeoclimatology, Palaeoecology, **170**: 261–289. doi:10.1016/S0031-0182(01)00259-0.

Schröder-Adams, C.J., Leckie, D.A., Bloch, J., Craig, J., McIntyre, D.J., and Adams, P.J. 1996. Paleoenvironmental changes in the Cretaceous (Albian to Turonian) Colorado Group of Western Canada: microfossil, sedimentological and geochemical evidence. Cretaceous Research, **17**: 311–365. doi:10.1006/cres.1996.0022.

Schwans, P. 1995. Controls on sequence stacking and fluvial to shallow-marine architecture in a foreland basin. *In* Sequence stratigraphy of foreland basin deposits. *Edited by* J.A. Van Wagoner and G.T. Bertram. American Association of Petroleum Geologists Memoir 64. American Association of Petroleum Geologists, Tulsa, OK. pp. 55–102.

Sharman, G.R., Sharman, J.P., and Sylvester, Z. 2018. detritalPy: a Python-based toolset for visualizing and analyzing detrital geothermochronologic data. Depositional Records, **4:** 202–215. doi:10.1002/dep2.45.

Silver, L.T., and Chappell, B. 1988. The Peninsular Ranges batholith: an insight into the Cordilleran batholiths of southwestern North America. Earth and Environmental Science Transactions of the Royal Society of Edinburgh, **79**: 105–121. doi:10.1017/S0263593300014152.

Silver, L.T., Taylor, H.P., Jr., and Chappell, B. 1979. Some petrological, geochemical and geochronological observations of the Peninsular Ranges batholith near the international border of the U.S.A. and Mexico. *In* Mesozoic crystalline rocks. *Edited by* P.L. Abbott and V.R. Todd. Department of Geological Sciences, California State University, San Diego, CA. pp. 83–110.

Sinclair, H.D. 1997. Tectonostratigraphic model for underfilled peripheral foreland basins: an alpine perspective. Geological Society of America Bulletin, **109**: 324–346. doi:10.1130/0016- 7606(1997)109⟨0324:TMFUPF⟩2.3.CO;2.

Singer, B.S., Jicha, B.R., Sawyer, D., Walaszczyk, I., Buchwaldt, R., and Mutterlose, J. 2021. Geochronology of Late Albian-Cenomanian strata in the U.S. western interior. Geological Society of America Bulletin, **133**: 1665–1678. doi:10.1130/B35794.1.

Skipp, B. 1987. Basement thrust sheets in the Clearwater orogenic zone, central Idaho and western Montana. Geology, **15**: 220–224. doi:10.1130/0091-7613(1987)15⟨220:BTSITC⟩2.0.CO;2.

Skipp, B., and Hait, M.H., Jr. 1977. Allochthons along the northeast margin of the Snake River Plain, Idaho. *In* Rocky Mountain thrust belt geology and resources. *Edited by* E.L. Heisey and D.E. Lawson. Annual Field Conference 29. Wyoming Geological Association, Casper, WY. pp. 499–516.

Spieker, E.M. 1946. Late Mesozoic and early Cenozoic history of central Utah. U.S. Geological Society Professional Paper 205-D. U.S. Geological Society, Denver, CO. pp. 117–161.

Sprinkel, D.A. 1994. Stratigraphic and time-stratigraphic cross sections: a north-south transect from near the Uinta mountains axis across the Basin and Range transition zone to the western margin of the San Rafael Swell, Utah. U.S. Geological Survey Miscellaneous Investigations Series I-2184-D. U.S. Geological Survey, Denver, CO. 31p. Scale 1:500,000.

Sprinkel, D.A., Madsen, S.K., Kirkland, J.I., Waanders, G.L., and Hunt, G.J. 2012. Cedar Mountain and Dakota formations around Dinosaur National Monument—evidence of the first incursion of the Cretaceous Western Interior seaway into Utah. Utah Geological Survey Special Study 143. Utah Geological Survey, Salt Lake City, UT. 21p. compact disc.

Sprinkel, D.A., Weiss, M.P., Fleming, R.W., and Waanders, G.L. 1999. Redefining the Lower Cretaceous stratigraphy within the central Utah foreland basin. Utah Geological Survey Special Studies **97**: 21p.

Stapp, R.W. 1967. Relationship of Lower Cretaceous depositional environment to oil accumulation, northeastern Powder River basin, Wyoming. AAPG Bulletin, **51**: 2044–2055. doi:10.1306/5D25C1F5-16C1-11D7-8645000102C1865D.

Stelck, C.R. 1962. Upper Cretaceous, Peace River area, British Columbia. *In* Peace River. *Edited by* E.E. Pelzer. Edmonton Geological Society Guidebook, Fourth Annual Field Trip. Edmonton Geological Society, Edmonton, AB. 10–21. pp.

Stelck, C.R. 1975. The upper Albian *Miliammina manitobensis* zone in northeastern British Columbia. *In* The Cretaceous system in the western interior of North America. *Edited by* W.G.E. Caldwell. Geological Association of Canada, Special Paper 13. Geological Association of Canada, St. John's, NL. pp. 253–275.

Stelck, C.R., and Koke, K.R. 1987. Foraminiferal zonation of the Viking interval in the Hasler Shale (Albian), northeastern British Columbia. Canadian Journal of Earth Sciences, **24**: 2254–2278. doi:10.1139/e87-212.

Stelck, C.R., and Leckie, D.A. 1990. Biostratigraphy of the Albian Paddy Member (Lower Cretaceous Peace River Formation). Canadian Journal of Earth Sciences, **27**: 1159–1169. doi:10.1139/e90-123.

Stockmal, G.S., and Beaumont, C. 1987. Geodynamic models of convergent margin tectonics: the southern Canadian Cordillera and the Swiss Alps. *In* Sedimentary basins and basin-forming mechanisms. *Edited by* C. Beaumount and A.J. Tankard. Canadian Society of Petroleum Geologists, Memoir 12 and Atlantic Geoscience Society, Special Publication 5. Canadian Society of Petroleum Geologists. Calgary, AB. pp. 393–411.

Stockmal, G.S., Beaumont, C., and Boutilier, R. 1986. Geodynamic models of convergent margin tectonics: transition from rifted margin to overthrust belt and consequences for foreland-basin development. American Association of Petroleum Geologists Bulletin, **70**: 181–190.

Stokes, W.L. 1976. What is the Wasatch line? *In* Geology of the Cordilleran hingeline. *Edited by* J.G. Hill. Rocky Mountain Association of Geologists, Denver, CO. pp. 11–25.

Stott, D.F. 1982. Lower Cretaceous Fort St. John Group and Upper Cretaceous Dunvegan Formation of the foothills and plains of Alberta, British Columbia, District of Mackenzie and Yukon Territory. Geological Survey of Canada Bulletin 328. Geological Survey of Canada, Ottawa, ON. 124p.

Stroup, C.N., Link, P.K., Janecke, S.U., Fanning, C.M., Yaxley, G.M., and Beranek, L.P. 2008. Eocene to Oligocene provenance and drainage in extensional basins of southwest Montana and east-central Idaho: evidence from detrital zircon populations in the Renova Formation and equivalent strata. *In* Ores and orogenesis: circum-Pacific tectonics, geologic evolution and ore deposits. *Edited by* J.E. Spencer and S.R. Titley. Arizona Geological Society Digest 22. Arizona Geological Society, Tucson, AZ. pp. 529–546.

Suarez, C.A., González, L.A., Ludvigson, G.A., Kirkland, J.I., Cifelli, R.L., and Kohn, M.J. 2014. Multi-taxa isotopic investigation of paleohydrology in the Lower Cretaceous Cedar Mountain Formation, eastern Utah, U.S.A.: deciphering effects of the Nevada Plano plateau on regional climate. Journal of Sedimentary Research, **84**: 975–987. doi:10.2110/jsr.2014.76.

Talavera-Mendoza, O., Ruiz, J., Gehrels, G. E., Valencia, V. A., and Centeno-García, E. 2007. Detrital zircon U/Pb geochronology of southern Guerrero and western Mixteca arc successions (southern Mexico): new insights for the tectonic evolution of the southwestern North America during the late Mesozoic. Geological Society of America Bulletin, **119**: 1052–1065. doi:10.1130/B26016.1.

Tardy, M., Lapierre, H., Freydier, C., Coulon, C., Gill, J.B., and Mercier De Lepinay, B., 1994. The Guerrero suspect terrane (western Mexico) and coeval arc terranes (the Greater Antilles and the Western Cordillera of Colombia): a Late Mesozoic intra-oceanic arc accreted to cratonal America during the Cretaceous. Tectonophysics, **230**: 49–73. doi:10.1016/0040-1951(94)90146-5.

Tesauro, M., Kaban, M.K., and Mooney, W.D. 2015. Variations of the lithospheric strength and elastic thickness in North America. Geochemistry, Geophysics, Geosystems, **16**: 2197–2220. doi:10.1002/2015GC005937.

Thomson, D., Schroëder-Adams, C.J., Hadlari, T., Dix, G., and Davis, W.J. 2011. Albian to Turonian stratigraphy and paleoenvironmental history of the northern Western Interior sea in the Peel Plateau region, Northwest Territories, Canada. Palaeogeography, Palaeoclimatology, Palaeoecology, **302**: 270–300. doi:10.1016/j.palaeo.2011.01.017.

Tizzard, P.G., and Lerbekmo, J.F. 1975. Depositional history of the Viking Formation, Suffield area, Alberta, Canada. Bulletin of Canadian Petroleum Geology, **23**: 715–752.

Troyer, R., Barth, A.P., Wooden, J.L., and Jacobson, C. 2006. Provenance and timing of Sevier foreland basin sediments in the Valley of Fire, southern Nevada, from U-Pb geochronology. Geological Society of America Abstracts with Programs, **38**(7): 369.

Tucker, R.T., Zanno, L.E., Huang, H-Q., and Makovocky, P.J. 2020. A refined temporal framework for newly discovered fossil assemblages of the upper Cedar Mountain Formation (Mussentuchit Member), Mussentuchit Wash, central Utah. Cretaceous Research, **110**: 104384. doi:10.1016/j.cretres.2020.104384.

Tulloch, A.J., and Kimbrough, D.L. 2003. Paired plutonic belts in convergent margins and the development of high Sr/Y magmatism: Peninsular Ranges batholith of Baja-California and Median batholith of New Zealand. *In* Tectonic evolution of northwestern Mexico and the southwestern USA. *Edited by* S.E. Johnson, S.R. Patterson, J.M. Fletcher, G.H. Girty, D.L. Kimbrough and A. Martín-Barajas. Geological Society of America Special Paper 374. Geological Society of America, Boulder, CO. pp. 275–295. doi:10.1130/0-8137-2374-4.275.

Turcotte, D.L. 1979. Flexure. *In* Advances in geophysics. *Edited by* B. Saltzman, B. Academic Press, New York, **v. 21**, pp. 51–86.

Turcotte, D.L., and Schubert, G. 1982. Geodynamics: Applications of continuum physics to geological problems. John Wiley & Sons, New York. 450p.

Tyagi, A., Plint, A.G., and McNeil, D.H. 2007. Correlation of physical surfaces, bentonites, and biozones in the Cretaceous Colorado group from the Alberta Foothills to southeast Saskatchewan, and a revision of the Belle Fourche – Second White Specks formational boundary. Canadian Journal of Earth Sciences, **44**: 871–888. doi:10.1139/e07-004.

Tysdal, R.G., Dyman, T.S., and Nichols, D.J. 1989. Correlation chart of Lower Cretaceous rocks, Madison Range to Lima Peaks area, southwestern Montana. United States Geological Survey, Miscellaneous Field Studies Map MF-2067. United States Geological Survey, Denver, CO. pp. 1–16.

Ullmann, P.V., Varricchio, D., and Knell, M.J. 2012. Taphonomy and taxonomy of a vertebrate microsite in the mid-Cretaceous (Albian-Cenomanian) Blackleaf Formation, southwest Montana. Historical Biology, **24**: 311–328.

van der Meulen, M.J., Kouwenhoven, T.J., van der Zwaan, G.J., Meulenkamp, J.E., and Wortel, M.J.R. 1999. Late Miocene uplift in the Romagnan Apennines and the detachment of subducted lithosphere. Tectonophysics, **315**: 319–335. doi:10.1016/S0040-1951(99)00282-6.

van der Meulen, M.J., Meulenkamp, J.E., and Wortel, M.J.R. 1998. Lateral shifts of Apenninic foredeep depocentres reflecting detachment of subducted lithosphere. Earth and Planetary Science Letters, **154**: 203–219. doi:10.1016/S0012-821X(97)00166-0.

Varricchio, D.J., Martin, A.J., and Katsura, Y. 2007. First trace and body fossil evidence of a burrowing, denning dinosaur. Proceedings of the Royal Society B: Biological Sciences, **274**: 1361–1368. doi:10.1098/rspb.2006.0443.

Vorobieva, O. 2000. A multidisciplinary subsurface study of the Albian Bow Island and Westgate formations in southwestern Alberta, Canada. M.S. thesis, Carleton University, Ottawa, ON, 202p.

Vuke, S.M. 1984. Depositional environments of the early Cretaceous Western Interior seaway in southwestern Montana and the northern United States. *In* The Mesozoic of middle North America. *Edited by* D.F. Stott and D.J. Glass. Canadian Society of Petroleum Geologists Memoir 9. Canadian Society of Petroleum Geologists, Calgary, AB. pp. 127–144.

Walaszczyk, I., and Cobban, W.A. 2016. Inoceramid bivalves and biostratigraphy of the Upper Albian and Lower Cenomanian of the United States Western Interior Basin. Cretaceous Research, **59**: 30–68. doi:10.1016/j.cretres.2015.10.019.

Walker, J.D., Burchfiel, B.C., and Davis, G.A. 1995. New age controls on initiation and timing of foreland belt thrusting in the Clark Mountains, southern California. Geological Society of America Bulletin, **107**: 742–750. doi:10.1130/0016-7606(1995)107⟨0742:NACOIA⟩2.3.CO;2.

Wallace, C.A., Lidke, D.J., and Schmidt, R.G. 1990. Faults of the central part of the Lewis and Clark line and fragmentation of the Late Cretaceous foreland basin in west-central Montana. Geological Society of America Bulletin, **102**: 1021–1037. doi:10.1130/0016-7606(1990)102⟨1021:FOTCPO⟩2.3.CO;2.

Waring, J. 1976. Regional distribution of environments of the Muddy Sandstone, southeastern Montana. *In* Geology and energy resources of the Powder River; 28th Annual Field Conference Guidebook. Wyoming Geological Association, Casper, WY. pp. 83–96.

Warzeski, E.R. 1987. Revised stratigraphy of the Mural Limestone: a lower Cretaceous carbonate shelf in Arizona and Sonora. *In* Mesozoic rocks of southern Arizona and adjacent areas. *Edited by* W.R. Dickinson and M.F. Klute. Arizona Geological Society Digest 18, Arizona Geological Society, Tucson, Arizona. pp. 335–363.

Weimer, R.J. 1986. Relationship of unconformities, tectonics, and sea level changes in the Cretaceous of the Western Interior, United States. *In* Paleotectonics and sedimentation in the Rocky Mountain Region, United States. *Edited by* J.A. Peterson. American Association of Petroleum Geologists, Memoir 41. American Association of Petroleum Geologists, Tulsa, OK. pp.397–422. doi:10.1306/M41456.

Wells, M.L. 2016. A major mid-Cretaceous shortening event in the southern Sevier orogenic belt: continental record of global plate reorganization. Geological Society of America Abstracts with Programs, **48**(7). doi:10.1130/abs/2016AM-287809.

Wetmore, P.H., and Ducea, M.N. 2009. Geochemical evidence of a near-surface history for source rocks of the central Coast Mountains batholith, British Columbia. International Geology Review **1**: 1–31.

Whalen, J.B., and Hildebrand, R.S. 2019. Trace element discrimination of arc, slab failure, and A-type granitic rocks. Lithos, **348-349**: 105179. doi:10. 1016/j.lithos.2019.105179.

Whiteford, Stanley D., Jr. 1962. Regional aspects of the Muddy Formation in the Wind River Basin, Wyoming. Proceedings of the Iowa Academy of Science, **69**: 411–430.

Wilson, J.T. 1968. Static or mobile earth: the current scientific revolution. Proceedings of the American Philosophical Society, **112**: 309–320.

Wulf, G.R. 1962. Lower Cretaceous Albian rocks in the northern Great Plains. Bulletin of the American Association of Petroleum Geologists, **46**: 1371–1415.

Yanagi, T., Baadsgaard, H., Stelck, C.R., and McDougall, I. 1988. Radiometric dating of a tuff bed in the middle Albian Hulcross Formation at Hudson's Hope, British Columbia. Canadian Journal of Earth Sciences, **25**: 1123–1127. doi:10.1139/e88-109.

Yang, T., and Gurnis, M. 2016. Dynamic topography, gravity and the role of lateral viscosity variations from inversion of global mantle flow. Geophysical Journal International. **207**: 1186–1202. doi:10.1093/gji/ggw335.

Yingling, V.L., and Heller, P.L. 1992. Timing and record of foreland sedimentation during the initiation of the Sevier orogenic belt in central Utah. Basin Research, **4**: 279–290. doi:10.1111/j.1365-2117.1992.tb00049.x.

Yonkee, W.A., and Weil, A.B. 2015. Tectonic evolution of the Sevier and Laramide belts within the North American Cordillera orogenic system. Earth-Science Reviews, **150**: 531–593. doi:10.1016/j.earscirev.2015.08.001.

Yonkee, W.A., Eleogram, B., Wells, M.L., Stockli, D.F., Kelley, S., and Barber, D.E. 2019. Fault slip and exhumation history of the Willard thrust sheet, Sevier fold-thrust belt, Utah: relations to wedge propagation, hinterland uplift, and foreland basin sedimentation. Tectonics, **38**: 2850–2893. doi:2018TC005444.

Yonkee, W.A., Parry, W.T., and Bruhn, R.L. 2003. Relations between progressive deformation and fluid-rock interaction during shear zone growth in a basement-cored thrust sheet, Sevier orogenic belt, Utah. American Journal of Science, **303**: 1–59. doi:10.2475/ajs.303.1.1.

Zartman, R.E., Dyman, T.S., Tysdal, R.G., and Pearson, R.C. 1995. U-Pb ages of volcanogenic zircon from porcellanite beds in the Vaughn Member of the mid-Cretaceous Blackleaf Formation, southwestern Montana. United States Geological Survey Bulletin 2113-B. United States Geological Survey, Denver, CO. pp. 1–16.

Zuber, M.T., Bechtel, T.D., and Forsyth, D.W. 1989. Effective elastic thicknesses of the lithosphere and mechanisms of isostatic compensation in Australia. Journal of Geophysical Research, **94**: 9353–9367. doi:10.1029/JB094iB07p09353.

Zupanic, J. 2017. Lateral heterogeneity and architectural analysis of the Wall Creek Member of the Upper Cretaceous (Turonian) Frontier Formation., Unpublished MSc Thesis. University of Montana, Missoula, MT. 145p.